

CRWMS/M&O

Design Analysis Cover Sheet

Complete only applicable items.

1.

QA: L

Page: 1 Of: 114

2. DESIGN ANALYSIS TITLE Evaluation of the Potential for Deposition of Uranium/Plutonium from Repository Waste Packages			
3. DOCUMENT IDENTIFIER (Including Rev. No.) BBA000000-01717-0200-00050 REV 00			4. TOTAL PAGES 114
5. TOTAL ATTACHMENTS 3 hardcopy, 1 tape - 3 ^{all} 10/13/97		6. ATTACHMENT NUMBERS - NO. OF PAGES IN EACH I-37, II-10, III-2	
	Printed Name	Signature	Date
7. Originator	P.L. Cloke, D.M. Jolley, D.H. Lester	<i>[Signature]</i> P. Cloke for D.M. Jolley Paul F. Cloke	9/16/97 9/16/97 9/16/97
8. Checker	P.L. Cloke D.H. Lester	P. Cloke for D.H. LESTER Paul F. Cloke	9/16/97 9/16/97
9. Lead Design Engineer	Peter Gottlieb	Peter Gottlieb	9/16/97
10. Department Manager	Hugh Benton	<i>[Signature]</i> H.A. BENTON	9/16/97
11. REMARKS			
<p><u>Originator Responsibilities</u> D. M. Jolley originated Section 7.3 D. H. Lester originated Sections 7.1.3, 7.1.1.3, 7.2.3, and 7.4, and Attachment III P. L. Cloke originated the remainder</p> <p><u>Checker Responsibilities</u> P. L. Cloke checked all sections originated by D.H. Lester and D. M. Jolley D. H. Lester checked all sections originated by P. L. Cloke</p> <p>Initial Issue</p> <p>EDITORIAL CHANGE IN BLOCK 5 all 10/13/97 HAB 10/14/97</p>			

Design Analysis Revision Record

Complete only applicable items.

1.

2. DESIGN ANALYSIS TITLE	
Evaluation of the Potential for Deposition of Uranium/Plutonium from Repository Waste Packages	
3. DOCUMENT IDENTIFIER (Including Rev. No.)	
BBA000000-01717-0200-00050 REV 00	
4. Revision No.	5. Description of Revision
00	Initial Issue

Table of Contents

1.	Purpose	7
2.	Quality Assurance	7
3.	Method	8
4.	Design Inputs	8
4.1	Design Parameters	8
4.1.1	WP Materials and Performance Parameters	9
4.1.1.1	Chemical Characteristics of Representative Commercial Spent Nuclear Fuel (SNF) Waste Packages	9
4.1.1.2	Chemical Characteristics of Representative Mixed Oxide (MOX) Spent Nuclear Fuel Waste Packages	10
4.1.1.3	Chemical Characteristics of Representative Codisposal Waste Packages for High Level Waste Glass (HLW) and Immobilized Plutonium Waste	11
4.1.2	Chemistry of the Invert	14
4.1.3	Chemical Characteristics of the Host Rock	17
4.1.4	Water Chemistry	19
4.1.5	Metal Chemistry	19
4.1.6	Thermodynamic Data	21
4.2	Criteria	22
4.3	Assumptions	23
4.4	Codes and Standards	26
5.	References	27
6.	Use of Computer Software	36
6.1	EQ3/6	36
6.2	Software Routines for Chaining Successive EQ6 Cases	37
6.2.1	File bldinpt.bat	37
6.2.2	File bldinput.c	37
6.2.3	File nxtinput.bat	37
6.2.4	File nxtinput.c	37
6.3	Spreadsheets	38
7.	Design Analysis	38
7.1	Potential Mechanisms for Development of High Concentrations of Fissile Elements External to the Waste Package	38
7.1.1	Consequences of Changes in Solution Chemistry	42
7.1.1.1	Solubility Effects	42
7.1.1.2	Adsorption	42
7.1.1.3	Colloid Formation	42
7.1.2	Mechanisms for Producing Change In Solution Chemistry	42

	7.1.2.1	Reaction of Solution with Solids along Pathway	42
	7.1.2.1.1	The Waste Package Invert	42
	7.1.2.1.2	Host Rock	43
	7.1.2.1.3	Organic Matter	43
	7.1.2.1.4	Metals	43
	7.1.2.2	Evaporation of Solution	43
	7.1.2.3	Reaction with Rock or Drift Gas	43
	7.1.2.4	Mixing with Pore and/or Fracture Water along the Pathway	43
	7.1.2.5	Cooling or Heating along the Pathway	44
	7.1.2.6	Pressure Drop	44
	7.1.3	Various Mineral Formation Processes	44
	7.1.4	Some scenario principles	45
7.2		Geochemical Analysis	45
	7.2.1	Techniques Used for EQ3/6 Computations	45
	7.2.2	Analysis Method for Sorption	47
	7.2.3	Evaluation Principles for Colloidal Transport	47
	7.2.4	Settling of Dense Particles Below a Waste Package	49
7.3		Evaluating Potential Far-Field Criticality Using Natural Analogs for Uranium Ore Deposition at Yucca Mountain	49
	7.3.1	Introduction Overview	49
	7.3.2	Short Overview of Uranium Geochemistry and Ore Deposition Environments and Mechanisms	50
	7.3.3	Abstraction of Yucca Mountain Geology to Natural Analog Geology	60
	7.3.4	Abstraction of Evaluated Scenarios from the TSPA Criticality Workshop to Natural Analogs	63
	7.3.5	Results of Natural Analog Study	68
	7.3.5.1	Unconformity	68
	7.3.5.2	Sandstone	71
	7.3.5.3	Calcrete	72
	7.3.6	Areas of Potential Concern	72
	7.3.7	Summary	73
7.4		Analyses of Interaction With External Features	74
	7.4.1	Water Entering the Waste Package	74
	7.4.2	Concentration From Solution Flowing Out Of A Waste Package Containing Immobilized Plutonium	77
	7.4.2.1	Solution From the Immobilized Plutonium Package	78
	7.4.2.1.1	Immobilized Plutonium Solution at pH 10	78
	7.4.2.1.2	Immobilized Plutonium Package Solution at pH 7	79
	7.4.2.1.3	Immobilized Plutonium Package Solution at pH 5	79
	7.4.2.2	Reaction of Immobilized Plutonium Solution with Crushed Tuff Invert	79
	7.4.2.2.1	Reaction of Immobilized Plutonium pH 10 Solution With Crushed Tuff Invert	79

- 7.4.2.2.2 Reaction of Immobilized Plutonium pH 7 Solution With Crushed Tuff Invert 86
- 7.4.2.2.3 Reaction of Immobilized Plutonium pH 5 Solution With Crushed Tuff Invert 86
- 7.4.2.3 Reaction of Immobilized Plutonium Package Solutions with Concrete or Grout 87
 - 7.4.2.3.1 Reaction of Immobilized Plutonium pH 10 Solution With Concrete 92
 - 7.4.2.3.2 Reaction of Immobilized Plutonium pH 5 Solution With Concrete 92
 - 7.4.2.3.3 Reaction of Immobilized Plutonium pH 7 Solution With Concrete 92
- 7.4.3 Concentration From Solution Flowing Out Of A Waste Package Containing Commercial Spent Nuclear Fuel (SNF) 92
 - 7.4.3.1 Solution From The Commercial SNF Package 92
 - 7.4.3.2 Reaction of Commercial SNF Solutions With Crushed Tuff Invert 93
 - 7.4.3.2.1 Reaction of pH 7 Commercial SNF Solutions With Tuff Invert 93
 - 7.4.3.2.2 Reaction of pH 4 Commercial SNF Solutions With Tuff Invert 93
 - 7.4.3.3 Reaction of Commercial SNF Solution With A Concrete Invert 94
 - 7.4.3.3.1 Reaction of Commercial SNF pH 7 Solution With Concrete 94
 - 7.4.3.3.2 Reaction of Commercial SNF pH 4 or 5 Solution With Concrete 95
- 7.4.4 Concentration From Solution Flowing Out Of A Waste Package Containing Mixed Oxide (MOX) Fuel 95
 - 7.4.4.1 MOX Package Solution 95
 - 7.4.4.2 Reaction of MOX Solutions With Crushed Tuff Invert 95
 - 7.4.4.2.1 Reaction of MOX pH 4 Solution With Crushed Tuff Invert 95
 - 7.4.4.2.2 Reaction of MOX pH 7 Solution With Tuff Invert 98
 - 7.4.4.3 Reactions Of MOX Package Solutions With Concrete 98
 - 7.4.4.3.1 Reaction of MOX pH 4 Solution With Concrete 98
 - 7.4.4.3.2 Reaction of MOX pH 7 Solution With Concrete 98
- 7.4.5 Reactions of Waste Package Effluents with other External Features . . . 98
 - 7.4.5.1 Reactions of Waste Package Effluents With Rock 98
 - 7.4.5.1.1 Topopah Springs welded tuff 98
 - 7.4.5.1.2 Calico Hills Formation 99
 - 7.4.5.1.3 Paleozoic Carbonates 99
 - 7.4.5.1.4 Veins and Minerals in Fractures 99

7.4.5.1.5 Host Rock Altered During Thermal Pulse 99

7.4.5.2 Reactions with Organic Matter in Drift or in Rock 99

7.4.5.3 Reaction of pH 10 Immobilized Plutonium Solution With Carbon Steel 99

7.4.5.3.1 Reaction of pH 10 Immobilized Plutonium Solution With Carbon Steel With No Gaseous Oxygen Present 100

7.4.5.3.2 Reaction of pH 10 Immobilized Plutonium Solution With Carbon Steel With 10% Normal Level of Gaseous Oxygen 101

7.4.5.3.3 Reaction of pH 10 Immobilized Plutonium Solution With Carbon Steel With Atmospheric Levels of Gaseous Oxygen 102

7.4.6 Other Phenomena 103

7.4.6.1 Evaporation 103

7.4.6.2 Reaction with Rock or Drift Gas 104

7.4.6.3 Mixing with Pore And/or Fracture Water 104

7.4.6.4 Cooling or Heating 105

7.4.6.5 Pressure Drop 105

7.4.6.6 Evaluation of Concentration by Sorption 105

7.4.7 Summary of Calculated Accumulations 110

8. Conclusions 112

8.1 Potential for Critical Near Field Accumulations 112

8.2 Potential for Far-Field Accumulations 112

9. Attachments 113

9.1 Hardcopy Attachments 113

9.2 Electronic Attachments 113

1. Purpose

This analysis is prepared by the Mined Geologic Disposal System (MGDS) Waste Package Development (WPD) department to provide input to an analysis on the probability of a criticality event external to the waste packages in the repository. The objective of this evaluation is to provide bounding calculations of the accumulation, external to the waste package in the near-field and the far-field, of fissile isotopes which have been transported out of the waste package. The further objective is the quantification of the accumulations for use as input to estimates of k_{eff} for the resulting configurations. The important parameters of this quantification include geometry of the deposits, mass of fissile material, isotopic composition, and admixture of alteration products. The ultimate products of these k_{eff} will be multivariate regressions which represent k_{eff} for the various degraded configurations as a function of the above mentioned parameters, as well as design options for reducing the k_{eff} of the degraded configurations. The analyses reported herein were not intended to, nor do they, address issues of waste containment and isolation.

2. Quality Assurance

The Quality Assurance (QA) program applies to this analysis. The work reported in this document is part of the preliminary WP design analysis that will eventually support the License Application Design phase. This activity, when appropriately confirmed, can impact the proper functioning of the Mined Geologic Disposal System waste package; the waste package has been identified as an MGDS Q-List item important to safety and waste isolation (pp. 4, 15, Ref. 5.1). The waste package is on the Q-List by direct inclusion by the Department of Energy (DOE), without conducting a QAP-2-3 evaluation. This analysis also relates to the functioning of some of the natural barriers, specifically, the Topopah Spring Welded Hydrologic Unit, the Calico Hills Nonwelded Hydrogeologic Unit, and the topmost part of the Saturated Zone (pp. 26, 27, 28, Ref. 5.1) As determined by an evaluation performed in accordance with QAP-2-0, *Conduct of Activities*, the work performed for this analysis is subject to *Quality Assurance Requirements and Description* (QARD; Ref. 5.2) requirements. The applicable procedural controls for this activity are indicated in the QAP-2-0 work control activity evaluation entitled *Perform Probabilistic Waste Package Design Analyses* (Ref. 5.3).

Unless otherwise stated, parameters and assumptions which are identified in this document are for preliminary design and shall be treated as unqualified data; these design parameters and assumptions will require subsequent qualification (or superseding inputs) as the waste package (WP) design proceeds. This document will not directly support any construction, fabrication or procurement activity and therefore is not required to be procedurally controlled in accordance with NLP-3-15 as TBV (to be verified). In addition, the inputs associated with this analysis are not required to be procedurally controlled as TBV. However, use of any data from this analysis for input into documents supporting procurement, fabrication, or construction is required to be controlled as TBV in accordance with the appropriate procedures.

3. Method

The method used for this analysis involves the following steps:

- Compilation of chemical characteristics of different kinds of waste packages, inverts, other engineered materials, rock at Yucca Mountain, and groundwater. Where relevant, this included degradation or alteration rates.
- Enumeration of the mechanisms for accumulating fissile mass with potential for criticality, including construction of an event tree showing alternative pathways and reaction scenarios that could produce deposits of fissile isotopes.
- Development of procedures for using geochemical modeling code (EQ3/6) to simulate/predict long term degradation and transport processes for materials containing neutronically active elements.
- Enumeration of the features of major uranium ore deposits and possible mechanisms of their formation. These natural formation mechanisms were intended to provide some guidance for the application of the geochemical modeling code (e.g., location of potential accumulation sites and associated rock characteristics).
- Preliminary EQ3/6 calculations to determine initial conditions which directly affect geochemical accumulation of fissile material (e.g., fissile content of outflow from the waste package, thermal pulse modification of invert material).
- Final EQ3/6 calculations to estimate precipitation of fissile material from the waste package outflow with the following scope: near-field and far-field, variety of waste forms, and range of pH for the outflow from the waste package.
- Estimation of the potential for accumulation of fissile material from the waste package outflow by processes other than chemical precipitation (e.g., sorption, colloid filtration).

Further detail on the specific methods employed for each step is available in Section 7 of this analysis.

4. Design Inputs

All design inputs are for preliminary design; these design inputs will require subsequent qualification (or superseding inputs) before this analysis can be used to support procurement, fabrication, or construction activities, unless otherwise noted.

4.1 Design Parameters

This section presents the design parameters used in the analysis.

4.1.1 WP Materials and Performance Parameters

This section provides a brief overview of the chemical characteristics of different waste packages. The emphasis is on the chemical composition and reactivity, rather than on the physical configurations within different waste packages, although the configurations were used for volume calculations to determine the overall chemistries.

4.1.1.1 Chemical Characteristics of Representative Commercial Spent Nuclear Fuel (SNF) Waste Packages

A commercial spent fuel waste package will consist of 21 PWR (pressurized water reactor) assemblies of spent fuel held in a basket and placed inside a corrosion barrier. The design for the corrosion barrier itself specifies an outer corrosion allowance and an inner corrosion resistant metal. For modeling of the chemical behavior of this system, the chemical compositions of each of these materials, their masses, their surface areas, and their corrosion or degradation rates are required. Tables 4.1.1.1-1 to 4.1.1.1-3 show the data used that are specific to commercial SNF.

Table 4.1.1.1-1 Representative Spent Commercial Nuclear Spent Fuel Composition

Element	Atom Fr.	At. Wt.*	Weight, g	Wt. %
O	6.70e-01	15.999	1.07e+01	1.21e+01
Mo	4.06e-04	95.94	3.89e-02	4.37e-02
Tc	4.00e-04	98.906	3.95e-02	4.44e-02
Ru	3.71e-04	101.07	3.75e-02	4.22e-02
Rh	2.40e-04	102.91	2.47e-02	2.78e-02
Ag	3.46e-05	107.87	3.73e-03	4.20e-03
Nd	5.64e-04	144.24	8.14e-02	9.15e-02
Sm	2.41e-04	150.4	3.62e-02	4.07e-02
Eu	3.74e-05	151.96	5.68e-03	6.40e-03
Gd	3.53e-06	157.25	5.55e-04	6.00e-04
U	3.25e-01	238.03	7.73e+01	8.69e+01
Np	3.31e-04	237.05	7.85e-02	8.83e-02
Pu	2.32e-03	239†	5.55e-01	6.24e-01
Am	6.90e-05	241†	1.66e-02	1.87e-02
Total	1.00e+00		88.96775351**	1.00e+02

Data from Ref. 5.4, p. 22. 1000 year old commercial PWR SNF, initial enrichment = 3%, burnup = 20 Gwd/MTU (which is representative of the most reactive SNF, with respect to criticality. Recalculated to atom fraction.

* Atomic weights from Ref. 5.5, inside front cover, except for Pu and Am, which correspond to mass numbers of most abundant isotope in the waste.

** "Molecular weight" of SNF.

† These weights are rounded for convenience and are slightly different for those given for MOX in Table 4.1.1.2-1 because of the difference in the initial fuel which generates them.

Table 4.1.1.1-2 Characteristics of a Commercial Spent Nuclear Fuel Waste Package 21 Assemblies; Refs. 5.6 and 5.7

Component	Mass, kg	Surface Area, cm ²
Spent fuel*	11054.2	4.38e+08
Carbon steel	5510.36	2.30e+06
Borated 316 stainless steel	1882.035	6.94e+05
304L stainless steel	343.56	1.27e+05
J-13 water**	4511	N/A

* 464 kg of heavy metal, from Ref. 5.6, p. 7. This was increased by the ratio 270/238 to include the oxygen in UO₂.

Density was taken as 96% of theoretical (Ref. 5.5, p. B-173) for use in calculating volume.

** J-13 well water is assumed to fill all void space, density assumed to be 1g/cm³.

Table 4.1.1.1-3 Rates of Reaction

Material	Rate, g/cm ² /yr	Rate, g/cm ² /sec	Rate, mols/cm ² /sec
PWR SNF*	1.24e-04	3.93e-12	4.42e-14
MOX fuel**	1.24e-04	3.93e-12	4.45e-14

Material	Rate, μm/yr	Area, cm ²	Rate, cm ³ /yr	Rate, cm ³ /sec	Density, g/cm ³	Rate, g/cm ² /sec	Rate, mols/cm ² /sec
B-SS***	8.00e-01	1.00e+00	8.00e-05	2.54e-12	7.745E+00	1.97e-11	3.78e-13
304L****	1.50e-01	1.00e+00	1.50e-05	4.76e-13	7.900E+00	3.76e-12	6.87e-14
C-steel*****	3.00e+01	1.00e+00	3.00e-03	9.51e-11	7.832E+00	7.45e-10	1.37e-11

* For pH 7.5 and 0.002 M CO₃²⁻, Ref. 5.6, p. 8.

** Assumed same rate as for commercial PWR SNF, initial enrichment = 3%, burnup = 20 GWd/MTU.

*** Borated stainless steel, Ref. 5.8, Section 4.1.4. A range of corrosion rates is presented. For the present purposes a conservative value equal to twice the middle of the range for 304/316 stainless steels, i.e. 0.2E-06 m/yr (μm/yr), times a conservatism factor of 4 for B-SS.

**** Ref. 5.9, p. 4-2. This is the mid point of the range given.

***** Ref. 5.8, p. 27. Corrosion rates are given a range of 10 to 50 μm/yr. The mid-point was chosen.

Compositional data for J-13 well water appear in Table 4.1.4-1, and compositions for the metals appear in Tables 4.1.5-1 to 4.1.5-2. Data for the corrosion barriers are not included in the tables nor used for calculations. See Section 4.3.4 for assumptions and bases for these choices.

4.1.1.2 Chemical Characteristics of Representative Mixed Oxide (MOX) Spent Nuclear Fuel Waste Packages

The configuration for a MOX waste package differs from that for commercial nuclear fuel only in respect to the fuel itself. The degradation rate has already, for convenience, been included in Table 4.1.1.1-3. A representative composition of the fuel is given in Table 4.1.1.2-1.

Table 4.1.1.2-1 Representative Composition for the MOX Waste Package
(MOX fuel at 1000 yr. Ref. 5.10, case wm221f)

Element	Atom Fr.	At. Wt.	Weight, g
O	6.72e-01	15.9994	1.08e+01
Mo	5.61e-04	95.94	5.38e-02
Tc	6.56e-04	98.9062	6.48e-02
Ru	6.82e-04	101.07	6.89e-02
Rh	5.96e-04	102.9055	6.14e-02
Ag	1.48e-05	107.868	1.59e-03
Nd	8.12e-04	144.24	1.17e-01
Sm	4.16e-04	150.4	6.25e-02
Eu	1.01e-04	151.96	1.54e-02
Gd	1.51e-05	157.25	2.38e-03
U	3.13e-01	238.029	7.44e+01
Np	1.51e-03	237.0482	3.59e-01
Pu	9.28e-03	240 †	2.23e+00
Am	4.49e-04	243 †	1.09e-01
Total	1.00e+00		8.83e+01 = "mol. wt." (weight of 1 "mole" of fuel)

†These weights are rounded for convenience and are slightly different for those given for commercial SNF in Table 4.1.1.1-1 because of the difference in the initial fuel which generates them.

4.1.1.3 Chemical Characteristics of Representative Codisposal Waste Packages for High Level Waste Glass (HLW) and Immobilized Plutonium Waste

A waste package for codisposal of HLW and immobilized plutonium is designed to consist of 20 cans containing immobilized plutonium arranged axially within a canister that is largely filled by HLW glass. Both the cans and the canisters are only partially filled, 80 to 85%, with glass, or, as the case may be, a ceramic form of waste. At the time that geochemical calculations for this type of glass waste package were begun, the concept was to place four such combined canisters inside the waste packages. From a chemical point of view this is more conservative than the current concept of placing one codisposal canister and four canisters containing only HLW inside the corrosion barriers. Results from the former calculations are discussed in Ref. 5.9. For compatibility with those results and to maintain the conservative approach the same configuration, i.e. four codisposal canisters per waste package, was retained for additional calculations performed for the present report.

Whereas the geochemical code EQ6 has been used for modeling the degradation of this glass (e.g., Ref. 5.13), attempts to combine this approach with the additional complexity required for an entire waste package have not succeeded. This appears to be caused by numerical difficulties in handling such a large computational problem. Instead, a conservative value (see Table 4.1.1.3-3) was chosen for the corrosion rate for the glasses, based on the initial rate of corrosion. Another reason for choosing initial rates is that some observations have shown, after a period of weeks to years during which the rate slows, a subsequent increase to rates resembling the initial value (Ref. 5.14 and 5.15). Whereas efforts have been made to design glasses that will not be subject to this eventual rate increase, it does not appear possible to guarantee that the rate will not

increase over the course of decades or centuries. Therefore, for this report high conservative rates have been selected. Data for these glasses are presented in Tables 4.1.1.3-1 to 4.1.1.3-3.

Table 4.1.1.3-1 Composition of HLW (HLW, Ref. 5.11, Attachment I, pp. 3-4, 3-9)

Component	Grams	Mol. Wt.	g-Atoms, 1st elem.	g-Atoms, 2nd elem.	2nd elem.	g-Atoms, oxygen
Ag	5.00e-02	1.08e+02				
Al2O3	3.96e+00	1.02e+02	7.77e-02			1.17e-01
B2O3	1.03e+01	6.96e+01	2.95e-01			4.43e-01
BaSO4	1.40e-01	2.33e+02	6.00e-04	6.00e-04	S	2.40e-03
Ca3(PO4)2	7.00e-02	3.10e+02	6.77e-04	4.51e-04	P	1.81e-03
CaO	8.50e-01	5.61e+01	1.52e-02			1.52e-02
CaSO4	8.00e-02	1.36e+02	5.88e-04	5.88e-04	S	2.35e-03
Cr2O3	1.20e-01	1.52e+02	1.58e-03			2.37e-03
Cs2O*						
CuO	1.90e-01	7.95e+01	2.39e-03			2.39e-03
Fe2O3	7.04e+00	1.60e+02	8.82e-02			1.32e-01
FeO	3.12e+00	7.19e+01	4.34e-02			4.34e-02
K2O	3.58e+00	9.42e+01	7.60e-02			3.80e-02
Li2O	3.16e+00	2.99e+01	2.12e-01			1.06e-01
MgO	1.36e+00	4.03e+01	3.37e-02			3.37e-02
MnO	2.00e+00	7.09e+01	2.82e-02			2.82e-02
Na2O	1.10e+01	6.20e+01	3.55e-01			1.77e-01
Na2SO4	3.60e-01	1.42e+02	5.07e-03	2.53e-03	S	1.01e-02
NaCl	1.90e-01	5.84e+01	3.25e-03	3.25e-03	Cl	
NaF	7.00e-02	4.20e+01	1.67e-03	1.67e-03	F	
NiO	9.30e-01	7.47e+01	1.24e-02			1.24e-02
PbS	7.00e-02	2.39e+02	2.93e-04	2.93e-04	S	
SiO2	4.56e+01	6.01e+01	7.59e-01			1.52e+00
ThO2*	2.10e-01	2.64e+02	7.95e-04			1.59e-03
TiO2*	9.90e-01	7.99e+01	1.24e-02			2.48e-02
U3O8	2.20e+00	8.42e+02	7.84e-03			2.09e-02
Zeolite*						
ZnO*	8.00e-02	8.14e+01	9.83e-04			9.83e-04
Np	7.51e-04	2.37e+02	3.17e-06			
Pu	1.23e-02	2.39e+02	5.16e-05			
Am*						
Tc	1.08e-02	9.99e+01	1.08e-04			
Zr	2.64e-02	9.12e+01	2.90e-04			
Pd*						
Sn*						
Ce	2.38e-02	1.42e+02	1.68e-04			
Ba	3.48e-02	1.37e+02	2.53e-04			
Nd	2.44e-02	1.44e+02	1.70e-04			
Sm	6.81e-03	1.50e+02	4.53e-05			
Total g-Atoms =						2.71e+00

* Not considered at this time in the interest of simplifying the calculations, because they were too small to be given by the source and/or they too small to effect pH or solubility of the fissile species. The number of chemical components must be limited to assure convergence of the EQ3/6 calculations.

Table 4.1.1.3-1 Composition of HLW (continued)

Element	g-Atoms	Atom Fr.	
Al	7.77e-02	1.64e-02	
B	2.95e-01	6.24e-02	
Ba	6.00e-04	1.27e-04	
Ca	1.64e-02	3.47e-03	
Cr	1.58e-03	3.34e-04	
Cu	2.39e-03	5.05e-04	
Fe	1.32e-01	2.78e-02	
K	7.60e-02	1.61e-02	
Li	2.12e-01	4.47e-02	
Mg	3.37e-02	7.12e-03	
Mn	2.82e-02	5.95e-03	
Na	3.65e-01	7.71e-02	
Cl	3.25e-03	6.87e-04	
F	1.67e-03	3.52e-04	
Ni	1.24e-02	2.63e-03	
P	4.51e-04	9.53e-05	
Pb	2.93e-04	6.18e-05	
S	4.01e-03	8.48e-04	
Si	7.59e-01	1.60e-01	
U	7.84e-03	1.66e-03	
O	2.71e+00	5.71e-01	
Np	3.17e-06	6.69e-07	
Pu	5.16e-05	1.09e-05	
Tc	1.01e-04	2.13e-05 Value from ORIGEN run used	
Zr	2.84e-04	6.01e-05 Value from ORIGEN run used	
Ce	1.68e-04	3.54e-05	
Nd	1.70e-04	3.59e-05	
Sm	4.53e-05	9.56e-06	
Total	4.74e+00	1.00e+00	2.11e+01 = "mol. wt." (weight of 1 "mole" of glass)

Table 4.1.1.3-2 Composition of Immobilized Plutonium

Pb-free immobilized plutonium.* Ref. 5.9

Oxide	Wt%	Mol. Wt.	g-Atoms, metal	g-Atoms, oxygen	At. fr. Metal	At. fr. oxygen
SiO ₂	25.8	60.08	4.29e-01	8.59e-01	1.19e-01	
B ₂ O ₃	10.4	69.62	2.99e-01	4.48e-01	8.28e-02	
Al ₂ O ₃	19.04	101.96	3.73e-01	5.60e-01	1.04e-01	
ZrO ₂	1.15	123.22	9.33e-03	1.87e-02	2.59e-03	
Gd ₂ O ₃	7.61	362.5	4.20e-02	6.30e-02	1.16e-02	
La ₂ O ₃	11.01	325.82	6.76e-02	1.01e-01	1.87e-02	
Nd ₂ O ₃	11.37	336.48	6.76e-02	1.01e-01	1.87e-02	
SrO	2.22	103.62	2.14e-02	2.14e-02	5.94e-03	
PuO ₂	11.39	274	4.16e-02	8.31e-02	1.15e-02	
Total	99.99		1.35e+00	2.26e+00	3.75e-01	6.25e-01

27.718577 = "mol. wt." (weight of 1 "mole" of glass)

*Specifically LaBS (lanthanide borosilicate) glass, which a recent decision (see Section 7.4.2) has been downgraded to a second choice behind immobilization in a ceramic medium.

Table 4.1.1.3-3 Rates of reaction for glass

Material	Rt, g/m ² /d	Rt, g/cm ² /s	Rt, mols/cm ² /s
HLW *	2.79e-02	3.23e-11	1.53e-12
Immobilized plutonium**	2.00e-03	2.32e-12	8.35e-14

*Ref. 5.14.

**Ref. 5.13.

4.1.2 Chemistry of the Invert

The current primary design for the invert will consist dominantly of concrete. Specifications for the concrete were taken from a preliminary draft of "Materials for Emplacement Drift Ground Support". From the perspective of what is needed for the present task, the specifications do not differ significantly from those in the final draft (Ref. 5.16). This section provides the composition of the cement used in this report, the proportion of cement to aggregate, and the physical characteristics of the aggregate, which was taken to be crushed tuff of the same composition as described for the host rock in Section 4.1.3. Tables 4.1.2-1 to 4.1.2-3 provide characteristics for the cement and concrete, and Table 4.1.3-1 contains compositions for crushed tuff aggregate.

Table 4.1.2-1 Composition of Cement Used in Concrete

Type V Portland cement, Ref. 5.94, p. 21

<u>Oxide</u>	<u>Wt%</u>
SiO ₂	25
Al ₂ O ₃	3.4
CaO	64.4
MgO	1.9
Na ₂ O	0
K ₂ O	0
Fe ₂ O ₃	2.8
SO ₃	1.6
<u>Total</u>	<u>99.1</u>

Table 4.1.2-2 Proportions of Components in Concrete

Concrete mix, Ref. 5.16, p. 54

<u>Material</u>	<u>Weight, kg/m³</u>
Type 5 cement	398
Water	160
Coarse aggregate	1003
Fine aggregate	777
Silica fume	59
Polyheed	3
Superplasticizer	7
Steel	39
<u>Total</u>	<u>2446</u>

Table 4.1.2-3 Characteristics of Coarse and Fine Aggregate

Size Distributions in Fine and 19 mm (Coarse) Aggregate, Ref. 5.17, pp. 2-3

Fine Aggregate

Sieve	Percent passing
9.5 mm	100
4.75 mm	95-100
2.36 mm	80-100
1.18 mm	50-85
600 μ m	25-60
300 μ m	10-30
150 μ m	2-10

Coarse Aggregate

Sieve	Percent passing
25 mm	100
19 mm	90-100
12.5 mm	20-55
9.5 mm	0-15
4.75 mm	0-5

4.1.3 Chemical Characteristics of the Host Rock

To obtain a representative composition for the welded tuff at the repository horizon, six analyses were chosen from Ref. 5.18, pp. F32-F33, and averaged. These compositions are shown in Table 4.1.3-1.

Table 4.1.3-1 Chemical Composition of Topopah Springs Tuff

Average of six analyses* from Ref. 5.18, pp. F-32-F-33, for typical Topopah Springs Tuff at repository level

Field No.	Weight Percentages									
	SiO ₂	Al ₂ O ₃	FeO**	MgO	CaO	Na ₂ O	K ₂ O	TiO ₂	P ₂ O ₅	MnO
63L-128-B-1	76.4	12.8	0.9	0.17	0.6	3.9	5	0.1	0	0.09
60ENH32	76.66	12.94	0.9	0.09	0.62	3.56	4.98	0.1	0.01	0.07
TO-41C	76.6	12.7	0.84	0.49	0.6	3.4	5.1	0.1	0.02	0.06
63L-17-I	76.9	13	0.89	0.23	0.55	3.5	4.7	0.09	0.02	0.05
33L-17-F	77	12.7	0.63	0.2	0.59	3.6	5	0.1	0.02	0.06
63L-17-H	77.4	12.3	0.89	0.29	0.4	3.6	4.8	0.1	0.02	0.07
Average	76.83	12.74	0.84	0.25	0.56	3.59	4.93	0.10	0.02	0.07

* These six analyses were recommended by David Vaniman at Los Alamos National Laboratory (LANL) as being reasonably representative of the tuff at the repository horizon.

** These values are reported in Ref. 5.18 as combined Fe₂O₃ and FeO, "Sum as FeO". Individual values of Fe₂O₃ and FeO are also given. For all 6 analyses, the reported wt% Fe₂O₃ exceeds that for FeO; however, the reader should bear in mind that analyses for ferrous iron in silicate rocks is difficult and uncertain owing to the difficulty of preventing air oxidation during dissolution of the rock.

For sample 63L-128-B-1, as an example, calculate total Fe as FeO per 100 g of sample:

Fe ₂ O ₃ , wt%	0.82
Mol. Wt. Fe ₂ O ₃	159.69
Gram-atoms Fe in 159.69 grams Fe ₂ O ₃	0.01
FeO, wt%	0.16
Mol. Wt. FeO	71.85
Gram-atoms Fe in 71.85 grams FeO	0.00
Total gram-atoms of Fe in sample	0.01
Total Fe as FeO, wt%	0.90

In addition to the chemical composition of the host rock, including formations well below the repository horizon, other chemical characteristics of the rock and its alteration products are needed. Specifically, coefficients for the distribution of fissile nuclides between the solution and minerals were used. The values used are compiled in Table 4.1.3-2. In view of the lack of data for adsorption for some minerals, and for high pH, other parameters were also employed; specifically, cation exchange capacities and data for the zero point of charge. These numbers are shown in Table 4.1.3-3.

Table 4.1.3-2 Sorption Coefficients (Kds) for Uranium and Plutonium

Maximum Values of Distribution Coefficients for U and Pu in milliliters/gram			
Solid	Kd for Plutonium	Kd for Uranium	Source
Goethite	70000	4000	Ref. 5.84
Clinoptilolite	800	30	Ref. 5.84
Zeolite *	Not determined	700	Ref. 5.89
Smectite	3000	50	Ref. 5.86
Vitric Tuff	80	4	Ref. 5.84
Marl	5000	1000	Ref. 5.85

* The zeolite used for the determination came from the Tono mine, Japan, and belongs to the clinoptilolite-heulandite group.

Table 4.1.3-3 Values of Zero Point of Charge for Selected Minerals

Adsorption Data for Specific Minerals *		
Mineral	Range Determined for Zero Point of Charge, pH	Cation Exchange Capacity, milliequivalents/100 grams
Hematite	4.2-6.9	
Goethite	5.9-6.7	
Amorphous Fe(OH) ₃	8.5-8.8	
Calcite	8.5, 10.8	
Montmorillonite (smectite)	≤2-3	80-150
Zeolites		100-400

* All values taken from Ref. 5.90, p. 351. Data entered only for values actually used in the report.

4.1.4 Water Chemistry

It was assumed that the composition of water entering the waste package would be the same as for water from well J-13 (Assumption 4.3.1). This water has been analyzed repeatedly over a span of at least two decades (Ref. 5.19). This composition is reproduced in Table 4.1.4-1.

Table 4.1.4-1 Analyzed Composition of J-13 Well Water

J-13 water	Molality	Mole Fr.
Na	1.99e-03	1.20e-05
Si	1.02e-03	6.11e-06
Ca	3.24e-04	1.95e-06
K	1.29e-04	7.74e-07
C	1.45e-04	8.69e-07
F	1.15e-04	6.89e-07
Cl*	2.15e-04	1.29e-06
N	1.42e-04	8.53e-07
Mg	8.27e-05	4.97e-07
S	1.92e-04	1.15e-06
B	1.24e-05	7.44e-08
P	1.27e-06	7.63e-09
H	1.11e+02	6.67e-01
O	5.55e+01	3.33e-01
Total	1.67e+02	1.00e+00

* Adjusted from the nominal value to produce electrical neutrality

4.1.5 Metal Chemistry

The following metals are considered directly in computer models for waste package degradation: Alloy 625 (currently selected for the inner corrosion resistant barrier), 304L stainless steel (used for containment of glass waste forms and support structures inside a waste package), borated stainless steel (used in basket structures for spent nuclear fuel), and carbon steel (used for support structures for spent nuclear fuel and for outer corrosion allowance barrier). Tables 4.1.5-1 and 4.1.5-2 show composition and reaction rate data for the metals.

Table 4.1.5-1 Composition of Metals

Alloy 625, Ref. 5.93, p. 3*		Borated 316 Stainless Steel 20% B removed, SS316B6A, Ref. 5.92, p. I-12		304L Stainless Steel, Ref. 5.92, p. I-4		Carbon Steel, Ref. 5.8, p. 12	
Element	Wt%	Element	Wt%	Element	Wt%	Element	Wt%
Cr	21.5	B	1.2841	C	0.03	Fe	98.535
Ni	65.85	C	0.0301	Mn	2	Mn	0.9
Mo	9	N	0.1003	P	0.045	S	0.035
Nb	3.65	Si	0.7524	S	0.03	P	0.035
	100	P	0.0451	Si	0.75	Si	0.275
		S	0.0301	Cr	19	C	0.22
		Cr	19.061	Ni	10		100
		Mn	2.0064	N	0.1		
		Fe	60.639	Fe	68.045		
		Ni	13.5433		100		
		Mo	2.508				
			99.9998				

*Analysis simplified by using values for Cr, Nb, and Mo and assigning the balance to Fe.

Table 4.1.5-2 Reaction Rates for Metals

Material	Rate, $\mu\text{m/yr}$	Rt, cm^3/sec^1	Density, g/cm^3	Rt, $\text{g/cm}^2/\text{s}$	Rt, $\text{mols/cm}^2/\text{s}$
304L ²	2.50e+00	7.93e-12	7.90e+00	6.26e-11	1.15e-12
304L ³	1.50e-01	4.76e-13	7.90e+00	3.76e-12	6.87e-14
Alloy 625 ⁴	2.54e+00	8.05e-12	8.44e+00	6.80e-11	1.13e-12
B-SS ⁵	8.00e-01	2.54e-12	7.75e+00	1.97e-11	3.78e-13
Carbon Steel ⁶	3.00e+01	9.51e-11	7.83e+00	7.45e-10	1.37e-11

¹per cm^2 of surface area.

² From Ref. 5.8, p. 12. Selected as reasonably conservative from the data; this value applied for cases with pH= 10.

³ Average of "general corrosion rate of" 0.1-0.2E-06 m/yr, Ref. 5.9, p. 4-2; this value applied for near neutral solutions.

⁴ No data available for relevant conditions. Rate conservatively assumed to be no more than 0.001 in. /yr (Assumption 4.3.10)

⁵ Ref. 5.8, p. 12.

⁶ Ref. 5.8, p. 27.

4.1.6 Thermodynamic Data

It was assumed that the data in the thermodynamic data bases provided in conjunction with the EQ3/6 computer code package (Refs. 5.22, 5.23, 5.24, and 5.25) are sufficiently accurate for the purposes of this report (Assumption 4.3.8).

A few exceptions or concerns, nevertheless, are worthy of comment. Initial runs showed that the Ca, Ba, and Sr zirconates were extremely insoluble. This was thought to be unrealistic and these solids were suppressed in the calculations. Instead, some other solid, such as zircon, occasionally shows up as a simulated precipitate. This suppression, consequently, has no impact on the results of interest.

Two other instances of doubtful data were identified, but in both cases use of the values is conservative. Consequently, the data were retained. These relate to: (1) the solid, $\text{Na}_4\text{UO}_2(\text{CO}_3)_3$, and (2) chromate/dichromate ion, as discussed below.

1. The modeling often predicts the formation of significant amounts of the solid, $\text{Na}_4\text{UO}_2(\text{CO}_3)_3$, [e.g. about 3.5% of the total mass of deposited material or 99.5% of the total mass of U plus Pu solids . This compound is not known as a mineral. This could mean simply the right conditions for its formation never occur in nature, but could also mean that there is some small error in the thermodynamic data for this solid. The impact on the results would be small, inasmuch as other uranium solids, which do occur as minerals, are very close to saturation under the conditions for which the models predict the formation of this carbonate. In the present instance, retaining the carbonate is conservative inasmuch as the calculations in this case will predict slightly more precipitate outside the waste package than would occur if only known minerals were allowed.
2. As noted in Ref. 5.9, the modeling of reactions with Cr-containing steels in the presence of air predicts the oxidation of the Cr to chromate or dichromate. This would result in the production of very significant quantities of acid. However, there appears to be no direct metallurgical evidence for the generation of this acid. It would appear that, if oxidation to chromate does occur, it must be very slow. It could be fast enough to be of consequence in the repository. Observations do indicate the attainment of low pH, e.g., 4 or less, in corrosion pits in such steels, but do not indicate whether this arises from the production of dichromate or from the hydrolysis of Cr^{+++} ion. Such hydrolysis does produce low pHs in solutions of CrCl_3 and $\text{Cr}(\text{NO}_3)_3$. Possibly the thermodynamic data for chromate ion are modestly in error, but enough to produce an erroneous modeling result. It is evidently difficult to obtain accurate thermodynamic data for chromate (see Ref. 5.20, pp. 355-357, and Ref. 5.21, pp. 249-250) owing to the great insolubility of CrO_3 and of chromates in general. Beyond this initial effort the accuracy of the thermodynamic data for Cr have not been investigated in conjunction with this report.

Conservatively, it is assumed that the data are sufficiently accurate because the production of acid will lower the pH more than would otherwise be true and this results in a somewhat higher

solubility of fissile material in the waste package and transport out to the surrounding environment where it has the potential to be precipitated.

4.2 Criteria

The *Engineered Barrier Design Requirements Document* (EBDRD; Ref. 5.95) contains several criteria which relate to criticality control. The "TBD" (To Be Determined) items identified in these criteria will not be carried to the conclusions of this analysis based on the rationale that the conclusions are for preliminary design, and will not be used as input in design documents supporting construction, fabrication, or procurement. A review of the EBDRD identified the following relevant requirements:

The EBDRD requirements 3.2.2.6 and 3.7.1.3.A both indicate that a waste package criticality shall not be possible unless at least two unlikely, independent, and concurrent or sequential changes have occurred in the conditions essential to nuclear criticality safety. These requirements also indicate that the design must provide for criticality safety under normal and accident conditions, and, that the calculated effective multiplication factor (k_{eff}) must be sufficiently below unity to show at least a five percent margin after allowance for the bias in the method of calculation and the uncertainty in the experiments used to validate the methods of calculation. The latter requirement contains a "TBD" at the end.

CDA Assumption EBDRD 3.7.1.3.A (Controlled Design Assumptions Document, Ref. 5.96, p. 4-32) clarifies that the above requirement is applicable to only the preclosure phase of the MGDS, in accordance with the current DOE position on postclosure criticality. This assumption also indicates that for postclosure, the probability and consequences of a criticality provide reasonable assurance that the performance objective of 10CFR60.112 is met. While the NRC has not yet endorsed any specific change for postclosure, they have indicated that they agree that one is necessary

Finally, EBDRD 3.3.1.G indicates that "The Engineered Barrier Segment design shall meet all relevant requirements imposed by 10CFR60." The NRC has recently revised several parts of 10CFR60 which relate to the identification and analysis of design basis events (Ref. 5.97) including the criticality control requirement, which was moved to 60.131(h). These changes are not reflected in the current versions of the EBDRD or the CDA. The change to the criticality requirement simply replaces the phrase "criticality safety under normal and accident conditions" with "criticality safety assuming design basis events."

This analysis contributes to satisfying the proposed postclosure requirement by supporting probabilistic analyses of external WP criticality. It does not deal with preclosure criticality. The probabilistic analysis, along with an estimate of internal criticality consequences to be performed in a separate analysis, will be considered in the Total System Performance Assessment (TSPA) - Viability Assessment (VA) to demonstrate compliance with the performance objective of §60.112 (or, as appropriate, other applicable performance objectives in effect or proposed by the NRC at the time the TSPA-VA analysis is performed).

4.3 Assumptions

All assumptions are for preliminary design; these assumptions will require verification before this analysis can be used to support procurement, fabrication, or construction activities.

- 4.3.1 It is assumed that J-13 well water fills all voids within waste packages. The basis is that this assumption provides the maximum amount of water and capacity to degrade the waste, thus providing the maximum potential to transport radionuclides from the waste package. This in turn maximizes the potential for a large deposit of fissile material external to the waste package. Thus, the assumption adds ultra conservatism to the analyses. The assumption applies throughout Section 7.4.
- 4.3.2 It is assumed that the density of J-13 well water is 1.0 g/cm^3 . The basis is that for dilute solutions the density differs extremely little from that for pure water and that any differences are insignificant in respect to other uncertainties in the data and calculations. Moreover, this number is used only initially in EQ3/6 to convert concentrations of dissolved substances from parts per million to molalities. The assumption applies throughout Section 7.4.
- 4.3.3 It is assumed that the corrosion rate of MOX fuel is the same as that for spent commercial nuclear fuel. The basis is that the chemical composition and physical characteristics of the two waste forms are very similar. No definitive data on the actual dissolution rate appear to be available, either in the United States (U.S.) or elsewhere. This assumption underlies the calculations in Sections 7.4.3 and 7.4.4
- 4.3.4 It is assumed that the infiltrating water will have only a minimal contact, if any at all, with undegraded metal in the corrosion allowance barrier. The basis is that this water should move rapidly enough through openings in the waste package barriers that its residence time in the corroded barrier will be too small for significant reaction to occur. Furthermore, the water flowing through the barriers will be in contact with the corrosion products left from the barrier corrosion which created the holes in the first place, but these corrosion products will closely resemble iron oxides and hydroxides in the overlying rock. Consequently, the water should already be close to equilibrium with these compounds and would be unaffected by further contact with them, even if it flowed slowly enough to permit significant reaction. This assumption applies throughout Section 7.4.
- 4.3.5 It was assumed that over the time frame of a few thousand years before waste package breach the cement in concrete would have reacted to equilibrium with the water and atmosphere, thereby obviating the need for a degradation rate. Most of the components of cements used in concretes are not thermodynamically stable and tend to react with the environment over the course of a few decades. This is evidenced by the loss of strength in concrete pavements, mortars used in brickwork, etc. Whereas some concretes have survived for a few millennia in Europe, they have nevertheless reacted to more stable phases, such as calcite instead of portlandite, even at low temperatures. In the higher temperature humid environment that is expected in the repository the reaction rate will be

greater. Consequently, it is believed that, by the time that effluent exits waste packages, the cement will have reacted to an equilibrium assemblage of solids. This assumption applies to Sections 7.4.2.3, 7.4.3.3, and 7.4.4.3.

- 4.3.6 It was assumed that the tuff aggregate would not undergo any significant chemical transformation by the time of expected waste package breach (3000 to 10000 years after emplacement). The basis for this assumption is that the temperature pulse experienced by the rock (less than 200°C) will be much less than any phase transformation temperatures of the rock (Ref. 5.5). Furthermore, it is highly unlikely that substantial change could occur in only a few thousand years, in spite of water chemistry which will change somewhat, mostly from the presence of alkaline conditions arising from reaction with the cement, because this alkalinity will be largely neutralized by reaction with atmospheric carbon dioxide. Some reaction will undoubtedly occur at the contact between cement and aggregate but will be limited because this reaction will in itself bring the composition back into the range which the tuff has experienced for millions of years. Moreover, the calculations performed for this report show that strongly alkaline solutions exiting some waste packages has little effect on underlying tuff. This assumption applies to Sections 7.4.2.3, 7.4.3.3, and 7.4.4.3.
- 4.3.7 It was assumed that the organic components added to the cement in concrete would all have decayed or altered to inorganic compounds, such as CO₂ and water, before waste package breach. The added organic compounds are thermodynamically unstable in the presence of air and will tend to degrade. Such degradation will be highly favored by the initial high temperatures during the thermal pulse and presence of oxygen. Whereas some organic compounds have survived for long periods, such as in petroleum and coal, this preservation occurs only when the organic material is isolated from air. Because these conditions are not expected in the repository, it is highly unlikely that these additives can survive the several thousand years before waste breach. This assumption applies to Sections 7.4.2.3, 7.4.3.3, and 7.4.4.3.
- 4.3.8 It has been assumed that the data base supplied with the EQ3/6 computer package is sufficiently accurate for the purposes of this report. The basis is that the data have been carefully scrutinized by many experts over the course of several decades and carefully selected by Lawrence Livermore National Laboratory (LLNL) for incorporation into the data base (Ref. 5.22). Every run of either EQ3 or EQ6 documents automatically what data base is used. The data bases include references internally for the sources of the data. The reader is referred to this documentation, included in electronic files labeled data0 that accompany this report, for details. Nevertheless, this review and documentation does not absolutely guarantee that all the data are adequate. In this connection, see discussion of the data for chromium in Section 4.1.5 and for uranium and plutonium in Section 4.1.6. The assumption applies throughout Section 7.4.
- 4.3.9 In general it is assumed that chromium and molybdenum will oxidize fully to chromate (or dichromate) and molybdate, respectively. This is based on the available thermodynamic data which indicate that in the presence of air the chromium and molybdenum would both oxidize to the +6 valence state. Laboratory observation of the

corrosion of Cr and Mo containing steels and alloys, however, indicates that this oxidation, if it in fact occurs at a significant rate in respect to the time frame of interest, is extremely slow. For the present analyses, the assumption is made that over the times of concern the oxidation will occur. This is conservative for times of several thousand years after waste package breach because it will cause acidification of the solution and consequent increase of solubility and transport of fissile material. It also has the consequence that the time interval during which the pH will remain at a particular value, e.g., 10 or 7, is limited. Such cases are considered separately. This assumption applies to Section 7.4 generally, except to a part of Section 7.5.6.6

- 4.3.10 It is assumed, in the absence of data for relevant conditions, that the corrosion rate of Alloy 625 is no more than 0.001 in/yr. The basis is that measured corrosion rates of this alloy under much more aggressive conditions than will exist in the repository are extremely slow, the highest being ≤ 0.001 in/yr (Ref. 5.102). Therefore, the highest rate was conservatively assumed. This assumption applies to Section 7.4.2.
- 4.3.11 It is assumed that both the inner corrosion resistant barrier and zircaloy cladding will react so slowly with the infiltrating water as to have negligible effect on the chemistry. The bases consist of the facts that both of these metals corrode very slowly compared to other reactions in the waste package, and to the rate at which soluble corrosion products will likely be flushed from the package. This assumption applies to Sections 7.4.3 and 7.4.4.
- 4.3.12 It is assumed for most calculations that the water will be in contact with air and will maintain equilibrium with the oxygen and carbon dioxide in the air. The basis for this assumption is that it is not expected that the repository will become flooded, thereby excluding air. The assumption applies throughout Section 7.4, except for Sections 7.4.5.3.1 and 7.4.5.3.2.
- 4.3.13 It is assumed that ^{235}U dissolved from the waste will mix with other isotopes of uranium, mostly ^{238}U , before the occurrence of any transport outside the waste package. Although this assumption is not conservative, the following basis arguments offer strong evidence that it is nearly correct: (1) The residence time of the water within the waste package is sufficiently long for convective or diffusional mixing to occur that the solution will be essentially isotopically homogeneous. (2) Even if some adsorption of newly released ^{235}U onto colloids occurs before it becomes mixed with the bulk of the solution, the colloidal particles will on average remain inside the waste package long enough for isotopic exchange to take place and result in the same isotopic ratio for adsorbed uranium as for that present in the bulk solution. (3) Adsorption onto immobile solids inside the waste package is not of concern for the present analysis, but even in that case isotopic exchange will result in homogenization. The assumption applies throughout Section 7.4.
- 4.3.14 It is assumed that, when calculating the maximum effect of sorption in the invert, each of several minerals may entirely fill the volume between the waste package and the host rock. The basis for this assumption is that it is highly conservative. The contribution of any single mineral cannot exceed that which it could provide if it alone were present.

Thus, the maximum possible contribution of each solid is considered in sequence. This assumption is used in Section 7.4.6.

- 4.3.15 It is assumed that the HLW glass will degrade at a rate no more than about 50% higher than the initial rate measured experimentally. The basis for this assumption is, whereas the initially observed rates of degradation always decrease with time, it has sometimes occurred that the rate subsequently increases (Ref. 5.14). The subsequent increase evidently depends upon nucleation of secondary phases. However, there is no satisfactory theory to predict when nucleation may start, which means that no matter how long an experiment is run, nucleation may still begin sometime later. To conservatively guard against underestimating release rates, hence the potential to form substantial deposits outside the waste package, the initial rate was increased by 50% as a conservative margin. This assumption applies to Sections 7.4.2, 7.4.5, and portions of 7.4.6.
- 4.3.16 It is assumed that the total estimated surface area of the invert material applies to all reactants including the invert. The basis for this assumption is that it is highly conservative. The contribution of any single material cannot exceed that which it could provide if it alone were present. Thus, the maximum possible contribution of each solid is considered combined with the maximum for all others. In reality there would be some subdivision of surface area among reactants. Thus this assumption overestimates the reaction effect. The assumption applies throughout Section 7.4.
- 4.3.17 It is assumed that the surface area of the invert lies at the high end of any conceivable area to volume ratio. The basis for this assumption is that it is highly conservative. The assumption applies throughout Section 7.4.
- 4.3.18 It is assumed that reaction rates are reasonable, but at the high end of applicable ranges. The basis for this assumption is that it is highly conservative. The assumption applies throughout Section 7.4.
- 4.3.19 It is assumed in the open system flow through modeling that all solids that are deposited remain in place; no solids are entrained or otherwise re-mobilized. The basis for this assumption is that it conservatively maximizes the size of potential deposits of fissile material. The assumption applies throughout Section 7.4.

4.4 Codes and Standards

No codes or standards were applicable to this analysis.

5. References

- 5.1 *Q-List*, YMP/90-55Q, REV 4, Yucca Mountain Site Characterization Project.
- 5.2 *Quality Assurance Requirements and Description*, DOE/RW-0333P, REV 7, Department of Energy (DOE) Office of Civilian Radioactive Waste Management (OCRWM).
- 5.3 *Perform Probabilistic Waste Package Design Analyses*, QAP-2-0 Activity Evaluations, WP-25, Civilian Radioactive Waste Management System (CRWMS) Management and Operating Contractor (M&O).
- 5.4 *SAS2H Generated Isotopic Concentrations for B&W 15x15 PWR Assembly*, Document Identifier Number (DI#): BBA000000-01717-0200-00012 REV 01, CRWMS M&O.
- 5.5 Weast, R. C., ed, *CRC Handbook of Chemistry and Physics, 58th Ed.*, 1977. CRC Press, Inc., Cleveland, OH.
- 5.6 *Probabilistic External Criticality Evaluation*, DI#: BB00000000-01717-2200-00037 REV 00, CRWMS M&O.
- 5.7 *PWR Assembly Source Terms for Waste Package Design*, DI#: BBA000000-01717-0200-00023 REV 00, CRWMS M&O.
- 5.8 *Criticality Evaluation of Degraded Internal Configurations for the PWR AUCF WP Designs*, DI#: BBA000000-01717-0200-00056 REV 00, CRWMS M&O.
- 5.9 *Degraded Mode Criticality Analysis of Immobilized Plutonium Waste Forms in a Geologic Repository*, DI#: A000000000-01717-5705-00014 REV 01, CRWMS M&O.
- 5.10 *Westinghouse 17x17 MOX PWR Assembly - Waste Package Criticality Analysis*, DI#: A000000000-01717-0200-00031 REV 00, CRWMS M&O.
- 5.11 *DHLW Glass Waste Package Criticality Analysis*, DI#: BBAC000000-01717-0200-00001 REV 00, CRWMS M&O.
- 5.12 Shaw, H., *Glass compositions*, E-mail to Peter Gottlieb, dtd. 08/09/96.
- 5.13 Bourcier, Wm. L., 1994, *Waste Glass Corrosion Modeling: Comparison with Experimental Results*, Materials Research Society Symposium Proceedings, v. 333, pp. 69-82.
- 5.14 Bates, J., Strachan, D., Ellison, A., Buck, E., Bibler, N., McGrail, B. P., Bourcier, W., Grambow, B., Sylvester, K., Wenzel, K., and Simonson, S., 1995, *Glass Corrosion and Irradiation Damage Performance*, Plutonium Stabilization & Immobilization Workshop, Washington, D. C., December 11-14.

- 5.15 Bates, John, 1996, *Viewgraph*, last in the set entitled "Leaching Studies", identifier ITT-96-051-LWG 5/2/96 -P -5. Identification number MOY-970911-13.
- 5.16 *Materials for Emplacement Drift Ground Support*, DI#: BCAA000000-01717-0200-00003 REV 00, CRWMS M&O.
- 5.17 *Standard Specification for Concrete Aggregates*, ASTM Designation C33-93, American Society for Testing and Materials, Philadelphia, PA.
- 5.18 Lipman, P. W., Christiansen, Robert L., and O'Connor, J. T., 1996, *A compositionally Zoned Ash-Flow Sheet in Southern Nevada*, U. S. Geological Survey Professional Paper 524-F, U. S. Government Printing Office, Washington, D.C.
- 5.19 Harrar, J. E., Carley, J. F., Isherwood, W. F., and Raber, E., 1990, *Report of the Committee to Review the Use of J-13 Well Water in Nevada Nuclear Waste Storage Investigations*, UCID-21867, Lawrence Livermore National Laboratory (LLNL), Livermore, CA.
- 5.20 Latimer, W. M., and Hildebrand, J. H., *Reference Book of Inorganic Chemistry, Revised Edition*, 1940. The MacMillan Co., New York.
- 5.21 Latimer, W. M., *The Oxidation States of the Elements and Their Potentials in Aqueous Solutions, 2nd ed.*, 1952. Prentice-Hall, Inc., New York.
- 5.22 Wolery, Thomas J., 1992, *EQ3/6, A Software Package for Geochemical Modeling of Aqueous Systems: Package Overview and Installation Guide (Version 7.0)*, UCRL-MA-110662 PT I, LLNL.
- 5.23 Daveler, Stephanie A., and Wolery, Thomas J., 1992, *EQPT, A Data File Preprocessor for the EQ3/6 Software Package: User's Guide, and Related Documentation (Version 7.0)*, UCRL-MA-110662 PT II, LLNL.
- 5.24 Wolery, Thomas J., 1992, *EQ3NR, A Computer Program for Geochemical Aqueous Speciation-Solubility Calculations: Theoretical Manual, User's Guide, and Related Documentation (Version 7.0)*, UCRL-MA-110662 PT III, LLNL.
- 5.25 Wolery, Thomas J., and Daveler, Stephanie A., 1992, *EQ6, A Computer Program for Reaction Path Modeling of Aqueous Geochemical Systems: Theoretical Manual, User's Guide, and Related Documentation (Version 7.0)*, UCRL-MA-110662 PT IV, LLNL.
- 5.26 Jensen, Mead, L., and Bateman, Alan M., 1981, *Economic Mineral Deposits, 3rd ed., Revised Printing*, John Wiley & Sons, New York.
- 5.27 Lichtner, P. C., 1985, "Continuum model for simultaneous chemical reactions and mass transport in hydrothermal systems", *Geochemica et Cosmochimica Acta*, vol. 49, pp. 779-800.

- 5.28 Lichtner, P. C., 1988, "The quasi-stationary state approximation to coupled mass transport and fluid-rock interaction in a porous medium", *Geochimica et Cosmochimica Acta*, vol. 52, pp. 143-165.
- 5.29 Knapp, R. B., 1989, *A Lagrangian Reactive Transport Simulator with Successive Paths and Stationary-States: Concepts, Implementation and Verification*, UCRL-100952 Rev 1, Preprin, LLNL.
- 5.30 Lloyd, M. H., and Haire, R. G., 1978, *The Chemistry of Plutonium in Sol-Gel Processes*, *Radiochimica Acta*, Vol 25, pp. 139-148.
- 5.31 Brunstad, A., Jan. 1959, *Polymerization and Precipitation of Plutonium(IV) in Nitric Acid*, *Industrial and Engineering Chemistry*, Vol 51, No. 1, pp. 38-40.
- 5.32 Newton, T. W., Hobart, D. E., and Palmer, P. D., 1986, *The Formation of Pu(IV) Colloid by the Alpha-reduction of Pu(V) or Pu(VI) in Aqueous Solutions*, *Radiochimica Acta*, Vol 39, pp. 139-147.
- 5.33 *Criticality Abstraction/Testing Workshop Results*, DI#: B000000000-01717-2200-00187 REV 00, CRWMS M&O.
- 5.34 Nash, J. T., Granger, H. C., and Adams, S. S., 1981, *Geology and Concepts of Genesis of Important Types of Uranium Deposits*, *Economic Geology*, 75th Anniversary Volume, pp. 63-116.
- 5.35 Guilbert, J. M., and Park, C. F. Jr., 1986, *The Geology of Ore Deposits*, W. H. Freeman and Company, New York, p. 985.
- 5.36 Hostetler, P. B., and Garrels, R. M., 1962, *Transportation and Precipitation of Uranium and Vanadium at Low Temperatures, with Special Reference to Sandstone Type Uranium Deposits*, *Economic Geology*, Vol 57, pp. 226-237.
- 5.37 Langmuir, D., 1978, *Uranium Solution-Mineral Equilibria at Low Temperatures with Applications to Sedimentary Ore Deposits*, in: *Uranium Deposits, Their Mineralogy and Origin*, M. N. Kimberly Ed., Mineralogical Association of Canada, Short Course Handbook, Volume 3, University of Toronto Press, Toronto, Canada, pp. 17-55.
- 5.38 Gruner, J. W., 1956, *Concentration of Uranium in Sediments by Multiple Migration-accretion*, *Economic Geology*, Vol. 51, p. 495-519.
- 5.39 Rackley, R. I., 1976, *Origin of Western-States Type Uranium Mineralization*, in: *Handbook of Strata-Bound and Stratiform Ore Deposits, II. Regional Studies and Specific Deposits, Volume 7, Au, U, Fe, Mn, Hg, Sb, W, and P Deposits*, Ed., K. H. Wolf, Elsevier Scientific Publishing Company, New York, pp. 89-156.

- 5.40 McKelvey, V. E., Everhart, D. L., and Garrels, R. M., 1955, Origin of Uranium Deposits, *Economic Geology 50th Anniversary Volume*, pp. 464-533.
- 5.41 Gauthier-Lafaye, F., and Weber F., 1989, The Francevillian (Lower Proterozoic) Uranium Ore Deposits of Gabon, *Economic Geology*, Vol. 84, pp. 2267-2285.
- 5.42 Percy, E. C., Prikryl, J. D., Murphy, W. M., and Leslie, B. W., 1994, Alteration of Uraninite from the Nopal I Deposit, Peña Blanca District, Chihuahua, Mexico, Compared to Degradation of Spent Nuclear Fuel in the Proposed U. S. High-level Nuclear Waste Repository at Yucca Mountain, Nevada, *Applied Geochemistry*, Vol. 9, pp. 713-732.
- 5.43 Clark, L. A., and Burrill, G. H. R., 1981, Unconformity-related Uranium Deposits Athabasca Area, Saskatchewan, and East Alligator Rivers Area, Northern Territory, Australia, *CIM Bulletin*, Vol 74, No. 831, pp. 63-72.
- 5.44 Devoto, R. H., 1978, Uranium in Phanerozoic Sandstone and Volcanic Rocks in: *Uranium Deposits, Their Mineralogy and Origin*, M. N. Kimberly Ed., Mineralogical Association of Canada, Short Course Handbook, Volume 3, University of Toronto Press, Toronto, Canada, pp. 293-305.
- 5.45 Mann, A. W., and Deutscher, R. L., 1978, Genesis Principles for the Precipitation of Carnotite in Calcrete Drainages in Western Australia, *Economic Geology*, Vol 73, pp. 1724-1737.
- 5.46 Langford, F. F., 1978, Mobility and Concentration of Uranium in Arid Surficial Environments, in: *Uranium Deposits, Their Mineralogy and Origin*, M. N. Kimberly Ed., Mineralogical Association of Canada, Short Course Handbook, Volume 3, University of Toronto Press, Toronto, Canada, pp. 383-394.
- 5.47 Scott, R. B., and Bonk, J., 1984, *Preliminary Geologic Map of Yucca Mountain, Nye County Nevada, with Geologic Sections*, Open File Report 84-494, U.S. Geological Survey.
- 5.48 Buesch, D. C., Spengler, R. W., Moyer, T. C., and Geslin, J. K., 1996, *Proposed Stratigraphic Nomenclature and Macroscopic Identification of Lithostatigraphic Units of the Paintbrush Group Exposed at Yucca Mountain, Nevada*, Open-File Report 94-469, U.S. Geological Survey, p. 45.
- 5.49 Moyer, T. C. and Geslin, J. K., 1995, *Lithostatigraphy of the Calico Hills Formation and Prow Pass Tuff (Crater Flat Group) at Yucca Mountain, Nevada*, Open-File Report 94-460, U. S. Geological Survey, p. 59.
- 5.50 Hoover, D. L., Swadley, W. C., and Gordon, A. J., 1981, *Correlation Characteristics of Surficial Deposits with a Description of Surficial Stratigraphy in the Nevada Test Site Region*, Open File Report 81-512, U. S. Geological Survey, p. 27.

- 5.51 Taylor, E. M., 1986, *Impact of Time and Climate on Quaternary Soils in the Yucca Mountain Area of the Nevada Test Site*, Unpublished Masters Thesis, University of Colorado, Boulder CO, p. 217.
- 5.52 Diehl, S. F., and Chornack, M. P., 1990, *Stratigraphic Correlation and Petrography of the Bedded Tuffs, Yucca Mountain, Nye County, Nevada*, Open File Report 89-3, U.S. Geological Survey, p. 152.
- 5.53 Bredehoeft, J. D., King, M. J., and Tangborn, W., 1996, *An Evaluation of the Hydrology at Yucca Mountain; The Lower Carbonate Aquifer and Amargosa River*, Yucca Mountain Project Oversight report for Inyo County California and Esmeralda County Nevada, P.O. Box 352 (234 Scenic Drive), LaHonda, CA, p. 28.
- 5.54 Vaniman, D. T., Bish, D. L., Chipera, S. J., Carlos, B. A., and Guthrie, Jr. G. D., 1996, *Summary and Synthesis Report on Mineralogy and Petrology Studies for the Yucca Mountain Site Characterization Project, Volume I, Chemistry and Mineralogy of the Transport Environment at Yucca Mountain*, Yucca Mountain Milestone report #3665, Los Alamos National Lab.
- 5.55 Barr, et al., 1997, *Geology of the Main Drift, Station 28-55, ESF, YMP, Yucca Mountain, Nevada*.
- 5.56 Beason, S., 1997, *Personal Communication*, 2 E-mail memos, subject Re: Fracture Info, from Steven Beason to Darren Jolley dated 8/19/1997 and 8/20/1997.
- 5.57 Shenker, A. R., Robey, T. M., Rautman, C. A., and Barnard, R. W., 1995, *Stochastic Hydrologic Units and Hydrologic Properties Development for Total-System Performance Assessments*, SAND94-0244, Sandia National Laboratory.
- 5.58 Bodvardson, G. S., and Bandurraga, T. M., 1996, *Development and Calibration of the Three-Dimensional Site-Scale Unsaturated Zone Model of Yucca Mountain, Nevada, Lawrence Berkeley National Laboratory report*.
- 5.59 Czarnecki, J. B., 1990, *Geohydrology and Evapotranspiration at Franklin Lake Playa, Inyo County, California*, Open-File Report 90-356, U.S. Geological Survey, p. 96.
- 5.60 Hoeve, J. and Sibbald, T. I. I., 1977, Rabbit Lake Uranium deposit, in: Dunn ed., *Uranium in Saskatchewan, Geological Society of Saskatchewan Special Publication. 3*, p. 331-354.
- 5.61 Hoeve, J. and Sibbald, T. I. I., 1978, On the Geneses of Rabbit Lake and Other Unconformity-type Uranium Deposits in Northern Saskatchewan Canada, *Economic Geology*, Vol 73, pp. 1450-1473.
- 5.62 Jones, B. E., 1980, The Geology of the Collins Bay Deposit, Saskatchewan, Canada, *CIM Bulletin*, Vol. 73, pp. 84-90.

- 5.63 Harper, C. T., 1978, The Geology of the Cluff Lake Uranium Deposits, Northern Saskatchewan, *CIM Bulletin*, Vol. 71, pp. 65-78.
- 5.64 Clark, R. J. McH., Homeniuk, L. A., and Bonner, R., 1982, Uranium Geology in the Athabasca and a Comparison with Other Canadian Proterozoic Basins, *CIM Bulletin*, Vol. 75, pp. 91-98.
- 5.65 Kerr, P. F., 1958, Uranium Emplacement in the Colorado Plateau. *Geological Society of America Bulletin*, Vol. 69, pp. 1075-1111.
- 5.66 Huff, L. C., and Lesure, F. G., 1962, Diffusion Features of Uranium-Vanadium Deposits in Montezuma Canyon, Utah, *Economic Geology*, Vol. 57, pp. 226-237.
- 5.67 Kimberley, M. M. 1978, Short Course in Uranium Deposits, their Mineralogy and Origin, *Mineralogical Association of Canada, Short Course Handbook 3*, p. 521.
- 5.68 Fischer, R. P., 1968, The Uranium and Vanadium Deposits of the Colorado Plateau Region, in: *Ore Deposits of the United States 1933/1967*, Graton-Sales Vols. New York: AIME, pp. 735-746.
- 5.69 Dodd, P. H., 1950, Happy Jack Mine, White Canyon Utah, RMO-660, U. S. Atomic Energy Commission, p. 23.
- 5.70 Kelley, D. R., and Kerr, P. F., 1958, Urano-organic Ore at Temple Mountain Utah, *Geological Society of America Bulletin*, Vol. 69, p. 701-756.
- 5.71 Geomatrix Consultants, 1996, *Probabilistic Volcanic Hazard Analysis for Yucca Mountain, Nevada*, Volume I of II, Draft Report, prepared for CRWMS M&O, Vienna, Va.
- 5.72 Perfect, D. L., Faunt, C. C., Steinkampf, W. C., and Turner, A. K., 1995, *Hydrochemical Data Base for the Death Valley Region, California and Nevada*, Open-File Report 94-305, U.S. Geological Survey.
- 5.73 Craig, R. W., and Johnson, K. A., *Geohydrologic Data for Test Well UE-25p#1, Yucca Mountain Area, Nye County, Nevada*, Open-File Report 84-450, U.S. Geological Survey.
- 5.74 Triay, I., Degueldre, C., Wistrom A., Cotter, C., and Lemons, W., 1996, *Progress Report on Colloid-Facilitated Transport at Yucca Mountain*, Los Alamos National Lab Yucca Mountain Milestone #3383.
- 5.75 Breger, I. A., 1974, *The role of Organic Matter in the Accumulation of Uranium, in Formation of Uranium Ore Deposits*, IAEA-SM-183/19, International Atomic Energy Agency.

- 5.76 Grow, J. A., Barker, C. E., and Harris, A. G., 1994, Oil and Gas Exploration Near Yucca Mountain, Southern Nevada, *Volume 3, Proceedings of the Fifth Annual High Level Radioactive Waste Management Conference*, American Nuclear Society, La Grange Park, IL, pp. 1298-1315.
- 5.77 Hess, F. L., 1933, Uranium, Vanadium, Radium, Gold, Silver, and Molybdenum Sedimentary Deposits, in: *Ore Deposits of the Western States*, Lindgren Volume of the American Institute of Mining and Metallurgical Engineers, New York.
- 5.78 Chenoweth, W. L., 1981, *The Uranium-vanadium Deposits of the Uravan Mineral Belt and Adjacent Areas, Colorado and Utah*, New Mexico Geological Society Guidebook, 32nd Field Conference, Western Slope Colorado, pp. 165-170.
- 5.79 Yamaguchi, D. K., and Hoblitt, R. P., 1995, *Tree-ring dating of pre-1980 volcanic flowage deposits at Mount St. Helens, Washington*, Geological Society of America Bulletin, Vol 107, pp. 1077-1093.
- 5.80 Klein, C., and Hurlbut Jr., C. S., 1985, *Manual of Mineralogy*, John Wiley and Sons, New York, p. 596.
- 5.81 Harris, Ann, and Tuttle, Esther, 1983, *Geology of National Parks, 3rd Edition*, Kendall-Hunt Publishing Company, Dubuque, IA.
- 5.82 Fleer, V. N., and Johnston, R. M., *A Compilation of Solubility and Dissolution Kinetics Data on Minerals in Granitic and Gabbroic Systems*, Atomic Energy of Canada Limited, Pinawa, Manitoba, Canada, AECL-TR-328-2.
- 5.83 Turner, G. D., Zachara, J. M., McKinley, J. P., and Smith, S. C., *Surface-charge properties and UO_2^{2+} adsorption of a subsurface smectite*, 1996, *Geochimica et Cosmochimica Acta*, Vol. 60, pp. 3399-3414.
- 5.84 Triay, I. R., Cotter, C. R., Kraus, S. M., Huddleston, M. H., Chipera, S. J., and Bish, D. L., *Radionuclide Sorption in Yucca Mountain Tuffs with J-13 Well Water: Neptunium, Uranium, and Plutonium*, 1996, Los Alamos National Laboratory, LA-12956-MS.
- 5.85 McKinley, I. G., and Scholtis, A., *Compilation and Comparison of Radionuclide Sorption Databases Used in Recent Performance Assessments*, in: *Radionuclide Sorption from the Safety Evaluation Perspective*, pp. 21-55, Proceedings of an NEA Workshop, Interlaken Switzerland, 16-18 October, 1991, Nuclear Energy Agency, Organisation for Economic Co-operation and Development, Publications Service, OECD, 2, rue André-Pascal, Paris, CEDEX, France.
- 5.86 Brandberg, F., and Skagius, K., *Porosity, sorption and diffusivity data compiled for the SKB 91 study*, SKB Technical Report 91-16, Swedish Nuclear Fuel and Waste Management Co., Stockholm.

- 5.87 Vandergraaf, T. T., Ticknor, K. V., and Melnyk, T. W., The Selection and Use of a Sorption Database for the Geosphere Model in the Canadian Nuclear Fuel Waste Management Program, in: *Radionuclide Sorption from the Safety Evaluation Perspective*, pp. 81-120, Proceedings of an NEA Workshop, Interlaken Switzerland, 16-18 October, 1991, Nuclear Energy Agency, Organisation for Economic Co-operation and Development, Publications Service, OECD, 2, rue André-Pascal, Paris, CEDEX, France.
- 5.88 *Total System Performance Assessment - 1995: An Evaluation of the Potential Yucca Mountain Repository*, DI#: B00000000-01717-2200-000136 REV 01, CRWMS M&O.
- 5.89 Katayama, N., Kubo, K., and Hirono, S., 1974, Genesis of Uranium Deposits of the Tono Mine, Japan, in: *Formation of Uranium Ore Deposits*, IAEA-SM-183/19, International Atomic Energy Agency, pp. 437-452.
- 5.90 Langmuir, D., 1996, *Aqueous Environmental Geochemistry*, Prentice-Hall, Upper Saddle River, NJ.
- 5.91 *Determination of Radionuclide Sorption for High-Level Nuclear Repositories*, 1986, Technical Position Paper, U. S. Nuclear Regulatory Commission.
- 5.92 *Material Compositions and Number Densities For Neutronics Calculations (SCPB: N/A)*, DI#: BBA000000-01717-0200-00002 REV 00, CRWMS M&O.
- 5.93 *Standard Specification for Nickel-Chromium-Molybdenum-Columbium Alloy (UNSN06625) Plate, Sheet, and Strip*, ASTM B443-93.
- 5.94 Yang, In C., Rattray, G. W., and Yu, P., 1996, *Interpretations of Chemical and Isotopic Data from Boreholes in the Unsaturated-Zone at Yucca Mountain, Nevada*, Water-Resources Investigations Report, U. S. Geological Survey WRIR 96-4058.
- 5.95 *Engineered Barrier Design Requirements Document*, YMP/CM-0024, REV 0, ICN 1, Yucca Mountain Site Characterization Project.
- 5.96 *Controlled Design Assumptions Document*, DI#: B00000000-01717-4600-0032 REV 04, ICN 02, CRWMS M&O.
- 5.97 *10CFR Part 60; Disposal of High-Level Radioactive Wastes in Geologic Repositories; Design Basis Events; Final Rule*, U.S. Nuclear Regulatory Commission, Federal Register, Volume 61, Number 234, January 1, 1997.
- 5.98 *Standard Specification for Concrete Aggregates*, American Society for Testing and Materials, ASTM Designation: C 33 - 93.
- 5.99 Crose, B., Perry, F., Geissman, J., McFadden, L., Wells, S., Murrell, M., Poths, J., Valentine, G. A., Bowker, L., and Finnegan, K., 1995, *Status of Volcanism Studies for the*

Yucca Mountain Site Characterization Project, Los Alamos National Laboratory, LA-12908-MS.

- 5.100 Krauskopf, Konrad B., *Introduction to Geochemistry, 2nd Ed.*, McGraw-Hill Book Co., New York.
- 5.101 Broxton, David E., Warren, Richard G., Hagan, Roland C., and Luedemann, 1986, *Chemistry of Diagenetically Altered Tuffs at a Potential Nuclear Waste Repository, Yucca Mountain, Nye County, Nevada*, Los Alamos National Laboratory, LA-10802-MS.
- 5.102 *Inconel Alloy 625*, 5th Edition, Inco Alloys International, Publication T-42, 1985.
- 5.103 *Electronic Media for BBA000000-01717-0200-00050 REV 00*, Colorado Trakker Tape, RPC Batch # MOY-970917-04, CRWMS M&O.

6. Use of Computer Software

This section describes the computer software used to carry out the analysis.

6.1 EQ3/6

The EQ3/6 software package originated in the mid-1970's at Northwestern University. Since 1978 Lawrence Livermore National Laboratory has been responsible for its maintenance. It has most recently been maintained under the sponsorship of the Civilian Radioactive Waste Management Program of the U.S. Department of Energy. The major components of the EQ3/6 package include: EQ3NR, a speciation-solubility code; EQ6, a reaction path code which models water/rock interaction or fluid mixing in either a pure reaction progress mode or a time mode; EQPT, a data file preprocessor; EQLIB, a supporting software library; and five supporting thermodynamic data files. The software deals with the concepts of the thermodynamic equilibrium, thermodynamic disequilibrium, and reaction kinetics. The five supporting data files contain both standard state and activity coefficient-related data. Three of the data files support the use of the Davies or B-dot equations for the activity coefficients; the other two support the use of Pitzer's equations. The temperature range of the thermodynamic data on the data files varies from 25°C only for some species to a full range of 0-300°C for others. EQPT takes a formatted data file (a data0 file) and writes an unformatted near-equivalent called a data1 file, which is actually the form read by EQ3NR and EQ6. EQ3NR is useful for analyzing groundwater chemistry data, calculating solubility limits and determining whether certain reactions are in states of partial equilibrium or disequilibrium. It is also required to initialize an EQ6 calculation.

EQ6 models the consequences of reacting an aqueous solution with a set of reactants which react irreversibly. It can also model fluid mixing and the consequences of changes in temperature. This code operates both in a pure reaction progress frame and in a time frame. In a time frame calculation, the user specifies rate laws for the progress of the irreversible reactions. Otherwise, only relative rates are specified. EQ3NR and EQ6 use a hybrid Newton-Raphson technique to make thermodynamic calculations. This is supported by a set of algorithms which create and optimize starting values. EQ6 uses an ODE integration algorithm to solve rate equations in time mode. The codes in the EQ3/6 package are written in FORTRAN 77 and have been developed to run under the UNIX operating system on computers ranging from workstations to supercomputers. Further information on the codes of the EQ3/6 package is provided in the following: (1) *EQ3/6, A Software Package for Geochemical Modeling of Aqueous Systems: Package Overview and Installation Guide* (Ref. 5.22); (2) *EQPT, A Data File Preprocessor for the EQ3/6 Software Package: User's Guide, and Related Documentation* (Ref. 5.23); (3) *EQ3NR, A Computer Program for Geochemical Aqueous Speciation-Solubility Calculations: Theoretical Manual, User's Guide, and Related Documentation* (Ref. 5.24); and (4) *EQ6, A Computer Program for Reaction Path Modeling of Aqueous Geochemical Systems: Theoretical Manual, User's Guide, and Related Documentation* (Ref. 5.25).

In this study EQ3/6 was used to provide: (1) a general overview of the nature of chemical reactions to be expected, (2) the degradation products likely to result from corrosion of the waste forms and containers, and (3) in indication of the minerals, and their amounts, likely to

precipitate in the various geologic environments likely to be encountered by the outflow from the waste package. The programs have not been used outside the range of parameters for which they have been verified. The EQ3/6 calculations reported in this document used version 7.0 of the code and were executed on the Hewlett-Packard 9000 Series 735 workstation.

The EQ3/6 package has been verified by its present custodian, Lawrence Livermore National Laboratory, but it has not been qualified under the Management and Operating Contractor Quality Administrative Procedure (M&O QAP). Therefore all the results are considered TBV with respect to any design or procurement decisions or specifications.

6.2 Software Routines for Chaining Successive EQ6 Cases

The following software routines were developed specifically for this study for the purpose of facilitating the setup and execution of successive cases of EQ6, by transforming the output of one case to the input of the following case, by diluting the solution constituents to reflect the inflow of fresh water. These routines were verified by visual inspection in accordance with QAP-SI-0, 5.3.2C, by an individual independent of the person doing the original development in accordance with QAP-SI-0, 5.3.2B, and are documented in Attachment II, in accordance with QAP-SI-0, 5.3.2D.

6.2.1 File bldinpt.bat

This is a UNIX shell script which does the following: (1) runs the program (EQ6) to build the initial input (bldinput.c); (2) executes the initial iteration of EQ6; (3) runs the program (nxtinput.c) to transfer the output from one iteration to the input of the next iteration; (4) runs the next iteration of EQ6; (5) repeats steps 3 and 4 until a specified number of iterations have been reached, or until an abnormal condition occurs (which causes nxtinput.c to write an error message to a file which is read and interpreted by this script file).

6.2.2 File bldinput.c

This C program builds the EQ3/6 input from a template and an input file containing casename, date, and maximum simulation time.

6.2.3 File nxtinput.bat

This shell script runs the same iteration loop as bldinput.bat, but starts from the output of a previous iteration.

6.2.4 File nxtinput.c

This C program reads the output and pickup files of an EQ3/6 iteration and generates the input file for the next iteration. In this process it makes two basic data changes: (1) the concentrations of all the species in solution are diluted to reflect an infusion of fresh water into the waste package, and (2) some alternative species are switched into, or out of, the basis set for the

chemical reactions, according to which member of the alternative set has achieved the largest concentration.

6.3 Spreadsheets

Spreadsheet analyses were done with Microsoft Excel version 7.0, loaded on a 486 PC. The specific spreadsheets used for results reported in this document are given, for reference in the attachments.

7. Design Analysis

The purpose of this section is to address the potentiality for the development of a nuclear criticality outside a waste package. Detailed consideration was given to all the ways in which a concentration of fissile material might develop outside a waste package. This was done while keeping in mind the concentration mechanisms recognized by economic geologists for the formation of ore deposits. Some modes of ore formation were eliminated, e.g., settling of U or Pu solids directly from an igneous melt (magma). Flow charts (Figures 7.0-1a and b) were developed incorporating these possibilities.

Section 7.1 discusses these potential mechanisms. Section 7.2 discusses the analysis to address the potential mechanisms; Section 7.3 presents a natural analog study of the mechanism in the context of ore body formation and Section 7.4 presents the results of analyses. Subsections of 7.1 are keyed to Sections in 7.3 and 7.4 which contain results related to the mechanisms.

7.1 Potential Mechanisms for Development of High Concentrations of Fissile Elements External to the Waste Package

This section discusses potential mechanisms for development of high concentration of fissile elements external to the waste package.

Any buildup of the concentrations of U and Pu external to the waste package (WP) must start with transport of these elements out of the degraded WP. Possible modes are :

1. In true solution (see discussion in the rest of this section)
2. In colloidal suspension (see Section 7.2.3 for discussion of this possibility)
3. Settling of dense particles downward (see Section 7.2.4 for discussion of this possibility)

For deposition from true solution, the chemistry of the solution must change as a consequence of some environmental change, such as contacting and reaction with different solids or cooling. Potential resultant changes include:

1. Change of pH

2. Change in oxidation potential (Eh)
3. Change in dissolved gases
4. Changes in other components within the solution
5. Change in temperature and/or pressure
6. Change in phases which the solution contacts. Generally this will in turn cause a change within the solution which could involve immobile solid phases, e.g., invert, host rock, minerals in fractures or veins. The change could involve suspended phases, e.g., colloidal clay particles

Over the lifetime of a given type of waste package, the chemistry of the water present in, and below, the waste package will change as a consequence of the balance among the rates of degradation of the various components of the package and the infiltration rate of the water. For the purposes of this analysis it has conservatively been assumed (Assumption 4.3.1) that the waste package becomes saturated with water and that the various components of the package degrade at conservatively high rates. For the most part it is also assumed (Assumption 4.3.9) that, in keeping with the available thermodynamic data, as distinguished from kinetic data, that Cr and Mo in the steels will oxidize fully to chromate and molybdate. This full oxidation results in the production of significant quantities of acid. Initially, however, the pH will rise substantially in those waste packages which contain HLW waste and this alkalinity will gradually be removed by reaction with the acid and/or by flushing out as additional water infiltrates through the package. Thus, achieving the objective of providing bounding calculations of fissile accumulation requires consideration of the range of chemical conditions in the effluent from a waste package and the manner in which it will react first with the invert and later, as the water percolates to deeper levels, with the host rock, and with minerals present in veins. Reactions with the invert will similarly depend upon the composition and physical parameters, such as porosity and distribution of fractures, within that structure.

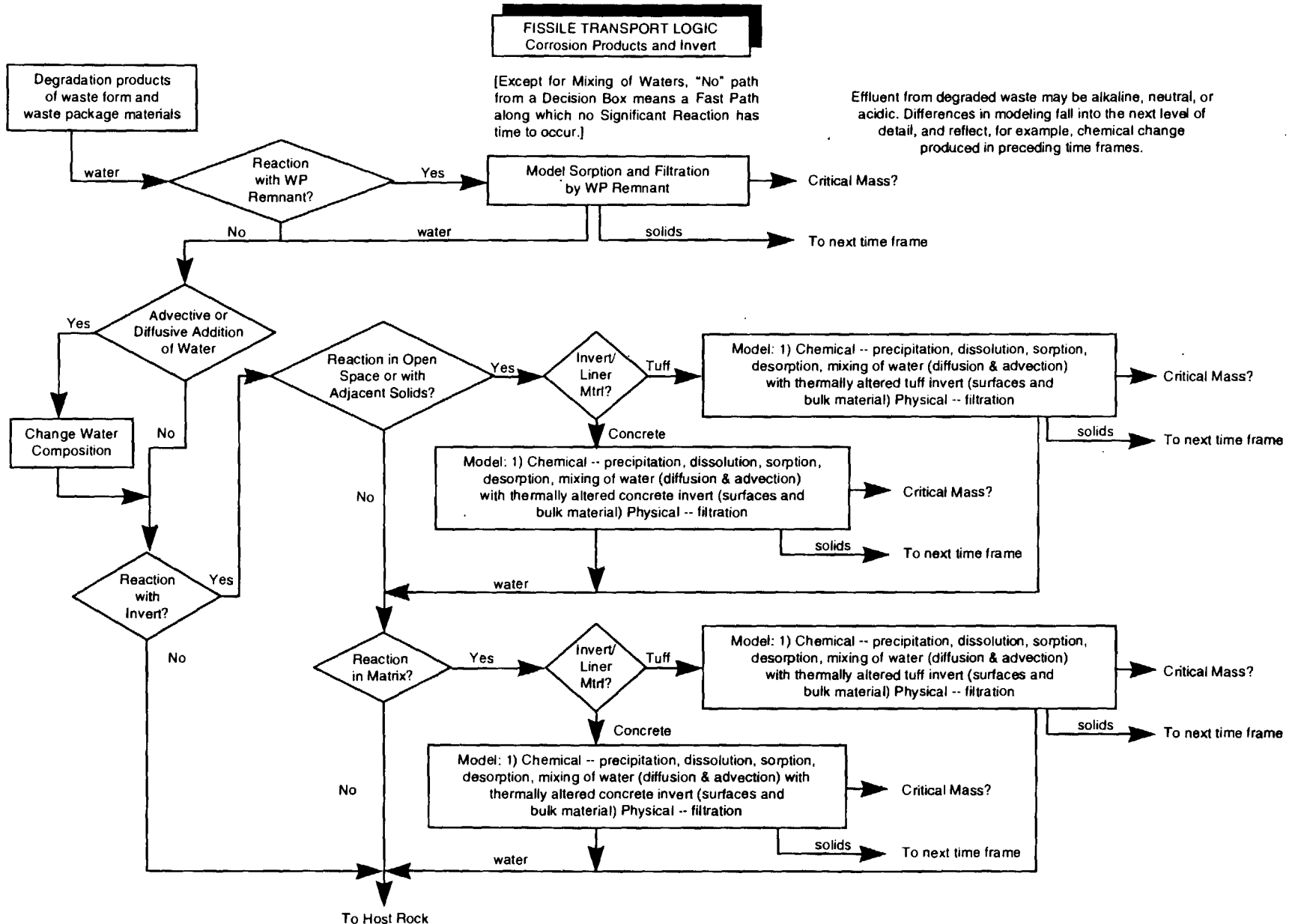


Figure 7.0-1a Flow Chart of Possible Mechanisms for External Criticality in Invert

FISSILE TRANSPORT LOGIC
Host Rock*

[Except for Mixing of Waters, "No" path from a Decision Box means a Fast Path along which no Significant Reaction has time to occur.]

* The same logic applies also to the underlying vitrophyre and Calico Hills

Effluent from degraded waste may be alkaline, neutral, or acidic. Differences in modeling fall into the next level of detail, and reflect, for example, chemical change produced in preceding time frames.

The pathway followed by water from the repository to the water table may be very complicated, possibly passing through a sequence of fractures, veins, and intervening matrix. However, for evaluation purposes migration through these features is considered in parallel rather than sequentially.

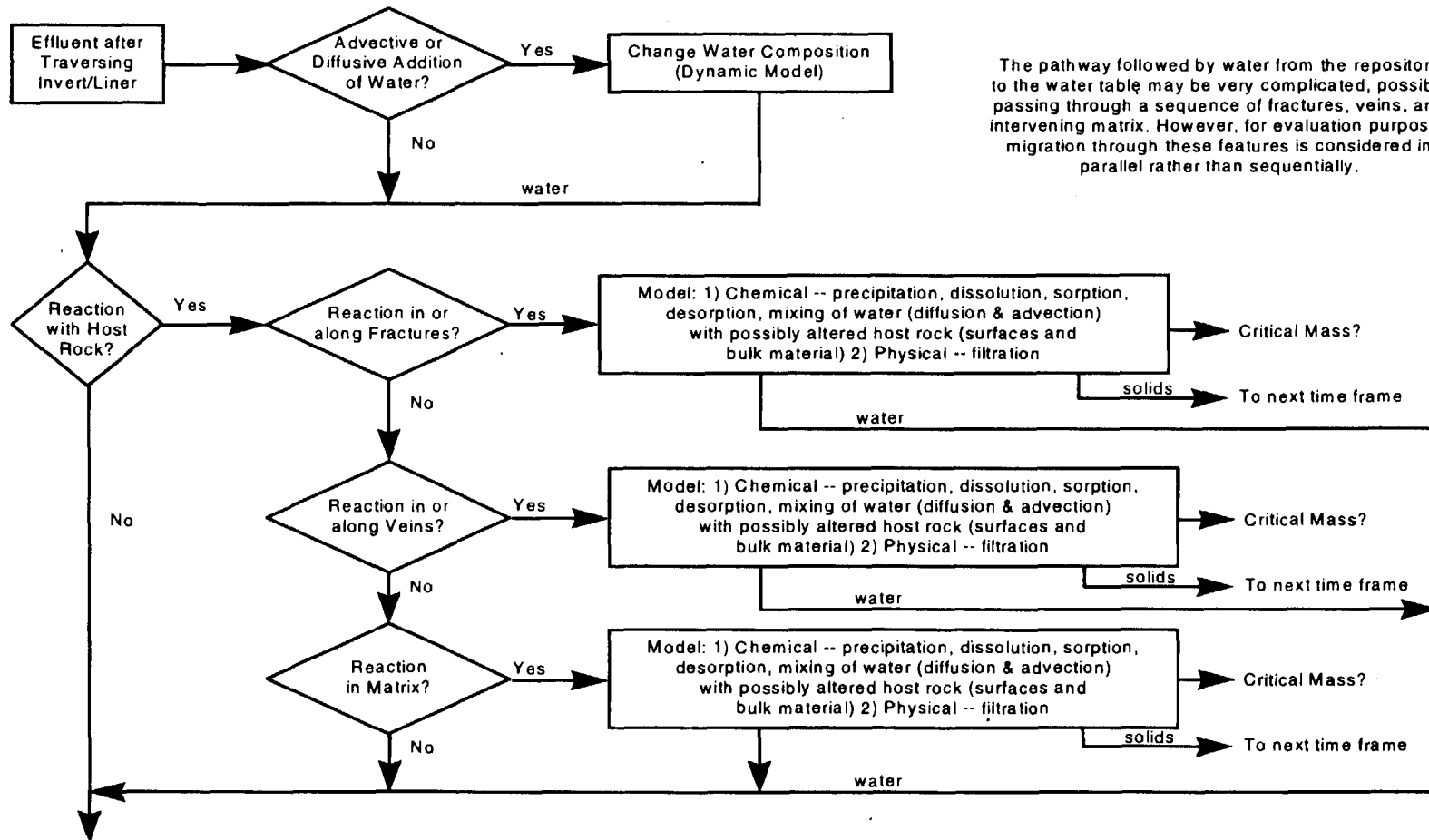


Figure 7.0-1b Flow Chart of Possible Mechanisms for External Criticality in Host Rock

7.1.1 Consequences of Changes in Solution Chemistry

The following sections describe the effects that can result from changing solution chemistry.

7.1.1.1 Solubility Effects

As solution chemistry changes (as the solution exits from the waste package), the solubilities of uranium and plutonium may decrease, leading to deposition; some simulations with EQ6, however, show increased, or nearly constant, solubility. Both a decrease in solubility and a sufficiently rapid rate of nucleation and growth are required to build up a high concentration of Pu and/or U through precipitation.

7.1.1.2 Adsorption

Adsorption and/or ion exchange may vary as a result of changes in solid phases in contact with water and changes in the water chemistry itself. This could result from other changes in solution chemistry, e.g., concentrations of ions that compete for adsorption sites, temperature. Results of adsorption analysis are presented in Section 7.4.6.6.

7.1.1.3 Colloid Formation

Changes in solution composition are likely to affect colloid stability which could cause coagulation and separation from the suspension. This could also cause peptization (redispersal of a previously coagulated colloid). An analysis of this is presented in Section 7.2.3.

7.1.2 Mechanisms for Producing Change In Solution Chemistry

The purpose of the following sections is to present the mechanisms that could possibly produce changes in the solution chemistry that might lead to accumulation of fissile material external to the waste package. Each of the sections is referenced to sections where results relating to the mechanism are presented.

7.1.2.1 Reaction of Solution with Solids along Pathway

There are several types of solids that the solution could encounter as it flows away from the waste package into repository features, host rock, and geologic structures beyond the repository (far-field). The sections below describe the types of interactions considered:

7.1.2.1.1 The Waste Package Invert

The horizontal emplacement concept includes a leveling foundation ("invert") which creates a level surface on the drift floor and supports the waste package mounting structure. The invert may be constructed of crushed tuff and/or of a concrete or grout material. The reaction of the solution with the invert may result in alteration of a major portion of the solid. In the case of concrete, it may already have been altered during the thermal pulse. In this case the fluid exiting

the package may react with concrete alteration products. Sections 7.4.2 to 7.4.4 present results related to this interaction of solution and invert.

7.1.2.1.2 Host Rock

After passing through the invert, the fluid may react with various rocks below the repository. The host rock both above and below the repository seems likely to be altered somewhat during the thermal pulse. These altered rocks need to be considered in the evaluation of far-field criticality. Intrusive igneous rocks, such as dikes and sills, need not be considered inasmuch as none have yet been identified. However, Yucca Mountain is in a volcanic region and some may be found. If so, there would also be some contact metamorphic, and possibly metasomatic, rocks. Section 7.4.5.1 addresses results of analyses of interaction of the fluid with host rocks.

7.1.2.1.3 Organic Matter

Another possible deposition mechanism is reaction with organic matter in drift or in rock which includes alteration during the thermal pulse. This possibility is discussed in Section 7.4.5.2.

7.1.2.1.4 Metals

The fluid may react with metals, e.g., rock bolts, rails, uncorroded chunks of metal that have fallen from the waste package into or onto the invert. This includes these materials being altered during the thermal pulse. Results of analyses of this possibility are presented in Section 7.4.5.3.

7.1.2.2 Evaporation of Solution

Evaporation of water from the solution will greatly change the concentrations of dissolved species. Results of analyses of this possibility are presented in Section 7.4.6.1.

7.1.2.3 Reaction with Rock or Drift Gas

Reaction with rock or drift gas would include gain or loss of dissolved gases as the fluid moves through drifts and rocks. Results of analyses of this possibility are presented in Section 7.4.6.2.

7.1.2.4 Mixing with Pore and/or Fracture Water along the Pathway

Mixing would include water in the saturated and unsaturated zones. Within the unsaturated zone, such waters are presumed to be oxidizing and at low temperature at the time of, and after, waste package breach. At some unspecified depth within the saturated zone, the waters are likely to be reducing, and may be warm as a consequence of circulation at greater depth and subsequent upwelling. High temperature (>200°C) hydrothermal conditions seem unlikely and are not considered. Results of analyses of this possibility are presented in Section 7.4.6.3.

7.1.2.5 Cooling or Heating along the Pathway

Possibly, in spite of small temperature differences, a convection cell could arise in the vicinity of emplacement drifts, but only if the repository becomes fully saturated. This would have the potential of dissolving fissile material from the waste package and concentrating it in a cooler zone nearby. The present analysis does not consider this case.

Heating or cooling could also involve changes in pH as a function of position along the drift, interactions with concrete, and consequent solubility changes.

A discussion of these phenomena is presented in Section 7.4.6.4.

7.1.2.6 Pressure Drop

As the fluid moves from pores in matrix to fractures it would probably exsolve dissolved gases to the voidspace (thereby generating rock gas) thus altering the fluid chemistry. Results of analyses of this possibility are presented in Section 7.4.6.5.

7.1.3 Various Mineral Formation Processes

By 5000 years, or more, the post-closure thermal pulse will have largely subsided. Consequently, there will be little driving force for hydrothermal action at times of concern for fissile transport out of a waste package. The various mineral formation processes include:

1. Hydrothermal deposition (not much thermal, but definitely changes in aqueous chemistry; principles are the same as noted above in Section 7.1.1 and 7.1.2).
2. Sedimentation (i.e., differential settling of dense grains through clay, settling of coagulated colloids, and any other physical processes).
3. Residual and mechanical concentration (included below, e.g., dissolution of matrix of fissile solids).
4. Evaporation.
5. Oxidation (coupled with supergene enrichment in Ref. 5.26). This is included in the sense that corrosion products of metals external to the waste package are considered.

Possibly applicable processes include:

1. Bacteriogenic: deposits formed by bacterial action, generally on the sea floor, but also in standing bodies of water. For example, bog iron ore in fresh water swamps involves bacteria.

Common mineral deposition processes which are inapplicable because they require the carrier of the elements to be at a high temperature or pressure:

1. Magmatic concentration -- this means deposition of ore forming minerals directly from an igneous magma. Intrusion of such a magma is highly improbable (Ref. 5.99).
2. Sublimation -- this requires high temperatures (Ref. 5.100), such as found in or near volcanoes. Future volcanic activity is not expected at Yucca Mountain.
3. Contact metasomatism -- this means magmatic intrusion into the repository, chemical changes in rocks adjacent to the intrusion, and concentration of fissile material into the altered rock. Magmatic intrusions are not expected.
4. Submarine exhalative and volcanogenic -- this means suboceanic volcanic extrusion accompanied by deposition of metal rich deposits where the emanations contact the water. This is very highly unlikely at Yucca Mountain for many millions of years.
5. Metamorphism -- this means regional metamorphism caused by deep burial and concomitant mobilization and redeposition of preexisting lower grade mineral deposits. This is very highly unlikely at Yucca Mountain for many millions of years.

7.1.4 Some Scenario Principles

1. If Pu or U solubility increases but there is no local source of Pu or U, the concentration in solution does not increase.
2. If Pu or U initially concentrate slightly at some point along the path, but solution characteristics later change, the Pu or U could be remobilized, possibly at a higher concentration.
3. Mixing of solutions of different dilutions may result in precipitation. It is fairly common for the solubility curve of a given solid as a function of the concentration of some other component (more generally of ionic strength) to be concave upward. In such a case mixing of a dilute solution with a more concentrated solution will result in precipitation. In other words, mixing of pore water, if it is close enough to saturation in some compound, with effluent from the waste package may produce a precipitate. Conversely, if the curve is convex upward, there is no precipitation, rather the solution becomes undersaturated.

7.2 Geochemical Analysis

This section describes the analysis used to address the processes described in Section 7.1. The natural analogs study was done separately and is described in Section 7.3.

7.2.1 Techniques Used for EQ3/6 Computations

The model was set up using the option for "Fluid-Centered Flow-Through Open System" in EQ6. In this type of simulation the solution is permitted to react with solid materials, in this case tuff or concrete, for some specified interval (time or reaction progress) and then moved away from the solid reaction products produced and allowed to react with the same initial solids for a further

interval. In this way the model simulates reaction of the solution as it percolates through a rock. Whereas this corresponds only to a single portion, or packet, of solution through the rock, successive modeling runs were set up that simulate successive packets through the now altered rock. In other words, the second packet would react both with remaining unaltered rock and with the alteration products produced by the first packet. This requires dividing the path through the rock into appropriate reaction zones, each with a characteristic mineralogy. The changing mineralogy from zone to zone necessitates several computer runs for the transit of the second packet through rock. The solution entering each zone was specified in the input file for each of these runs to be the same as that exiting the preceding upstream zone. A more detailed discussion of the modeling scheme can be found in Attachment III. Fortunately, prior studies have shown that zones of consistent mineralogy will develop which migrate slowly downstream as successive packets of solution are passed through (Refs. 5.27, 5.28, and 5.29). Some further verification of this was done during the simulations of reactions of immobilized plutonium package solutions with crushed tuff. The results are discussed in the section on immobilized plutonium-tuff reactions. (Section 7.4.2.2)

The output from the EQ6 calculations was then processed in spreadsheets. Data from the EQ6 output file was transferred electronically over the network as text files which were then converted to input spreadsheets. These input spreadsheets were then processed in summary spreadsheets by linking formulas. All of the spreadsheets used are documented electronically as Microsoft Excel® files in Section 9.2. The tables in the results section are condensed versions of these spreadsheets.

Two types of results were handled somewhat differently in the spreadsheets. The first type of result was a deposit which extended over a significant distance due to slow reactions between the water and the reactant. The second was a surface deposition of material on the reactant (in this case, metal fragments on the floor of the drift).

The spreadsheets for the extended distance deposit calculate the deposition profile through the flow path as each successive kg of water flows through. The build up of the deposit and its composition of fissile material is tabulated as a function of distance, infiltration rate, and total duration of the deposition period. The deposition period is the smallest of: the period during which the pH condition persists, or the time it takes for the solid to plug the flow path, or the time it takes to remove all fissile material from the package (this limit did not occur for any of the cases). The fraction of voids filled with the total solid and the fraction filled with fissile material are also tabulated versus distance.

The spreadsheets for the surface deposition are used to calculate the deposit as a slab with an area equal to the footprint of the waste package. The thickness of the slab is calculated for the infiltration rate and the duration of the pH condition. The time would also be limited by the inventory of the package (this limit did not occur in any of the cases).

The tables in the results section are condensed versions of these spreadsheets.

7.2.2 Analysis Method for Sorption

It would be best to use a computer code that couples the type of geochemical calculations done in EQ3/6 with sorption and ion exchange. However, these latter capabilities have not been incorporated into the most recently released version of that code package.

To obtain an approximate answer, the so-called K_d approach has been used. This method has often been employed in hydrological flow and transport codes to provide a simple approximation to sorption along flow paths. Nevertheless, it suffers from serious drawbacks in some cases because it does not place an upper bound on the amount adsorbed, whereas in fact no more can be adsorbed than can fit onto adsorption sites on the solid surface (substrate). It also does not take into account changes in solution chemistry, such as whether or not the dissolved element becomes incorporated into complexes, or surface chemistry, such as competition with other ions. Application of available data to cases of interest in evaluating criticality external to waste packages shows that in some cases the calculated amount of adsorption using K_d s is unrealistic.

7.2.3 Evaluation Principles for Colloidal Transport

The purpose of this section is to summarize the conditions for colloidal transport of fissile material and the possibility of formation of fissile deposits to critical mass levels outside the waste package. This possible mechanism was proposed in Section 7.1.

Generally, colloids will form by peptization where a previously precipitated solid is resuspended as an extremely small (<10 angstrom) particles. Such a suspension behaves like a solution in many respects. If Pu or U form such a colloid in the water, then the concentration of Pu and/or U in mobile form could greatly exceed that of the dissolved species. This would allow more rapid transport of fissile material out of the package. Colloids can be filtered from solution by very fine beds of solids (unlike dissolved ions which pass through filters owing to their much smaller size). Transport followed by filtration outside the package thus sets up the potential for a critical mass outside the package.

The fissile species do not have a unique tendency for colloid formation when compared with the many other species present. The dissolution of materials in the waste package gives rise to a variety of clay and other minerals which are prone to form colloids. This is especially true of clay minerals which form from the breakdown of glass waste forms and oxides that are formed during metal corrosion. To generate an approximation to the likely proportions of different types of colloids, one may look at EQ6 simulations. For example, during the dissolution of the immobilized plutonium waste package, the solids at pH 10.003 include 30 g $\text{Na}_4\text{UO}_2(\text{CO}_3)_3$ and 4.7 g PuO_2 in 895 g of other material including 448 g smectite (a material with large tendency to form colloids) (see EQ6 output file "j13awp50.6o" in Section 9.2). The same package exhibits similarly diluted material at pH = 7 with 51 g Sodydyite and 25.6 g PuO_2 in 2098 g of other solids which tend to form colloids (EQ6 output file "j13avwp45.6o"). At pH 5 the immobilized plutonium package will contain 55.8 g Sodydyite and 51.3 g PuO_2 in 3970 g of other solids including over 1 kg of smectite (EQ6 output file "j13avwpsoly40.6o"). The commercial SNF package at pH 4 will contain 83.9 g of Sodydyite and 2450 g of $\text{UO}_3 \cdot 2\text{H}_2\text{O}$ which appears to be a large percentage of the 4340 g of other solids. However, the U only include 4% fissile material

(see EQ6 output file j13avaugfa1.6o). The MOX SNF package at pH 4 contains only 35.7 g PuO₂ and 82.6 g of Soddyite, but it does contain 1330 g of UO₃·2H₂O. However, the low U enrichment (0.1675%) means that the total fissile material is very small compared to the 3230 g of other colloid forming solids (see EQ6 output file "j13avmoxa1.60", Section 9.2). Thus it would be expected that any colloids formed will be a mixture typical of all the minerals formed in the waste package - not pure suspensions of only fissile material. Subsequent filtration would result in a solid deposit of very low fissile content - probably similar to degradation products described in the altered rock products from the reaction of solutions with rocks (see Section 7.4). Characteristically such materials consist of large amount of diluent minerals compared to the amount of U or Pu minerals.

Colloids of Pu polymer are well known both as a safety concern and as a useful form for preparing very precise particulates for nuclear fuels (Ref. 5.30). The sol-gel processes have been used to prepare colloidal solutions of Pu which can be used for a variety of purposes. At the same time Pu polymer has been cited as a safety concern. Precipitates from high acid (such as nitric) concentration solutions) when exposed to water can peptize into colloidal suspensions of material which can then transport to process equipment and possibly accumulate in critical geometries. Pu polymer forms from Pu(IV). This polymeric form of Pu(IV) is a hydrolytic form of Pu(IV) that is characterized by a bright green color and distinctive absorption spectrum which differs markedly from the ionic Pu(IV) (Ref. 5.30). One type of sol-gel process involves preparation of "high-nitrate" sols from solutions of Pu(NO₃)₄ in HNO₃. The HNO₃ is removed from solution either by adding NH₄OH and washing the precipitate to remove NH₃ and nitrate or by solvent extraction of the HNO₃ with n-hexanol. In either case the solids are then peptized by digestion with dilute nitric acid. Highly stable solutions can be prepared with NO₃/Pu ratios of about 1.0. The resultant particles are typically 10 to 20 angstroms in size and can exist in amorphous or crystalline form (Ref. 5.30). An essential step in the process was found to be an aging process where the washed crystalline material was heated in water for an hour at 100°C prior to peptization. Without such a step, depolymerization occurred in a significant amount of the material. Significant peptization does not occur unless the initial solution has a NO₃/Pu ratio of at least 0.8. Similar effects can be obtained in sulfuric acid (Ref. 5.31). In the immobilized plutonium package as dissolution proceeds an initial acid solution resulting from chromate formation is made alkaline as the glass degrades. This might conceivably replicate the precipitate formation step of the sol-gel process, but the levels of acidity are not appropriate. Furthermore, there is no scenario for the aging step. The continued flushing by J-13 water might supply an appropriate washing step and possibly produce peptization. As mentioned above, while Pu polymer is somewhat unique, peptization of clay precipitates is just as likely to occur. A pure form of a fissile colloid is not envisioned.

Data are not available to indicate whether U could form colloids. One unique aspect of ²³⁹Pu is that it decays with a 5.15 MeV alpha which has been found to foster the disproportionation of Pu(V) into Pu(VI) and Pu(IV) enabling colloid formation (Ref. 5.32). Uranium does not have a corresponding mechanism. It is conceivable that oxides of U in the precipitates formed during degradation could be peptized in some similar manner to form U colloids. In any case there is no reason to believe such colloids would be exclusive of other diluting colloidal material.

Clearly more investigation of this issue is desirable, but there is currently no evidence that this could be a significant driver for the formation of a critical mass external to the waste package.

7.2.4 Settling of Dense Particles Below a Waste Package

This mechanism applies only to particles of greater than colloidal size. Nevertheless, they will be small. This possibility has not been analyzed quantitatively in this report. Qualitatively, a significant separation of fissile material from other solids by this mechanism seems to be very unlikely because: (1) The particle size of precipitates of fissile material will almost certainly be so small that the difference in density between fissile and clay particles will provide little driving force for the dense particles to settle differentially through the mass of other degradation products inside the waste package; (2) Precipitates formed inside are unlikely to exit the waste package; (3) Outside the waste package there will likewise be little tendency for fissile particles to settle differentially; (4) Within the invert or underlying host rock only a very small amount of new precipitate of fissile material will form (see Section 7.4) mixed with a much larger proportion of non-fissile solids. At most, only a very thin layer could form.

7.3 Evaluating Potential Far-Field Criticality Using Natural Analogs for Uranium Ore Deposition at Yucca Mountain

The purpose of this section is to present an analysis of the mechanisms proposed in Section 7.1.3. The analogies between ore body formation and potential far-field criticality configurations are explored.

7.3.1 Introduction Overview

As a result of the TSPA Abstraction/Testing workshop on criticality held on March 18-20, 1997 in Las Vegas, NV, a series of potential scenarios was developed and later refined that potentially could result in a future criticality event in the far-field (the far-field being defined in this case as encompassing the host rock from the drift wall up to and including the accessible environment). A plan was developed to look at these scenarios with the hypothesis that many of the possible scenarios for external criticality could be screened out on the basis of available literature and simple physical or geochemical calculations (Ref. 5.33). In this section, the available literature is screened for comparison to the physical environment at Yucca Mountain and conclusions are drawn with respect to the scenarios that were identified previously.

One concern of the far-field problem is that the waste placed in the repository, over geologic time, will act as a source of transportable uranium, thus enabling one of the conditions needed for uranium mineral deposition in the far-field. The hypothesis is that epigenetic (i.e. mineralization deposited much later than the host rock) uranium ore deposits documented in the literature should provide some understanding as to the environmental conditions/setting necessary for significant uranium mineral deposition in the far-field and define the mechanisms of precipitation that would be necessary to accumulate enough fissile material to produce a critical assemblage. The second major concern is that this depositional process will operate over geologic time and ^{239}Pu will have sufficient time to decay to ^{235}U . In this section the transport and deposition of plutonium is not evaluated.

7.3.2 Short Overview of Uranium Geochemistry and Ore Deposition Environments and Mechanisms

Uranium never occurs naturally as a native element because it would react with water in a geologically short time to form an oxide and elemental hydrogen. Because all uranium minerals contain oxygen, and this marked affinity for oxygen plays a dominant role in determining uranium geochemical properties, uranium occurs only in the oxidation states of U^{+4} , U^{+5} and U^{+6} . Most of the geochemical reactions are adequately described in terms of either the reduced U^{+4} or the oxidized U^{+6} state.

At low temperatures and pressures, uranium in rocks and minerals undergoing weathering and leaching is oxidized from U^{+4} to U^{+6} and becomes soluble in groundwater as UO_2^{2+} ion, as one of the uranyl carbonate complex ions (Figure 7.3.2-1), or as any of a number of other complexes; among these are complexes with PO_4^{-3} , SO_4^{-2} and AsO_4^{-3} (Ref. 5.34). As long as groundwaters containing these complexes remain oxidizing, the hexavalent uranium ions will remain mobile; but when they encounter and percolate through reducing environments, the uranyl ions are reduced to tetravalent uranium and are reprecipitated as uraninite, pitchblende, coffinite, or some other reduced uranium mineral. Vanadium may also be deposited by this same sort of reductive mechanism as tetravalent V in montroseite, roscoelite, etc. (Ref. 5.35). Reduction of mobile uranyl species to U^{+4} with precipitation of highly insoluble uraninite or coffinite normally reflects the concurrent oxidation of proportionate amounts of more abundant species in nature, such as ferrous iron, sulfides, and/or organic carbon (Ref. 5.37). Reactions for vanadium are similar. Subsequent to this deposition process, the minerals containing reduced vanadium may oxidize along with the minerals with reduced uranium to produce uranyl vanadate minerals such as carnotite and tyuyamunite.

Epigenetic uranium mineral deposits vary in size and grade, depending on geology, but one fact remains: the need for a reducing environment (or vanadium) for the primary mineral(s) to precipitate. Gruner (Ref. 5.38) stated that the oxidation-reduction potential is so low at pH values expected in nature that only carbonaceous matter or H_2S could reduce uranyl solutions at temperatures below about $100^\circ C$. Other authors explicitly state that the precipitation mechanism for epigenetic uranium ore deposits is reduction (Ref. 5.38, Ref. 5.35, Ref. 5.34). To further illustrate the need for reduction as the precipitation mechanism in epigenetic deposits, a pH of 3 or less would be required to provide the acidity necessary to dissolve more than a few parts per million from pitchblende without oxidizing it (Ref. 5.40).

Therefore, without sufficient reducing potential in the depositional environment, the precipitation of uranium by reduction of uranyl ions cannot occur, and only minor amounts would precipitate in cases of low reducing potentials or small reducing capacity. Once there is sufficient reducing capacity within the host rock, uranium will accumulate in sufficient quantities to form ore grade deposits if other conditions necessary for mineral deposition are present, e.g., sufficient porosity, favorable host rock, stable groundwater flow, etc.

Uranium deposits normally are classified based on one of the following criteria: host rock type, structural setting, mineralogy, deposit form, or geochemistry; however, for this report, the classification scheme is kept simple based on the review of the available literature. Ore body

type descriptions found in Nash et al (Ref. 5.34) include 11 different types which are based on depositional environment. They are as follows: quartz-pebble conglomerate, unconformity, ultrametamorphic, classical vein, alkalic plutons, contact, volcanogenic, sandstone, calcrete, black shale, and phosphorite. Three of these depositional environments can be associated with the local geology at Yucca Mountain and form the basis for this study; namely unconformity, sandstone, and calcrete deposits. The uranium deposits at Oklo, Gabon and Peña Blanca, Mexico have often been cited as natural analogs to Yucca Mountain. However, these two deposits did not utilize epigenetic processes to accumulate the uranium ore. The Oklo deposit falls under the quartz-pebble-conglomerate type deposit (Ref. 5.41) and the Peña Blanca deposit is classified as a hydrothermal type deposit (Ref. 5.42). Therefore, neither of these two deposits apply to this study. Below is a brief description of the three types of deposits that seem to apply to epigenetic ore deposition.

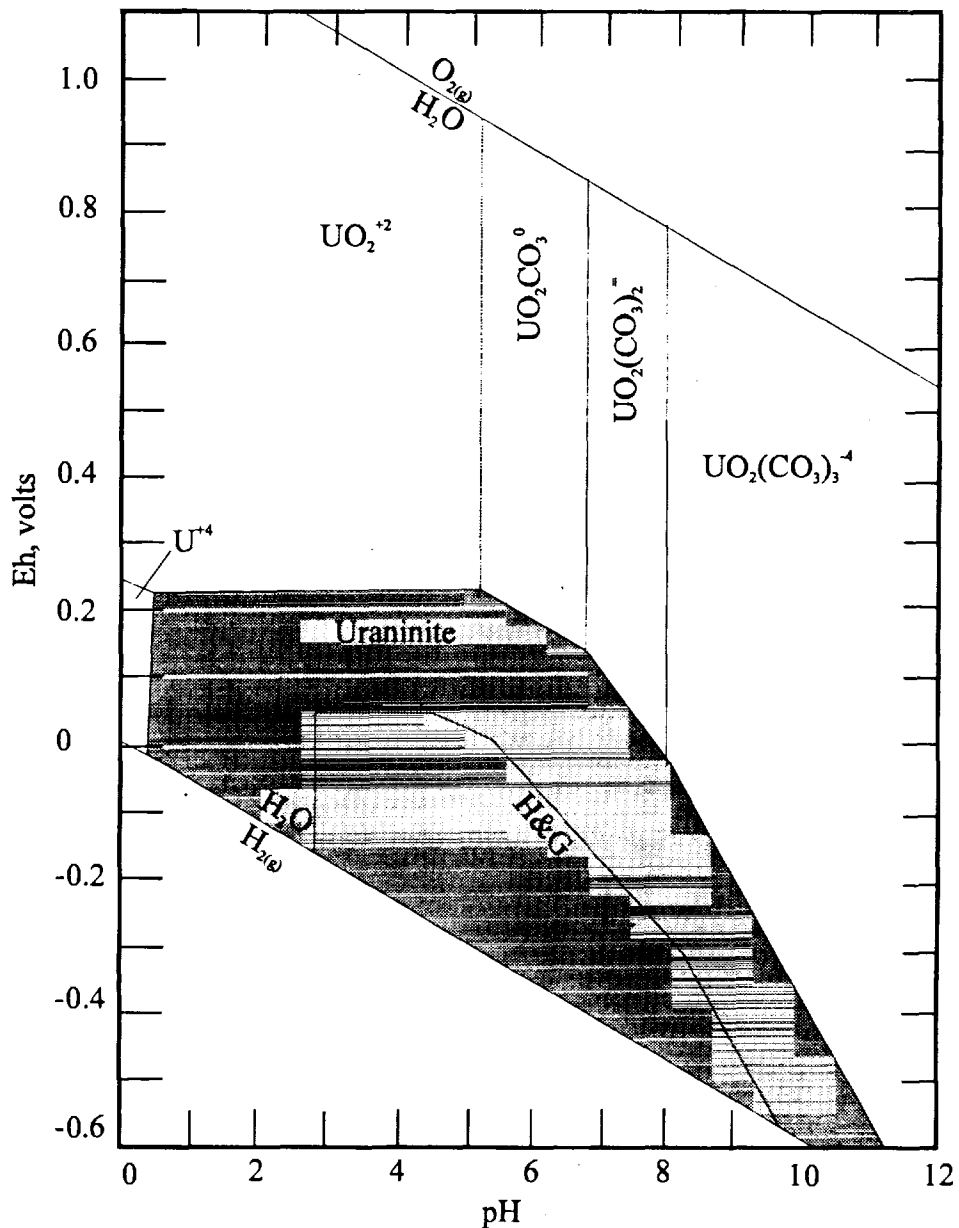


Figure 7.3.2-1 Eh-pH diagram of the U-O₂-CO₂-H₂O system at 25°C and $p\text{CO}_2 = 10^{-2}$ atm. The shading represents U⁺⁶ ion dominance and solubility from that of U⁺⁴ and uraninite precipitation. H&G denotes boundary of the uraninite stability field according to Hostetler and Garrels (Ref. 5.36). The figure was modified from Guilbert and Park (Ref. 5.35).

Unconformity:

The key to the formation of these deposits, and thus to their geologic characteristic, is the interplay of dissolved U^{+6} ions reacting with a reducing environment. The general mechanism seems to be a leaching of uranium into oxidizing groundwaters and flowing in a permeable sandstone/conglomerate above an unconformity. The reductant consists of methane or other hydrocarbon charged fluids moving upward along faults from the basement rock and through the unconformable contact boundary (Figure 7.3.2-2). The criteria for unconformity type deposits consist of the following (Ref. 5.35, which is based on Ref. 5.43):

1. The basement rocks (usually metamorphosed) are commonly topped with a weathered soil zone, a regolith or perhaps a paleosol, although the paleosol is not essential.
2. The host rocks above the unconformity are normally fluvial-deltaic sandstones or siltstones, thus providing a high porosity location (relative to rocks below the unconformity) for ore deposition.
3. The deposits occur at or within a few tens to hundreds of meters above the unconformity or a few meters below it and are horizontally elongated, ribbonlike deposits along faults through the unconformity.
4. The deposits are epigenetic, with predominant open space filling textures in faults, breccia zones and fractures. Low pressures and low to moderate temperatures are indicated. Where reported, lead-lead isotopic dates are those of the cover rocks above the unconformity or younger.
5. The uranium mineralogy is simple, generally pitchblende with coffinite or thucolite.
6. The altered wall rocks show fine-grained chloritization, argillization, albitization, hematization, and veinlets of carbonates.

Sandstone:

Generally there are two major types of epigenetic sandstone uranium deposits; those associated with organic material as a reducing agent and those deposited without organic material (includes mineral deposits formed by sorption). However the general mechanisms seem to be similar and the requirements for ore deposition are the same; namely (Figure 7.3.2-3) (Ref. 5.35):

1. A source of uranium,
2. Oxidation, mobilization and transportation of the uranium,
3. Sufficient permeability in the host rock,

4. Reducing capacity (or sorptive capacity) in the host rock, and
5. Stable, sustained groundwater flow.

Uranium sources seem to vary, including magmatic and meteoric hydrothermal solutions, leaching of host rocks, and leaching of granitic rocks. Of most interest to the present study case, many of the sandstone ore deposits seem to have their uranium source as devitrified volcanic ash (Figure 7.3.2-3). In fact, there is a striking correlation between the presence of volcanic ash and ore (Ref. 5.34, Ref. 5.35).

The ore is mainly deposited in the sandstones or conglomeratic facies (either in confined or semi-confined aquifers; Figure 7.3.2-3) where the oxidized uranium bearing fluids interact with a reducing agent or fluid. The ore is normally deposited along what is termed a roll-front (Ref. 5.44, Ref. 5.34, Ref. 5.35) or a geochemical cell (Ref. 5.39) where the reducing agent or fluid is in contact with the oxidized groundwater (Figure 7.3.2-4). The reducing agent may or may not be organic, however the result is the same.

Common organic reducing environments seem to be fluvial organic debris and/or buried logs (Figure 7.3.2-5); however, lignite or petroleum bearing sands or shales can also lead to deposition. Common inorganic redox environments tend to be associated with reduced iron or sulfide based minerals (Figure 7.3.2-4). An alternate mechanism for formation of a few of these types of deposits can be attributed to sorption onto zeolites and clays (Ref. 5.34).

Calcrete:

These epigenetic deposits occur in areas of internal drainage where evaporation exceeds rainfall. The general locations for these types of deposits occur along the lower ends of alluvial valleys, at playa lakes, and at desiccated calcrete terraces. One proposed mechanism for precipitation is related to evaporitic processes by which potassium is concentrated, uranyl ion activity is increased, as carbonate complexes are weakened by common ion effects (i.e., other ions compete for the carbonate), and pH is decreased. The precipitation occurs as groundwater is constricted by barriers and caused to move upward where V^{+4} is oxidized to V^{+5} thus allowing the precipitation of the oxidized uranium mineral carnotite (Ref. 5.45, Figure 7.3.2-6). This precipitation mechanism is unlikely to occur at Yucca Mountain because of the low concentrations of vanadium in the environment (less than 10 to about 60 parts per million, Ref. 5.101, Appendix C). An alternate mechanism of precipitation (one that should operate in the arid environment of the Yucca Mountain region) is that of upward diffusion of uranyl ions into the unsaturated soil where evaporation can concentrate the uranyl complexes, thus allowing precipitation to occur (Ref. 5.46). The only ore that has been found deposited in this type of depositional environment is carnotite. This mineral requires vanadium to precipitate; the chemical formula for carnotite is $K_2(UO_2)_2(VO_4) \cdot 3H_2O$ and is located in regolith, fluvial detritus, or in fractures and voids in the calcretes. (Ref. 5.45, Ref. 5.34, Ref. 5.46)

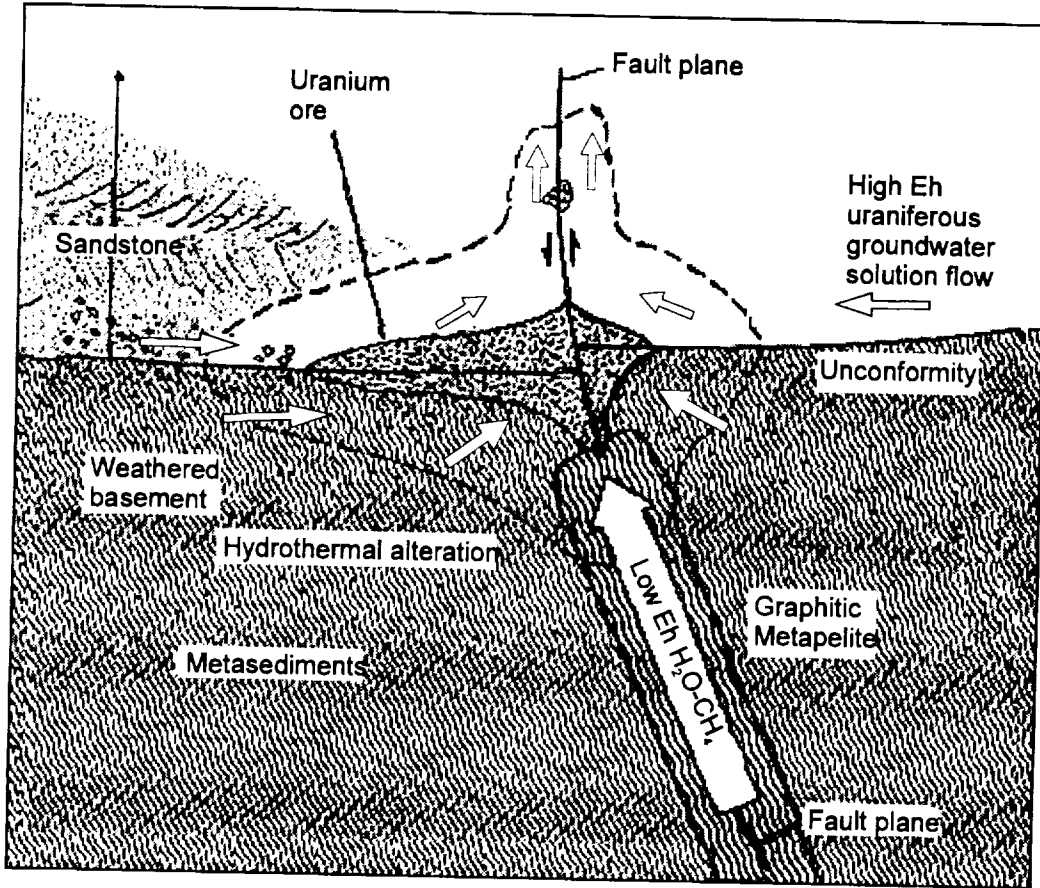
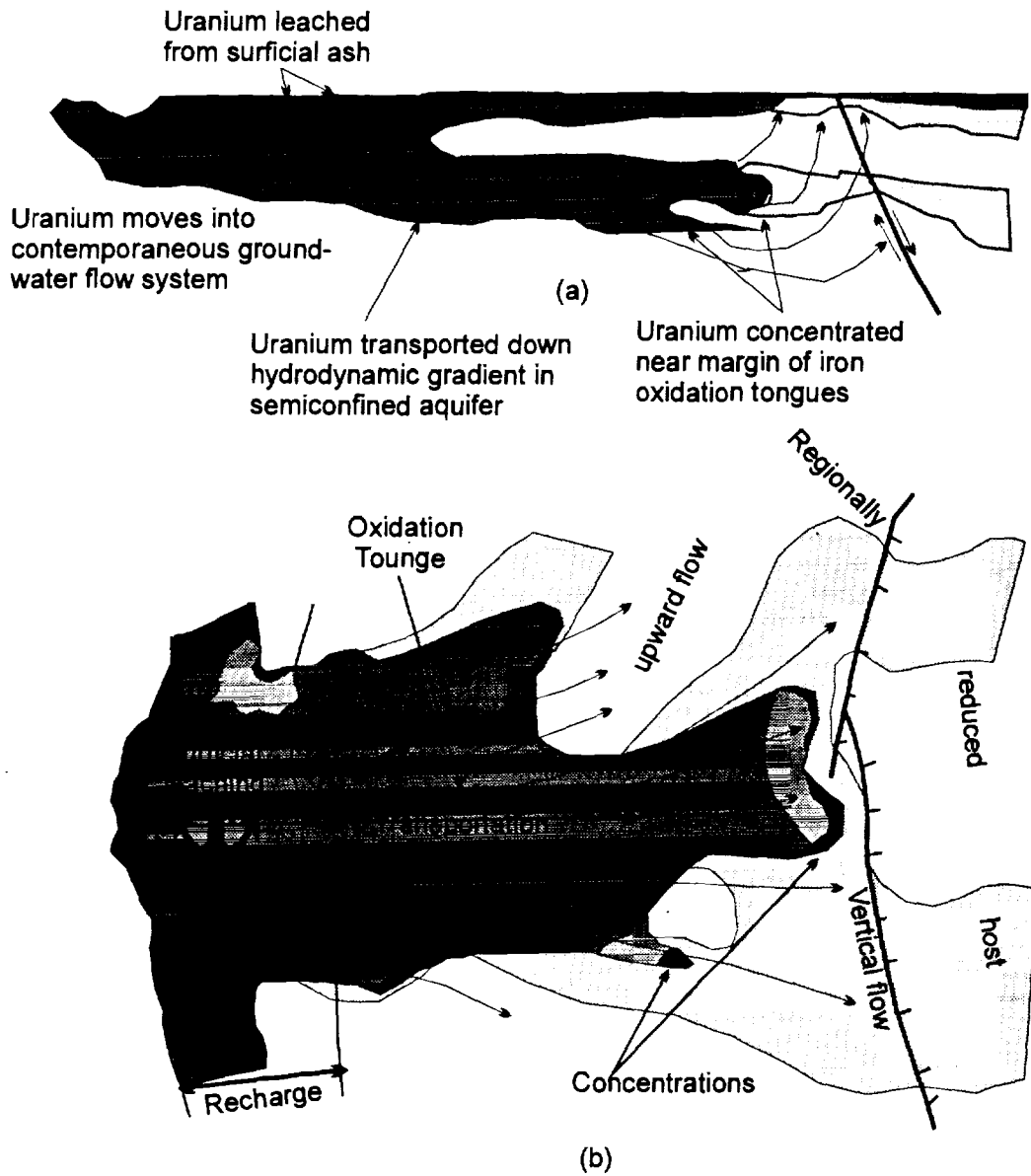


Figure 7.3.2-2. Schematic cross section of the formative processes of an unconformity-type uranium deposit. The diagram is based on an Athabasca deposit, but is applicable elsewhere. Modified from Clark and Burrill (Ref. 5.43).



- Dispersed mineralization
 - Concentrated mineralization
 - Schematic flow lines
- Scale: variable

Figure 7.3.2-3 (a) Conceptual cross section and (b) plan view of a roll-front type system. Modified from Guilbert and Park (Ref. 5.35).

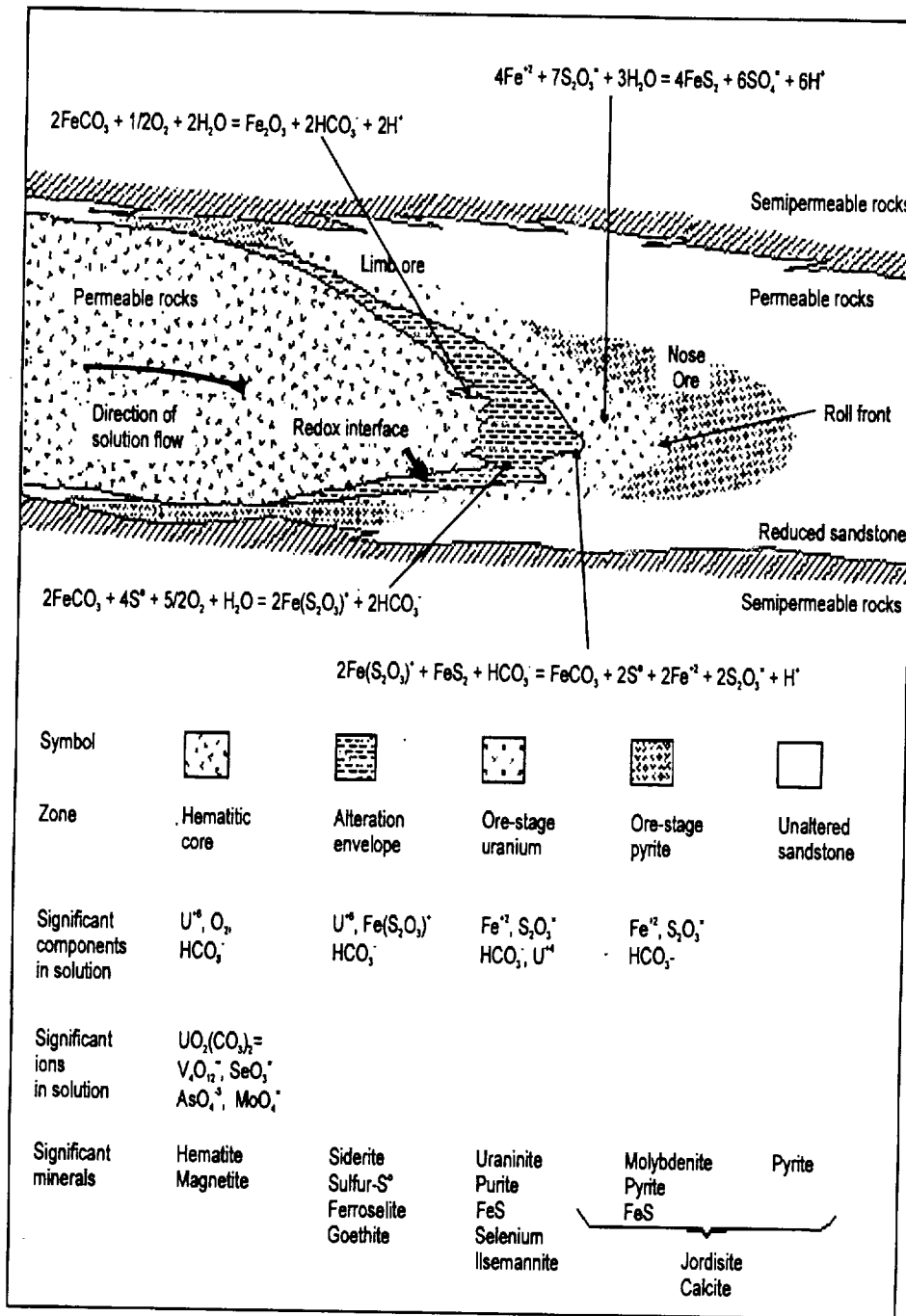
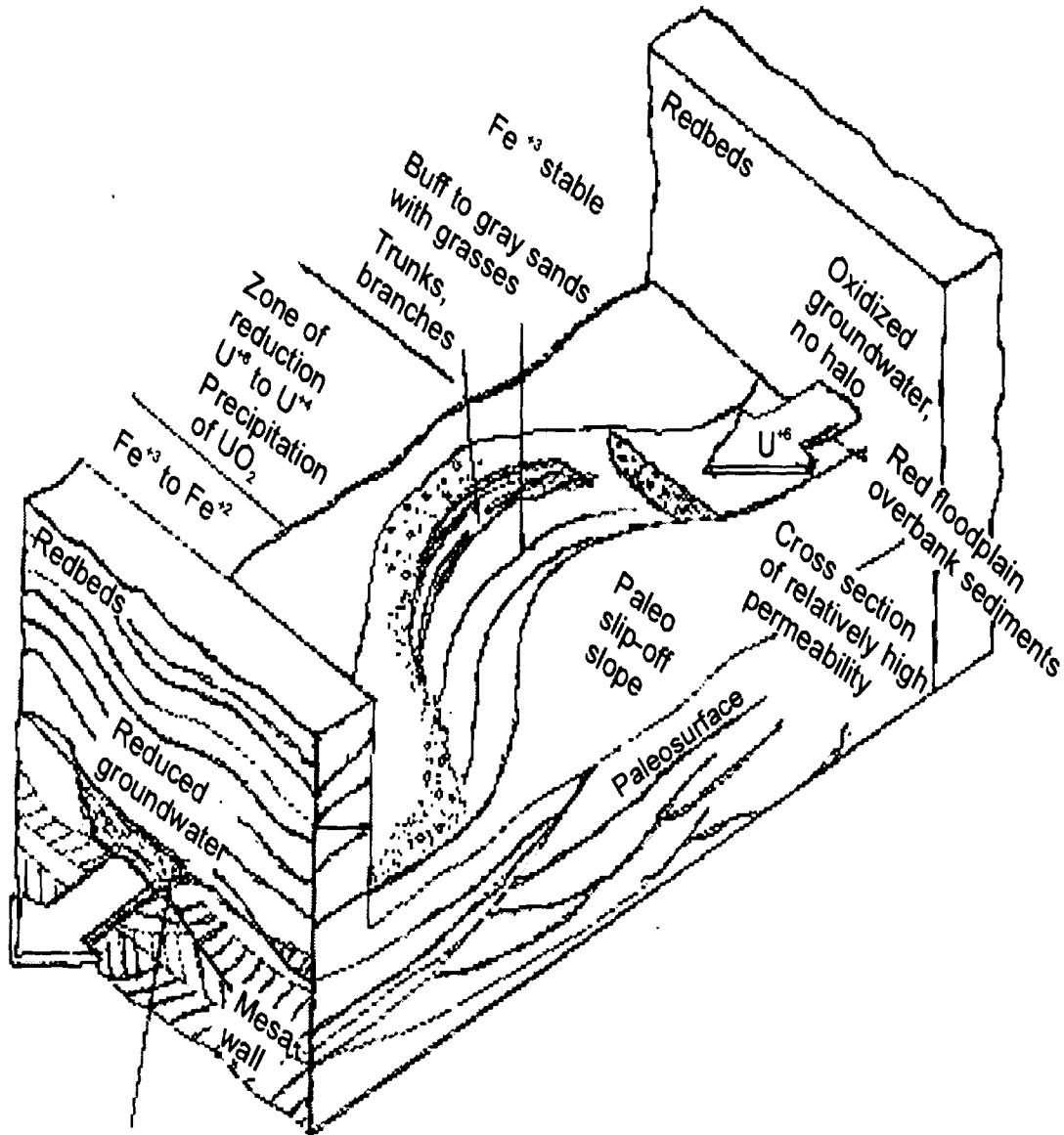


Figure 7.3.2-4. Diagram of a roll-front uranium deposit advancing to the right. Groundwater moves through the roll front, which advances slowly downdip at a rate determined by the oxidative capacity of the solution versus the reductive capacity of the permeable host rock. Reactions shown are for iron species. Modified from Guilbert and Park (Ref. 5.35).



"Bleached"
halo of green buff reduced
clays around paleochannel
short distance downstream

Figure 7.3.2-5. Oxidation-reduction dynamics in sandstone type paleostream channel mineralization. The buffering capacity of the "zone of reduction" is gradually diminished with the accumulation of U^{+4} and other reduced species. Oxidation may ultimately overwhelm the zone of reduction. Modified from Guilbert and Park (Ref. 5.35).

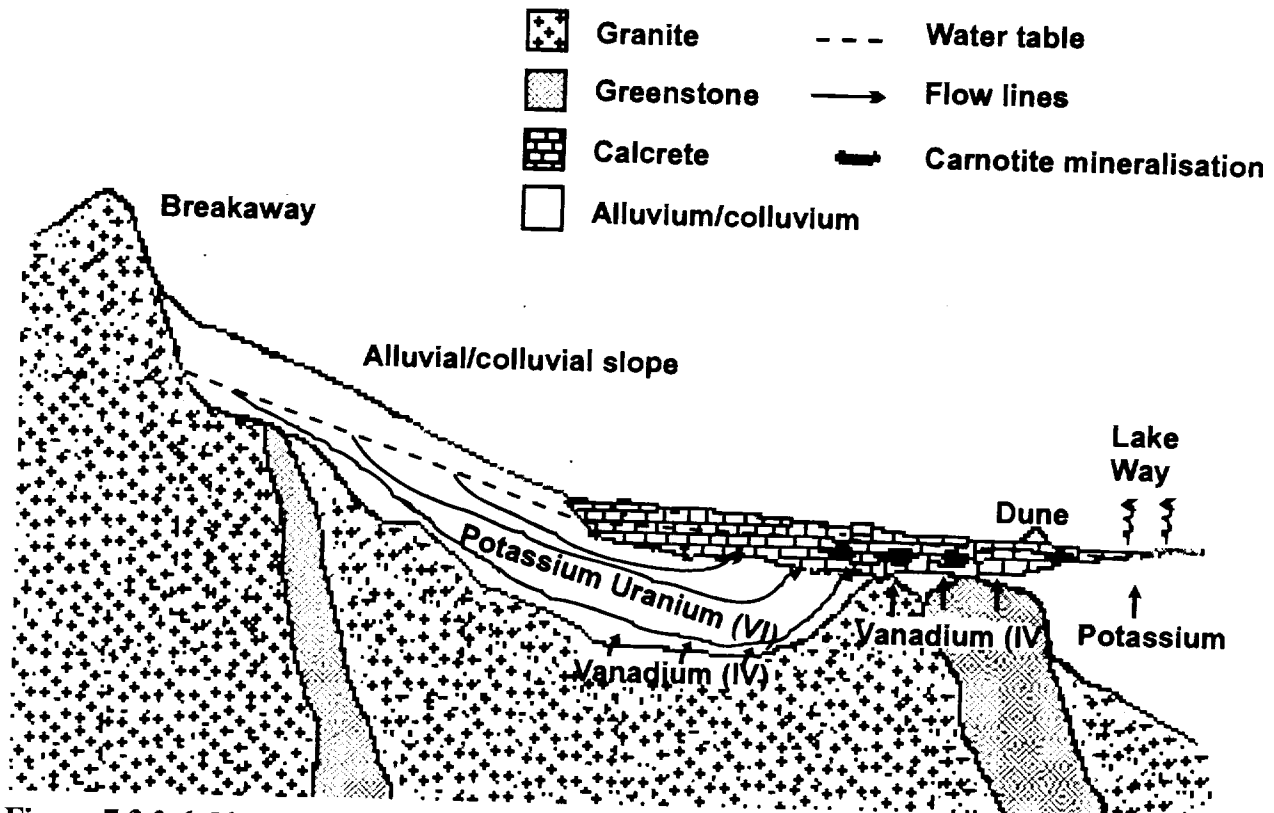


Figure 7.3.2-6. Idealized section along a representative catchment showing the postulated redox-controlled genesis of carnotite in calcrete. Reducing groundwaters supplying vanadium for precipitation at the redox front can be either localized beneath, or laterally displaced, from the precipitation site. Modified from Mann and Deutscher (Ref. 5.45).

7.3.3 Abstraction of Yucca Mountain Geology to Natural Analog Geology

The geology/geomorphology of the Yucca Mountain region includes block-faulted hills consisting of easterly dipping units from the Miocene (Tertiary) age Timber Mountain Tuff, the Paintbrush Group, the Calico Hills Formation, and the Crater Flat Group (Ref. 5.47, Ref. 5.48, and Ref. 5.49), and fault-angle depressions (valleys) filled with alluvial fan and other surficial deposits consisting of Holocene, Pleistocene, Pliocene and Late Miocene age alluvium, colluvium, and eolian deposits. The surficial deposits, including fill in gullies and washes, consist of poorly sorted boulders, gravels, cobbles, and sands that are partially cemented with pedogenic carbonates (Ref. 5.50). Soil development is relatively thin, consists of various soil and paleosol horizons, and is typical of an arid climate (Ref. 5.51).

Outcropping bedrock, generally classified as quartz latite and rhyolite tuff, was deposited via multiple ash-fall (non-welded, bedded and/or reworked tuffs) and ash-flow (welded tuffs) volcanic deposition events (Ref. 5.47, Ref. 5.52). At depth in the subsurface the Tertiary volcanogenic materials are deposited unconformably on Paleozoic carbonates of the Roberts Mountains Dolomite and Lone Mountain Dolomite (Silurian in age; Ref. 5.53). The multiple eruptive events have deposited the various units of the Tertiary ash fall and ash flow tuffs. Between these events there have been relatively long periods of quiescence that have produced erosional surfaces and paleosols that are subsequently interbedded between the multiple ash fall and ashflow events (Ref. 5.48 and Ref. 5.49).

The Paleozoic carbonates and the Tertiary volcanics tend to change facies somewhat with distance away from the proposed repository, but the overall rock types (e.g., tuff, alluvium, and carbonate sequences) remain the same. In the direction of regional groundwater flow, the Quaternary sediments thicken to several hundreds of meters of alluvial sediment due to subsidence and range flank erosion. These basin fill sequences including Frenchman Flat, Yucca Flat, Mid Valley, and Crater Flat basin include not only the debris flow, colluvium, and fan sheet gravels described above, but also lakebed-playa deposits that include siliceous clays, marls, and evaporates (Ref. 5.50).

The structural control of the bedrock is dominated by basin and range faulting and folding including the typical uplifted horst and downthrown graben blocks that make up the general topography of Nevada. Some of the major north-south striking faults that cross the proposed repository site include Windy Wash, Fatigue Wash, Solitario Canyon, Ghost Dance, Bow Ridge, and Paintbrush Canyon faults. These faults dip steeply towards the west. Several smaller northwest-southeast striking faults also exist including the Drill Hole Wash fault (Ref. 5.57).

The bulk mineralogy of the Tertiary tuffs includes cristobalite and alkali feldspars through much of the Topopah Spring formation with smectite and glass appearing in the basal vitrophyre. In the Calico Hills and Prow Pass formations, the bulk mineralogy consists of alkali feldspars, opal-CT or cristobalite, and smectite, as well as major abundances of two zeolites; clinoptilolite and mordenite. Deeper, in the Bullfrog formation, the zeolite analcime begins to appear. Fracture lining minerals throughout the tuff formations seem to consist of calcite, smectite, various zeolites (mainly stellerite, heulandite, mordenite, and clinoptilolite, hematite and various manganese oxides including rancieite, lithiophorite, and cryptomelane (Ref. 5.54).

The possible depositional environments that apply to both Yucca Mountain and the three classifications described above are discussed below.

Unconformity:

There are abundant unconformities and faults present in the far-field at Yucca Mountain. Within the Tertiary volcanic deposits present beneath the potential repository horizon there are at a minimum, five unconformable contacts (others exist including the contact between the Tertiary volcanics and the Silurian carbonates) commonly classified as bedded tuffs. These bedded tuffs commonly consist not only of reworked ash-fall and ash-flow deposits but contain sandstone, breccia, and paleosols. These bedded tuffs are sandwiched between units of both welded and nonwelded tuff (Ref. 5.49, Ref. 5.52).

Within the welded tuff, highly fractured and brecciated zones are present that could be used as void space/porosity for ore deposition. According to Barr et al (Ref. 5.55), the maximum fracture frequency in exploratory studies facility (ESF) tunnel occurred between station 4200 and 5250. This is based on a maximum fracture density of mapped fractures (minimal length of 1 meter) in the ESF tunnel. The average fracture density in this interval was around 8/m. According to Steve Beason (Ref. 5.56), the ESF Geologic Mapping Lead, there are more fractures that were not mapped; these unmapped fractures fell outside the criteria for mapping (i.e. not greater than a meter in length). If these fractures are included, the worst case fracture density would be on the order of 19/m within several locations in the ESF. This information, coupled with average fracture porosity values of 0.001 for repository host rock (Ref. 5.57) and aperture values on the order of 200 μm (Ref. 5.58), indicates that there could be sufficient void space to precipitate mineral phases in the fractures.

The above factors fulfill the geological requirements for advection of mineralizing solutions that are common to unconformity type ore deposition (i.e., an unconformity; a source fluid that could enter a higher porosity sandstone, breccia, or paleosol; and sufficient porosity and/or fracturing and brecciation along faults or fractures).

Sandstone:

The analog to sandstone deposits can be made in three locations. First, as described above, there are sandstone and bedded tuff layers that are or could be the more permeable aquifer units within two semi-confining welded tuff units. An example was shown in Figure 7.3.2-4.

Second, at some location down gradient of the proposed repository, the tuff aquifer pinches out and becomes an alluvial aquifer. There are fluvial and/or eolian sediments, debris flows, etc., which could provide a preferential flow path within the alluvial aquifer that could be semi-confined within cemented paleosols overbank sediments, or other less permeable alluvium (example was shown in Figure 7.3.2-5). Because these deposits dip away from the repository and uranium charged groundwater could be flowing down dip in a semi-confined state, or there exist within the alluvium deposits themselves preferential

flow channels that follow paleostreams, the geologic advection conditions are present for uranium deposition in the alluvium.

Third, there are sufficient sorbing sites on or in: a) the smectite clays associated with the basal vitrophyre of the Topopah Spring formation, b) significant zeolite facies in the Calico Hills, Prow Pass, and Bullfrog formations, and c) the zeolites, smectite clays, hematite, and manganese oxide minerals lining the fractures.

Calcrete:

Calcrete uranium ore deposits are very similar to the sandstone deposits except for the uranium reconcentration mechanism (example was shown in Figure 7.3.2-6). Here, there is an evaporitic mechanism. In the arid environment and with known deposits of pedogenic carbonate in the alluvium deposited near Yucca Mountain and the presence of playa lake deposits at Franklin lakes the geologic conditions are present, but the possibility for this type of ore deposit to form is unlikely due to the fact that there is no known source of vanadium in the area that is required to precipitate carnotite. However, due to the fact that Franklin Lakes playa is the currently expected location for surficial discharge of groundwaters flowing beneath Yucca Mountain (Ref. 5.58), one could expect some accumulation of uranium mineralization via the same evaporative mechanisms that have formed the playa.

7.3.4 Abstraction of Evaluated Scenarios from the TSPA Criticality Workshop to Natural Analogs

The general geology of the Yucca Mountain area provides background for the abstraction to the three potential types of mineral deposits. Most of the far-field scenarios discussed in a previous section fall within or are somewhat analogous to one of the three previously described ore deposit classifications. These include both the M and N branches of the Features, Events, and Processes (FEP) diagram produced as a result of the TSPA criticality abstraction workshop (Figures 7.3.4-1 to 7.3.4-4).

Table 7.3.4-1 below shows the correlation between the scenarios on the FEP diagram and the natural analogs described in this section.

Table 7.3.4-1 TSPA FEP Scenarios and their associated natural analogs

Analog	Unconformity	Sandstone	Calcrete
Scenario	FF-3a, 3b, 4a,	FF-3c, 3d, 3e, 4b, 4c, 4d, 1b, 1d, (1a), (1c)	FF-3f, 3g, 4e, 4f

FEPs FF-1a and FF-1c (Figure 7.3.4-1) are somewhat analogous to the sandstone or calcrete type deposits. Although the scenarios are somewhat different, the mechanisms for uranium precipitation do not differ from the standard saturated zone geochemical processes. By definition scenarios FF-1a and FF-1c (Figure 7.3.4-1) need either a roll-front/geochemical cell or a sorption mechanism in order to precipitate the uranium minerals.

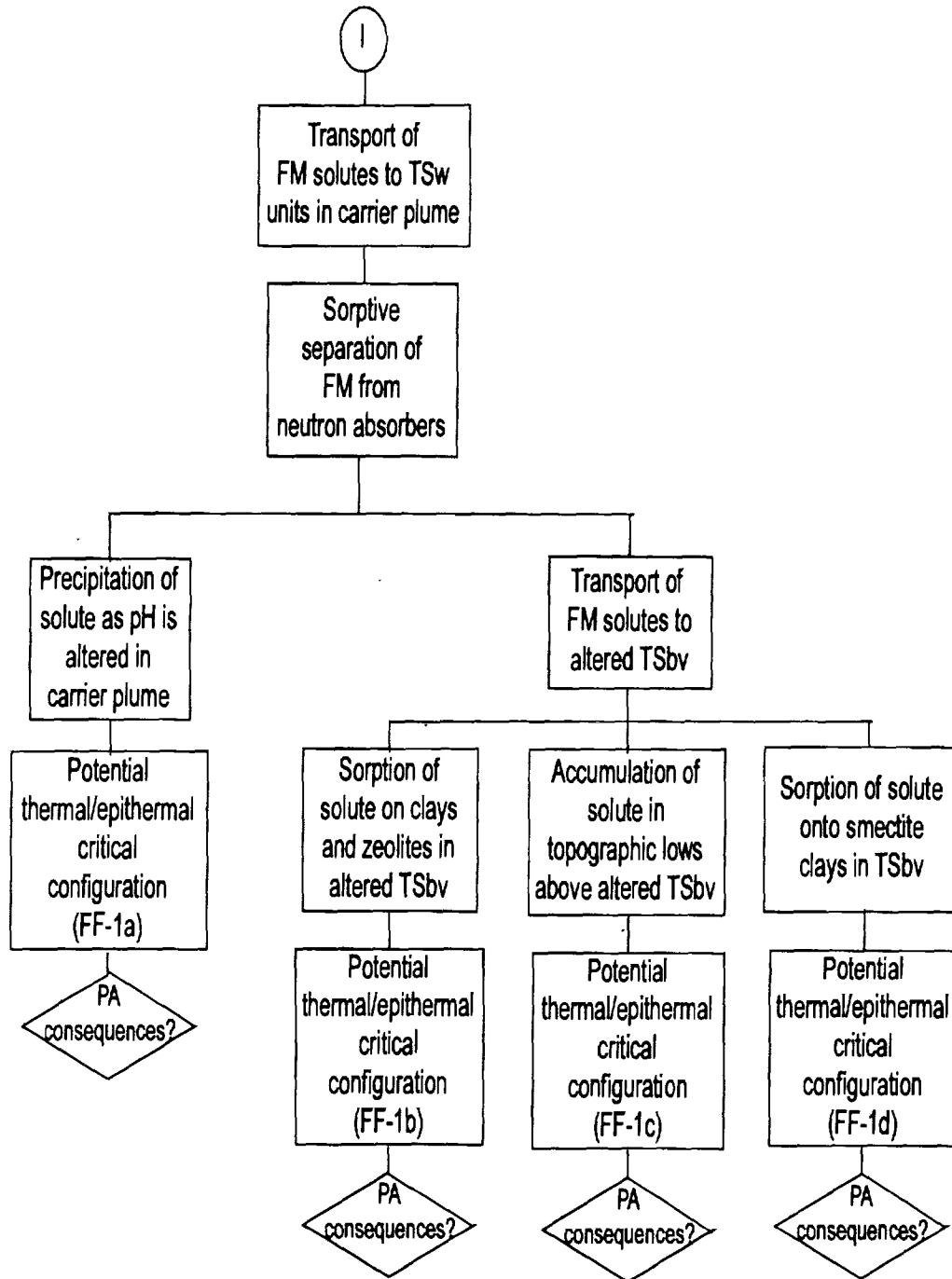


Figure 7.3.4-1. I portion of the FEP diagram created from the TSPA criticality abstraction workshop. The I portion consists of the fissile material solutes scenarios that are of concern in the unsaturated zone.

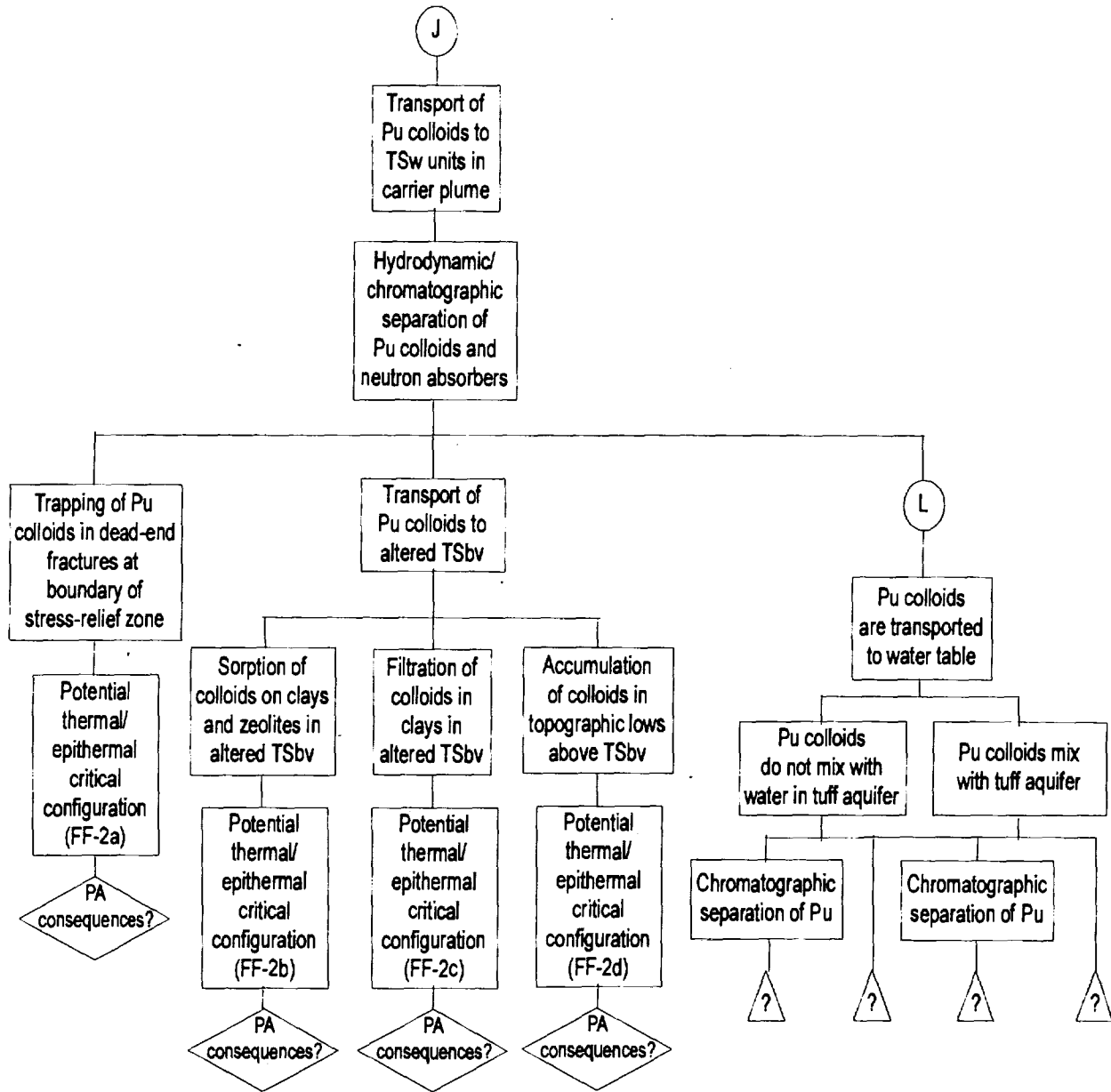


Figure 7.3.4-2. J and L portions of the FEP diagram created from the TSPA criticality abstraction workshop. The two portions represent colloid transport in both the saturated and unsaturated zones.

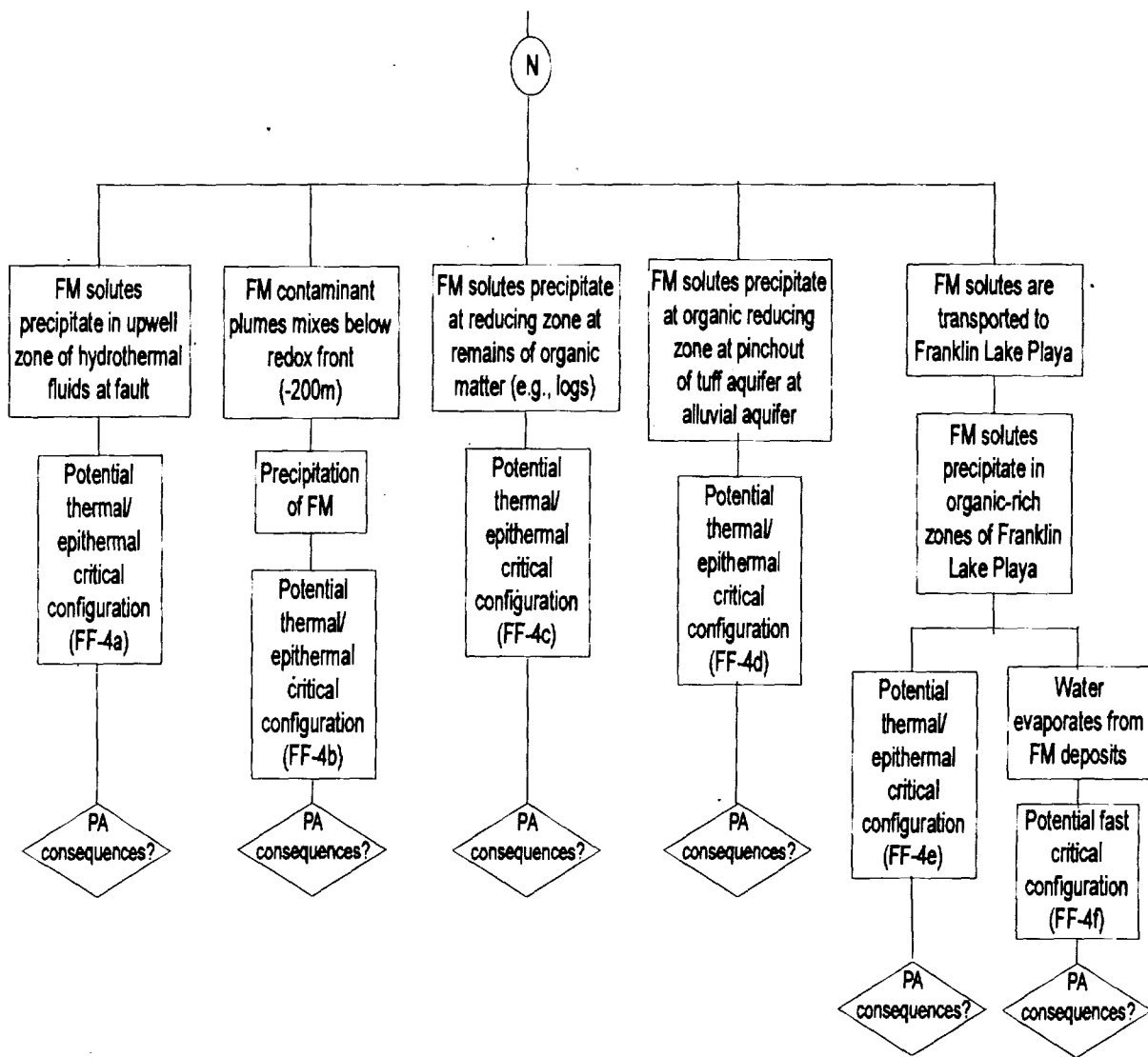


Figure 7.3.4-3. N portion of the FEP diagram created from the TSPA criticality abstraction workshop. The N portion includes the fissile material solutes that are transported to the water table which undergo no mixing with the aquifer and are not separated by chromatographic separation.

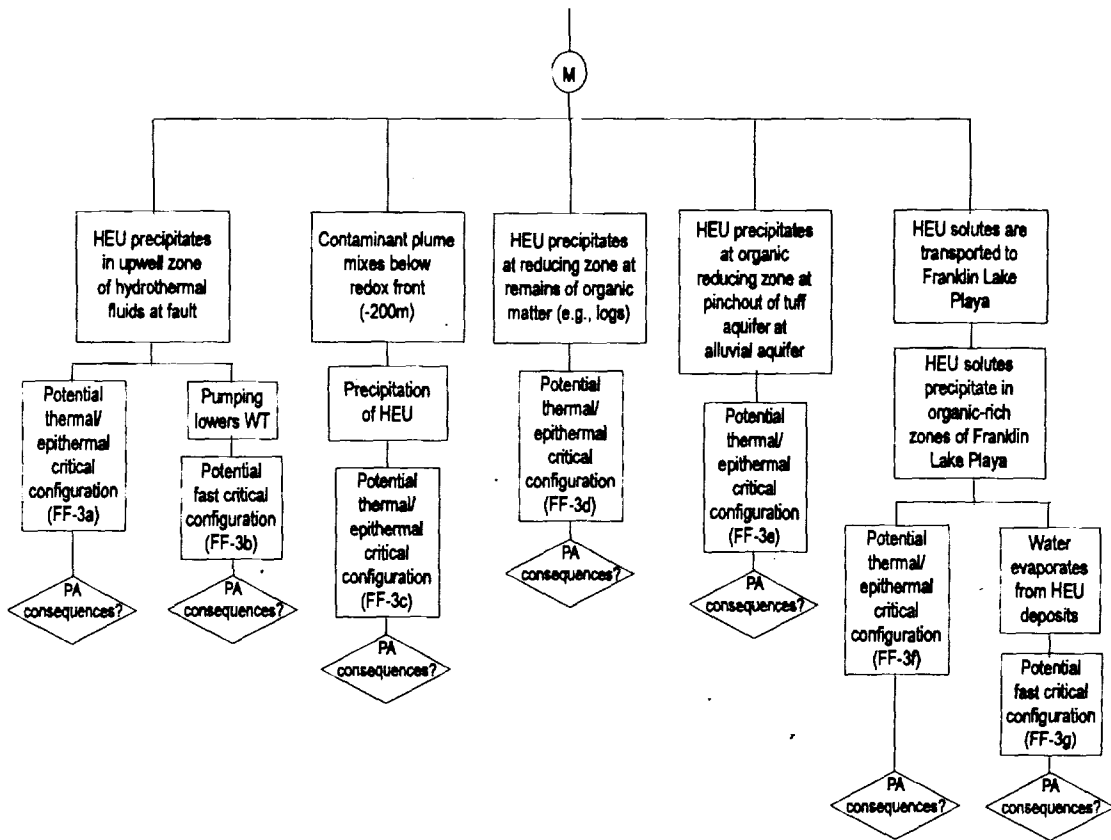


Figure 7.3.4-4. M portion of the FEP diagram created as a result of the TSPA criticality abstraction workshop. The M portion relates to the fissile material solutes that are transported to the water table which do not mix with the water in the tuff aquifer and undergo chromatographic separation.

Those scenarios that are not easily defined or classified into one of the three types are the colloid scenarios (FF-2a to -2d; Figure 7.3.4-2), mainly because they do not deal with saturated groundwater flow systems and are associated with colloidal transport mechanisms of accumulation. Colloidal transport and agglomeration is less well known. It is uncertain, at this time, how the Pu colloids behave in the far-field environment. Therefore, this effort does not address their effects. See discussion of colloids in Section 7.2.3.

7.3.5 Results of Natural Analog Study

The key factor in this study (as with all epigenetic uranium ore deposition) is the need for either a sufficient localized reducing capacity or a source of vanadium within the Yucca Mountain regional geology and aquifer system to precipitate sufficient quantities of ore grade uranium. Without a mechanism or source to either reduce the oxidized uranium species in the groundwater or the vanadium to precipitate oxidized uranium minerals there can be no substantial accumulation of uranium minerals, thus no possible way for a critical assemblage to form. If the required reducing capacity (or presence of vanadium) in the natural system at Yucca Mountain (which is yet unknown or uncharacterized) does not exceed the reducing capacity (or presence of vanadium) that has produced the accumulated known quantities of epigenetic uranium ore in the past, the potential uranium precipitation at Yucca Mountain over geologic time is bounded to that found in ores that occur in similar settings. The three natural analogs are discussed below in this light.

7.3.5.1 Unconformity

A deposit at or near Yucca Mountain resembling an unconformity analog has the highest potential for developing a criticality. On average, ore grade is much higher for the unconformity type than either the sandstone or the calcrete type deposits. The average ore grade for an unconformity type deposit can be 2% (Table 7.3.5-1) whereas the other analogs have a much lower grade, usually no greater than 0.35% (Table 7.3.5-2). The percentage of U_3O_8 in these high grade ores seems to dwarf those in the other two analogs. The high grade ores reported in the Athabasca region (Collins Bay, Rabbit Lake, Cluff Lake, Midwest Lake, and Key Lake) have produced localized mineralizations that have high grade ores ranging between 30 and 80% U_3O_8 . These high grades are persistent over several meters of the orebody. Certainly these types of deposits, if formed at Yucca Mountain, could potentially result in a criticality. However, the reducing conditions necessary to produce such large concentrated masses of fissile material are evidently absent. See Section 7.4 for evaluations of what chemical reactions might actually occur.

Indications of the fluid geochemistry that was migrating up the faults and reacting with the uranium charged oxidized waters above the unconformity in the Athabasca region, give bounding conditions of what type of fluid is needed to react with the potential uranium rich oxidized waters at Yucca Mountain (Figure 7.3.2-2). Gas samples associated with a characteristic odor at Collins bay were analyzed and found to contain short chain aliphatic hydrocarbon gases, hydrogen, and

Table 7.3.5-1 Collected Information on Selected Unconformity Type Deposits
Global average ore grade (% U₃O₈) runs between 0.2 to 2.0%

Deposit	High Grade (% U ₃ O ₈)	Average Ore Grade (% U ₃ O ₈)	Ore Body Dimensions	Ore Deposition Age (m.y.)
Collins	80 ^a	0.6	3000 ft x 300 x 100 ft	1238 ^e
Rabbit	NA	0.4	215 m x 540 m x 200 m	1075 ^e
Cluff	29.3 ^b	1.9	1200 m x 200 m x 150 m	1050 ^e
Key Lake	35 ^c	2.0	3.6 km x 100 m x NA	1160 ^e
Midwest	NA	3.4	2 km x 200 m x NA	
East	2.47	0.4	NA	
Jabiluka II	NA	0.39	1500 m x 500 m x 150 m	
Nabarlek	5 to 72 ^d			1770 to 800

^aHigh grade ore: 7 ft. Section of 80% U₃O₈, 30 ft section of 60% U₃O₈; ^bD zone ores have an average grade of 7% with a high grade of 29.3% U₃O₈; ^cHigh grade ore reported in one case at 35% U₃O₈ over 2 m; ^dWithin a 10 meter wide crush zone; ^eGeneral time interval of mineralization for all of the Athabasca deposits runs about 250 m.y. Table compiled using information from Nash et al. (Ref. 5.34), Hoeve and Sibbald (Ref. 5.60 and Ref. 5.61), Jones (Ref. 5.62), Harper (Ref. 5.63), Clark et al. (Ref. 5.64) and Clark and Burrill (Ref. 5.43). NA means not readily available in the literature.

Table 7.3.5-2 Collected Information on Selected Sandstone and Calcrete Type Deposits

Deposit	High Grade (% U ₃ O ₈)	Average Ore Grade (% U ₃ O ₈)	Ore Body Dimensions	Ore Deposition Age (m. y.)
<i>Sandstone Type</i>	Global Ave. 2.0%	Global Ave. 0.10 to 0.35%		
Olympic Dam	NA	0.05 to 0.1	NA	NA
Fieberbaunn	2.3	NA	A few m x 11 km x 3m	NA
Montezuma	b	0.25	80 ft x several 1000 ft ^e	NA
Happy Jack ^a	1.3 ^b	0.39	20 ft x 500 ft x 3500 ft	65 m. y.
Temple	15 ^c		NA	84 m. y.
<i>Calcrete Deposits</i>		Global Avg 0.1 to 0.3%		
Yeelirrie	0.36 ^d	0.15	8 m x 6 km x 0.05 km	

^aColorado Plateau deposits average an ore grade of about 0.25% U₃O₈. ^bColorado Plateau deposits have an average high grade ore of about 2.0% U₃O₈. ^cTemple Mountain has a unique ore chemistry as uranium ore is directly associated with petroleum products such as tar and is not directly associated with the normal uranium ore deposits on the Colorado Plateau. ^dHalf of the ore at Yeelirrie grades better than 0.36% U₃O₈; no high grade numbers are given. Table compiled using information from Kerr (Ref. 5.65), Huff and Lesure (Ref. 5.66), Kimberly (Ref. 5.67), Fisher (Ref. 5.68), Dodd (Ref. 5.69), Kelley and Kerr (Ref. 5.79), and Nash et al. (Ref. 5.34). ^eCovers a broad area, of several thousand feet dimension. NA means not readily available in the literature.

carbon dioxide. Also associated with the ore deposits are hard glassy hydrocarbon buttons (Ref. 5.62). With these indications, the waters that were migrating up the fault were certainly charged with methane and carbon dioxide. For other unconformity type deposits some sort of hydrothermal fluid, which often has H_2S gas, is cited as the reductant. These two gases (methane and H_2S) are very reducing (Ref. 5.38) and can potentially promote the formation of very high grade ore deposits.

One potential source of very reducing fluids could be hydrothermal activity. A volcanogenic hazard analysis done on Yucca Mountain suggests that the probability is extremely low for having a volcanic event. Thus, because of the necessary physical and temporal correlation between hydrothermal activity and volcanism, a hydrothermal event is unlikely (Ref. 5.71). This low probability rules out a hydrothermal event as a likely source of reducing fluids.

Another potential source of very reducing fluids is that are associated with petroleum. However, there are no known petroleum deposits at Yucca Mountain (Ref. 5.75). This does not preclude mineralization from this mechanism at Yucca Mountain. A big uncertainty with current site characterization data lies in the saturated zone geochemistry at Yucca Mountain. There is a lack of measured data from the carbonate aquifer, but with the data that are available, a known chemical gradient exists between the composition of the Paleozoic aquifer and the Tuff aquifer (Table 7.3.5-3). The measurements found on Table 7.3.5-3 are not sufficiently reducing; however, there is no measurement for Eh nor are there measurements for CH_4 and H_2S in these waters.

The information presented above seems to indicate that the only geochemical mechanism that could potentially create an unconformity type of deposit at Yucca Mountain is a nonhydrothermal source of methane (or other hydrocarbon) migrating up a fracture zone or fault plane to react with an oxidized uranium-rich fluid. Without a water chemistry sampling from the Paleozoic aquifer that could yield information on potential petroleum or methane migration from depth, this type of ore deposit cannot be entirely ruled out, although a nonhydrothermal unconformity type deposit due to petroleum migration seems very unlikely in view of the current geochemical understanding of the site.

Table 7.3.5-3. Water Chemistry for well UE-25 P#1 (Paleozoic Aquifer) and Average J-13 (Tuff Aquifer) Compositions

<i>Source</i>	<i>LA-101188- MS</i>	<i>OFR-84- 450</i>	<i>OFR-94- 305</i>	<i>AVG</i>	<i>J-13</i>
Si	30	41	44	38.3	28.5
Al	0.1				
Fe	<0.1				
Mn	<0.1				
Mg	32	39	31	34.0	2.01
Ca	88	100	94	94.0	13.0
Na	171	150	150	157.0	45.8
K	13.4	7.2	12	10.9	5.0
Li	0.32	0.59	0.31	0.4	0.048
HCO ₃ ⁻	698	710	890	766.0	129
F ⁻	3.5	4.7	4.9	4.4	2.18
Cl ⁻	37	28	26	30.3	7.1
SO ₄ ⁻	129	160	78	122.3	18.4
NO ₃ ⁻	0.1				8.8
pH (field)	6.7	6.6	6.7	6.7	7.4
Temp °C		56	57	56.5	31.0

Values found on this table are taken from References 5.19, 5.72, 5.73, and 5.74.

7.3.5.2 Sandstone

Sandstone type deposits in the U.S. comprise about one third of all the known minable uranium reserves in the world of which the majority are located on the Colorado Plateau (Ref. 5.34). Under normal occurrence the high grade ores in sandstone deposits seldom exceed 2% U₃O₈ (Table 7.3.5-2). The average ore grade for a typical sandstone deposit seems to range somewhere between 0.1 and 0.35% U₃O₈ with the deposits on the Colorado Plateau averaging about 0.25% (Table 7.3.5-2). However, there are known occurrences of high grade ore that are directly associated with either petroleum (tar and asphalt type materials) or buried logs. The Table Mountain deposit is associated with tar and asphalt like substances as the reducing agent. This deposit has a maximum ore grade of 15% (Ref. 5.70). Other uranium deposits on the Colorado Plateau have occurrences of petrified logs that have been replaced with uranium minerals. These localized log deposits average around 1.88% uranium with maximum concentrations in individual logs of reaching 16.5 to 20% uranium (Refs. 5.75, 5.77, and 5.78).

Without the presence of either logs or petroleum, no other mechanism is known wherein a sandstone type deposit can precipitate mineral grades much greater than 2% (Ref. 5.22). Therefore, basic sandstone type deposits, without the reducing capacity of either buried logs or petroleum, will not accumulate enough fissile material to go critical. However, as demonstrated above, uranium deposition in the presence of logs or petroleum products could accumulate

enough high grade mineralization wherein sufficient fissile material could precipitate to go critical.

Within the bedded Tuff (ash-fall or reworked) deposits at Yucca Mountain, where there are known sandstone and paleosol deposits, there is the possibility of buried logs. As an example, a study done at Mount St. Helens (Ref. 5.79) looked at dating ash fall deposits from eruptive events using buried logs within associated lahar and debris flow deposits. Logs tended to be highly disseminated within each deposit; however, within some of the sampled debris flows and lahar deposits, between 17-30 logs were sampled for dating. These logs ranged in ages between 1355 and 1885 AD. Although Yamaguchi and Hoblitt (Ref. 5.79) do not give a distribution nor the abundance of buried logs in the Mount St. Helens deposits, their study documents the presence of buried logs within volcanic deposits. The possible occurrence of logs within ashfall type deposits cannot be discredited at Yucca Mountain. In Reference 5.6, a probabilistic analysis done for far-field criticality suggested that the likelihood a criticality event would occur as a result of uranium mineral precipitation with buried logs is very small. Unless there is either a petroleum deposit or migration event, such as is needed in the unconformity case described above, the likelihood of criticality occurring in a sandstone type mineral deposit is small.

In conjunction with the burial of logs within or in close proximity to volcanic deposits, it should be borne in mind that they tend to become petrified in a geologically short time. For example, about 20 petrified forests have been identified in Specimen Ridge in Yellowstone National Park (Ref. 5.81, pp. 313-314). This is closely related to the release of silica from the weathering of volcanic glass giving rise to waters supersaturated in quartz, chalcedony, and other silica minerals, which may then precipitate within the cells of the wood. Thus, it is quite likely that any wood buried in the volcanic pile at Yucca Mountain, or in the soils between ash falls, may be petrified, thereby severely limiting its capacity to provide a reducing environment.

7.3.5.3 Calcrete

Calcrete type deposits have similar ore grades as the sandstone type deposits. The average ore grade ranges between 0.1 and 0.3% U_3O_8 (Table 7.3.5-2). The arguments described above that exclude the sandstone deposits from consideration are the same in this case (i.e., an insufficient amount of vanadium in this environment to precipitate high grade quantities of uranium ore); thus, the likelihood of a critical assemblage is small. Other potential arguments that help in this case include both the potential accumulation of known nuclear fuel poisons and the evaporitic loss of moderating water. The most likely location in the vicinity of Yucca Mountain for this type of deposit is at or near Franklin Lake playa (believed to be a groundwater discharge location for the groundwater flowing beneath Yucca Mountain, Ref. 5.58). Playa deposits are known to accumulate borates as evaporite deposits (Ref. 5.80). Boron is a known reactor fuel poison and will be a constituent of the high level waste planned to be disposed at Yucca Mountain. Last of all, due to evaporation, there may be insufficient water to act as a moderator for criticality.

7.3.6 Areas of Potential Concern

At Yucca Mountain conditions in the rock, specifically fracture density and aperture as well as possibly some buried organic material, might permit high-grade mineral deposits to accumulate.

However, these locations will have to be in areas where either the reducing capacity or source of vanadium in the host rock is sufficiently high over extended periods of geologic time to accumulate a high percentage of U_3O_8 . The analogs to Yucca Mountain described above associate the realistic precipitation capacity for epigenetic deposits to either H_2S gas, some type of organic accumulation in the host rock, or presence of vanadium in the environment. Thus, the potential areas of concern at Yucca Mountain seem to be associated with locations where there potentially could be these types of gas or organic accumulations (i.e., for logs in the paleosols, bedded tuffs, and in the alluvium; and for petroleum and H_2S gas, along faults and fracture zones). Otherwise, the probability of high grade uranium accumulations in the potential Yucca Mountain radionuclide pathway seems very small (see Table 7.3.5-4).

Table 7.3.5-4 Summary of Geologic Reducing Zone Occurrence Requirements, and Likelihood at Yucca Mountain

Formation type	Reducing media	Occurrence at Yucca Mountain
Unconformity	Hydrothermal fluid	Requires volcanic activity; highly unlikely
	Other methane source	Incredibly low probability
Sandstone	Organic logs	Very unlikely*
	Petroleum	None observed, nor likely to be
Calcrete	Vanadium	None observed

* This case has been shown to have incredibly low probability for low enriched uranium (LEU) commercial SNF with the log occurrence frequency of the Colorado Plateau (Ref. 5.6).

7.3.7 Summary

The obvious potential criticism to this discussion is that alteration of the ambient geologic environment would occur with placement of a highly enriched source of fissile material in Yucca Mountain. Over time, the repository would act as a source for potential mineral deposition in the far-field. This highly enriched source is unlike any source of uranium for mineral deposits found in nature. However, the fact remains that there still has to be either a persistent reducing agent (one strong enough to resist the invasion of oxidizing solutions) or a source of vanadium within the host rock for the uranium to accumulate. If the precipitation conditions are not persistent, there may be short term accumulation followed by remobilization.

One cannot fully rule out the possibility of any of the FEP scenarios (Figures 7.3.4-1 to 7.3.4-4) occurring, because of the nature of the geologic environment and the infeasibility to characterize the entire geologic system at Yucca Mountain deterministically. However, the potential for Yucca Mountain to have the required persistent reducing capacity seems minimal given the current site characterization data. Some of the currently accepted characterization data are as

follows: a) there are no known petroleum deposits in the vicinity of Yucca Mountain (Ref. 5.75); b) the probability of a hydrothermal event has been determined to be very small (Ref. 5.71); and c) the probability of uranium ore deposits from log replacement has been determined to be very unlikely (Ref. 5.6). The three items discussed above cover the main areas of concern for potential criticality in the far-field. Therefore, the potential for far-field criticality seems small.

7.4 Analyses of Interaction With External Features

The purpose of this section is to report the results of analyses of interactions of waste package fluids with external features. The findings summarized in these sections are supplied in detail in the electronic and hard copy attachments.

For analyses of the reaction of effluent from a waste package the open system option in EQ6 was utilized. This was implemented successively, as described in detail in Attachment III. The composition of the effluent itself as a function of time was calculated using the titration mode in EQ6, normally in the chemical sense of a closed system. This corresponds to maximum impacts on the aqueous chemistry because the solution inside the waste package is not diluted by newly infiltrating water, nor flushed from the package. Nevertheless, an alternative scheme was devised, using the option available in EQ6 of mixing of two solutions, whereby the solution inside the package was first diluted for some specified time interval, and then part of the solution removed, thereby simulating to some degree advection of new ground water and transport out of the package. Details of this procedure are described in Attachment II.

The uncertainties in the calculations stem mainly from lack of definitive knowledge of reaction rates and the pathways which the effluent from waste packages may take. The reaction rates are very slow and hard to measure. Some insight into the pathways and reactions along them may be gained by use of a suitable code and model incorporating both geochemistry and hydrology. Because a great deal of conservatism has been built into the data used, it seems unlikely that the calculations will yield answers more than an order of magnitude low. To a degree this has been taken into account by spread sheet calculations ten times more extreme. Whereas uncertainties also exist in the thermodynamic data, see, for example, Section 4.1.6, These data have been much more thoroughly reviewed and selected and seem to introduce less uncertainty than do the data for rates.

7.4.1 Water Entering the Waste Package

Examination of the analytical results for J-13 well water by the use of the geochemical code EQ3 reveals that the measurements are compatible with well established thermodynamic data only if the partial pressure of CO₂ is markedly higher than in the atmosphere. This situation is discussed in more detail in Ref. 5.9, pp. 5-18 to 5-19. For the present application, the pH values in Ref. 5.19 were converted approximately to hydroxide concentrations, those values averaged, and the average converted back to an average pH of 7.64. To achieve agreement between analytical and thermodynamic data, the average for alkalinity was adjusted by about half of its analytical standard deviation (8.6 mg/L) from 128.9 mg/L to 133.0 mg/L. These adjusted values were used in modeling the degradation of waste packages containing commercial spent nuclear fuel and for MOX fuel waste packages. In addition during the modeling runs, normal atmospheric partial

pressures of CO₂ were used. This results in an immediate adjustment of pH and corresponding loss of carbonate concentration in the water. In other words, the implicit assumption is that not long after entering the open space of a repository, the water will come to equilibrium with the atmosphere, rather than with rock gas which may have a higher concentration of CO₂. Table 7.4.1-1, first three columns, shows the composition of the water actually used for the SNF and MOX calculations. The initial water composition for modeling the degradation of immobilized plutonium was the same as given in Ref. 5.19 along with EQ3 input constraints for being in equilibrium with atmospheric CO₂ and O₂ and the electrical balance adjusted by modifying the total chloride ion concentration as needed. Chloride was chosen for the electrical balancing because it tends to have little effect on the chemical calculations; this results from the facts that with most elements it forms only weak complexes and that the solids present in the system under consideration contain little or no chloride. This resulted in a solution very nearly the same as described above, except for a significant change in chloride concentration (last 3 columns of Table 7.4.1-1). This difference in chloride concentration has little effect because the dissolution of the HLW glass very quickly results in substantial changes that dominate the aqueous chemistry.

Table 7.4.1-1 Calculation of J-13 Water Composition

J-13 water	Molality	Mole Fr.	J-13 water	Molality	Mole Fr.
Na	1.99e-03	1.20e-05	Na	1.99e-03	1.20e-05
Si	1.02e-03	6.11e-06	Si	1.02e-03	6.11e-06
Ca	3.24e-04	1.95e-06	Ca	3.24e-04	1.95e-06
K	1.29e-04	7.74e-07	K	1.29e-04	7.74e-07
C	2.18e-03	1.31e-05	C	1.45e-04	8.69e-07
F	1.15e-04	6.89e-07	F	1.15e-04	6.89e-07
Cl	2.01e-04	1.21e-06	Cl	2.15e-04	1.29e-06
N	1.42e-04	8.53e-07	N	1.42e-04	8.53e-07
Mg	8.27e-05	4.97e-07	Mg	8.27e-05	4.97e-07
S	1.92e-04	1.15e-06	S	1.92e-04	1.15e-06
B	1.24e-05	7.44e-08	B	1.24e-05	7.44e-08
P	1.27e-06	7.63e-09	P	1.27e-06	7.63e-09
H	1.11e+02	6.67e-01	H	1.11e+02	6.67e-01
Al	1.48e-08	8.90e-11	O	5.55e+01	3.33e-01
Ba	1.00e-10	6.00e-13	Totals	1.67e+02	1.00e+00
Ce	1.00e-24	6.00e-27			
Cr	3.45e-07	2.07e-09			
Cu	1.00e-10	6.00e-13			
Cs	1.00e-10	6.00e-13			
Fe	1.15e-04	6.89e-07			
Gd	1.00e-14	6.00e-17			
La	1.00e-14	6.00e-17			
Li	1.00e-10	6.00e-13			
Mn	7.28e-07	4.37e-09			
Mo	1.00e-10	6.00e-13			
Nd	1.00e-14	6.00e-17			
Ni	1.00e-10	6.00e-13			
Pb	1.00e-10	6.00e-13			
Pu	1.00e-14	6.00e-17			
Sm	1.00e-10	6.00e-13			
Sr	1.00e-10	6.00e-13			
Ti	1.00e-10	6.00e-13			
U	1.00e-14	6.00e-17			
Zn	1.00e-10	6.00e-13			
Zr	1.00e-20	6.00e-23			
O	5.55e+01	3.33e-01			
Totals	1.67e+02	1.00e+00			

J-13 water. Columns A-C: Adjusted for pH 7.6397 and log fO₂ = -2.5390 to be consistent with thermodynamic data. Original molalities from Ref. 5.19; adjustments in EQ6 run j13avg20.60. These data used for oxide fuel calculations. Col. E-G correspond to original data, balanced on Cl- and for log fO₂ = -3.500. These data were used for runs with glass waste before a method was devised to make a suitable adjustment to the raw data. The effect on the results is insignificant because the dissolution of the HLW quickly dominates the chemistry.

The concentrations of dissolved U and Pu are not sensitive to differences in chloride concentration nor, except at high pH, to differences in sodium or carbonate concentrations. Consequently, the results of the calculations provided in Ref. 5.9 were used for calculations evaluating the possible deposition of fissile isotopes dissolved in neutral or acidic effluent from immobilized plutonium waste packages in invert or rock below the waste package.

7.4.2 Concentration From Solution Flowing Out Of A Waste Package Containing Immobilized Plutonium

The reactions with invert discussed in Section 7.1.2.1.1 for the case of the immobilized plutonium package were modeled. As indicated in Section 4, this waste form was modeled as plutonium and gadolinium in a lanthanum-borosilicate (LaBS) glass because this was the one form for which there was the most data. As this analysis was in the final publication process (September 1997) a downselection process chose ceramic as the matrix for immobilized plutonium. The potential accumulations from the ceramic waste form will be analysed in subsequent studies; however, it is expected that the analyses for LaBS glass reported here will be conservative with respect to the ceramic waste form, because of the expected lower dissolution rate for the ceramic waste form. Therefore, it is appropriate to present the results of the LaBS glass waste form analyses.

At early times, the composition of the effluent was taken from a stage in the simulation of the reaction inside the waste package at which the pH had risen nearly to its maximum value, but before the ionic strength had increased to the point that no confidence could be placed in the result. This composition and the time of its occurrence are discussed in more detail in subsections below. For later times, compositions were calculated on the basis that most of the high ionic strength alkaline initial solution would have been flushed out and that the chemistry was essentially the same as would result from influx of J-13 water with the oxidized uranium and plutonium solids that would exist at a given pH at saturation as discussed in Ref. 5.9. Nevertheless, the newly developed algorithm for simulating flushing and transport, noted above in Section 7.4, was exercised for an infiltration rate of 10 mm/yr (see files allinglsI10mm, allinglsII10mm, allinglsIII10mm, allinglsIV10mm, allinglsV10mm, alloutglsI10mm, alloutglsII10mm, alloutglsIII10mm, alloutglsIV10mm, and alloutglsV10mm) with the assumption that Cr would oxidize fully (Assumption 4.3.9). This analysis showed that the pH still rose to a high value, 9.9274, in about 250 years (see file alloutglsII10mm) compared to 10.04 for the closed system case, but was no longer highly alkaline after about 330 years (see file alloutglsIII10mm), about half as long as in the closed system case. Ionic strength reached a high of 1.456 in marked contrast to the continually increasing value to totally unrealistic values for the closed system; in the closed system at 250 years the ionic strength was calculated as 4.25, and, because this is too high to model correctly, even approximately, with the available data for activity coefficients, the solution characteristics for this stage were not used. Thus, the flushing has a large effect on the total dissolved solids in the system, but only a modest effect on the pH as compared to the highly conservative case of a closed system. The largest causes of the initial rapid rise in pH and ionic strength, as well as the very low pH that could result from complete oxidation of Cr and Mo, thus appear to be the high (conservative) rates of degradation used in the models.

7.4.2.1 Solution From the Immobilized Plutonium Package

As the contents of the package degrade in J-13 water the pH gradually begins to increase as alkaline glass degradation products are formed. The solution composition was modeled by EQ6 as the contents of the waste package were dissolved. For about 600 years the effluent from the package was simulated to have a pH of about 10. The effluent becomes neutral (about pH 7) after the high pH period. The neutral condition lasts about 1200 years after which the effluent pH is approximately 5 for another 8000 years. During the entire degradation period the solution remains oxidizing. Solutions with these three conditions were used as feed solutions for reactions with the environment external to the waste package.

7.4.2.1.1 Immobilized Plutonium Solution at pH 10

For the present analysis, a solution composition near the maximum pH, but at a low enough ionic strength to stay within reasonable bounds, was chosen (see step 824 of EQ6 output file j13avwp50.6o, Section 9.2). Specifically, this was pH 10.0031 and ionic strength 2.51 at 140 years post-closure. Under these conditions the solubilities of U and Pu are near their maximum values; consequently, solutions resembling the one chosen are the most likely to produce a sufficient concentration of fissile material to give rise to a criticality in the invert. The pH will remain high for 600 years, which is a short time compared to time-frames of interest. Consequently, the total mass of ^{235}U and ^{239}Pu that could be released while the pH is high may be small. The simulated solution chosen contains 6111 ppm total U and 78.3 ppm Pu. All the Pu would have been released from the LaBS glass as would all the ^{235}U . The ^{235}U arises from the decay of ^{239}Pu , here simulated as at 5000 years post-closure. It is assumed that the ^{235}U from the LaBS glass will mix with the ^{238}U from the HLW glass before any U or Pu solids precipitate or are otherwise immobilized within the waste package. In this case the percentage of ^{235}U in the effluent from the waste package will be about 3.31%, which is conservative in view of the fact that no preferential early removal of ^{235}U would occur immediately upon release from the LaBS glass.

The composition described above is very conservative because it was developed for no flow through the package during the dissolution. With no flow, the concentrations become much higher than with the flushing effect of a flow through situation. At infiltration rates up to 1 mm per year the flushing effect may be minimal. However, some results below were reported for 5 mm/yr and 10 mm/yr infiltration rates. A dissolution case with flushing (EQ6 output files alloutglsI10mm, alloutglsII10mm, alloutglsIII10mm, alloutglsIV10mm, and alloutglsV10mm -- see Section 9.2) were run to test the sensitivity of the results. It was found that at 10 mm/yr infiltration that the pH 10 (actually 9.93) condition would last less than 300 years (compared with 600 years for the non-flushing cases). It would also be expected that the pH 10 condition would last less than 400 years at 5 mm/yr due to the same effect. The flushing dissolution case at 10 mm/yr gave at the same length of dissolution time (140 years), a higher maximum concentration of uranium, 7263 ppm versus 6111 ppm, and a lower maximum plutonium concentration, 10.1 ppm versus 78.3.

7.4.2.1.2 Immobilized Plutonium Package Solution at pH 7

For the simulations of the reactions, a representative solution chemistry was chosen. The results from EQ6 output file j13avwpsoly45.6o was taken. This solution at pH 7.01 an ionic strength of 3.5E-03 (molality scale). The solution contained 1.929E-03 ppm U and 1.56E-07 ppm Pu.

7.4.2.1.3 Immobilized Plutonium Package Solution at pH 5

For the simulations of the reactions, a representative solution chemistry was chosen. The results from Step 14 of EQ6 output file j13avwpsoly40.6o was taken. This solution at pH 5.5 has an ionic strength of 2.4 molal. The solution contained 4.71E-03 ppm U and 6.15E-06 ppm Pu.

7.4.2.2 Reaction of Immobilized Plutonium Solution with Crushed Tuff Invert

This section presents results of modeling analyses of immobilized plutonium package solution reacting with crushed tuff invert.

To simulate a vitric tuff, the average composition of six analyses shown in Table 4.1.3-1 was recalculated to the form of a "special reactant" for input to EQ6. To model a devitrified tuff, this composition was used as input to a petrological calculation of the norm, i.e. a calculation to distribute the various components of the rock among minerals that are found in welded tuff.

For modeling of the chemical behavior of this system, the chemical compositions of tuff, its mass, surface areas, and degradation rate are required. Tables 4.1.3-1 to 4.1.3-3 show the data used.

7.4.2.2.1 Reaction of Immobilized Plutonium pH 10 Solution With Crushed Tuff Invert

A simulation of this reaction in EQ6 (output file wp10t0a.6o) shows that when the solution first enters the invert, its composition changes slowly as it reacts with the tuff producing small quantities of alteration minerals, but neither uranium nor plutonium solids are produced. The alteration of the tuff principally consists of a recrystallization of the tuff to a mixture of quartz and feldspar. As the solution flows deeper into the invert and finally into the host rock below, there is further reaction and change of solution composition. At this time, a small quantity of solid $\text{Na}_4\text{UO}_2(\text{CO}_3)_3$ is simulated to form primarily due to dissolution of additional sodium from the tuff. The small decrease in pH causes a concomittent shift in the proportions of carbonate and bicarbonate ions in solution and consequent destabilization of the plutonyl carbonate aqueous complex primarily responsible for the solubility of plutonium. Thus, PuO_2 also precipitates. Table 7.4.2-1 shows the results for the reaction of the alkaline solution with the tuff. The table shows the deposition profile over a 600-year period (the duration of pH 10 condition) for an infiltration rate of 1 mm/yr. The deposit is distributed over a distance of 18.2 m extending through the 0.7 m invert and into the rock fractures below. This path was discretized into finite lengths or "cells". The boundaries of these cells are points where there is a significant shift in the mineralogy of the deposit. (The choice of boundaries is detailed workbook WP10T0A.XLS,

worksheet "All Solids".) The first cell extends from the entry point to where the uranium and plutonium species begin to precipitate. The second cell extends to the point where a new mineral, borax, is added to the precipitating solid. (Note: while borax is predicted as a product, large infiltration rates above 1 mm/yr would be expected to flush this out of the waste package before this reaction takes place.) The third cell extends to where another new mineral, Albite (low temperature type) is added to the solid composition. Cell 4 extends to a somewhat arbitrary point where no significant additional uranium plus plutonium solids are forming. Cell 5 extends to the point where the water is in equilibrium with the rock and no further reactions will take place. The first four cells in the profile are in the crushed tuff of the invert. Cell 5 is in the rock. Note that in the first three cells there is a steady decrease in the fraction of void space filled with solids. A sudden increase in cell 4 of the fractures filled is due to a shift in the mineralogy (onset of more solid solutions and low density minerals). A further shift in cell 5 is a combination of changing mineralogy and a different availability of void space (different porosity).

The total amount of fissile material deposited in the invert and rock is only 356 g distributed over the 18 m flow path with most of it concentrated in the first 200 cm (see Figure 7.4.2-1). Throughout the deposition path, the percent of void space filled with fissile material is extremely small (less than 0.01%). The highest distribution point (near the top) has only about 0.5 g of fissile material in a 1 mm depth distributed over a 5.5 m² area. This small deposit of fissile material could not give rise to a criticality under any conditions postulated.

Table 7.4.2-1. Deposition From The Reaction of pH 10 Solution From the Immobilized Plutonium Package with a Crushed Tuff Invert for a 600-year Duration of pH 10 Conditions and 1 mm/yr Infiltration Rate (EQ6 Output File wp10t0a.6o)

Cell No.	Travel Time Into Rock days	Distance Traveled mm	Accumulation During The Deposition Time				% Void Filled With Solids	% Void Filled With Fissile	Fissile wt% of U+Pu	
			Total Solids grams	Uranium grams	Plutonium grams	Fissile grams				
1	2.19E+03	2.00E+01	1.67E+04	2.60E+02	2.48E+00	1.06E+01	5.30E-01	19.1726%	0.0122%	4.05%
2	5.73E+03	5.23E+01	2.70E+04	4.12E+02	4.11E+00	1.70E+01	5.25E-01	11.8405%	0.0075%	4.09%
3	2.11E+04	1.93E+02	1.17E+05	1.70E+03	1.67E+01	7.00E+01	4.99E-01	14.0116%	0.0084%	4.07%
4	9.65E+04	1.09E+03	5.43E+05	4.51E+01	3.45E+01	3.59E+01	4.00E-02	24.7499%	0.0016%	45.13%
5	9.65E+05	1.82E+04	6.26E+06	0.00E+00	2.22E+02	2.22E+02	1.30E-02	17.0949%	0.0006%	100.00%
Total			6.96E+06	2.42E+03	2.80E+02	3.56E+02				13.18%

Calculations were made for a factor of 10 difference in pH duration which would correspond to a factor of 10 decrease in rate constants for reaction with the tuff. Table 7.4.2-2 shows the same scenario as Table 7.4.2-1 but with a deposition pattern for 6000 years duration of pH and infiltration rate of 1 mm/yr. The large increase in pH duration does not have so large an effect as it might since the flow path is sealed by deposits after 2420 years. The maximum amount of fissile material in the flow path is less than 0.05% at the highest point. While there is nearly 1.5 kg of fissile material in the deposit, it is distributed over the flow path. Over 60% of the total fissile material is in a region (Cells 4 and 5) where the fissile material per mm of depth is less than 0.2 g/mm and the % voids filled with fissile material is less than 0.01%. Therefore, this case does not present a scenario which would support a criticality. A separate package dissolution run was made (discussed above in Section 7.4.2.1.1) to investigate what happens to pH duration and concentrations when the infiltration rate is very high. The high-flushing rate run

showed that duration of pH 10 was reduced by half and plutonium and uranium concentrations were reduced by a factor of 5. Therefore, if the infiltration rate were 10 mm/yr, a higher deposition rate is predicted but at such a high infiltration the pH duration drops to 300 years and there is less total deposit than for the 10 mm/year case as shown in Table 7.4.2-3. If the 10 mm/yr selection is combined with a factor of 10 increase in pH duration (to 3000 yr) the result shown in Table 7.4.2-4 is obtained. In this case the voids are nearly filled but the fraction of voids filled with fissile material is still less than 0.07% at the highest point, and, while the total amount of fissile material in the deposit is nearly 18 kg, it is distributed over 190 m of depth. It should be noted that this result is actually high by a factor of nearly 5 since the high flushing rates in the package during dissolution would have greatly reduced concentrations of all species in solution. Figure 7.4.2-2 shows a graphical representation of the buildup of solids and fissile material for the 10 mm/yr, 3000 yr case.

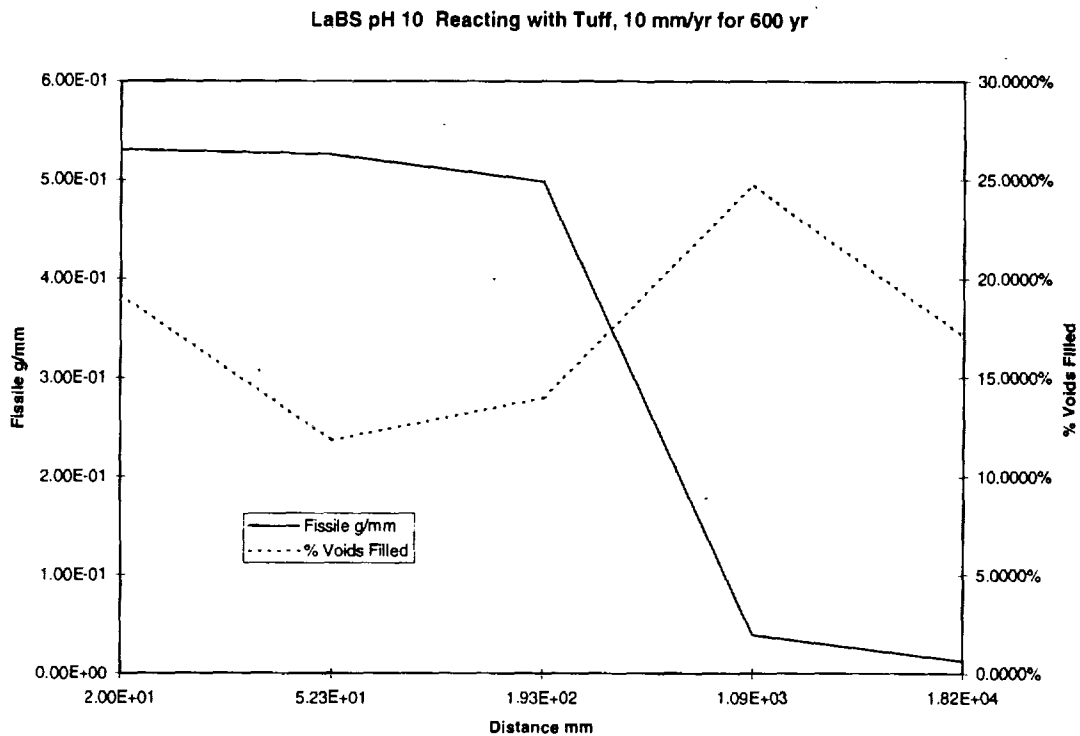


Figure 7.4.2-1. Amount of Fissile Material and Percentage of Voids Filled for Immobilized Plutonium pH 10 Reacting With Tuff at 1 mm/yr for 600 years.

Table 7.4.2-2. Deposition From The Reaction of pH 10 Solution From the Immobilized Plutonium Package with a Crushed Tuff Invert For a 6000-year Duration of pH 10 Conditions and 1 mm /yr infiltration rate (EQ6 Output File wp10t0a.6o).

Cell No.	Travel Time Into Rock days	Distance Traveled mm	Accumulation During The Deposition Time					% Void Filled With Solids	% Void Filled With Fissile	Fissile wt% of U+Pu
			Total Solids grams	Uranium grams	Plutonium grams	Fissile grams	Fissile g/mm			
1	2.19E+03	2.00E+01	6.74E+04	1.05E+03	1.00E+01	4.28E+01	2.14E+00	77.4653%	0.0492%	4.05%
2	5.73E+03	5.23E+01	1.09E+05	1.66E+03	1.66E+01	6.87E+01	2.12E+00	47.8407%	0.0301%	4.09%
3	2.11E+04	1.93E+02	4.74E+05	6.88E+03	6.74E+01	2.83E+02	2.01E+00	56.6130%	0.0338%	4.07%
4	9.65E+04	1.09E+03	2.19E+06	1.82E+02	1.39E+02	1.45E+02	1.62E-01	100.0000%	0.0066%	45.13%
5	9.65E+05	1.82E+04	2.53E+07	0.00E+00	8.98E+02	8.98E+02	5.25E-02	69.0706%	0.0025%	100.00%
Total			2.81E+07	9.77E+03	1.13E+03	1.44E+03				13.18%

Table 7.4.2-3. Deposition From The Reaction of pH 10 Solution From the Immobilized Plutonium Package with a Crushed Tuff Invert For a 10mm /yr infiltration rate and 300 year Deposition time (EQ6 Output File wp10t0a.6o).

Cell No.	Travel Time Into Rock days	Distance Traveled mm	Accumulation During The Deposition Time					% Void Filled With Solids	% Void Filled With Fissile	Fissile wt% of U+Pu
			Total Solids grams	Uranium grams	Plutonium grams	Fissile grams	Fissile g/mm			
1	2.19E+03	2.00E+02	8.35E+04	1.30E+03	1.24E+01	5.30E+01	2.65E-01	9.5863%	0.0061%	4.05%
2	5.73E+03	5.23E+02	1.35E+05	2.06E+03	2.05E+01	8.50E+01	2.63E-01	5.9203%	0.0037%	4.09%
3	2.11E+04	3.35E+03	5.86E+05	8.52E+03	8.34E+01	3.50E+02	1.24E-01	8.7024%	0.0052%	4.07%
4	9.65E+04	1.82E+04	2.71E+06	2.25E+02	1.73E+02	1.80E+02	1.21E-02	7.4133%	0.0005%	45.13%
5	9.65E+05	1.89E+05	3.13E+07	0.00E+00	1.11E+03	1.11E+03	6.49E-03	8.2180%	0.0003%	100.00%
Total			3.48E+07	1.21E+04	1.40E+03	1.78E+03				13.18%

Table 7.4.2-4. Deposition From The Reaction of pH 10 Solution From the Immobilized Plutonium Package with a Crushed Tuff Invert For a 10mm /yr infiltration rate and 3000 year Deposition time. (EQ6 Output File wp10t0a.6o)

Cell No.	Travel Time Into Rock days	Distance Traveled mm	Accumulation During The Deposition Time					% Void Filled With Solids	% Void Filled With Fissile	Fissile wt% of U+Pu
			Total Solids grams	Uranium grams	Plutonium grams	Fissile grams	Fissile g/mm			
1	2.19E+03	2.00E+02	8.35E+05	1.30E+04	1.24E+02	5.30E+02	2.65E+00	95.8628%	0.0609%	4.05%
2	5.73E+03	5.23E+02	1.35E+06	2.06E+04	2.05E+02	8.50E+02	2.63E+00	59.2026%	0.0373%	4.09%
3	2.11E+04	3.35E+03	5.86E+06	8.52E+04	8.34E+02	3.50E+03	1.24E+00	87.0240%	0.0519%	4.07%
4	9.65E+04	1.82E+04	2.71E+07	2.25E+03	1.73E+03	1.80E+03	1.21E-01	74.1326%	0.0049%	45.13%
5	9.65E+05	1.89E+05	3.13E+08	0.00E+00	1.11E+04	1.11E+04	6.49E-02	82.1795%	0.0029%	100.00%
Total			3.48E+08	1.21E+05	1.40E+04	1.78E+04				13.18%

LaBS pH 10 Reacting with Tuff, 10 mm/yr for 3000 yr

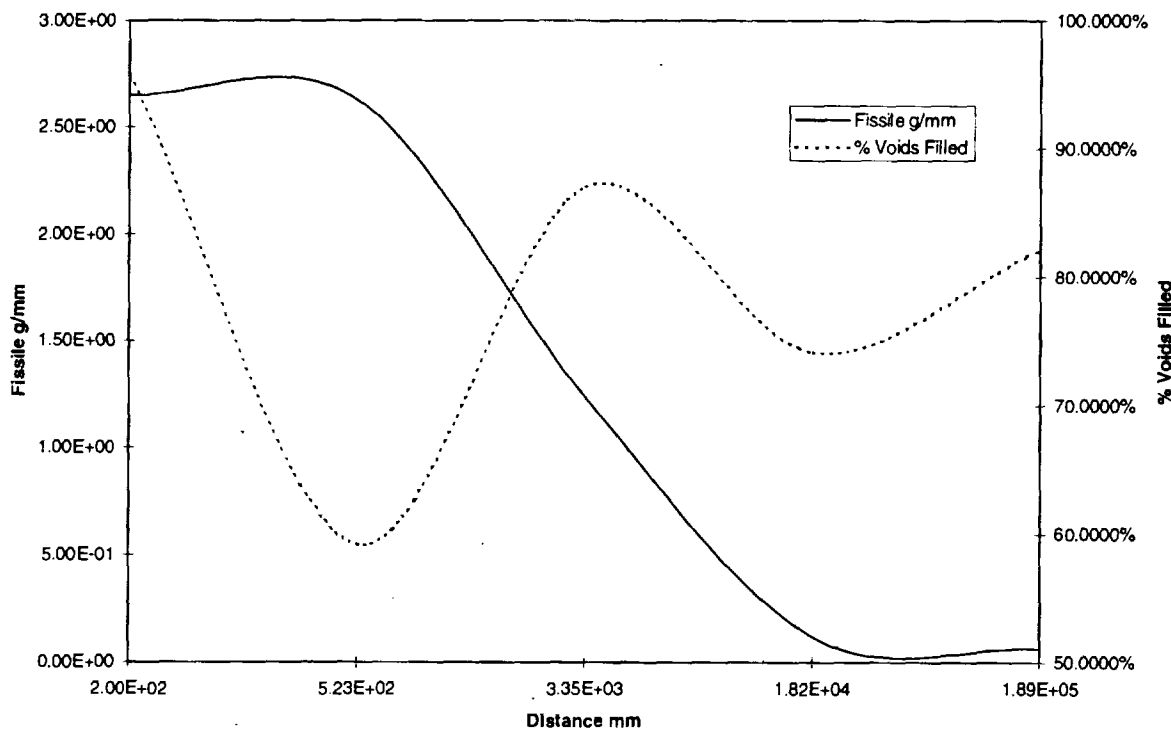


Figure 7.4.2-2. Amount of Fissile Material and Percentage of Voids Filled for Immobilized Plutonium pH 10 Reacting With Tuff at 10 mm/yr for 3000 years.

The chemistry modeling results discussed above do not account for further decay of ^{239}Pu to ^{235}U . The duration of 6000 years is about 1/4 the half-life, and some significant amount of plutonium will have become uranium. This will likely increase the fissile contents by some small amount since more uranium tends to deposit than plutonium. The effect of decay is not sufficient to change the likelihood of any criticality condition.

Studies were done to explore whether the presence of reaction products from the first path would have a significant effect on the behavior of the second pass fluid, etc. The original modeling scheme considered the need to model each pass if necessary (see Attachment III for detailed discussion of modeling scheme). Table 7.4.2-5 shows the deposition pattern for the two subsequent passes in cell 2. During the course of the three passes, $1.929\text{E}-02$ g of fissile material is deposited in 24.1 g of altered tuff, which amounts to 0.08 wt%. In other words, the rate of deposition is slightly less on the second and third passes. Thus, gradually the tuff invert would be converted to altered material, mostly quartz and feldspar, with a fissile content amounting to less than 0.1 wt%. Because cells deeper than cell 2 would already be partially altered before fissile bearing solution could reach them, the amount of reaction, hence amount of precipitated U and Pu, would be smaller, i.e. less than 0.1%. The chemical calculations do not permit modeling the geometry. In fact it is difficult to establish the ratio of reactive solution to invert and the manner of contact between them. This means that the cells may be layers that

develop on crushed tuff fragments, or altered pieces of tuff that lie above others, or, more likely, some combination of both. The results indicate some small increase in fissile material but it is not a significant increase in terms of criticality concerns. This result confirms the results of Lichtner (Refs. 5.27 and 5.28) that were discussed above in Section 7.2.1.

Table 7.4.2-5. Deposition in Cell 2 From Three Passes for Reaction of Immobilized Plutonium pH 10 Solution With Crushed Tuff

	Uranium grams	Plutonium grams	Total Solids grams	Fissile grams	Fissile wt% of U+ Pu
Pass 0	1.24E-01	1.24E-03	8.14E+00	5.13E-03	4.0877%
Pass 1	3.36E-01	3.29E-03	1.80E+01	1.38E-02	4.0686%
Pass 2	4.70E-01	4.58E-03	2.41E+01	1.93E-02	4.0660%

(Each "pass" is one kg of water flowing through the system).

Whereas subsequent to deposition of Pu or U it is conceivable that through flowing water could dissolve the minerals of the invert faster than the fissile solids, leaving behind a residual concentration, the modeling scheme and results described above provide no hint that this will in fact occur. Moreover, the simulation indicates that 90% or more of the invert would need to be dissolved even to reach a concentration of fissile material of 1%. This is highly unlikely in view of the low solubility of the clay minerals, quartz, and feldspar.

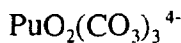
As was discussed above, a special case with a large area of reactants was also run. Table 7.4.2-6 presents the Large Area results with deposition history for 600-years and 1 mm/yr infiltration rate. The depositions occur much sooner (near the entrance to the invert). The change in area (and thus the effective reaction rate) seems only to change the position, not the composition, of the deposited material. This would be expected since the relative rates for the reactants has not changed, only the overall rate. Because the deposits occur over a short distance, they soon plug the flow path (in less than 6 years). This results in diversion of flow and consequent spreading out of the deposit over a larger area. Thus, the result would be even less likely to cause any criticality than the smaller area case.

Table 7.4.2-6. Large Area Case For Reaction of pH10 Immobilized Plutonium Package Effluent With Crushed Tuff Invert, 600 year duration of pH 10 and 1mm/yr infiltration rate (EQ6 Output File wp10t0la.6o)

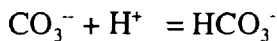
Cell No.	Travel Time Into Rock dayss	Distance Traveled mm	Accumulation During The Deposition Time				% Void Filled With Solids	% Void Filled With Fissile	Fissile wt% of U+Pu	
			Total Solids grams	Uranium grams	Plutonium grams	Fissile grams				
1	1.10E+01	1.01E-01	4.38E+02	6.72E+00	6.61E-02	2.76E-01	2.75E+00	99.9999%	0.0632%	4.07%
2	3.82E+01	3.49E-01	1.03E+03	1.57E+01	1.54E-01	6.45E-01	2.37E-02	71.4143%	0.0426%	4.07%
3	1.75E+02	1.60E+00	5.13E+03	4.26E+01	3.26E-01	3.39E-01	2.49E-03	73.9871%	0.0049%	45.13%
4	1.75E+03	1.60E+01	5.91E+04	0.00E+00	2.10E+00	2.10E+00	1.33E-03	85.3051%	0.0030%	100.00%
Total			6.57E+04	2.28E+01	2.64E+00	3.36E+00				13.18%

Mechanism of the Immobilized Plutonium pH 10 Solution Reaction with Tuff:

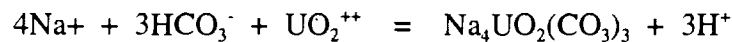
In the reaction between the alkaline effluent and tuff, the controlling factors for the system appear to be the sodium and carbonate solution content conditions. During the passage of fluid, the pH change is minor but decreasing. The carbonate species result from the presence of atmospheric levels of CO₂ in the repository air which is in contact with the solution. The dominant carbonate solution species (which is typical for the various runs), is CO₃²⁻. The dominant aqueous species for U and Pu are the carbonate complexes:



Seven reactions involving aqueous Pu and U consume H⁺ and one such reaction generates H⁺. In addition the carbonate system promotes a large buffering capacity. The consumption of H⁺ by the tuff dissolution processes coupled with the combining of H⁺ with aqueous species is compensated by the generation of H⁺ from processes forming Pu and U solids. The pH remains nearly constant owing to buffering by the reaction:

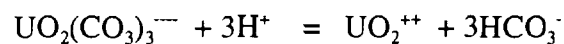
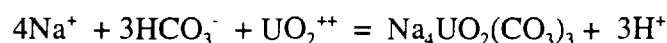


The U solid formation reaction, in terms of EQ6 basis species, is:



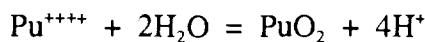
This shows the precipitation of UO₂²⁺ as Na₄UO₂(CO₃)₃ solid is dependent on the fourth power of the Na⁺ and the third power of the HCO₃⁻ solution content. Furthermore, the dissolution of Na₄UO₂(CO₃)₃ is dependent on the third power of the H⁺ solution content. Generation of H⁺ would drive this reaction in the Na₄UO₂(CO₃)₃ dissolution direction. Generation of H⁺ is not a significant driving force for Na₄UO₂(CO₃)₃ dissolution. Generation of HCO₃⁻ would drive the reaction to form Na₄UO₂(CO₃)₃ solid. The HCO₃⁻ solution content decreases as the reaction proceeds, which would be expected to promote dissolution of Na₄UO₂(CO₃)₃. Since Na₄UO₂(CO₃)₃ solid does form, HCO₃⁻ cannot be a dominant driving force for Na₄UO₂(CO₃)₃ formation under the constant CO₂(g) pressure conditions (assumed in the modeling to apply to the repository system). However, as discussed below, the generation of Na⁺ can be a significant driving force.

The dominant aqueous species in the high pH effluent-tuff system is UO₂(CO₃)₃⁴⁻. Therefore the following set of reactions applies to the formation of Na₄UO₂(CO₃)₃ solid:



Here, in terms of the net reaction, the formation of Na₄UO₂(CO₃)₃ solid is dependent on the fourth power of the solution Na⁺ content.

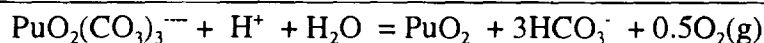
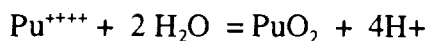
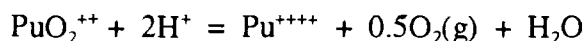
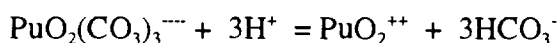
The Pu solid formation reaction, in terms of EQ6 basis species, is:



Here the PuO_2 dissolution is dependent on the fourth power of the H^+ solution content.

Generation of H^+ , if it underwent a significant concentration increase, would drive the reaction to dissolve PuO_2 solid. However, the dominant Pu species in solution is $\text{PuO}_2(\text{CO}_3)_3^{---}$ not Pu^{++++} .

Therefore, the following set of reactions apply to the formation of PuO_2 solid:



Whereas subsequent to deposition of Pu or U it is conceivable that through flowing water could dissolve the minerals of the invert faster than the fissile solids, leaving behind a residual concentration. The modeling scheme and results described above provide no hint that this will in fact occur. Moreover, the simulation indicates that 90% or more of the invert would need to be dissolved even to reach a concentration of fissile material of 1%. This is highly unlikely in view of the low solubility of the clay minerals, quartz, and feldspar.

7.4.2.2.2 Reaction of Immobilized Plutonium pH 7 Solution With Crushed Tuff Invert

The same analysis was done for the pH 7 solution as was done for the pH 10 solution. The results are documented in EQ6 output file "wp7t0.6o". The EQ6 calculations showed that no uranium or plutonium was deposited by the solution. The dissolved uranium and plutonium are instead carried out of the system by the flowing water. Some alteration of the tuff occurred but this did not foster any deposition of any fissile material. No further analysis was performed.

These results indicated that no pH 7 solution from any of the waste packages is likely to produce a deposit of any uranium or plutonium in the invert or rock when it reacts with tuff. Based on this, all other modeling of pH 7 solutions was suspended.

7.4.2.2.3 Reaction of Immobilized Plutonium pH 5 Solution With Crushed Tuff Invert

A pH 5 solution will flow from the degrading immobilized plutonium package for over 8000 years. Modeling of the reaction of this solution with crushed tuff was also carried out. The results are documented in EQ6 output file "wp5t0.6o". Table 7.4.2-7 shows how a deposit will build up for a 1 mm/yr infiltration rate. A large deposit of alteration products is produced which plugs the flow path about 22 cm into the invert after about 2440 years. At the time the flow path is plugged, a 1.5E+04 kg deposit has formed which contains a total of only 0.0016 g of fissile material. The fraction of voids filled with fissile material is then less than 0.0001%. At higher

infiltration rates the results are of course the same: plugged path at 2440 years. This reaction will not produce a significant accumulation of fissile material and will not result in any criticality.

Table 7.4.2-7. Deposition Resulting From Reaction of Immobilized Plutonium pH 5.5 Solution With Crushed Tuff Invert, 1 mm/yr infiltration rate, 2440 year deposition (EQ6 Output File wp5t0.6o).

Cell No.	Travel Time Into Rock days	Distance Traveled mm	Accumulation During The Deposition Time				% Void Filled With Solids	% Void Filled With Fissile	Fissile wt% of U+Pu	
			Total Solids grams	Uranium grams	Plutonium grams	Fissile grams				
1	3.84E-03	3.51E-05	1.92E-02	0.00E+00	0.00E+00	0.00E+00	0.00E+00	9.8572%	0.0000%	0.00%
2	3.84E+03	3.51E+01	1.24E+05	5.10E-04	0.00E+00	1.60E-05	4.55E-07	75.6864%	0.0000%	3.13%
3	1.53E+05	2.20E+03	4.70E+06	1.77E-02	2.54E-05	5.78E-04	2.67E-07	100.0000%	0.0000%	3.27%
4	5.01E+05	9.07E+03	1.03E+07	2.85E-02	6.34E-05	9.57E-04	1.39E-07	55.5012%	0.0000%	3.34%
Total			1.51E+07	4.67E-02	8.88E-05	1.55E-03				100.00%

7.4.2.3 Reaction of Immobilized Plutonium Package Solutions with Concrete or Grout

This section presents results of modeling analyses of the reaction of immobilized plutonium solutions with a concrete or grout invert.

The composition for the cement was put into the form of a “special reactant” for input to EQ6 and the code run to ascertain the likely makeup of the cement at long times in the presence of J-13 well water and atmospheric CO₂. For this purpose, rates of reaction were not needed; it was instead assumed that over the time frame of a few thousand years before waste package breach the cement would have reacted to equilibrium with the water and atmosphere (Assumption 4.3.5). This degraded cement, which contained mostly calcite with lesser amounts of clay minerals, zeolites, and quartz, was then combined with an appropriate proportion of crushed tuff as aggregate. Because the silicate minerals, or glass, of the tuff react much more slowly than cement, it was assumed that the tuff aggregate would not have changed before waste package breach (Assumption 4.3.6). It was also assumed that the organic components added to the cement would all have decayed or altered to inorganic compounds, such as CO₂ and water, before waste package breach (Assumption 4.3.7). Consequently, the organics were not included in the chemistry for modeling the degradation of the cement. The size distribution of the aggregate was taken from Ref. 5.17, pp. 2 and 3. These data were used to estimate the surface area of aggregate needed for modeling the rates of reaction. Attachment I shows the details of this calculation. The chemical and mineralogical compositions of the tuff were the same as described in Section 4.1.3. Table 7.4.2-8 provides details of the composition, masses, surface areas, and corrosion or degradation rates of the cement and aggregate, and physical parameters for the concrete.

Table 7.4.2-8 Calculation of composition of degraded grout, last step of run j13avmix1.60

Mineral	Moles	g-Atoms of Element													Totals	
		O	Al	Ca	F	Fe	H	C	P	K	Mg	Mn	Na	Si		
Fluorapatite	4.24E-07	5.08E-06		2.12E-06	4.24E-07				1.27E-06							
Pyrolusite	9.83E-11	1.97E-10										9.83E-11				
Quartz	2.59E-02	5.18E-02													2.59E-02	
Stilbite	4.08E-05	1.03E-03	8.90E-05	4.16E-05			5.99E-04			2.45E-07			5.55E-06	2.79E-04		
Calcite	9.55E-02	2.86E-01		9.55E-02				9.55E-02								
Magnesite	3.51E-03	1.05E-02						3.51E-03								
Montmor-Ca	3.42E-07	4.10E-06	5.71E-07	5.64E-08			6.84E-07				1.13E-07			1.37E-06		
Montmor-K	1.13E-08	1.36E-07	1.89E-08				2.27E-08			3.74E-09	3.74E-09			4.54E-08		
Montmor-Mg	2.31E-07	2.77E-06	3.86E-07				4.62E-07				1.14E-07			9.25E-07		
Montmor-Na	2.20E-08	2.64E-07	3.67E-08				4.39E-08				7.25E-09		7.25E-09	8.79E-08		
Nontronite-Ca	5.63E-03	6.76E-02	1.86E-03	9.29E-04		1.13E-02	1.13E-02							2.07E-02		
Nontronite-K	1.14E-04	1.37E-03	3.77E-05			2.29E-04	2.29E-04			3.77E-05				4.20E-04		
Nontronite-Mg	2.34E-03	2.81E-02	7.73E-04			4.69E-03	4.69E-03				3.87E-04			8.60E-03		
Nontronite-Na	2.27E-04	2.73E-03	7.49E-05			4.54E-04	4.54E-04						7.49E-05	8.34E-04		
Total g-atoms		4.50E-01	2.83E-03	9.64E-02	4.24E-07	1.66E-02	1.72E-02	9.90E-02	1.27E-06	3.80E-05	3.87E-04	9.83E-11	8.05E-05	5.67E-02	7.39E-01	
At fr.		6.08E-01	3.84E-03	1.31E-01	5.73E-07	2.25E-02	2.33E-02	1.34E-01	1.72E-06	5.14E-05	5.24E-04	1.33E-10	1.09E-04	7.67E-02	1.00E+00	
At. Wt.		1.60E+01	2.70E+01	4.01E+01	1.90E+01	5.58E+01	1.01E+00	1.20E+01	3.10E+01	3.91E+01	2.43E+01	5.49E+01	2.30E+01	2.81E+01		
Grans		7.19E+00	7.65E-02	3.87E+00	8.05E-06	9.29E-01	1.74E-02	1.19E+00	3.94E-05	1.48E-03	9.40E-03	5.40E-09	1.85E-03	1.59E+00	1.49E+01	
Wt. fr.		4.84E-01	5.14E-03	2.60E-01	5.41E-07	6.24E-02	1.17E-03	7.99E-02	2.65E-06	9.98E-05	6.32E-04	3.63E-10	1.24E-04	1.07E-01	1.00E+00	

Waste Package Development

Design Analysis

Title: Evaluation of the Potential for Deposition of U/Pu from a Repository Waste Package

Document Identifier: BBA000000-01717-0200-00050 REV 00

Page 89 of 114

Approximate calculation of surface of aggregate in concrete proposed for the invert.											
Fine aggregate per Ref. 5.98, ASTM specifications, C 33-93, 0759510 0531853 341											
Area to be modeled in two ways:											
1) From specifications for sieve analysis in Section 6.1, use the average of the nominal sizes between sieves as the diameter of spherical particles and take the average of the percentage between that size and the next larger.											
2) Use the average of the nominal sizes as the smaller dimension of rectangular parallelepipeds and twice that size as the length											
Sieve size, mm		Percent Passing				Surface area, mm ²		Volume, mm ³		Area/vol, cm ² /cm ³	
Larger	Smaller	Average	Larger	Smaller	% of total*	Sphere	Piped	Sphere	Piped	Sphere	Piped
9.5	4.75	2.375	100	95	5	0.89	2.82	2.81	2.68		
4.75	2.36	1.195	100	80	15	0.67	2.14	1.07	1.02		
2.36	1.18	0.59	85	80	80	0.87	2.78	0.69	0.66		
1.18	0.6	0.29	60	25	25	0.07	0.21	0.03	0.02		
0.6	0.3	0.15	30	10	15	0.01	0.03	0.00	0.00		
0.3	0.15	0.075	10	2	10	0.00	0.01	0.00	0.00		
					150	2.51	8.00	4.59	4.39	5.47	18.23
* Calculated as the percentage passing through the smaller sieve minus the amount that also goes through the next larger sieve, except for the except for the smallest size for which it is believed that all pass through the larger sieve.											
A reasonable value is thought to be the average of the two values for area/vol, i.e.											
11.85											
Coarse aggregate per ASTM specifications, C 33-93, 0759510 0531853 341+A5.											
Area to be modeled in two ways:											
1) From specifications for sieve analysis in Section 6.1, use the average of the nominal sizes between sieves as the diameter of spherical particles and take the average of the percentage between that size and the next larger. Use column for 3/8" in Table 2 in Ref. 5.98. This is because the proposed coarse aggregate will have a maximum size of 3/4", and this is the first column in the table for which the sieve analysis specifications are all less than this.											
2) Use the average of the nominal sizes as the smaller dimension of rectangular parallelepipeds and twice that size as the length											
Sieve size, mm		Percent Passing				Surface area, mm ²		Volume, mm ³		Area/vol, cm ² /cm ³	
Larger	Smaller	Average	Larger	Smaller	% of total*	Sphere	Piped	Sphere	Piped	Sphere	Piped
19	9.5	4.75	100	85	15	10.63	33.84	67.34	64.30		
9.5	2.36	3.57	85	0	85	34.03	108.33	162.00	154.70		
						44.67	142.18	229.34	219.00	1.95	6.49
A reasonable value is thought to be the average of the two values for area/vol+A62, i.e.											
4.22											

Waste Package Development

Design Analysis

Title: Evaluation of the Potential for Deposition of U/Pu from a Repository Waste Package

Document Identifier: BBA000000-01717-0200-00050 REV 00

Page 91 of 114

Calcite		37.37	0.96	10352.63							
Magnesite		1.37	0.04	380.08							
Nontronite-Ca		2.20	0.68	2796.68							
Nontronite-K		0.04	0.01	0.00							
Nontronite-Mg		0.92	0.28	0.26							
Nontronite-Na		0.09	0.03	0.00							

7.4.2.3.1 Reaction of Immobilized Plutonium pH 10 Solution With Concrete

The reaction of the immobilized plutonium pH 10 solution with a concrete invert was also investigated. The results are documented in the EQ6 output file "LaBSconcrete1simp7.6o" (see Section 9.2). This was a difficult case to obtain results in EQ6 largely because there is very little reactivity between the alkaline solution and the alkaline concrete. About 77 grams of solid are produced per kg of water reacted with no uranium in the deposit. The solid contains less than 0.001% plutonium. The pH 10 condition lasts for 600 years and the flow cross section is $5.52E+04 \text{ cm}^2$. Based on this, there would be 33 kg of water contacting the solid during the pH 10 period. This gives 2.55 kg of solid containing less than 0.03 g of Pu and no uranium. No further analysis was carried out because it was clear that this mechanism would produce no significant deposit of fissile material over any realistic time frame.

7.4.2.3.2 Reaction of Immobilized Plutonium pH 5 Solution With Concrete

The reaction of the immobilized plutonium pH 5 solution with a concrete invert was also investigated. The results are documented in the EQ6 output file "LaBSconcrete5t0.6o" (see Section 9.2). This was a difficult case to obtain results in EQ6 largely because there is very little reactivity between solution and the concrete. About 200 grams of solid are produced per kg of water reacted with no uranium in the deposit. The 200 g of solid contains only $6.8 E-09 \text{ g}$ of plutonium. At an infiltration rate of 1 mm/yr with a flow cross section (package footprint) of $5.52E+04 \text{ cm}^2$, and an 8000-yr duration of pH 5, the total amount of water reacting is 440 kg. Therefore about 88 kg of solid is deposited containing $2.9E-06 \text{ g}$ of plutonium and no uranium. No further analysis of the was carried out because it was clear that this mechanism would produce no significant deposit of fissile material over any realistic time frame.

7.4.2.3.3 Reaction of Immobilized Plutonium pH 7 Solution With Concrete

Based on the results obtained with tuff reactions modeling of this case was suspended. It is not expected that any effect will be obtained from reaction of a neutral solution such as this with concrete.

7.4.3 Concentration From Solution Flowing Out Of A Waste Package Containing Commercial Spent Nuclear Fuel (SNF)

The reactions with invert discussed in Section 7.1.2.1.1 for the case of the commercial nuclear spent fuel package were modeled. This section presents the results of those analyses.

7.4.3.1 Solution From The Commercial SNF Package

The solution composition was modeled by EQ6 as the contents of the waste package were dissolved. The solution at step 530 of the EQ6 output file j13avaucfa1.6o (see Section 9.2) was taken. The degradation of package contents by J-13 water was modeled with the assumption that the chromium oxidizes to chromate. For the simulations of the reactions a representative solution chemistry was chosen at pH 3.9 and an ionic strength of 0.295 molal. The solution contained 1416 ppm U and 0.002 ppm Pu. At 1000 years post-closure the uranium is

characteristic of depleted uranium with a ²³⁵U content of about 1.4335 wt% (see workbook WPOX4T0.XLS, worksheet "Enrichment"). Very little new ²³⁵U arises from decay of the small quantity of plutonium, since only a small fraction of half-life has elapsed.

7.4.3.2 Reaction of Commercial SNF Solutions With Crushed Tuff Invert

This section presents modeling results for the reaction of the commercial nuclear spent fuel package solutions with the tuff invert.

7.4.3.2.1 Reaction of pH 7 Commercial SNF Solutions With Tuff Invert

Results obtained with immobilized plutonium pH 7 solutions indicated that no significant uranium or plutonium would be deposited by any pH 7 solution reacting with concrete. Therefore, no detailed modeling of this case has been carried out.

7.4.3.2.2 Reaction of pH 4 Commercial SNF Solutions With Tuff Invert

The reaction of a pH 4 solution from the Commercial SNF package with a crushed tuff invert was modeled. The results are summarized in Table 7.4.3-1. A very small

Table 7.4.3-1. Deposition From The Reaction of pH 4 Solution From the Commercial SNF Package with a Crushed Tuff Invert For a 600-year Duration of pH 4 Conditions and 1mm/yr Infiltration Rate (EQ6 Output File wpoX4t0.6o)

Cell No.	Travel Time Into Rock days	Distance Traveled mm	Accumulation During The Deposition Time				% Void		Fissile wt% of U+ Pu	
			Total Solids grams	Uranium grams	Plutonium grams	Fissile grams	Filled With Solids	Filled With Fissile		
1	9.65E-07	8.81E-09	7.28E-05	5.19E-05	0	7.44E-07	8.44E+01	79.5783%	0.8127%	1.43%
2	2.42E-02	2.21E-04	1.76E+00	1.26E+00	0	1.80E-02	8.13E+01	76.7237%	0.7826%	1.43%
3	9.65E-01	8.81E-03	6.85E+01	4.87E+01	0	6.98E-01	8.13E+01	74.8217%	0.7632%	1.43%
4	1.14E+01	1.04E-01	1.06E+03	7.27E+02	0	1.04E+01	1.09E+02	99.9999%	0.9826%	1.43%
5	6.50E+02	5.94E+00	1.04E+04	3.40E+03	6.13E-05	4.87E+01	8.35E+00	30.4690%	0.1433%	1.43%
6	9.65E+02	8.81E+00	5.72E+03	4.74E+00	3.72E-03	7.17E-02	2.50E-02	8.4328%	0.0001%	1.51%
7	9.65E+05	1.82E+04	8.73E+06	9.48E-01	0	1.36E-02	7.47E-07	18.1937%	0.0000%	1.43%
Total			8.75E+06	4.18E+03	3.78E-03	5.99E+01				

plugging point can be seen at 0.1 mm. A total of only 60 g of fissile material is deposited in the 18 m flow path. Even if the pores of the invert did not plug, there would not be sufficient material to cause any possible instance of criticality. The calculated amount of fissile material is deposited in a fairly large quantity of deposited alteration products. Sufficient deposition of the alteration products is simulated to occur, even at the low infiltration rate of 1 mm/yr, to plug the upper portion of the invert at about a 0.1 mm depth (see data in Table 7.4.3-1 and in Attachment I). This process presumes that the water moves uniformly, but very slowly, and that in only 11 days a kilogram of solids can be deposited over a path length of 0.1 mm (and the area of the waste package footprint, 6.8 m² (see Table 7.4.3-1, cell 4). This is a very conservative result. This deposition is sufficient to fill the small void space in the invert beneath the waste package, based on the fracture density and aperture estimated for this case.

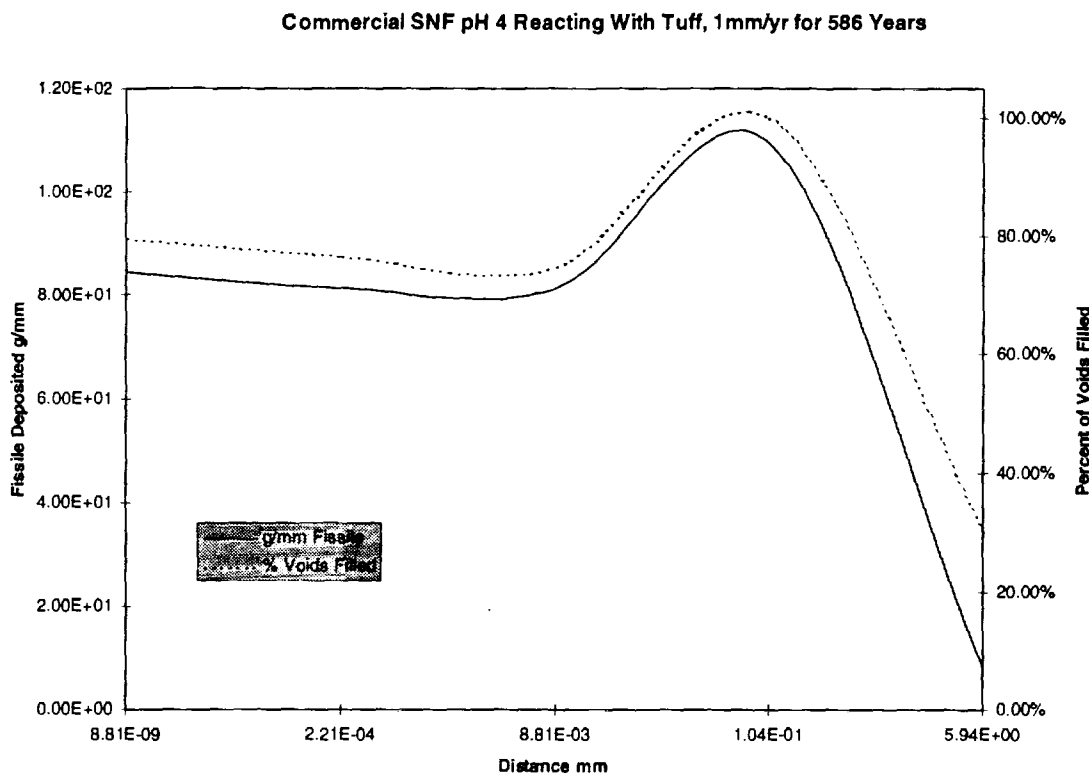


Figure 7.4.3-1. Amount of Fissile Material and Percentage of Voids Filled for Commercial SNF pH 4 Reacting With Tuff at 1 mm/yr for 600 years.

Thus, while this pH condition may persist for about 600 years, the plugging stops the process in slightly less than 600 years. Figure 7.4.3-1 displays the result graphically. The sudden increase of total solids in cell 7 is not plotted on Figure 7.4.3-1 but can be seen in Table 7.4.3-1. This increase occurs because the solution has entered the rock below the invert (the invert is 700 mm deep). The rock has a much lower porosity (0.139) as opposed to the invert (0.3). There is also a marked change in the mineralogy to include solid solutions which tend to be less dense than minerals precipitated earlier.

7.4.3.3 Reaction of Commercial SNF Solution With A Concrete Invert

The same cement composition was used as for the reaction of immobilized plutonium solutions (see Section 7.4.2.3).

7.4.3.3.1 Reaction of Commercial SNF pH 7 Solution With Concrete

Results obtained with immobilized plutonium pH 7 solutions indicated that no significant uranium or plutonium would be deposited by any pH 7 solution reacting with concrete. Therefore, no detailed modeling of this case has been carried out.

7.4.3.3.2 Reaction of Commercial SNF pH 4 or 5 Solution With Concrete

Results obtained with immobilized plutonium pH 5 solutions indicated that no significant uranium or plutonium would be deposited by any 4 to 5 pH range solution reacting with concrete. Therefore, no detailed modeling of this case or pH 5 has been carried out.

7.4.4 Concentration From Solution Flowing Out Of A Waste Package Containing Mixed Oxide (MOX) Fuel

The reactions with invert discussed in Section 7.1.2.1.1 for the case of the MOX spent fuel package were modeled. This section presents the results of those analyses.

7.4.4.1 MOX Package Solution

For the simulations of the reactions a representative solution chemistry was chosen. The results from Step 632 of EQ6 output file j13avmoxa1.6o was taken. The degradation of package contents by J-13 water was modeled with the assumption that the chromium oxidizes. For the simulations of the reactions with tuff a representative solution chemistry was chosen at pH 4.09 and an ionic strength of 0.173 molal. The solution contained 782.6 ppm U and 1.3E-03 ppm Pu. At 1000 years post-closure the uranium is characteristic of depleted uranium with a ²³⁵U content of about 0.1675 wt%. Very little new ²³⁵U arises from decay of the small quantity of plutonium since only a small fraction of half-life has elapsed.

7.4.4.2 Reaction of MOX Solutions With Crushed Tuff Invert

This section presents the results of modeling of the reaction of MOX package solutions with a crushed tuff invert. The same crushed tuff invert composition was used as for the immobilized plutonium form reactions (see Section 7.4.2.2).

7.4.4.2.1 Reaction of MOX pH 4 Solution With Crushed Tuff Invert

A pH 4 solution will flow from the dissolving MOX package contents for about 50 years. The reaction of this solution with the crushed tuff invert was modeled.

The results for a 1 mm/yr infiltration rate are summarized in Table 7.4.4-1. A very large quantity of solid is formed over a 286 mm path in the invert. This solid contains only about 0.38 g of fissile material over the entire path and fills less than 8% of voids at the highest point of accumulation. Figure 7.4.4-1 shows the pattern of fissile accumulation and the filling of the voids. Most of the material is located in the first mm of the invert but it does not represent a significant amount of fissile material.

Table 7.4.4-1. Deposition From The Reaction Of MOX Package pH 4 Solution With Tuff Invert, 1 mm/yr infiltration rate for 50 years (EQ6 Output File wpmox4t0.6o).

Cell No.	Travel Time Into Rock days	Distance Traveled mm	Accumulation During The Deposition Time				Fissile g/mm	% Void Filled With Solids	% Void Filled With Fissile	Fissile wt% of U+Pu
			Total Solids grams	Uranium grams	Plutonium grams	Fissile grams				
1	9.65E-07	8.81E-09	6.49E-06	4.62E-06	0.00E+00	7.75E-09	8.79E-01	7.0934%	0.0085%	0.168%
2	3.84E+02	3.51E+00	5.86E+02	2.27E+02	0.00E+00	3.81E-01	1.09E-01	2.6439%	0.0017%	0.168%
3	1.53E+03	1.40E+01	1.40E+03	2.15E+00	3.50E-04	3.96E-03	3.78E-04	1.4075%	0.0000%	0.184%
4	6.09E+03	5.56E+01	3.44E+03	1.62E-02	2.29E-05	5.01E-05	1.20E-06	1.0121%	0.0000%	0.309%
5	3.13E+04	2.86E+02	1.90E+04	0.00E+00	1.06E-06	1.06E-06	4.60E-09	1.1675%	0.0000%	100.000%
Total			2.45E+04	2.30E+02	3.74E-04	3.85E-01				

If the dissolution rates in the package were overestimated by a factor of 10, the pH 4 condition could persist for as much as 500 years. This case is shown in Table 7.4.4-2 and is plotted in Figure 7.4.4-2. About 4 kg of solid accumulates in the top 3.5 mm of the invert filling about 71% of the void space at the highest point. But the total fissile material in this region is less than 1 g. The total fissile material in the whole deposit (spread over a 286 mm depth) is only 3.9 g. If the infiltration were 10 mm/yr and the pH were 10 for 500 years, this total would be 39 g. As previously discussed, the flushing effects at 10 mm/yr would greatly reduce the time of pH 10 and the fissile material concentrations so that the 39 g figure would be considerably less. Therefore, even in the largest bounding cases, this reaction does not produce a significant quantity of fissile material.

Table 7.4.4-2. Deposition From The Reaction Of MOX Package pH 4 Solution With Tuff Invert, 1 mm/yr infiltration rate for 500 years (EQ6 Output File wpmox4t0.6o).

Cell No.	Travel Time Into Rock days	Distance Traveled mm	Accumulation During The Deposition Time				Fissile g/mm	% Void Filled With Solids	% Void Filled With Fissile	Fissile wt% of U+Pu
			Total Solids grams	Uranium grams	Plutonium grams	Fissile grams				
1	9.65E-07	8.81E-09	6.49E-05	4.62E-05	0.00E+00	7.75E-08	8.79E+00	70.9337%	0.0846%	0.168%
2	3.84E+02	3.51E+00	5.86E+03	2.27E+03	0.00E+00	3.81E+00	1.09E+00	26.4390%	0.0172%	0.168%
3	1.53E+03	1.40E+01	1.40E+04	2.15E+01	3.50E-03	3.96E-02	3.78E-03	14.0750%	0.0000%	0.184%
4	6.09E+03	5.56E+01	3.44E+04	1.62E-01	2.29E-04	5.01E-04	1.20E-05	10.1211%	0.0000%	0.309%
5	3.13E+04	2.86E+02	1.90E+05	0.00E+00	1.06E-05	1.06E-05	4.60E-08	11.6751%	0.0000%	100.000%
Total			2.45E+05	2.30E+03	3.74E-03	3.85E+00				

MOX pH 4 Solution reacting with tuff, 1mm/yr, for 50yr

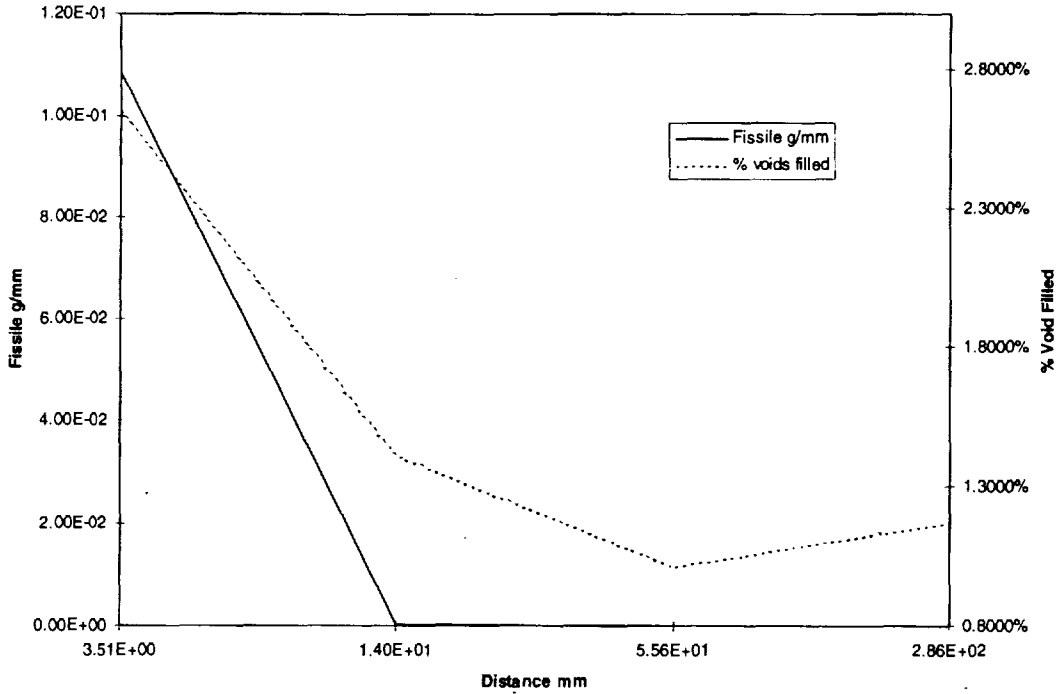


Figure 7.4.4-1. Amount of Fissile Material and Percentage of Voids Filled for MOX pH 4 Reacting With Tuff at 1 mm/yr for 50 years

MOX pH 4 Solution Reacting With Tuff, 1mm/yr for 500 Years

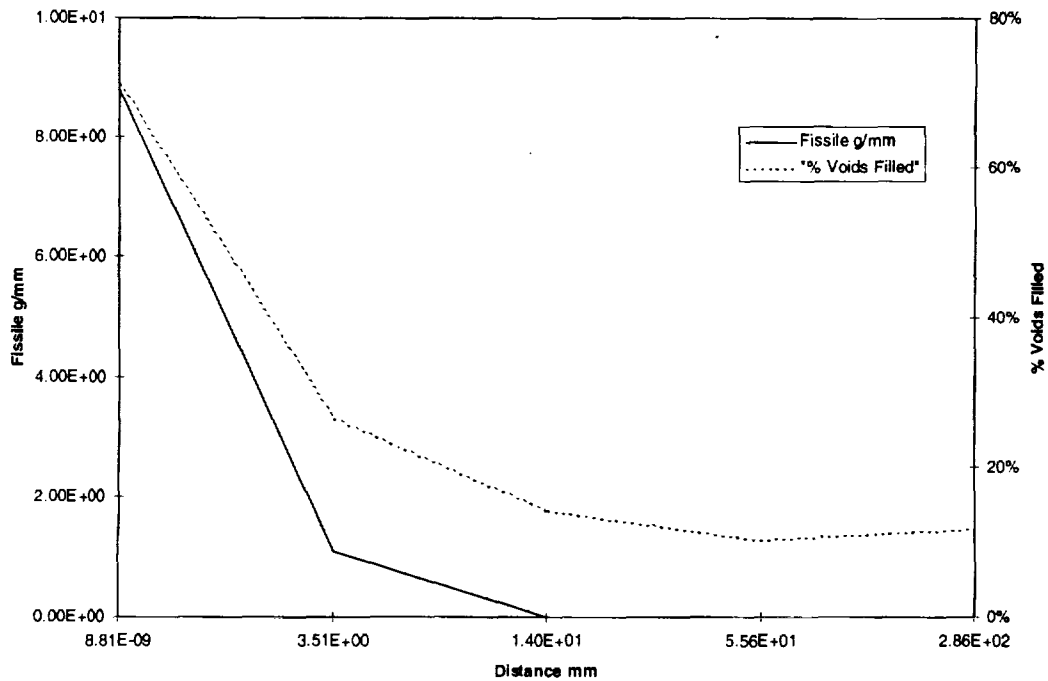


Figure 7.4.4-2. Amount of Fissile Material and Percentage of Voids Filled for MOX pH 4 Reacting With Tuff at 1 mm/yr for 500 years

7.4.4.2 Reaction of MOX pH 7 Solution With Tuff Invert

This case was not run. The results with neutral solutions for the immobilized plutonium package indicated that little or no fissile material would be formed from any neutral solutions.

7.4.4.3 Reactions Of MOX Package Solutions With Concrete

Reactions of MOX package solutions with concrete are discussed in the following section.

7.4.4.3.1 Reaction of MOX pH 4 Solution With Concrete

Based on results obtained for immobilized plutonium and the results for pH 4 with tuff this case was not run since no significant deposition of fissile material would be expected.

7.4.4.3.2 Reaction of MOX pH 7 Solution With Concrete

This case was not run. The results with neutral solutions for the Immobilized Plutonium package indicated that little or no fissile material would be formed from any neutral solutions.

7.4.5 Reactions of Waste Package Effluents with other External Features

This section discusses the interaction of waste package solutions with features other than the waste package invert.

7.4.5.1 Reactions of Waste Package Effluents With Rock

The reactions with various rocks were discussed in Section 7.1.2.1.2. This section presents the results of analyses of such reactions.

7.4.5.1.1 Topopah Springs welded tuff

Devitrified tuff This case, tuff host rock lying between the drifts, was in effect modeled during the investigation of reaction of effluent with crushed tuff. The only difference would be the ratio of water to tuff, which was already taken into account by means of different choices for the surface area of tuff in relation to one kilogram of water. The modeling focused on vitric tuff owing to the inefficiency of the modeling with devitrified mix of minerals. Thus, the results are conservative.

Vitric tuff This case was also effectively considered during early simulations of the reaction of effluent with the "special reactant" tuff. In those cases the tuff was already included as a glass, and a much higher rate of reaction was chosen, using a rate from Fler (Ref. 5.82) that was subsequently rejected as being unrealistic (it corresponded to feldspar dissolution in a solution of hydrofluoric and hydrochloric acids) (EQ6 output file WPT10LA0.60 in Section 9.2). For these simulations also the percentage of precipitated fissile material was very low (8.3E-04 moles Pu and 1.6E-03 moles U). The main effect of a higher rate constant is simply to shorten the time of reaction but not greatly alter the chemistry of the result.

7.4.5.1.2 Calico Hills Formation

The most likely concentration mechanism that could be effective for this formation is sorption, which is discussed in Section 7.4.6.6. Otherwise the consequences of reaction would parallel those for unaltered tuff already discussed. An EQ6 simulation with pH 10 Immobilized Plutonium package effluent was run with clinoptilolite (which is the principal ingredient of Calico Hills formation tuff). The results are documented in EQ6 output file "clino10t.6o" in Section 9.2. The same amounts of Pu solids are formed as with the tuff invert calculations (see Section 7.4.2.2). The principal difference is the formation of Soddyite as a product in about 10 times the amount of uranium seen in the tuff invert calculations. However, even this large increase in uranium results in an insignificant amount of total fissile material.

7.4.5.1.3 Paleozoic Carbonates

In this case the Eh is likely to be low, leading to precipitation of any Pu or U that makes it this far. The results would be comparable to the reaction of solutions with concrete (i.e. calcite) which indicated not significant deposit of fissile material.

7.4.5.1.4 Veins and Minerals in Fractures

This case was not specifically analyzed. However, reaction with the wall rocks of a vein or fracture will closely resemble the situation for reaction with crushed tuff invert. Reactions with zeolites and clay minerals in the fractures will parallel those with the Calico Hills formation, discussed above. Reaction with calcite in veins will parallel that with calcite in degraded concrete.

7.4.5.1.5 Host Rock Altered During Thermal Pulse

In this case the likely alteration products are clay minerals, zeolites, silica (e.g., quartz), and possibly calcite probably in zones with different proportions of minerals, such as a clay zone, a zeolitic zone, and a silicified zone. Reactions with all these minerals have been discussed above.

7.4.5.2 Reactions with Organic Matter in Drift or in Rock

This possible mechanism was presented in Section 7.1.2.1.3. This is not likely to be a consideration at Yucca Mountain. See the discussion of natural analogs in Section 7.3.5.

7.4.5.3 Reaction of pH 10 Immobilized Plutonium Solution With Carbon Steel

The reaction with metal objects were discussed in Section 7.1.2.1.4. This section presents the results of analyses of such a reaction.

This scenario includes the existence of altered steel fragments in a pool of water below the waste package. If the pool is sufficiently deep a no or low free oxygen condition may be maintained. The cases investigated covered a range of oxygen contents of the water ranging from an anoxic condition to atmospheric oxygen content. It was hypothesized that fragments of iron existed in

the pool. These fragments would act as a reducing agent to the solution entering especially if there was a limited oxygen supply. The deposit is envisioned as a slab covering the bottom of the pond in the footprint of the package. The model visualizes a slab forming on the layer of steel fragments forming a slab at the bottom of the pond. The thickness of such a slab is calculated.

7.4.5.3.1 Reaction of pH 10 Immobilized Plutonium Solution With Carbon Steel With No Gaseous Oxygen Present

This case was investigated because of the potential of precipitation of fissile material due to direct reduction of uranium and plutonium species by the iron in an anoxic environment.

The oxygen fugacity is never lowered enough to reduce the uranium to where it would precipitate. However, at a 10 mm/yr infiltration rate, a significant amount of plutonium is reduced and precipitated reaching equilibrium in about 3 years as the fluid contacts the iron. Table 7.4.5-1 shows the accumulated deposit for various infiltration rates. At 10 mm/yr, the pH condition will last about 300 years. For this case, deposit was calculated to contain nearly 1.5 kg of fissile material (all as PuO₂). However, note that the concentrations would probably be reduced by a factor of 5 due to flushing effects during dissolution at this very high infiltration rates. Thus the deposit is likely to contain about 500 g of Pu. The slab scenario views the deposit as a very thin (0.05 mm) slab. However, if the steel fragments were more local the deposit could be much thicker with a smaller areal extent (approaching a cube or sphere). In any case this extreme bounding case should not pose a criticality concern.

Table 7.4.5-1. Deposition From Reaction of pH 10 Solution From the Immobilized Plutonium Package With Carbon Steel Fragments With No Gaseous Oxygen Present (Anoxic Condition)

Deposition Time yr*	Infiltration Rate mm/yr	Accumulation For The Deposition Period				Fissile wt% of U+Pu	Slab Deposit** Thickness cm
		Total Solids grams	Uranium grams	Plutonium grams	Fissile grams		
600	1.00E-01	4.73E+01	0	2.94E+01	2.94E+01	100.00%	1.10E-04
600	1.00E+00	4.73E+02	0	2.94E+02	2.94E+02	100.00%	1.10E-03
400	5.00E+00	1.58E+03	0	9.81E+02	9.81E+02	100.00%	3.65E-03
300	1.00E+01	2.36E+03	0	1.47E+03	1.47E+03	100.00%	5.48E-03

* Equals the duration of pH 10 condition which is less at higher infiltrations due to flushing effects.

** The deposit is viewed as a slab of this thickness spread out over an area = to the package footprint.

The deposit could be accumulated in a smaller area (where there is iron).

As with other cases, the possibility that the pH 10 condition could endure longer was investigated. Table 7.4.5-2 shows results if the duration of pH 10 conditions should last 10 times longer. In this case, large quantities of Pu are formed even at 1 mm/yr infiltration rates. A deposit of 14.7 kg of PuO₂ (about 10% of the total Pu in the package) in a slab 0.5 mm thick is shown for a 10 mm/yr infiltration rate. This could be a significant material for a criticality. Even considering flushing effects this would still represent nearly 5 kg of Pu and would be a definite criticality concern. However, anoxic conditions are probably not realistic for a duration of 3000 years due to diffusion of oxygen into the system. Such long times are probably more consistent with a partial atmosphere of oxygen (see the 10% atmosphere case in Section 7.4.5.3.2).

Table 7.4.5-2. Deposition From Reaction of pH 10 Solution From the Immobilized Plutonium Package With Carbon Steel Fragments With No Gaseous Oxygen Present (Anoxic Condition) - long duration of pH 10

Deposition Time yr*	Infiltration Rate mm/yr	Accumulation For The Deposition Period				Fissile wt% of U+Pu	Slab Deposit** Thickness cm
		Total Solids grams	Uranium grams	Plutonium grams	Fissile grams		
6000	1.00E-01	4.73E+02	0	2.94E+02	2.94E+02	100.00%	1.10E-03
6000	1.00E+00	4.73E+03	0	2.94E+03	2.94E+03	100.00%	1.10E-02
4000	5.00E+00	1.58E+04	0	9.81E+03	9.81E+03	100.00%	3.65E-02
3000	1.00E+01	2.36E+04	0	1.47E+04	1.47E+04	100.00%	5.48E-02

* Equals the duration of pH 10 condition which is less at higher infiltrations due to flushing effects.

** The deposit is viewed as a slab of this thickness spread out over an area = to the package footprint.

The deposit could be accumulated in a smaller area (where there is iron).

7.4.5.3.2 Reaction of pH 10 Immobilized Plutonium Solution With Carbon Steel With 10% Normal Level of Gaseous Oxygen

The interaction of the solution with steel fragments was also investigated for the case where there are small amounts of oxygen present (10% of atmospheric). The results are shown in Table 7.4.5-3. In this case plutonium is not reduced as with the anoxic case. The iron oxidizes and the pH steadily reduces. Note that the time to equilibrium is nearly 2000 years. In such a case the water may flush out of the pond before significant reaction. In the model, the water does react with the steel, which is probably a very conservative scenario. The principal uranium product in the simulation is $\text{Na}_4\text{UO}_2(\text{CO}_3)_3$ which is a small percentage of a very large accumulation of minerals (the uranium metal represents about 0.2% of the total weight of solid). At an infiltration rate of 10 mm/yr there is a kg of fissile material in a slab which is 63 cm thick. There are several problems with the result in view of the scenario:

1. The slab is so thick that the iron would long have been masked from the solution and reaction rates would likely have become near zero early in the process.
2. The slab is so thick as to have displaced all the water from the pond and the steel under the slab would have reacted with all the oxygen dissolved in the interstitial water in the slab, or, if the pore water has dried up, been exposed to enough atmosphere that all the steel has corroded. In either case the 10% oxygen assumption is not valid.
3. The 2000 year reaction time is almost 10 times longer than the calculated duration of the pH condition.
4. The amount of iron required to produce the deposit is $9.3\text{E}+06$ g. The total mass of the corrosion allowance vessel is $8.2\text{E}+06$ g. Therefore it would take more than all the iron available to produce the deposit. In view of the difficulties, the result is viewed as not realistic.

Table 7.4.5-3. Deposition From Reaction of pH 10 Solution From the Immobilized Plutonium Package With Carbon Steel Fragments With 10% Of Normal Atmospheric Gaseous Oxygen Level, Expected Duration of pH Condition

Deposition Time yr*	Infiltration Rate mm/yr	Accumulation For The Deposition Period				Fissile wt% of U+Pu	Slab Deposit** Thickness cm
		Total Solids grams	Uranium grams	Plutonium grams	Fissile grams		
600	1.00E-01	2.96E+05	6.33E+02	2.82E-01	2.01E+01	3.17%	1.26E+00
600	1.00E+00	2.96E+06	6.33E+03	2.82E+00	2.01E+02	3.17%	1.26E+01
400	5.00E+00	9.86E+06	2.11E+04	9.41E+00	6.70E+02	3.17%	4.19E+01
300	1.00E+01	1.48E+07	3.16E+04	1.41E+01	1.00E+03	3.17%	6.28E+01

* Equals the duration of pH 10 condition which is less at higher infiltrations due to flushing effects.

** The deposit is viewed as a slab of this thickness spread out over an area = to the package footprint.
The deposit could be accumulated in a smaller area (where there is iron).

Table 7.4.5-4 shows the result if the duration of pH 10 is increased by a factor of 10. At infiltration rates of 5 mm/yr and above the modeling results would indicate that the entire uranium inventory of the package (1.32E+02 moles) is seen as deposited on the steel as Na₄UO₂(CO₃)₃ (7.15e+04 g). In view of the conflict between the result and requisite conditions (see discussion above), the result is not considered realistic.

Table 7.4.5-4. Deposition From Reaction of pH 10 Solution From the Immobilized Plutonium Package With Carbon Steel Fragments With 10% Of Normal Atmospheric Gaseous Oxygen Level, Duration of pH Condition Increased by a Factor of 10

Deposition Time yr	Infiltration Rate mm/yr	Accumulation For The Deposition Period				Fissile wt% of U+Pu	Slab Deposit*** Thickness cm
		Total Solids grams	Uranium grams	Plutonium grams	Fissile grams		
6000*	1.00E-01	2.96E+06	6.33E+03	2.82E+00	2.01E+02	3.17%	1.26E+01
6000*	1.00E+00	2.96E+07	6.33E+04	2.82E+01	2.01E+03	3.17%	1.26E+02
1356**	5.00E+00	3.34E+07	7.15E+04	3.19E+01	2.27E+03	3.17%	1.42E+02
678**	1.00E+01	3.34E+07	7.15E+04	3.19E+01	2.27E+03	3.17%	1.42E+02

* Equals the duration of pH 10 condition which is less at higher infiltrations due to flushing effects.

**Uranium supply in the package is used up before pH condition is over.

*** The deposit is viewed as a slab of this thickness spread out over an area = to the package footprint.
The deposit could be accumulated in a smaller area (where there is iron).

7.4.5.3.3 Reaction of pH 10 Immobilized Plutonium Solution With Carbon Steel With Atmospheric Levels of Gaseous Oxygen

The reaction of the solution with steel under atmospheric conditions was also investigated. Table 7.4.5-5 shows the results. The time to equilibrium was only about 3 years. No uranium was precipitated and small quantities of plutonium were precipitated. At the highest infiltration rate there was only 243 g of fissile material (all PuO₂) in a slab 89 cm thick. This large thickness poses difficulties of conflict with the scenario. If the slab were this thick, the solution would be completely isolated from the steel. This would be the case for a very long time and reaction rates

would have fallen to near zero early in the process. Such a large slab would divert all the water away from the region early in the process. The case of a pH 10 duration of times longer produces a 1 kg quantity of fissile material (all PuO₂), but it is contained in a 4.5 m thick slab containing 1.3E+05 kg of deposit. This result is even more implausible than the shorter duration case.

Table 7.4.5-5. Deposition From Reaction of pH 10 Solution From the Immobilized Plutonium Package With Carbon Steel Fragments With Normal Atmospheric Gaseous Oxygen Level

Deposition Time yr*	Infiltration Rate mm/yr	Accumulation For The Deposition Period				Fissile wt% of U+Pu	Slab Deposit** Thickness cm
		Total Solids grams	Uranium grams	Plutonium grams	Fissile grams		
600	1.00E-01	2.58E+05	0	2.43E+00	2.43E+00	100.00%	8.91E-01
600	1.00E+00	2.58E+06	0	2.43E+01	2.43E+01	100.00%	8.91E+00
600	5.00E+00	1.29E+07	0	1.22E+02	1.22E+02	100.00%	4.46E+01
600	1.00E+01	2.58E+07	0	2.43E+02	2.43E+02	100.00%	8.91E+01

* Equals the duration of pH 10 condition which is less at higher infiltrations due to flushing effects.

** The deposit is viewed as a slab of this thickness spread out over an area = to the package footprint.

The deposit could be accumulated in a smaller area (where there is iron).

7.4.6 Other Phenomena

7.4.6.1 Evaporation

The possibility of an effect due to evaporation was discussed in Section 7.1.2.2. This section presents the results of analyses of such reactions.

As water evaporates the pH is likely to stay the same or increase. This means that carbonate complexation will, if anything, rise, keeping U and Pu in solution. Hence, it is expected that there will be no precipitation unless evaporation is nearly total, which in turn is unlikely. A single evaporation simulation was run, starting from the effluent from an immobilized plutonium waste package at a pH of 10.003, as for the runs described in Section 7.4.2. This solution was already very concentrated, but was chosen because it had the highest concentrations of Pu and U of any considered. Consequences of choosing this solution are, among others, that little evaporation could be reasonably simulated before the ionic strength increased to the point that not even qualitative results are reliable and that the run did not go to completion because of numerical difficulties. Nevertheless, the results are in general accord with those noted above as to be expected. At about 2% evaporated the pH had increased to 10.006 and about 7% of the dissolved uranium had precipitated as Na₄UO₂(CO₃)₃. No plutonium had precipitated. Ionic strength increased from 2.51 to 2.54. At the point when about 12% had evaporated the pH had increased to 10.02, and the ionic strength to 2.72. About 13% of the U had precipitated, but no Pu. The results show that, in spite of the evaporation, the amount of solvent water had increased substantially. Inasmuch as the solids initially present had been removed from this evaporation run, this cannot result from dehydration of hydrous solid phases. Instead it most likely means that the aqueous solution chemistry is not being modeled correctly because of the high ionic

strength. Hence, any further results from this simulation are unreliable. (See EQ6 output file evapglsl10.6o, See Section 9.2.)

The results do appear to indicate that dilution of the highly concentrated pH 10 solution can result in a modest precipitation of U. Because of the limited time frame of this high pH stage and the low percentage of ^{235}U in the solution during this time frame, this is not viewed as sufficient to produce a critical accumulation. Because the effect is small and the concentrations at other pHs are much less, dilution is also not thought to be capable of producing a critical accumulation under those conditions.

7.4.6.2 Reaction with Rock or Drift Gas

The reactions with rock or drift gases were discussed in Section 7.1.2.3. This section presents the results of analyses of such reactions.

The loss of CO_2 is important only for the highly alkaline conditions. Because, for immobilized plutonium or ceramic, very little fissile is released during the high pH period, the maximum amount of deposit is too limited to produce a criticality. It is suggested that this be used as the resolution, rather than running EQ6 for loss of CO_2 , which could, nevertheless, be done. For Al based fuel the importance is less obvious for some of the scenarios that have been discussed. This has not yet been evaluated. A significant effect is not anticipated but this should be analyzed in the future.

O_2 concentrations are expected to remain essentially at atmospheric throughout the unsaturated zone. This means that neither U nor Pu would precipitate as a consequence of reduction of Eh in the rock as a consequence of O_2 loss. Because of the high O_2 concentration, other gases, such as methane and hydrogen sulfide seem unlikely to occur. The existing data on rock gas (Ref. 5.94) indicate no such gases. Thus, there would be no effect in the unsaturated zone. During the short calculated period of high pH, the amount of alkaline water will be small. Consequently, it seems unlikely that interactions in the saturated zone need to be taken into account.

7.4.6.3 Mixing with Pore And/or Fracture Water

Another mechanism for changing the waste package effluent chemistry is mixing with pore water. This was discussed in the potential mechanisms in Section 7.1.2.4.

An EQ6 simulation was carried out in which one kg of immobilized plutonium pH 10 solution was mixed with one kg of J-13 water. The products were very similar to those produced in the simulation of the reaction of immobilized plutonium pH10 solution with tuff invert. This is not surprising since J-13 water is likely to be close to equilibrium with tuff. The quantities of product were much less than in the case of the reaction with tuff. (See EQ6 output file wp10dil.6o Section 9.2.) At the end of the simulation no U had precipitated and 0.07 g of PuO_2 from the 2 kg mixture (67% of the initially dissolved Pu). The pH decreased to 9.937 from 10.003 which reduced the solubility of silica resulting in precipitation dominantly (according to the simulation, which did not suppress quartz in favor of other silica phases) of 0.11 g of quartz

together with lesser amounts of carbonates. The total mass of precipitate was about 0.23 g. Thus, the percentage of Pu in the total precipitate would be about 27 wt%.

7.4.6.4 Cooling or Heating

Another mechanism for changing the waste package effluent chemistry is cooling and heating. This was discussed in the potential mechanisms in Section 7.1.2.5.

Temperature effects haven't been evaluated in this report. However, the high solubility of Pu and U at high pH results from the high carbonate. This in turn comes about from the dissolution of atmospheric CO₂. As temperature increases, CO₂ solubility in water decreases rapidly. Thus, one would expect that carbonate complexation of Pu and U would decrease causing a decrease in solubilities. Thus, on moving away from a repository that is somewhat warmer than the underlying rock the solubility should increase as the solution cools. This would tend to mitigate the potential precipitation mechanisms noted above. However, most data needed for good computations of solubility of Pu as a function of temperature are lacking and only a limited set exists for U.

7.4.6.5 Pressure Drop

Another mechanism for changing the waste package effluent chemistry is pressure drop. This was discussed in the potential mechanisms in Section 7.1.2.6.

This is generally the inverse of the temperature effect. This was not evaluated for this report. It is likely to be dominated by changes in dissolved CO₂. The effect of pressure in the absence of a gas phase (i.e. with dissolved gases remaining constant) is not easy to evaluate in the present case. Some solids, e.g., calcite, have higher solubility at higher pressure -- and, correspondingly, lower solubility at higher temperature, in the absence of a gas phase; loss of CO₂ adds to this effect. Because carbonate complexes are involved, relationships for U and Pu may be the inverse of what normally happens. Data to resolve this, are not likely to be available, but the effect is almost certainly too small to worry about under the pressure changes that could occur in the unsaturated zone.

7.4.6.6 Evaluation of Concentration by Sorption

Adsorption was proposed as a possible accumulation mechanism in Section 7.1.1. This section describes results of analyses of this mechanism using the techniques discussed in Section 7.2.2. The parameters used in this section (7.4.6.6), with the exception of data cited from Ref. 5.89 (which were not used for calculations), may be treated as qualified data, as may the calculations based upon them.

A good example of the complexity of modeling sorption appears in Ref. 5.83, which deals with the adsorption of uranyl ion onto smectite, but in the absence of carbonates. This paper utilized equations for 34 chemical equilibria in order to model the observed sorption reasonably well. Unfortunately, because of the lack of consideration of carbonate complexes, this paper has little value for the present application except to confirm in a qualitative way the general order of

magnitude for the sorption relevant for conditions likely to be present within or near a repository at Yucca Mountain. In particular it is clear that the adsorption of UO_2^{++} is significantly reduced by the presence of moderate to high concentrations of Na^+ and by complexation in solution. Carbonate species in solution were rigorously excluded from the experiments described in this paper in order to avoid this effect. Thus, low values of adsorption for UO_2^{++} are appropriate for the present application.

Data from Los Alamos National Laboratory (Ref. 5.84), the NEA sorption data base (Ref. 5.85), a Swedish data set (Ref. 5.86), a Canadian set (Ref. 5.87), and TSPA 95 (Ref. 5.88) were used for obtaining data. For conservatism maximum values were chosen. Table 7.4.6-1 documents the calculations.

Data chosen are for goethite ($FeOOH$), which represents the degradation products of steel; zeolite, both a value for clinoptilolite from Ref. 5.84 and one for a zeolite of the heulandite-clinoptilolite family from Ref. 5.89, and smectite, which represent degradation products of glass waste forms as well as degradation products of tuff and aggregate in concrete; tuff from Yucca Mountain; and marl, which resembles the degradation products of the cement in concrete. Adsorption onto other materials, e.g., quartz and feldspar, is significantly less than on these solids (Ref. 5.84), or otherwise similar to that for tuff, and has not been included in the analyses. The geometric relationships among these solids as they may lie in the repository, i.e. a mix of two or more of them, or segregation of one into a separate pocket, has not been considered. In effect the analyses conducted assume that each occupies the entire region of the invert below a waste package. Because none of these individually gives rise to a condition in which a criticality could arise, none could arise from any mixture of them.

The analysis covers a full range of anticipated pH and materials. In no case was a critical condition approached. Below the repository only tuff, sometimes altered to zeolite and/or smectite, together with minor amounts of other materials is present. In view of the analysis here it is apparent that a criticality could not arise there as a consequence of adsorption unless some mechanism could occur that would greatly increase the concentration in the solution. In this connection it should be borne in mind that at least an approximate equilibrium between the concentration in solution and that in or on the solids will prevail. Thus, a solution with a low concentration of fissile material moving through the rock for a long time cannot increase the amount adsorbed. Conversely, if a solution with a low concentration of UO_2^{++} percolates through a region which had previously been enriched in uranium by adsorption from a solution with a higher uranium concentration, the adsorbed uranium will be at least partially desorbed and flushed out. These relations differ in principle from possibilities that might arise through precipitation of uranium or plutonium.

The only circumstance recognized to date in which the K_d approach is clearly inappropriate for the present application is during the relatively brief time span that highly alkaline solution is expected to exit the "can-in-can" glass waste package, i.e. immobilized plutonium cans embedded in HLW glass canisters. This case can be evaluated independently, as is done below. The amount of adsorbed fissile material in all other cases is too low to lead to a criticality.

Table 7.4.6-1 Calculations of Uranium and Plutonium Sorption

This table provides basic relations (estimates) for input to specific configurations. The data are very uncertain. This sheet uses European and Canadian data. The estimations will be based on a simple Kd approach. Concentration units for solutions are mg/kg; densities chosen to be unity, which will be low and conservative. For solids are g element/kg adsorbing substrate. Kd is in ml/g, i.e. solid conc.*1000/soln. conc. The Kd approach used here has limitations. Specifically, at sufficiently high concentrations in solution all adsorption sites on the solid may be occupied. This means that the concentration in the solid is in fact limited, but that this simple model is incapable of showing that.

Solid	Kd, Pu	Kd, U	Plutonium		Uranium		Comm.SNF pkg effluent Soln. conc	Comm.SNF pkg effluent Solid conc
			Pu gls. effluent, pH 8.01 Soln. conc	Solid conc	Pu gls. effluent, pH 8.01 Soln. conc	Solid conc		
FeOOH	70000	4000	5.34E-08	3.74E-06	4.78E-03	1.91E-02		
Clinoptilolite	800	30	5.34E-08	4.27E-08	4.78E-03	1.43E-04		
Zeolite		700			4.78E-03	3.35E-03		
Smectite	3000	50	5.34E-08	1.60E-07	4.78E-03	2.39E-04		
Vitric Tuff	80	4	5.34E-08	4.27E-09	4.78E-03	1.91E-05		
Marl	5000	1000	5.34E-08	2.67E-07	4.78E-03	4.78E-03		
			Pu gls. effl., pH 7.01		Pu gls. effl., pH 7.01			
FeOOH	70000	4000	1.56E-07	1.09E-05	1.93E-03	7.72E-03		
Clinoptilolite	800	30	1.56E-07	1.25E-07	1.93E-03	5.79E-05		
Zeolite		700			1.93E-03	1.35E-03		
Smectite	3000	50	1.56E-07	4.68E-07	1.93E-03	9.65E-05		
Tuff	80	4	1.56E-07	1.25E-08	1.93E-03	7.72E-06		
Marl	5000	1000	1.56E-07	7.80E-07	1.93E-03	1.93E-03		
			Pu gls. effl., pH 6		Pu gls. effl., pH 6			
FeOOH	70000	4000	1.48E-06	1.04E-04	2.31E-03	9.24E-03		
Clinoptilolite	800	30	1.48E-06	1.18E-06	2.31E-03	6.93E-05		
Zeolite		700			2.31E-03	1.62E-03		
Smectite	3000	50	1.48E-06	4.44E-06	2.31E-03	1.16E-04		
Tuff	80	4	1.48E-06	1.18E-07	2.31E-03	9.24E-06		
Marl	5000	1000	1.48E-06	7.40E-06	2.31E-03	2.31E-03		
			Pu gls. effl., pH 5.5		Pu gls. effl., pH 5.5		Comm.SNF pkg pH 6	
FeOOH	70000	4000	6.15E-06	4.31E-04	1.87E-06	1.31E-04	4.71E-03	1.88E-02
Clinoptilolite	800	30	6.15E-06	4.92E-06	1.87E-06	1.50E-06	4.71E-03	1.41E-04
Zeolite		700					4.71E-03	3.30E-03
Smectite	3000	50	6.15E-06	1.85E-05	1.87E-06	5.61E-06	4.71E-03	2.36E-04
Tuff	80	4	6.15E-06	4.92E-07	1.87E-06	1.50E-07	4.71E-03	1.88E-05
Marl	5000	1000	6.15E-06	3.08E-05	1.87E-06	9.35E-06	4.71E-03	4.71E-03
							2.19	8.76E+00
							2.19	6.57E-02
							2.19	1.53E+00
							2.19	1.10E-01
							2.19	8.76E-03
							2.19	2.19E+00

Data for FeOOH, clinoptilolite, and vitric tuff taken from Ref. 5.84.

Data for zeolite taken from Ref. 5.89.

Data for smectite taken from Ref. 5.86.

Data for marl taken from Ref. 5.85.

Under highly alkaline conditions both Pu and U will be dissolved primarily as tricarbonate complexes, $\text{PuO}_2(\text{CO}_3)_3^-$, and $\text{UO}_2(\text{CO}_3)_3^-$. The large negative charge on these ions is of special importance because the silicate crystalline structure of clays and zeolites carries a net negative charge. This arises from the substitution of Al^{+++} for Si^{++++} in the silicate lattice; within the crystal structure this is compensated by the presence of other metal ions, such as Na^+ and Ca^{++} . On the surface, however, this negative charge isn't balanced by firmly held ions, but by adsorbed positive ions. Negative ions will be repelled. This will effectively prevent the adsorption of the tricarbonate complexes of plutonyl or uranyl ions onto zeolites or clays. These tricarbonate ions are also very large and cannot penetrate into the crystal structures, i.e. into the channels in zeolite or between layers in smectite. Even if they could, they would be repelled because of the net negative charge which limits the ionic exchange to positive ions (cations), not negative ones (anions).

The nature of adsorption onto goethite and calcite differs markedly from that on the clays. For these minerals the crystal lattice itself does not incorporate a charge imbalance that intrinsically creates a net surface charge. Instead the nature of the surface chemistry changes with pH. This is conveniently viewed in terms of major structural cations, e.g., Fe^{+++} , just below the surface firmly bonded to a surface oxide ion. This can be represented as $\equiv\text{FeO}^-$, where the triple equal sign represents bonding to the rest of the structure. The $\equiv\text{FeO}^-$ then signifies an active surface chemical group, which interacts with the solution. At low pH hydrogen ions from the solution will become bound to it, producing the group $\equiv\text{FeOH}_2^+$. In other words at low pH ferric oxides and hydroxides, such as goethite, will have a net positive charge, and will readily adsorb anions. At an intermediate pH the surface group changes to $\equiv\text{FeOH}$, and at high pH to $\equiv\text{FeO}^-$, which adsorbs cations. The transition between the first and last of these groups is known as the zero point of charge. For hematite this occurs in the pH range 4.2 to 6.9; for goethite in the range 5.9 to 6.7, and for amorphous $\text{Fe}(\text{OH})_3$ in the range 8.5 to 8.8 (Ref. 5.90, p. 351). Thus in any case the ferric oxyhydroxides will tend to repel the plutonyl and uranyl tricarbonate complexes, which are of importance only at still higher values of pH. It is not yet clear whether calcite will similarly not adsorb Pu and U at high pH; Ref. 5.90, p. 351 lists two values for the zero point of charge, 8.5 and 10.8. If the latter applies to the situation for Yucca Mountain, potentially large concentrations of these elements could be adsorbed in a concrete invert. Literature searches conducted to date have not found any experimental measurements of adsorption of Pu or U on calcite under highly alkaline oxidizing conditions. (Clay minerals can also exhibit the phenomena of zero point of charge, e.g., for montmorillonite it occurs over a range of ≤ 2 to 3, Ref. 5.90, p. 351.) It should be kept in mind that the high pH condition applies only to waste packages containing alkali rich borosilicate glasses.

In contrast to the implications of the preceding paragraph, large quantities of fissile material will not be available because of the limited duration of the high pH phase of waste package degradation. This brevity would arise either because of acid production within the waste package through the potential oxidation of Cr to chromate, or simply because of flushing of the contents of the waste package by infiltrating water. Depending upon these factors the pH might remain high for periods ranging from 300 to several hundred years (Ref. 5.9) at an infiltration rate of 1 mm/yr. Higher infiltration rates will, of course, shorten the length of the high pH period. The maximum mass of fissile material that could be released during 1000 years will be about 1500 grams per waste package. If this is all adsorbed uniformly in the invert immediately below the

package, the maximum concentration could reach only 0.05 wt%. For higher infiltration rates the time during which the pH will remain high will be proportionately reduced. Table 7.4.6-2 shows the results of calculations for several infiltration rates and times. Other distributions of the fissile material in the invert would produce variations in the concentration, e.g., 0.5% fissile material distributed uniformly in the top 10 % of the invert. These are very conservative values because a very high dissolution rate was chosen for the HLW glass.

Table 7.4.6-2 Calculation of Maximum Amount of Fissile Material Exiting an Immobilized Plutonium Waste Package at pH 10

Dimensions and Transport Characteristics					
Flow Width	171 cm	"shadow" of waste package			
Flow Length	323 cm	"shadow" of waste package			
Flow Cross Section	55200 sq cm	same as slab deposit area			
Water density	1 g/cm ³	estimated same as pure water			
Porosity of Invert	0.3				
Depth of Invert	700 mm				
Solid vol. of invert	1160000 ⁰				
Density of invert	2.65 g/cm ²				
Mass of invert	3070000				
Pu conc. in effluent	78.3 ppm				
U conc. in effluent	6110 ppm				
Infiltration rate, mm/yr	Vol./yr ⁰	Transport g/yr,	Time, yr	Fissile mass, g	Conc. in invert, %
1	5520	1.49	300	446.37	0.01
1	5520	1.49	1000	1487.90	0.05
5	27600	7.44	200	1487.90	0.05
10	55201	14.88	100	1487.90	0.05

The results presented above differ markedly from some of those presented in Ref. 5.89. The experimental results were interpreted to mean that up to about 1 wt% uranium may be adsorbed and/or ion-exchanged by zeolites of the heulandite-clinoptilolite group. The experimental work is described only briefly. The Kd derived from the adsorption experiments is surprisingly high, about 700 ml/g. Some idea of how high the Kd might be can be obtained by utilizing data from a table in Ref. 5.90, p 351. In this table the cation exchange capacity of smectite-montmorillonite is given as ranging from 80 to 150 meq/100g, and that of zeolites from 100 to 400 meq/100g.

Evidently this table includes the combined effects of adsorption and cation exchange within the crystal structure. From these data one may conclude that the capacity of zeolites may be up to about 2½ times that for smectite-montmorillonite. This implies that, believing that the data in Table 7.4.6-1 are reasonable, one may expect the maximum Kd for zeolites to be about 125ml/g. It is evident from statements made by the authors of Ref. 5.89 that they understand the need to perform reversed experiments; however, they made determinations of the Kd only from adding a uranyl containing solution to the zeolite, but not from taking a zeolite previously charged with uranium from a reasonably concentrated solution and reequilibrating the zeolite with a solution with a lower uranium concentration. This casts some doubt on the reliability of the results. Nevertheless, the value of 700 ml/g is also included in Table 7.4.6-1. The concentrations of U in the aqueous solutions in these experiments are of interest. Calculations performed with the code, EQ6, indicate solubilities in the pH range from 5.5 to 6 or 0.005 to 0.002 ppm (Ref. 5.9), are far less than those used in the experiments. This article makes no mention of the possibility of precipitation of an insoluble U solid during the course of the experiments. On the other hand the experiments reported in Ref. 5.84 used similar concentrations and times of reaction, but obtained much smaller values for the distribution coefficient. In summary the results reported in Ref. 5.89 are questionable. So far as can be determined, Ref. 5.89 does not properly take into account the principles recommended by the Nuclear Regulatory Commission (NRC) (Ref. 5.91).

The paper (Ref. 5.89) also includes a plot comparing the "adsorption ratio" as a function of pH, evidently the percentage of the uranium adsorbed, and "the ratio of residual uranium in H-C zeolite" against pH. (H-C refers to heulandite-clinoptilolite.) This latter ratio refers to results after leaching tests, for which no details are provided. Points from the second determination fall very close to the curved line drawn through the first set. Nevertheless, percent adsorbed does not permit a calculation of the Kd unless the solution concentration is also given, which is not done. Thus, this graph does not correlate directly with the one from which the Kd was estimated and the significance of the comparison is lost. This plot is compatible with the interpretation that uranyl ion is displaced from the zeolite at low pH by hydrogen ion, and that it is prevented from adsorbing, or is removed from the solid, by complexation with carbonate at high pH. However, over the range of pH from about 4 to about 8, where 100% of the U is "adsorbed", it is not possible to tell from the data presented whether it is truly adsorbed or is precipitated. In any case the high percentage of about 0.9% found in the zeolite would be relevant to the issues in this report only for the brief initial period of high pH, and even then only a small percentage of the uranium would consist of ²³⁵U. In other words it is not a concern.

7.4.7 Summary of Calculated Accumulations

Table 7.4.7-1 summarizes the potential accumulations beneath the waste package footprint calculated in the computer simulations described in preceding sections.

Table 7.4.7-1 Accumulations of Fissile Material Calculated by EQ3/6 Simulations Tuff or Concrete Inverts from Waste Packages Containing Immobilized Plutonium, Commercial SNF, and MOX

Waste form	pH	Invert medium	Accumulation duration (yrs)	Max accumulation of fissile (g)*	Section
1. Immobilized Pu	10	Tuff	300	1780 (350)†	7.4.2.2.1
2. Immobilized Pu	10	Tuff	600	356 (36)†	7.4.2.2.1
3. Immobilized Pu	10	Tuff	3000	17800 (3500)†	7.4.2.2.1
4. Immobilized Pu	10	Tuff	6000	1440 (145)†	7.4.2.2.1
5. Immobilized Pu	7	Tuff	600	Nil	7.4.2.2.2
6. Immobilized Pu	5	Tuff	8000	0.0016	7.4.2.2.3
7. Immobilized Pu	10	Concrete	600	0.03	7.4.2.3.1
8. Immobilized Pu	7	Concrete	N/A	Smaller than case 5	7.4.2.3.3
9. Immobilized Pu	5	Concrete	8000	2.9x10 ⁻⁶	7.4.2.3.2
10. Cmmrcl SNF	7	Tuff	N/A	Smaller than case 5	7.4.3.2.1
11. Cmmrcl SNF	4	Tuff	600	60	7.4.3.2.2
12. Cmmrcl SNF	7	Concrete	N/A	Smaller than case 5	7.4.3.3.1
13. Cmmrcl SNF	5	Concrete	N/A	Smaller than case 9	7.4.3.3.2
14. MOX	7	Tuff	N/A	Smaller than case 5	7.4.4.2.2
15. MOX	4	Tuff	500	3.85	7.4.4.2.1
16. MOX	7	Concrete	N/A	Smaller than case 5	7.4.4.3.2
17. MOX	5	Concrete	N/A	Smaller than case 9	7.4.4.3.1

* Maximum accumulation in the invert, over an area equal to the waste package footprint: 5.5 m² for the immobilized Pu emplacement and 6.8 m² for the commercial SNF waste package.

† The values in parentheses are distributed over less than 3 meters path length, the other values are distributed over tens of meters, which greatly reduces the potential for criticality.

Notes:

- All cases are for infiltration rate = 1 mm/yr, except cases 1 and 3 which are for 10 mm/yr.
- The expression N/A has been used to indicate that a time period is not relevant for those cases which were not run because they are completely dominated by cases already shown to have negligible fissile accumulation.

The above table summarizes all but the sensitivity cases: Tables 7.4.2-1 to 7.4.3-7, and the cases with steel resting in a pond of water: Tables 7.4.5-1 to 7.4.5-5.

8. Conclusions

In compliance with the M&O Quality Administrative Procedures, the design results presented in this document cannot be used for procurement, fabrication, or construction unless properly identified, tracked as TBV, and controlled by the appropriate procedures.

8.1 Potential for Critical Near-Field Accumulations

Extensive simulations of the range of physically possible dissolution/transport/deposition scenarios, using the geochemical code package EQ3/6, have shown very little potential for the accumulation of potentially critical amounts of fissile material in the repository near-field (drift invert) for the following reasons:

- Significant deposition from true solution requires a high pH (both to carry a significant concentration of fissile material in the fluid, and to support a sufficiently strong deposition caused by reaction with invert or rock or by dilution with ambient water outside the waste package). The physicochemical conditions required to support this high pH will only last for a few hundred years (or a few thousand years at most). (Sections 7.4.2, 7.4.3, and 7.4.4)
- Colloids containing fissile material may be released from the waste form and waste package. Most likely this degradation and transport will be accompanied by a much larger amount of non-fissile colloidal material, which will greatly dilute the fissile material in any aggregate that may accumulate within the waste package, where most of it is likely to collect, or outside where it will be further diluted by being dispersed within degraded invert or host rock.
- Void space is largely filled with competing precipitates which have higher concentrations in solution and stronger reactions with the rock. (Sections 7.4.2, 7.4.3, and 7.4.4)

8.2 Potential for Far-Field Accumulations

The evaluation of natural uranium deposits with respect to Yucca Mountain geology has shown that there is very little likelihood for neutronically significant accumulations of uranium in the repository far-field for two fundamental reasons: (1) There has to be a reducing agent (one strong enough to resist the invasion of oxidizing solutions) or a source of vanadium within the host rock; (2) Precipitation conditions must be persistent over the geologic time scale required to accumulate significant amounts, otherwise there will only be short term accumulation followed by remobilization. The specific conditions which would be required for (1) are listed in Table 7.4.7-1. The reasons why either of these conditions are unlikely at Yucca Mountain are summarized in Section 7.3.7.

9. Attachments

This section contains general supporting information for the design analysis presented in the sections above. The section includes hardcopy of several spreadsheets and other supporting files and descriptive information. These attachments are supplied to allow detailed review of the analysis and provide detailed understanding of the analysis approach

9.1 Hardcopy Attachments

Supporting spreadsheets and other information provided as hardcopy are listed in Table 9-1. The files presented in this section are also available as electronic copies on tape (see Section).

Table 9-1. List of Attachments

Attachment No.	Title	Date	No. of Pages
I	Composition and Characteristics of Concrete	9/16/97	37
II	Algorithm for Successive Runs Simulating Flow and Transport	9/12/97	10
III	Description of the Modeling Approach between Effluent from the Waste Package and Invert of Rock, Using EQ6	9/12/97	2

9.2 Electronic Attachments

The following supporting documents are in electronic form on a Colorado Trakker® tape (Ref. 5.103) and are listed below.

```

..\eq36
BLDINPUT BAT          538 09-09-97 2:33p bldinput.bat
BLDINPUT C            2,241 09-09-97 2:33p bldinput.c
BLDINPUT IN           100 09-09-97 2:33p bldinput.in
CLINO10T 60          5,883,348 09-09-97 2:33p clinol0t.6o
J13AVA~1 60          2,762,533 09-09-97 2:33p j13avaucfa1.6o
J13AVA~1 6P          1,494,273 09-09-97 2:33p j13avaucfa1.6p
J13AVM~1 60          2,988,089 09-09-97 2:33p j13avmoxa1.6o
J13AVM~1 6P          1,595,680 09-09-97 2:33p j13avmoxa1.6p
J13AVW~1 60          5,357,036 09-09-97 2:33p j13avwp50.6b
J13AVW~2 60           130,717 09-09-97 2:33p j13avwpsoly40.6o
J13AVW~3 60           200,263 09-09-97 2:33p j13avwpsoly45.6o
J13AVW~1 6P          127,516 09-09-97 2:33p j13avwpsoly45.6p
LABSCO~1 60          7,941,124 09-09-97 2:33p LaBSconcretelsimp7.6o
LABSCO~2 60          8,512,162 09-09-97 2:34p LaBSconcrete5t0.6o
NXTINPUT BAT          328 09-09-97 2:34p nxtinput.bat
NXTINPUT C            9,939 09-09-97 2:34p nxtinput.c
WP10CS~1 60          3,222,649 09-09-97 2:34p wp10CSatm.6o
WP10CSLG 60          3,359,937 09-09-97 2:34p wp10CSLG.6o
    
```

Waste Package Development

Design Analysis

Title: Evaluation of the Potential for Deposition of U/Pu from a Repository Waste Package

Document Identifier: BBA00000-01717-0200-00050 REV 00

Page 114 of 114

WP10CSNG	60	4,638,047	09-09-97	2:34p	wp10CSNG.6o
WP10T0A	60	3,250,223	09-09-97	2:34p	wp10t0a.6o
WP10T0LA	60	3,250,879	09-09-97	2:34p	wp10t0LA.6o
WP5T0	60	2,715,943	09-09-97	2:34p	wp5t0.6o
WP7T0	60	2,614,801	09-09-97	2:34p	wp7t0.6o
WPMOX4T0	60	5,791,113	09-09-97	2:34p	wpmox4t0.6o
WPMOX4T0	TAB	408,850	09-09-97	2:34p	wpmox4t0.tab
WPOX4T0	60	4,710,691	09-09-97	2:34p	wpox4t0.6o
WPOX4T0	TAB	343,720	09-09-97	2:34p	wpox4t0.tab
WPT10LA	60	2,838,422	09-09-97	2:34p	WPT10LA.6o
WP10T1E	60	2,530,755	09-09-97	2:37p	wp10t1e.6o
WP10T2R	60	1,924,380	09-09-97	2:38p	wp10t2r.6o
EVAPGL~1	60	2,612,082	09-09-97	2:38p	evapglsl0.6o
WP10DIL	60	1,132,538	09-09-97	2:39p	wp10dil.6o
ALLING~1		826,876	09-09-97	2:40p	allinglsI10mm
ALLING~2		829,500	09-09-97	2:40p	allinglsII10mm
ALLING~3		832,206	09-09-97	2:40p	allinglsIII10mm
ALLING~4		919,174	09-09-97	2:40p	allinglsIV10mm
ALLING~5		3,120,055	09-09-97	2:40p	allinglsV10mm
ALLOUT~1		5,893,599	09-09-97	2:40p	alloutglsl10mm
ALLOUT~2		4,399,515	09-09-97	2:40p	alloutglslII10mm
ALLOUT~3		5,103,336	09-09-97	2:40p	alloutglslIII10mm
ALLOUT~4		5,578,022	09-09-97	2:40p	alloutglslIV10mm
ALLOUT~5		15,275,287	09-09-97	2:40p	alloutglslV10mm
.. \excel					
WPOX4T0	XLS	136,192	09-01-97	12:47p	WPOX4T0.XLS
SORPTAB	XLS	25,600	09-08-97	6:16p	SORPTAB.XLS
CONCRETE	XLS	43,008	09-08-97	6:06p	CONCRETE.XLS
STEELTAB	XLS	27,136	09-09-97	5:21p	STEELTAB.XLS
WPMOX4T0	XLS	183,808	09-05-97	3:43p	WPMOX4T0.XLS
OXIDETAB	XLS	19,968	09-05-97	3:20p	OXIDETAB.XLS
GLASSTAB	XLS	27,136	09-05-97	3:10p	GLASSTAB.XLS
CEL2PASS	XLS	25,600	09-05-97	2:28p	CEL2PASS.XLS
WP5T0	XLS	75,776	09-10-97	9:42a	WP5T0.XLS
WP10T0LA	XLS	86,528	09-05-97	1:36p	WP10T0LA.XLS
WP10T0A	XLS	137,728	09-05-97	1:33p	WP10T0A.XLS
TUFF	XLS	28,672	09-09-97	12:24p	TUFF.XLS
WP10CSAT	XLS	35,840	08-22-97	5:48p	WP10CSAT.XLS
WP10CSNG	XLS	33,280	08-22-97	5:29p	WP10CSNG.XLS
WP10CSLG	XLS	55,296	08-22-97	5:29p	WP10CSLG.XLS
WATERTAB	XLS	22,528	08-18-97	4:25a	WATERTAB.XLS

I.1 Composition and characteristics of concrete

This attachment uses data from Refs. 5.16, 5.17, and 5.18 to estimate the composition, surface area of aggregate used, and other properties of concrete intended for use in the invert.

Workbook CONCRETE.XLS, Sheet "Cement"

Calculation of composition of degraded grout, last step of run j13avmix1.6o															
Gram-atoms of element															
Mineral	Moles	O	Al	Ca	F	Fe	H	C	P	K	Mg	Mn	Na	Si	Totals
Fluorapatite	4.24e-07	5.08e-06		2.12e-06	4.24e-07				1.27e-06						
Pyrolusite	9.83e-11	1.97e-10										9.83e-11			
Quartz	2.59e-02	5.18e-02												2.59e-02	
Stilbite	4.08e-05	1.03e-03	8.90e-05	4.16e-05			5.99e-04			2.45e-07			5.55e-06	2.79e-04	
Calcite	9.55e-02	2.86e-01		9.55e-02				9.55e-02							
Magnesite	3.51e-03	1.05e-02						3.51e-03							
Montmor-Ca	3.42e-07	4.10e-06	5.71e-07	5.64e-08			6.84e-07				1.13e-07			1.37e-06	
Montmor-K	1.13e-08	1.36e-07	1.89e-08				2.27e-08			3.74e-09	3.74e-09			4.54e-08	
Montmor-Mg	2.31e-07	2.77e-06	3.86e-07				4.62e-07				1.14e-07			9.25e-07	
Montmor-Na	2.20e-08	2.64e-07	3.67e-08				4.39e-08				7.25e-09		7.25e-09	8.79e-08	
Nontronite-Ca	5.63e-03	6.76e-02	1.86e-03	9.29e-04		1.13e-02	1.13e-02							2.07e-02	
Nontronite-K	1.14e-04	1.37e-03	3.77e-05			2.29e-04	2.29e-04			3.77e-05				4.20e-04	
Nontronite-Mg	2.34e-03	2.81e-02	7.73e-04			4.69e-03	4.69e-03				3.87e-04			8.60e-03	
Nontronite-Na	2.27e-04	2.73e-03	7.50e-05			4.54e-04	4.54e-04						7.50e-05	8.34e-04	
Total g-atoms		4.50e-01	2.83e-03	9.64e-02	4.24e-07	1.66e-02	1.72e-02	9.90e-02	1.27e-06	3.80e-05	3.87e-04	9.83e-11	8.05e-05	5.67e-02	7.39e-01
At. fr.		6.08e-01	3.84e-03	1.31e-01	5.73e-07	2.25e-02	2.33e-02	1.34e-01	1.72e-06	5.14e-05	5.24e-04	1.33e-10	1.09e-04	7.67e-02	1.00e+00
At. Wt.		1.60e+01	2.70e+01	4.01e+01	1.90e+01	5.58e+01	1.01e+00	1.20e+01	3.10e+01	3.91e+01	2.43e+01	5.49e+01	2.30e+01	2.81e+01	
Grams		7.19e+00	7.65e-02	3.87e+00	8.05e-06	9.29e-01	1.74e-02	1.19e+00	3.94e-05	1.48e-03	9.40e-03	5.40e-09	1.85e-03	1.59e+00	1.49e+01
Wt. fr.		4.84e-01	5.14e-03	2.60e-01	5.41e-07	6.24e-02	1.17e-03	7.99e-02	2.65e-06	9.98e-05	6.32e-04	3.63e-10	1.24e-04	1.07e-01	1.00e+00

Workbook CONCRETE.XLS, Sheet "Mix"

Concrete mix	Weight,kg	Component	Wt.	Wt. % of components
Type 5 cement	392.00	Cement mix	490.00	21.53
Water	160.00	Aggregate	1786.00	78.47
Coarse aggregate	1003.00		2276.00	
Fine aggregate	783.00			
Silica fume	59.00			
Polyheed	0.63			
Superplasticizer	1.56			
Steel	39.00			
	2438.19			

Workbook CONCRETE.XLS, Sheet "Concrete"

Concrete mix, total						
From Cement sheet of this file:						
78 wt% aggregate						
22 wt% cement mix						
Material	Weight, g	Moles	Moles in concrete	Vol%	Rel. vol**	Mol/kg wat
Cmt mix	2.20e+01	1.05e+00	1.05e+00			
Aggreg	7.80e+01	3.79e+00	3.79e+00			9.04e+02
Aggregate						
Mineral	Moles*	Mol/100g	Moles in concrete	Vol%	Rel. vol**	Mol/kg wat
Quartz	5.88e-01	5.81e-01	4.53e-01	3.48e+01	2.72e+01	1.08e+02
K-spar	1.00e-01	9.92e-02	7.74e-02	2.81e+01	2.19e+01	1.85e+01
Albite	1.16e-01	1.15e-01	8.94e-02	3.04e+01	2.37e+01	2.13e+01
Anorthite	9.63e-03	9.52e-03	7.43e-03	2.55e+00	1.99e+00	1.77e+00
Biotite	4.31e-03	4.26e-03	3.32e-03	2.51e+00	1.95e+00	7.92e-01
Magnetite	1.52e-03	1.51e-03	1.17e-03	1.28e-01	1.00e-01	2.80e-01
Ilmenite	1.23e-03	1.22e-03	9.49e-04	1.63e-01	1.27e-01	2.26e-01
Apatite	7.04e-05	6.96e-05	5.43e-05	3.43e-02	2.67e-02	1.30e-02
Kaolinite	5.03e-03	4.98e-03	3.88e-03	1.30e+00	1.02e+00	9.26e-01
				1.00e+02		
*Moles of mineral per 101.19 g of rock -- cf. file c:\pau\invert\tuffmin.xls						
** Approx. equal to wt% = rel. rate in concrete						
Degraded cement mix						
Mineral		Moles/100g	Moles in concrete	Wt%	Rel. vol**	Mol/kg wat
Fluorapatite		3.16e-06	6.95e-07	1.59e-03	3.51e-04	1.66e-04
Pyrolusite		7.33e-10	1.61e-10	6.38e-08	1.40e-08	3.85e-08
Quartz		1.93e-01	4.25e-02	1.16e-08	2.55e-09	1.01e+01
Stilbite		3.05e-04	6.70e-05	2.18e-01	4.79e-02	1.60e-02
Carbonate-Calcite		7.38e-01	1.62e-01	7.35e+01	1.62e+01	3.87e+01
Calcite		7.12e-01	1.57e-01			3.74e+01
Magnesite		2.62e-02	5.75e-03			1.37e+00
Rhodochrosite		1.26e-11	2.76e-12			6.59e-10
Siderite		3.25e-20	7.16e-21			1.71e-18
Smectite-di		6.20e-02	1.36e-02	2.63e+01	5.78e+00	3.26e+00
Beidellite-Ca		7.56e-11	1.66e-11			3.97e-09
Beidellite-K		1.53e-12	3.38e-13			8.05e-11
Beidellite-Mg		3.14e-11	6.92e-12			1.65e-09
Beidellite-Na		3.05e-12	6.71e-13			1.60e-10

Montmor-Ca			2.55e-06	5.61e-07			1.34e-04
Montmor-K			8.46e-08	1.86e-08			4.44e-06
Montmor-Mg			1.72e-06	3.79e-07			9.05e-05
Montmor-Na			1.64e-07	3.61e-08			8.60e-06
Nontronite-Ca			4.20e-02	9.24e-03			2.20e+00
Nontronite-K			8.53e-04	1.88e-04			4.48e-02
Nontronite-Mg			1.75e-02	3.85e-03			9.17e-01
Nontronite-Na			1.69e-03	3.73e-04			8.89e-02
Normalization to mass of water:							
Assume 10% void space. Need to get confirmation later.							
				Vol	Wt	Normalize to 1000 g H2O	
100 g concrete will occupy about $100/2.65 \text{ cm}^3 =$				3.77e+01	1.00e+02	2.39e+04	
10% void =				4.19e+00	4.19e+00	1.00e+03	
total				4.19e+01			
Calculation of relative rates using equations 40-43 in the EQ6 users manual:							
Mineral	rk1	sk	dzi/dt	Rel. Rt.	dzi/dt	Rel. Rt.	
Calcite	6.50e-03	1.08e+04	7.04e+01	1.00e+00			
Quartz	1.67e-20	2.03e+04	3.39e-16	4.81e-18	1.63e-33	3.64e-19	
Sanidine	2.50e-15	1.49e+04	3.74e-11	5.31e-13	1.98e-23	4.44e-09	
Plagiocl	3.20e-11	1.75e+04	5.61e-07	7.97e-09	4.47e-15	1.00e+00	
			7.04e+01		4.47e-15		

Workbook CONCRETE.XLS. Sheet "Surface"

Approximate calculation of surface of aggregate in concrete proposed for the invert.											
Fine aggregate per ASTM specifications, C 33-93, 0759510 0531853 341											
Area to be modeled in two ways:											
1) From specifications for sieve analysis in Section 6.1, use the average of the nominal sizes between sieves as the diameter											
of spherical particles and take the average of the percentage between that size and the next larger.											
2) Use the average of the nominal sizes as the smaller dimension of rectangular parallelepipeds and twice that size as the length											
Sieve size, mm			Percent Passing			Surface area, mm ²		Volume, mm ³		Area/vol, cm ² /cm ³	
Larger	Smaller	Average	Larger	Smaller	% of total*	Sphere	Piped		Piped	Sphere	Piped
9.500	4.750	2.375	100.000	95.000	5.000	0.886	2.820	2.806	2.679		
4.750	2.360	1.195	100.000	80.000	15.000	0.673	2.142	1.072	1.024		
2.360	1.180	0.590	85.000		80.000	0.875	2.785	0.688	0.657		
1.180	0.600	0.290	60.000	25.000	25.000	0.066	0.210	0.026	0.024		
0.600	0.300	0.150	30.000	10.000	15.000	0.011	0.034	0.002	0.002		
0.300	0.150	0.075	10.000	2.000	10.000	0.002	0.006	0.000	0.000		
					150.000	2.512	7.997	4.594	4.387	5.469	18.22
* Calculated as the percentage passing through the smaller sieve minus the amount that also goes through the next larger sieve, except for the											
except for the smallest size for which all must have passed through the larger sieve.											

Value used in further calculations taken as the average of the two values for area/vol, i.e.								11.848			
Coarse aggregate per ASTM specifications, C 33-93, 0759510 0531853 341+A5											
Area to be modeled in two ways:											
1) From specifications for sieve analysis in Section 6.1, use the average of the nominal sizes between sieves as the diameter											
of spherical particles and take the average of the percentage between that size and the next larger. Use column for 3/8" in											
Table 2. This is because the proposed coarse aggregate will have a maximum size of 3/4", and this is the first column in the											
table for which the sieve analysis specifications are all less than this.											
2) Use the average of the nominal sizes as the smaller dimension of rectangular parallelepipeds and twice that size as the length											
Sieve size, mm			Percent Passing			Surface area, mm ²		Volume, mm ³		Area/vol, cm ² /cm	
Larger	Smaller	Average	Larger	Smaller	% of total*	Sphere	Piped	Sphere	Piped	Sphere	Piped
19.000	9.500	4.750	100.000	85.000	15.000	10.632	33.844	67.338	64.303		
9.500	2.360	3.570	85.000	0.000	85.000	34.033	108.332	161.999	154.698		
						44.666	142.175	229.337	219.001	1.948	6.4
Value used in further calculations taken as the average of the two values for area/vol+A62, i.e.								4.220			
Combinatio n											
Wt coarse	Wt fine	Total	%coarse	%fine							
1003.000	783.000	1786.000	0.562	0.438	7.564						
Surface area of cement mix:											
Spheres of 0.001cm, 0.0001cm, and 1.0E-08 cm diameter chosen for calculations:											
Diam, cm.	0.001	0.000	0.000	0.100							
Area=	0.000	0.000	0.000	0.031							
Volume=	0.000	0.000	0.000	0.004							
Area/vol=	7.50e+02	7.50e+03	7.50e+07	7.50e+00							
Aggregate											
Mineral	Moles***	Vol%	Density	Mol. Wt.	cm ³ /mol	Moles/kg water	cm ² /kg water				
Quartz	0.588	34.84	2.650	60.060	1.71e+02	1.08e+02	1.85e+04				
K-spar	0.100	28.09	2.600	278.340	8.10e+02	1.85e+01	1.49e+04				
Albite	0.116	30.39	2.615	262.220	7.59e+02	2.13e+01	1.62e+04				
Anorthite	0.010	2.55	2.750	278.210	7.65e+02	1.77e+00	1.36e+03				
Biotite	0.004	2.51	3.000	667.360	1.68e+03	7.92e-01	1.33e+03				
Magnetite	0.002	0.13	7.180	231.540	2.44e+02	2.80e-01	6.83e+01				
Ilmenite	0.001	0.16	4.720	239.600	3.84e+02	2.26e-01	8.69e+01				
Apatite	0.000	0.03	2.710	504.310	1.41e+03	1.30e-02	1.82e+01				
Kaolinite	0.005	1.30	2.610	258.160	7.48e+02	9.26e-01	6.93e+02				
							5.32e+04				
*** Moles/100 g tuff											
Degraded cement mix											

Workbook CONCRETE.XLS, Sheet "Molefr"

Cement							
Oxide	Wt%	Mol. Wt.	g-at metal	g-at O	Ele. mol fr	At wt. ele.	Wt% ele.
SiO2	25.000	60.060	0.416	0.833	0.105	28.086	11.69
Al2O3	3.400	101.940	0.067	0.100	0.017	26.982	0.90
CaO	64.400	56.080	1.148	1.148	0.289	40.080	46.03
MgO	1.900	40.320	0.047	0.047	0.012	24.305	1.15
Na2O	0.000	61.990	0.000	0.000	0.000	22.990	0.00
K2O	0.000	94.190	0.000	0.000	0.000	39.098	0.00
Fe2O3	2.800	159.700	0.035	0.053	0.009	55.847	0.98
SO3	1.600	80.060	0.020	0.060	0.005	32.060	0.64
Sums	99.100		1.733	2.241			
O					0.564	15.999	37.72
Totals					1.000		99.10
Molecular weight			24.937				

I.2 Sorption Calculations

Workbook SORPTAB.XLS, Sheet "Sorption"

This sheet provides basic relations for input to specific configurations. The data are very uncertain. This sheet uses European and Canadian data.										
The estimations will be based on a simple Kd approach. Concentration units for solutions are mg/kg; densities taken to be unity, which will be low and conservative, and for solids are g element/kg adsorbing substrate. Kd is in ml/g, i.e. solid conc. * 1000/soln. conc..										
The Kd approach used here has limitations. Specifically, at sufficiently high concentrations in solution all adsorption sites on the solid may be occupied. This means that the concentration in the solid is in fact limited, but that this simple model is incapable of showing that.										
			Plutonium				Uranium			
Solid	Kd, Pu	Kd, U	Pu gls. effluent, pH 8.01		Comm.SNF pkg effluent		Pu gls. effluent, pH 8.01		Comm.SNF pkg effluent	
			Soln. conc	Solid conc	Soln. conc	Solid conc	Soln. conc	Solid conc	Soln. conc	Solid conc
FeOOH	70000	4000	5.34E-08	3.74E-06			4.78E-03	1.91E-02		
Clinoptilolite	800	30	5.34E-08	4.27E-08			4.78E-03	1.43E-04		
Zeolite		700					4.78E-03	3.35E-03		
Smectite	3000	50	5.34E-08	1.60E-07			4.78E-03	2.39E-04		
Vitric Tuff	80	4	5.34E-08	4.27E-09			4.78E-03	1.91E-05		
Marl	5000	1000	5.34E-08	2.67E-07			4.78E-03	4.78E-03		
			Pu gls. effl., pH 7.01				Pu gls. effl., pH 7.01			
FeOOH	70000	4000	1.56E-07	1.09E-05			1.93E-03	7.72E-03		
Clinoptilolite	800	30	1.56E-07	1.25E-07			1.93E-03	5.79E-05		
Zeolite		700					1.93E-03	1.35E-03		
Smectite	3000	50	1.56E-07	4.68E-07			1.93E-03	9.65E-05		
Tuff	80	4	1.56E-07	1.25E-08			1.93E-03	7.72E-06		
Marl	5000	1000	1.56E-07	7.80E-07			1.93E-03	1.93E-03		
			Pu gls. effl., pH 6				Pu gls. effl., pH 6			
FeOOH	70000	4000	1.48E-06	1.04E-04			2.31E-03	9.24E-03		
Clinoptilolite	800	30	1.48E-06	1.18E-06			2.31E-03	6.93E-05		
Zeolite		700					2.31E-03	1.62E-03		
Smectite	3000	50	1.48E-06	4.44E-06			2.31E-03	1.16E-04		
Tuff	80	4	1.48E-06	1.18E-07			2.31E-03	9.24E-06		
Marl	5000	1000	1.48E-06	7.40E-06			2.31E-03	2.31E-03		
			Pu gls. effl., pH 5.5		Comm.SNF pkg pH 6		Pu gls. effl., pH 5.5		Comm.SNF pkg pH 6	
FeOOH	70000	4000	6.15E-06	4.31E-04	1.87E-06	1.31E-04	4.71E-03	1.88E-02	2.19	8.76E+00
Clinoptilolite	800	30	6.15E-06	4.92E-06	1.87E-06	1.50E-06	4.71E-03	1.41E-04	2.19	6.57E-02
Zeolite		700					4.71E-03	3.30E-03	2.19	1.53E+00
Smectite	3000	50	6.15E-06	1.85E-05	1.87E-06	5.61E-06	4.71E-03	2.36E-04	2.19	1.10E-01
Tuff	80	4	6.15E-06	4.92E-07	1.87E-06	1.50E-07	4.71E-03	1.88E-05	2.19	8.76E-03
Marl	5000	1000	6.15E-06	3.08E-05	1.87E-06	9.35E-06	4.71E-03	4.71E-03	2.19	2.19E+00
Data for FeOOH, clinoptilolite, and vitric tuff taken from Ref. 5.84										
Data for zeolite taken from Ref. 5.89										
Data for smectite taken from Ref. 5.86										
Data for marl taken from Ref. 5.85										

I.3 Tuff Chemistry

Several spreadsheets were used to obtain an average tuff composition and convert this into forms suitable for input to EQ6. They are presented here and are also available electronically.

Workbook Tuff.xls, Sheet Avg. Comp.

Average of six analyses supplied by LANL from USGS Prof. Paper 524-F (1966) for typical Topopah Tuff at repository level										
Weight Percentages										
Field No.	SiO2	Al2O3	FeO**	MgO	CaO	Na2O	K2O	TiO2	P2O5	MnO
63L-128-B-1	76.40	12.80	0.90	0.17	0.60	3.90	5.00	0.10	0.00	0.09
60ENH32	76.66	12.94	0.90	0.09	0.62	3.56	4.98	0.10	0.01	0.07
TO-41C	76.60	12.70	0.84	0.49	0.60	3.40	5.10	0.10	0.02	0.06
63L-17-I	76.90	13.00	0.89	0.23	0.55	3.50	4.70	0.09	0.02	0.05
33L-17-F	77.00	12.70	0.63	0.20	0.59	3.60	5.00	0.10	0.02	0.06
63L-17-H	77.40	12.30	0.89	0.29	0.40	3.60	4.80	0.10	0.02	0.07
Average	76.83	12.74	0.84	0.25	0.56	3.59	4.93	0.10	0.02	0.07
* This number is for Fe2O3										
** These values are reported in Prof. Paper 524-F as combined Fe2O3 and FeO, "Sum as FeO"; Individual values of Fe2O3 and FeO are also given. For all 6 analyses the reported wt% Fe2O3 exceeds that for FeO; however, the reader should bear in mind that analyses for ferrous iron in silicate rocks is difficult and uncertain owing to the difficulty of preventing air oxidation during dissolution of the rock.										
For sample 63L-128-B-1, as an example, calculate total Fe as FeO per 100 gm of sample										
Fe2O3			0.82							
Mol. Wt. Fe2O3			159.69							
Gram-atoms Fe in 159.69 grams Fe2O3			0.01							
FeO			0.16							
Mol. Wt. FeO			71.85							
Gram-atoms Fe in 71.85 grams FeO			0.00							
Total gram-atoms of Fe in sample			0.01							
Total Fe as FeO			0.90							
These six analyses were recommended by David Vaniman at LANL as being reasonably representative of the tuff at the repository horizon.										

Workbook Tuff.xls, Sheet, Norm

Norm for average of six analyses of Topopah Spring Tuff										
Oxide	Wt%	Mol. Wt.	g-at metal	g-at. O2	Mol. Fr.*					
SiO2	76.83	60.06	1.28	2.56	0.26					
Al2O3	12.74	101.94	0.25	0.37	0.05					
FeO	0.84	71.85	0.01	0.01	0.00					

CaO	0.56	56.08	0.01	0.01	0.00								
MgO	0.25	40.32	0.01	0.01	0.00								
TiO2	0.10	79.90	0.00	0.00	0.00								
Na2O	3.59	61.99	0.12	0.06	0.02								
K2O	4.93	94.19	0.10	0.05	0.02								
P2O5	0.02	141.96	0.00	0.00	0.00								
MnO	0.07	70.93	0.00	0.00	0.00								
	99.92		1.78	3.08		Molecular weight	20.58						
O					0.63								
Total					1.00								
* Gram-atom fraction of the corresponding metal or oxygen													
Element	gram-atoms	ilm	ap	bi	mag	Balance	Kspar	Ab	An	Balance	Kaol	Qz	Balance
Si	1.28			0.01		1.27	0.30	0.35	0.02	0.60	0.01	0.59	0.00
Al	0.25			0.00		0.25	0.10	0.12	0.02	0.01	0.01		0.00
Fe	0.01	0.00		0.01	0.00	0.00				0.00			0.00
Ca	0.01		0.00			0.01			0.01	0.00			0.00
Mg	0.01			0.01		0.00				0.00			0.00
Ti	0.00	0.00				0.00				0.00			0.00
Na	0.12					0.12		0.12		0.00			0.00
K	0.10			0.00		0.10	0.10			0.00			0.00
P	0.00		0.00			0.00				0.00			0.00
Mn	0.00			0.00		0.00				0.00			0.00
F**	0.00		0.00			0.00				0.00			0.00
Calculation scheme: Matrix, assumed to be finely crystalline. Scheme resembles that used to calculate the petrologic norm													
All Ti assigned to ilmenite, FeTiO3													
All phosphate assigned to fluorapatite, Ca5F(PO4)3, and fluoride assumed from this.													
All Mg assigned to biotite. Mg/(Mg+Fe) taken to be 0.47; this corresponds to 47% Mg & 53% Fe. Fe is assumed to include Mn for this purpose.													
Remainder of Fe assigned to magnetite.													
This leaves K, Na, Ca, and Al to be assigned to k-feldspar and plagioclase (solid solution of albite and anorthite)													
The excess aluminum assigned to kaolinite.													
The excess of Si assigned to quartz.													
Summary, by mineral component. E.g. K-spar includes potassium component of sanidine and matrix k-feldspar.													
Mineral	Moles	Mol. Wt.	Weight, g	Wt%	Density	Volume #	Vol%						
Quartz	0.59	60.06	35.31	34.90	2.65	13.33	34.84						
K-spar	0.10	278.34	27.94	27.61	2.60	10.75	28.09						
Albite	0.12	262.22	30.40	30.04	2.62	11.63	30.39						
Anorthite	0.01	278.21	2.68	2.65	2.75	0.97	2.55						
Biotite	0.00	667.36	2.88	2.84	3.00	0.96	2.51						
Magnetite	0.00	231.54	0.35	0.35	7.18	0.05	0.13						
Ilmenite	0.00	239.60	0.29	0.29	4.72	0.06	0.16						
Apatite	0.00	504.31	0.04	0.04	2.71	0.01	0.03						
Kaolinite	0.01	258.16	1.30	1.28	2.61	0.50	1.30						
			101.19	100.00		38.25	100.00						
# Volume for the calculated weight of 101.191g.													
Density = 2.65													

I.4 Waste Package Composition Calculations

Several spreadsheets were used to develop the chemical composition of waste package components and representative degradation rate constants. This information was used in the package dissolution modeling to produce representative solutions to react with external features. The spreadsheets are presented here and are also available electronically (see Section 9.2)

Workbook OXIDE.TAB, Sheet "SNF1"

Representative Spent Commercial Nuclear Fuel Composition ¹				
Element	Atom Fr.	At. Wt. 2	Weight, g	Wt. %
O	6.70E-01	1.60E+01	1.07E+01	1.21E+01
Mo	4.06E-04	9.59E+01	3.89E-02	4.37E-02
Tc	4.00E-04	9.89E+01	3.95E-02	4.44E-02
Ru	3.71E-04	1.01E+02	3.75E-02	4.22E-02
Rh	2.40E-04	1.03E+02	2.47E-02	2.78E-02
Pd	3.46E-05	1.08E+02	3.73E-03	4.19E-03
Ni	5.64E-04	1.44E+02	8.14E-02	9.15E-02
Sm	2.41E-04	1.50E+02	3.62E-02	4.07E-02
Eu	3.74E-05	1.52E+02	5.68E-03	6.39E-03
Gd	3.53E-06	1.57E+02	5.55E-04	6.23E-04
U	3.25E-01	2.38E+02	1.73E+01	8.69E+01
Np	5.31E-04	2.37E+02	7.85E-02	8.83E-02
Pu	2.32E-03	2.39E+02	5.55E-01	6.24E-01
Am	6.90E-05	2.41E+02	1.66E-02	1.87E-02
	1.00E+00		8.90E+01	1.00E+02

¹ Data from Ref. 5.4, p. 22. 1000 year old PWR SNF. Recalculated to atom fraction.

² Atomic weights from Ref. 5.5, inside front cover, except for Pu and Am, which correspond to mass numbers of most abundant isotope in the waste.

Workbook OXIDE.TAB, Sheet "SNF WP"

Characteristics of a Commercial Spent Nuclear Fuel Waste Package		
21 assemblies; Refs. 5.6 & 5.7		
Component	Mass, kg	Surface Area, cm ²
Spent Fuel*	11054.2	4.38e+08
Carbon steel	5510.36	2.30e+06
Boron steel	1882.035	6.94e+05
304L steel	343.56	1.27e+05
J-13 water**	4511	N/A

* 464 kg of heavy metal, from Ref. 5.6, p. 7. This was increased by the ratio 270/238 to include the oxygen in UO₂. Density was taken as 96% of theoretical (Ref. 5.5, p. B-173) for use in calculating volume.

** J-13 well water is assumed to fill all void space, density assumed to be 1g/cm³

Workbook OXIDE.TAB, Sheet "SNF Rates"

Rates of reaction								
Mat'l	Rate, g/cm ² /yr	Rate, g/cm ² /sec	Rate, g/cm ² /sec	Rt,mols/cm ² /sec				
PWR SNF*	0.00012	3.9E-12	3.9E-12	4.4E-14				
MOX fuel**	0.00012	3.9E-12	3.9E-12	4.5E-14				
Mat'l	R a t e , um/yr	Rt,g/m2/d	Area,cm ²	R a t e , cm ³ /yr	R a t e , cm ³ /sec	Density	Rate,g/cm ² /sec	Rate,mols/cm ² /sec
B-SS***	0.8		1	0.00008	2.5E-12	7.745	2E-11	3.8E-13
304L****	0.15		1	1.5E-05	4.8E-13	7.9	3.8E-12	6.9E-14
C-steel*****	30		1	0.003	9.5E-11	7.832	7.5E-10	1.4E-11
* For pH 7.5 and 0.002 M CO ₃ --, Ref. 5.6, p. 8								
** Assumed same rate as for commercial PWR SNF, initial enrichment = 3%, burnup = 20 GWd/MTU								
*** Ref. 5.8, Section 4.1.4. A range of corrosion rates is presented. For the present purposes a conservative value equal to twice the middle of the range for 304/316 stainless steels, i.e. 0.2E-06 m/yr (um/yr), times a conservatism factor of 4 for B-SS.								
**** Ref. 5.9, p. 4-2. This is the mid point of the range given..								
***** Ref. 5.8, p. 27. Corrosion rates are given a range of 10 to 50 um/yr. The mid-point was chosen.								

Workbook OXIDE.TAB. Sheet "MOX"

MOX fuel at 1000 yr. Ref. 5.10, case wm221f				
Element	Atom Fr.	At. Wt.	Weight, g	
O	6.72e-01	15.9994	1.08e+01	
Mo	5.61e-04	95.94	5.38e-02	
Tc	6.56e-04	98.9062	6.48e-02	
Ru	6.82e-04	101.07	6.89e-02	
Rh	5.96e-04	102.9055	6.14e-02	
Ag	1.48e-05	107.868	1.59e-03	
Nd	8.12e-04	144.24	1.17e-01	
Sm	4.16e-04	150.4	6.25e-02	
Eu	1.01e-04	151.96	1.54e-02	
Gd	1.51e-05	157.25	2.38e-03	
U	3.13e-01	238.029	7.44e+01	
Np	1.51e-03	237.0482	3.59e-01	
Pu	9.28e-03	240	2.23e+00	
Am	4.49e-04	243	1.09e-01	
Sum	1.00e+00		8.83e+01	= "mol. wt." (weight of 1 "mole" of fuel)

Workbook GLASSTAB.XLS, Sheet "DHLW"

HLW, Ref. 5.11, Attachment I, pp. 3-4, 9						
Component	Grams	Mol. Wt.	g-Atoms, 1st element	g-Atoms, 2nd element	2nd element	g-Atoms, oxygen
Ag	0.05	107.868				
Al ₂ O ₃	3.96	101.96	7.77e-02			1.17e-01
B ₂ O ₃	10.28	69.62	2.95e-01			4.43e-01
BaSO ₄	0.14	233.4	6.00e-04	6.00e-04	S	2.40e-03
Ca ₃ (PO ₄) ₂	0.07	310.18	6.77e-04	4.51e-04	P	1.81e-03
CaO	0.85	56.08	1.52e-02			1.52e-02
CaSO ₄	0.08	136.14	5.88e-04	5.88e-04	S	2.35e-03
Cr ₂ O ₃	0.12	151.99	1.58e-03			2.37e-03
Cs ₂ O*						
CuO	0.19	79.54	2.39e-03			2.39e-03
Fe ₂ O ₃	7.04	159.69	8.82e-02			1.32e-01
FeO	3.12	71.85	4.34e-02			4.34e-02
K ₂ O	3.58	94.2	7.60e-02			3.80e-02
Li ₂ O	3.16	29.88	2.12e-01			1.06e-01
MgO	1.36	40.31	3.37e-02			3.37e-02
MnO	2	70.94	2.82e-02			2.82e-02
Na ₂ O	11	61.98	3.55e-01			1.77e-01
Na ₂ SO ₄	0.36	142.04	5.07e-03	2.53e-03	S	1.01e-02
NaCl	0.19	58.44	3.25e-03	3.25e-03	Cl	
NaF	0.07	41.99	1.67e-03	1.67e-03	F	
NiO	0.93	74.71	1.24e-02			1.24e-02
PbS	0.07	239.25	2.93e-04	2.93e-04	S	
SiO ₂	45.57	60.06	7.59e-01			1.52e+00
ThO ₂ *	0.21	264.04	7.95e-04			1.59e-03
TiO ₂ *	0.99	79.9	1.24e-02			2.48e-02
U ₃ O ₈	2.2	842.09	7.84e-03			2.09e-02
Zeolite*						
ZnO*	0.08	81.37	9.83e-04			9.83e-04
Np	0.000751	237.048	3.17e-06			
Pu	0.01234	239.052	5.16e-05			
Am*						
Tc	0.010797	99.906	1.08e-04			
Zr	0.026415	91.22	2.90e-04			
Pd*						
Sn*						
Ce	0.023811	141.909	1.68e-04			
Ba	0.034794	137.33	2.53e-04			
Nd	0.024435	143.9099	1.70e-04			
Sm	0.00681	150.4	4.53e-05			
						2.71e+00
* Not considered at this time in the interest of simplifying the calculations						
Element	g-at.	Atom fr.				
Al	7.77e-02	1.64e-02				
B	2.95e-01	6.24e-02				
Ba	6.00e-04	1.27e-04				
Ca	1.64e-02	3.47e-03				
Cr	1.58e-03	3.33e-04				
Cu	2.39e-03	5.04e-04				
Fe	1.32e-01	2.78e-02				
K	7.60e-02	1.61e-02				
Li	2.12e-01	4.47e-02				
Mg	3.37e-02	7.12e-03				
Mn	2.82e-02	5.95e-03				

Na	3.65e-01	7.71e-02				
Cl	3.25e-03	6.87e-04				
F	1.67e-03	3.52e-04				
Ni	1.24e-02	2.63e-03				
P	4.51e-04	9.53e-05				
Pb	2.93e-04	6.18e-05				
S	4.01e-03	8.48e-04				
Si	7.59e-01	1.60e-01				
U	7.84e-03	1.66e-03				
O	2.71e+00	5.71e-01				
Np	3.17e-06	6.69e-07				
Pu	5.16e-05	1.09e-05				
Tc	1.01e-04	2.13e-05	Value from ORIGEN run used			
Zr	2.84e-04	6.00e-05	Value from ORIGEN run used			
Ce	1.68e-04	3.54e-05				
Nd	1.70e-04	3.59e-05				
Sm	4.53e-05	9.56e-06				
Total	4.74e+00	1.00e+00	2.11e+01	= "mol. wt." (weight of 1 "mole" of glass)		

Workbook GLASSTAB.XLS, Sheet "LaBS"

Pb-free LaBS glass. Ref. 5.12						
Oxide	Wt%	Mol. Wt.	g-Atoms, metal	g-Atoms, oxygen	Atom Fr. metal	Atom Fr. oxygen
SiO2	25.8	60.08	4.29e-01	8.59e-01	1.19e-01	
B2O3	10.4	69.62	2.99e-01	4.48e-01	8.28e-02	
Al2O3	19.04	101.96	3.73e-01	5.60e-01	1.04e-01	
ZrO2	1.15	123.22	9.33e-03	1.87e-02	2.59e-03	
Gd2O3	7.61	362.5	4.20e-02	6.30e-02	1.16e-02	
La2O3	11.01	325.82	6.76e-02	1.01e-01	1.87e-02	
Nd2O3	11.37	336.48	6.76e-02	1.01e-01	1.87e-02	
SrO	2.22	103.62	2.14e-02	2.14e-02	5.94e-03	
PuO2	11.39	274	4.16e-02	8.31e-02	1.15e-02	
	99.99		1.35e+00	2.26e+00	3.75e-01	6.25e-01
			1 = Check sum of at. fr.			
		27.71858	= "mol. wt." (weight of 1 "mole" of glass)			

Workbook GLASSTAB.XLS, Sheet "Rates"

Rates of reaction for glass			
Mat'l	Rt, g/m ² /d	Rt, g/cm ² /s	Rt, mols/cm ² /s
PWR SNF *	2.79e-02	3.23e-11	1.53e-12
LaBS**	2.00e-03	2.32e-12	8.35e-14
* Ref. 5.14. The rate for SRL 165 Frit [20] times conservation factor of about 1.5 was used			
** Ref. 5.15. The 7 day PCT test for Lan(B) was selected			

I.5 Data Reduction for EQ6 Effluent-Solids Reactions

Two types of results were handled somewhat differently in the spreadsheets. The first type of result was a deposit which extended over a significant distance due to slow reactions between the water and the reactant. As noted under the description of the modeling approach, Attachment III, sometimes successive "passes" were computed for this type. The second was a surface deposition of material on the reactant (in this case, metal fragments on the floor of the drift). The spreadsheets shown here are samples of the two types used. All spreadsheets are in the electronic attachments (Section 9.2).

In both types of results the cumulative products at a specific time were extracted electronically from the EQ6 output file by cutting and pasting text files and then parsing the text files into spreadsheets using Excel's parsing utilities. Each time point is called a "cell" (see discussion of modeling approach in Attachment III). These cumulative inventories are presented below as spreadsheets with names "Cell x". Thus the inventory in a particular cell is the cumulative amount at the end time of the cell minus the cumulative amount at the end time of the previous cell. This electronically extracted information then formed the basis for processing the data in a final results spreadsheet which follows a different format for the two types of results.

I.5.1 Extended Deposit

The example used is the reaction of immobilized plutonium waste package solution with tuff (WP1010A.XLS) for the case of 1mm/yr infiltration for 600 years. The first spreadsheets shown are the cumulative solids at time points that represent the last time in a "cell". This is followed by the summary sheet with the resultant numbers. Following this is a set of spreadsheets for a representative second pass. Next is the enlarged view of the summary sheet showing the formulas. All of the spreadsheets of this type used the same template.

Workbook WP10T0.XLS, Sheet "Cell 1"

pH 10 solution from LaBS pkg reacting with crushed tuff invert				
EQ6 Output File wp10t0a.6o				
Phase/End-member	Log moles	Moles	Mass, g	Volume, cc
Celadonite	-3.5566	2.78E-04	1.10E-01	4.36E-02
Maximum_Microcline	-1.9461	1.13E-02	3.15E+00	1.23E+00
Na4UO2(CO3)3	-3.4825	3.29E-04	1.78E-01	4.83E-02
PuO2	-5.5039	3.13E-06	8.65E-04	7.47E-05
Pyrolusite	-4.3561	4.40E-05	3.83E-03	7.57E-04
Quartz	-1.6246	2.37E-02	1.43E+00	5.39E-01
Rutile	-4.2408	0.000057442	0.0045884	1.08E-03
Carbonate-Calcite	-3.325	4.73E-04		
Calcite	-3.3311	4.67E-04	4.67E-02	1.72E-02
Magnesite	-5.1763	6.66E-06	5.62E-04	1.87E-04
Rhodochrosite	-14.0944	8.05E-15	9.25E-13	2.50E-13
Siderite	-22.6556	2.21E-23	2.56E-21	6.49E-22
Smithsonite	-15.8471	1.42E-16	1.78E-14	4.02E-15
Strontianite	-8.8731	1.3393E-09	1.9772E-07	5.22E-08
Smectite-di	-3.5624	2.74E-04		
Beidellite-Ca	-36.378	4.19E-37	1.54E-34	5.43E-35
Beidellite-K	-33.5074	3.11E-34	1.16E-31	4.16E-32
Beidellite-Mg	-36.9639	1.09E-37	3.96E-35	1.34E-35
Beidellite-Na	-33.0481	8.95E-34	3.29E-31	1.17E-31
Montmor-Ca	-25.4995	3.17E-26	1.16E-23	1.58E-23
Montmor-K	-22.4156	3.84E-23	1.43E-20	1.92E-20
Montmor-Mg	-25.8745	1.34E-26	4.85E-24	6.68E-24
Montmor-Na	-21.9676	1.08E-22	3.95E-20	5.39E-20
Nontronite-Ca	-7.0221	9.50E-08	4.03E-05	1.25E-05
Nontronite-K	-4.1506	7.07E-05	3.04E-02	9.56E-03
Nontronite-Mg	-7.6077	2.47E-08	1.04E-05	3.20E-06
Nontronite-Na	-3.6923	0.00020311	0.086375	2.68E-02
Rhabdophane-ss	-5.7575	1.75E-06		
LaPO4:H2O	-6.4123	3.87E-07	9.75E-05	0.00E+00
CePO4:H2O	-20.0467	8.98E-21	2.27E-18	0.00E+00
NdPO4:H2O	-6.4768	3.34E-07	8.58E-05	0.00E+00
GdPO4:H2O	-6.3132	4.86E-07	1.31E-04	0.00E+00
SmPO4:H2O	-6.2666	5.4125E-07	1.43E-04	0.00E+00
			5.04E+00	1.92E+00

Workbook WP10T0.XLS, Sheet "Cell 2"

pH 10 solution from LaBS pkg reacting with crushed tuff invert				
EQ6 Output File wp10t0a.6o				
Phase/End-member	Log moles	Moles	Mass, g	Volume, cc
Celadonite	-3.1386	7.27E-04	2.88E-01	1.14E-01
Fluorapatite	-5.4076	3.91E-06	1.97E-03	6.17E-04
Maximum_Microcline	-1.5283	2.96E-02	8.25E+00	3.22E+00
Na4UO2(CO3)3	-3.0699	8.51E-04	4.61E-01	1.25E-01
PuO2	-5.0796	8.33E-06	2.30E-03	1.98E-04
Pyrolusite	-3.9383	1.15E-04	1.00E-02	1.98E-03
Quartz	-1.2068	6.21E-02	3.73E+00	1.41E+00
Rutile	-3.823	1.50E-04	1.20E-02	2.83E-03
Tenorite	-6.5238	2.9939E-07	0.000023815	3.66E-06
Carbonate-Calcite	-2.9139	1.22E-03		
Calcite	-2.9201	1.20E-03	1.20E-01	4.44E-02
Magnesite	-4.7653	1.72E-05	1.45E-03	4.81E-04
Rhodochrosite	-13.6833	2.07E-14	2.38E-12	6.44E-13
Siderite	-22.2507	5.62E-23	6.51E-21	1.65E-21
Smithsonite	-15.8471	1.42E-16	1.78E-14	4.02E-15
Strontianite	-8.8731	1.3393E-09	1.9772E-07	5.22E-08
Smectite-di	-3.1446	7.17E-04		
Beidellite-Ca	-35.5085	3.10E-36	1.14E-33	4.02E-34
Beidellite-K	-32.7131	1.94E-33	7.22E-31	2.59E-31
Beidellite-Mg	-36.0944	8.05E-37	2.93E-34	9.91E-35
Beidellite-Na	-32.1783	6.63E-33	2.44E-30	8.66E-31
Montmor-Ca	-24.7772	1.67E-25	6.11E-23	8.35E-23
Montmor-K	-21.7618	1.73E-22	6.44E-20	8.65E-20
Montmor-Mg	-25.1522	7.04E-26	2.56E-23	3.52E-23
Montmor-Na	-21.2449	5.69E-22	2.09E-19	2.84E-19
Nontronite-Ca	-6.5926	2.56E-07	1.08E-04	3.35E-05
Nontronite-K	-3.7691	1.70E-04	7.33E-02	2.30E-02
Nontronite-Mg	-7.1782	6.63E-08	2.80E-05	8.61E-06
Nontronite-Na	-3.2625	0.00054634	0.23234	7.22E-02
Rhabdophane-ss	-5.6892	2.05E-06		
LaPO4:H2O	-6.4058	3.93E-07	9.90E-05	0.00E+00
CePO4:H2O	-20.0109	9.75E-21	2.47E-18	0.00E+00
NdPO4:H2O	-6.4255	3.75E-07	9.66E-05	0.00E+00
GdPO4:H2O	-6.193	6.41E-07	1.73E-04	0.00E+00
SmPO4:H2O	-6.1965	6.3609E-07	1.68E-04	0.00E+00
			1.32E+01	5.02E+00

Workbook WP10T0.XLS, Sheet "Cell 3"

pH 10 solution from LaBS pkg reacting with crushed tuff invert				
EQ6 Output File wp10t0a.6o				
Phase/End-member	Log moles	Moles	Mass, g	Volume, cc
Borax	-3.4987	3.17E-04	1.21E-01	7.06E-02
Celadonite	-2.5725	2.68E-03	1.06E+00	4.20E-01
Fluorapatite	-4.5668	2.71E-05	1.37E-02	4.27E-03
Maximum_Microcline	-0.9624	1.09E-01	3.04E+01	1.19E+01
Na4UO2(CO3)3	-2.5212	3.01E-03	1.63E+00	4.42E-01
PuO2	-4.5318	2.94E-05	8.11E-03	7.00E-04
Pyrolusite	-3.3723	4.24E-04	3.69E-02	7.29E-03
Quartz	-0.6408	2.29E-01	1.37E+01	5.19E+00
Rutile	-3.257	5.53E-04	4.42E-02	1.04E-02
Tenorite	-5.9676	1.08E-06	8.57E-05	1.32E-05
Carbonate-Calcite	-2.3541	4.43E-03		
Calcite	-2.3602	4.36E-03	4.37E-01	1.61E-01
Magnesite	-4.2056	6.23E-05	5.25E-03	1.75E-03
Rhodochrosite	-13.1235	7.53E-14	8.65E-12	2.34E-12
Siderite	-21.7511	1.77E-22	2.06E-20	5.21E-21
Smithsonite	-15.8471	1.42E-16	1.78E-14	4.02E-15
Strontianite	-8.8731	1.34E-09	1.98E-07	5.22E-08
Smectite-di	-2.5786	2.64E-03		
Beidellite-Ca	-27.3583	4.38E-28	1.61E-25	5.68E-26
Beidellite-K	-25.7932	1.61E-26	6.00E-24	2.15E-24
Beidellite-Mg	-27.9444	1.14E-28	4.14E-26	1.40E-26
Beidellite-Na	-24.0261	9.42E-25	3.46E-22	1.23E-22
Montmor-Ca	-19.0846	8.23E-20	3.01E-17	4.12E-17
Montmor-K	-17.2851	5.19E-18	1.93E-15	2.59E-15
Montmor-Mg	-19.4597	3.47E-20	1.26E-17	1.73E-17
Montmor-Na	-15.5502	2.82E-16	1.03E-13	1.41E-13
Nontronite-Ca	-5.9685	1.08E-06	4.56E-04	1.41E-04
Nontronite-K	-3.4789	3.32E-04	1.43E-01	4.49E-02
Nontronite-Mg	-6.5542	2.79E-07	1.18E-04	3.62E-05
Nontronite-Na	-2.6372	2.31E-03	9.80E-01	3.05E-01
Rhabdophane-ss	-5.6881	2.05E-06		
LaPO4:H2O	-6.4057	3.93E-07	9.90E-05	0.00E+00
CePO4:H2O	-20.0104	9.76E-21	2.47E-18	0.00E+00
NdPO4:H2O	-6.4248	3.76E-07	9.67E-05	0.00E+00
GdPO4:H2O	-6.1912	6.44E-07	1.74E-04	0.00E+00
SmPO4:H2O	-6.1954	6.38E-07	1.68E-04	0.00E+00
			4.86E+01	1.85E+01

Workbook WP10T0.XLS, Sheet "Cell 4"

pH 10 solution from LaBS pkg reacting with crushed tuff invert				
EQ6 Output File wpl0t0a.6o				
Phase/End-member	Log moles	Moles	Mass, g	Volume, cc
Albite_low	-0.6395	2.29E-01	6.01E+01	2.30E+01
Borax	-2.9435	1.14E-03	4.34E-01	2.54E-01
Celadonite	-1.9123	1.22E-02	4.85E+00	1.92E+00
Fluorapatite	-3.8517	1.41E-04	7.10E-02	2.22E-02
Maximum_Microcline	-0.5698	2.69E-01	7.49E+01	2.93E+01
Na4UO2(CO3)3	-2.513	3.07E-03	1.66E+00	4.51E-01
PuO2	-4.1367	7.30E-05	2.01E-02	1.74E-03
Pyrolusite	-2.7122	1.94E-03	1.69E-01	3.33E-02
Quartz	0.0195	1.05E+00	6.28E+01	2.37E+01
Rutile	-2.5969	2.53E-03	2.02E-01	4.76E-02
Tenorite	-5.5167	3.04E-06	2.42E-04	3.72E-05
Carbonate-Calcite	-1.6958	2.01E-02		
Calcite	-1.7019	1.99E-02	1.99E+00	7.34E-01
Magnesite	-3.5479	2.83E-04	2.39E-02	7.94E-03
Rhodochrosite	-12.4652	3.43E-13	3.94E-11	1.06E-11
Siderite	-21.2194	6.03E-22	6.99E-20	1.77E-20
Smithsonite	-15.8471	1.42E-16	1.78E-14	4.02E-15
Strontianite	-8.8731	1.34E-09	1.98E-07	5.22E-08
Smectite-di	-1.9185	1.21E-02		
Beidellite-Ca	-23.727	1.88E-24	6.87E-22	2.43E-22
Beidellite-K	-22.4296	3.72E-23	1.39E-20	4.97E-21
Beidellite-Mg	-24.3133	4.86E-25	1.77E-22	5.99E-23
Beidellite-Na	-20.4157	3.84E-21	1.41E-18	5.01E-19
Montmor-Ca	-15.9959	1.01E-16	3.70E-14	5.05E-14
Montmor-K	-14.4853	3.27E-15	1.22E-12	1.64E-12
Montmor-Mg	-16.3714	4.25E-17	1.55E-14	2.13E-14
Montmor-Na	-12.4825	3.29E-13	1.21E-10	1.65E-10
Nontronite-Ca	-5.2494	5.63E-06	2.39E-03	7.38E-04
Nontronite-K	-3.3744	4.22E-04	1.82E-01	5.71E-02
Nontronite-Mg	-5.8354	1.46E-06	6.16E-04	1.90E-04
Nontronite-Na	-1.9342	1.16E-02	4.95E+00	1.54E+00
Rhabdophane-ss	-5.685	2.07E-06		
LaPO4:H2O	-6.4054	3.93E-07	9.90E-05	0.00E+00
CePO4:H2O	-20.009	9.80E-21	2.48E-18	0.00E+00
NdPO4:H2O	-6.4226	3.78E-07	9.72E-05	0.00E+00
GdPO4:H2O	-6.1857	6.52E-07	1.76E-04	0.00E+00
SmPO4:H2O	-6.1924	6.42E-07	1.69E-04	0.00E+00
			2.12E+02	8.10E+01

Workbook WP10T0.XLS, Sheet "Cell 5"

pH 10 solution from LaBS pkg reacting with crushed tuff invert				
EQ6 Output File wp10t0a.6o				
Phase/End-member	Log moles	Moles	Mass, g	Volume, cc
Albite_low	0.4603	2.89E+00	7.57E+02	2.89E+02
Borax	-1.8373	1.45E-02	5.55E+00	3.24E+00
Celadonite	-0.9122	1.22E-01	4.86E+01	1.92E+01
Fluorapatite	-2.839	1.45E-03	7.31E-01	2.28E-01
Maximum_Microcline	0.3221	2.10E+00	5.84E+02	2.28E+02
Na4UO2(CO3)3	-2.513	3.07E-03	1.66E+00	4.51E-01
PuO2	-3.4514	3.54E-04	9.76E-02	8.43E-03
Pyrolusite	-1.7122	1.94E-02	1.69E+00	3.33E-01
Quartz	1.0195	1.05E+01	6.29E+02	2.37E+02
Rutile	-1.5969	2.53E-02	2.02E+00	4.76E-01
Tenorite	-4.5819	2.62E-05	2.08E-03	3.20E-04
Carbonate-Calcite	-0.6963	2.01E-01		
Calcite	-0.7024	1.98E-01	1.99E+01	7.33E+00
Magnesite	-2.5549	2.79E-03	2.35E-01	7.81E-02
Rhodochrosite	-11.4657	3.42E-12	3.93E-10	1.06E-10
Siderite	-20.262	5.47E-21	6.34E-19	1.61E-19
Smithsonite	-15.8471	1.42E-16	1.78E-14	4.02E-15
Strontianite	-8.8731	1.34E-09	1.98E-07	5.22E-08
Smectite-di	-0.9185	1.21E-01		
Beidellite-Ca	-19.8784	1.32E-20	4.85E-18	1.71E-18
Beidellite-K	-18.9681	1.08E-19	4.01E-17	1.44E-17
Beidellite-Mg	-20.4681	3.40E-21	1.24E-18	4.19E-19
Beidellite-Na	-16.9541	1.11E-17	4.09E-15	1.45E-15
Montmor-Ca	-12.9278	1.18E-13	4.32E-11	5.90E-11
Montmor-K	-11.8045	1.57E-12	5.84E-10	7.84E-10
Montmor-Mg	-13.3066	4.94E-14	1.79E-11	2.47E-11
Montmor-Na	-9.8013	1.58E-10	5.80E-08	7.90E-08
Nontronite-Ca	-3.8541	1.40E-04	5.94E-02	1.83E-02
Nontronite-K	-2.8351	1.46E-03	6.29E-01	1.98E-01
Nontronite-Mg	-4.4433	3.60E-05	1.52E-02	4.68E-03
Nontronite-Na	-0.9244	1.19E-01	5.06E+01	1.57E+01
Rhabdophane-ss	-5.6277	2.36E-06		
LaPO4:H2O	-6.402	3.96E-07	9.98E-05	0.00E+00
CePO4:H2O	-19.9869	1.03E-20	2.61E-18	0.00E+00
NdPO4:H2O	-6.3886	4.09E-07	1.05E-04	0.00E+00
GdPO4:H2O	-6.0807	8.30E-07	2.24E-04	0.00E+00
SmPO4:H2O	-6.142	7.21E-07	1.90E-04	0.00E+00
			2.10E+03	8.02E+02

Workbook WP10T0.XLS, Sheet "1 mm per year 600 yr"

pH 10 solution from LaBS pkg reacting with crushed tuff invert														
EQ6 Output File wp10t0a.6o														
Package Inventory														
	moles	grams	wt% fissile											
U	1.32E+02	3.13E+04	3.1300%											
Pu	5.90E+02	1.41E+05	100.0000%											
Porosity of Invert		0.3												
Porosity of Rock		0.139												
Depth of Invert		7.00E+02 mm												
flow	width	170.9 cm		"shadow" of waste package										
flow	length	323 cm		"shadow" of waste package										
	Flow Cross Section	5.52E+04 sq cm												
	1.00E+00	mm/yr infiltration rate												
	6.00E+02	yr Deposition Time (time for pH 10 condition to persist)												
Cell	Travel Time	Distance	Accumulation During The Deposition Time								% Void	% Void	Fissile	
No.	Into Rock	Traveled	Total Solids	Total Solids	Uranium	Plutonium	Uranium	Plutonium	Fissile	Fissile	Filled With	Filled With	wt% of	
	d	nm	cc	g	Moles	Moles	g	g	g	g/mm	Solids	Fissile	U+Pu	
1	2.19E+03	2.00E+01	6.3500E+03	1.67E+04	1.09E+00	1.04E-02	2.60E+02	2.48E+00	1.06E+01	5.30E-01	19.1726%	0.0122%	4.05%	
2	5.73E+03	5.23E+01	1.0262E+04	2.70E+04	1.73E+00	1.72E-02	4.12E+02	4.11E+00	1.70E+01	5.25E-01	11.8405%	0.0075%	4.09%	
3	2.11E+04	1.93E+02	4.4712E+04	1.17E+05	7.16E+00	6.98E-02	1.70E+03	1.67E+01	7.00E+01	4.99E-01	14.0116%	0.0084%	4.07%	
4	9.65E+04	1.09E+03	2.0704E+05	5.43E+05	1.89E-01	1.44E-01	4.51E+01	3.45E+01	3.59E+01	4.00E-02	24.7499%	0.0016%	45.13%	
5	9.65E+05	1.82E+04	2.3872E+06	6.26E+06	0.00E+00	9.30E-01	0.00E+00	2.22E+02	2.22E+02	1.30E-02	17.0949%	0.0006%	100.00%	
Total			2.6556E+06	6.96E+06			2.42E+03	2.80E+02	3.56E+02					

Workbook WP10T0.XLS, Sheet "1 mm per year 600 yr" (Formulas Displayed)

	A	B	C	D
1		pH 10 solution from LaBS pkg reacting with crushed tuff invert		
2		EQ6 Output File wp10t0a.6o		
3				
4			Package Inventory	
5			moles	grams
6				
7		U	131.57	=238*D8
8		Pu	589.92	=239*D9
9				
10		Porosity of Invert		0.3
11		Porosity of Rock		0.139
12		Depth of Invert		700
13		flow	width	170.9
14		flow	length	323
15			Flow Cross Section	=E14*E15
16				
17				
18				
19			l	mm/yr infiltration rate
20			600	yr Deposition Time (time for pH 10 condition to persist)
21				
22				
23		Cell	Travel Time	Distance
24		No.	Into Rock	Traveled
25			d	mm
26		1	2190	=IF(D27*\$D\$20/365/\$E\$11>\$E\$13,\$E\$13+(D27/365-\$E\$13*\$E\$11/\$D\$20)*\$D\$20/\$E\$12,D27*\$D\$20/365/\$E\$11)
27		2	5731	=IF(D28*\$D\$20/365/\$E\$11>\$E\$13,\$E\$13+(D28/365-\$E\$13*\$E\$11/\$D\$20)*\$D\$20/\$E\$12,D28*\$D\$20/365/\$E\$11)
28		3	21100	=IF(D29*\$D\$20/365/\$E\$11>\$E\$13,\$E\$13+(D29/365-\$E\$13*\$E\$11/\$D\$20)*\$D\$20/\$E\$12,D29*\$D\$20/365/\$E\$11)
29		4	96450	=IF(D30*\$D\$20/365/\$E\$11>\$E\$13,\$E\$13+(D30/365-\$E\$13*\$E\$11/\$D\$20)*\$D\$20/\$E\$12,D30*\$D\$20/365/\$E\$11)
30		5	964500	=IF(D31*\$D\$20/365/\$E\$11>\$E\$13,\$E\$13+(D31/365-\$E\$13*\$E\$11/\$D\$20)*\$D\$20/\$E\$12,D31*\$D\$20/365/\$E\$11)
31		Total		

	E	F
1		
2		
3		
4		
5	wt% fissile	
6		
7	0.0313	
8	l	
9		
10		
11		
12	mm	
13	cm	"shadow" of waste package
14	cm	"shadow" of waste package
15	sq cm	
16		
17		
18		
19		
20		
21		
22		
23		Accumulation During The Deposition Time
24	Total Solids	Total Solids
25	cc	g
26	=Cell 1!E42*E16*\$D\$21*\$D\$20/10000	=Cell 1!D42*\$E\$16*\$D\$21*\$D\$20/10000
27	=(Cell 2!E44-Cell 1!E42)*E16*\$D\$21*D20/10000	=(Cell 2!D44-Cell 1!D42)*E16*\$D\$21*D20/10000
28	=(Cell 3!F46-Cell 2!E44)*E16*\$D\$21*D20/10000	=(Cell 3!E46-Cell 2!D44)*E16*\$D\$21*D20/10000
29	=(Cell 4!F47-Cell 3!F46)*E16*\$D\$21*\$D\$20/10000	=(Cell 4!E47-Cell 3!E46)*E16*\$D\$21*\$D\$20/10000
30	=(Cell 5!F47-Cell 4!F47)*E16*\$D\$21*\$D\$20/10000	=(Cell 5!E47-Cell 4!E47)*E16*\$D\$21*\$D\$20/10000
31	=SUM(F27:F31)	=SUM(G27:G31)

	F	G	H
23	Accumulation During The Deposition Time		
24	Total Solids	Uranium	Plutonium
25	g	Moles	Moles
26	=Cell 1!D42*\$E\$16*\$D\$21*\$D\$20/10000	=Cell 1!C8*E16*\$D\$21*D20/10000	=Cell 1!C9*E16*\$D\$21*D20/10000
27	=(Cell 2!D44-Cell 1!D42)*E16*\$D\$21*D20/10000	=(Cell 2!C9-Cell 1!C8)*E16*\$D\$21*D20/10000	=(Cell 2!C10-Cell 1!C9)*E16*\$D\$21*D20/10000
28	=(Cell 3!E46-Cell 2!D44)*E16*\$D\$21*D20/10000	=(Cell 3!D11-Cell 2!C9)*E16*\$D\$21*D20/10000	=(Cell 3!D12-Cell 2!C10)*E16*\$D\$21*D20/10000
29	=(Cell 4!E47-Cell 3!E46)*E16*\$D\$21*\$D\$20/10000	=(Cell 4!D12-Cell 3!D11)*E16*\$D\$21*\$D\$20/10000	=(Cell 4!D13-Cell 3!D12)*E16*\$D\$21*D20/10000
30	=(Cell 5!E47-Cell 4!E47)*E16*\$D\$21*\$D\$20/10000	=(Cell 5!D12-Cell 4!D12)*E16*\$D\$21*\$D\$20/10000	=(Cell 5!D13-Cell 4!D13)*E16*\$D\$21*D20/10000
31	=SUM(G27:G31)		

	I	J	K	L	M
23					% Void
24	Uranium	Plutonium	Fissile	Fissile	Filled With
25	g	g	g	g/mm	Solids
26	=H27*238	=I27*239	=(F\$8*J27+K27)	=L27/E27	=IF(E27<\$E\$13,F27/(E16*E27/10*\$E\$11),F27/(E16*E27/10*\$E\$12))
27	=H28*238	=I28*239	=(F\$8*J28+K28)	=L28/(E28-E27)	=IF(E28<\$E\$13,F28/(E16*E28/10*\$E\$11),F28/(E16*E28/10*\$E\$12))
28	=H29*238	=I29*239	=(F\$8*J29+K29)	=L29/(E29-E28)	=IF(E29<\$E\$13,F29/(E16*E29/10*\$E\$11),F29/(E16*E29/10*\$E\$12))
29	=H30*238	=I30*239	=(F\$8*J30+K30)	=L30/(E30-E29)	=IF(E30<\$E\$13,F30/(\$E\$16*E30/10*\$E\$11),F30/(\$E\$16*E30/10*\$E\$12))
30	=H31*238	=I31*239	=(F\$8*J31+K31)	=L31/(E31-E30)	=IF(E31<\$E\$13,F31/(\$E\$16*E31/10*\$E\$11),F31/(\$E\$16*E31/10*\$E\$12))
31	=SUM(J27:J31)	=SUM(K27:K31)	=SUM(L27:L31)		

	N	O
23	% Void	Fissile
24	Filled With	wt% of
25	Fissile	U+Pu
26	=(F\$8*J27+K27)*N27/G27	=(F\$8*J27+K27)/L27
27	=(F\$8*J28+K28)*N28/G28	=(F\$8*J28+K28)/L28
28	=(F\$8*J29+K29)*N29/G29	=(F\$8*J29+K29)/L29
29	=(F\$8*J30+K30)*N30/G30	=(F\$8*J30+K30)/L30
30	=(F\$8*J31+K31)*N31/G31	=(F\$8*J31+K31)/L31
31		=(F\$8*J32+K32)/L32

I.5.2 Surface Deposit

The example used is the reaction of immobilized plutonium waste package solution with iron with no free oxygen (WPCSNGL.XLS) for the 600-year deposition case. The first spreadsheets shown are the cumulative solids at time points that represent the last time in a "cell". This is followed by the summary sheet with the resultant numbers. Next is the enlarged view of the summary sheet showing the formulas. All of the spreadsheets are provided in the electronic attachments.

Workbook CELL2PASS.XLS, Sheet "Pass 0"

pH 10 solution from LaBS pkg reacting with crushed tuff invert									
Run wp10t0a.6i									
Duration of pH = 10: 600 yr									
Flow rate for 1 mm/yr infiltration= 4.00E+00 kg/yr									
Invert Vol (cc) = 2.00E+06									
void fraction = 0.300									
Void Vol (cc) = 6.00E+05									
Package Inventory									
moles grams wt% fissile									
U 1.32E+02 3.13E+04 3.1300%									
Pu 5.90E+02 1.41E+05 100.0000%									
Deposition Profile for Each 1 kg of Water									
Cell	Time (d)	Moles U	Moles Pu	Total Solids	Uranium	Plutonium	Fissile	Fissile	
				g	g	g	g	wt%	
1	2.19E+03	3.29E-04	3.13E-06	5.04E+00	7.84E-02	7.49E-04	3.20E-03	0.0635%	
2	5.73E+03	5.22E-04	5.19E-06	8.14E+00	1.24E-01	1.24E-03	5.13E-03	0.0630%	
3	2.11E+04	2.16E-03	2.11E-05	4.35E+01	5.14E-01	5.03E-03	2.11E-02	0.0485%	
4	9.65E+04	5.72E-05	4.36E-05	1.64E+02	1.36E-02	1.04E-02	1.08E-02	0.0066%	
5	9.65E+05	0.00E+00	2.81E-04	1.89E+03	0.00E+00	6.71E-02	6.71E-02	0.0036%	
Total				2.11E+03	7.30E-01	8.45E-02	1.07E-01		
Total Volume (cc)				8.02E+02					
Deposition of Solid for 600 year period at various infiltration rates									
Infiltration Rate		Total Vol		Total Solids	Uranium	Plutonium	Fissile	Fissile	
mm/yr	kg/yr	cc	g	g	g	g	g	wt%	
1.00E-01	4.00E-01	1.92E+05	5.06E+05	1.75E+02	2.03E+01	2.58E+01	0.0051%		
1.00E+00	4.00E+00	6.00E+05	1.58E+06	5.47E+02	6.33E+01	8.04E+01	0.0051%		
*	5.00E+00	2.00E+01	6.00E+05	1.58E+06	5.47E+02	6.33E+01	8.04E+01	0.0051%	
*	1.00E+01	4.00E+01	6.00E+05	1.58E+06	5.47E+02	6.33E+01	8.04E+01	0.0051%	

		*At these infiltration rates part of the deposit would be spread into the rock and the available volume						
		would be less than that used because of the different porosity.						

Workbook CELL2PASS.XLS, Sheet "Pass 1"

Fissile Material Content of Deposited Solids - Pass 1					
	Moles	MW	grams	g fissile	% mass fissile
U	1.4109E-03	2.3800E+02	3.3579E-01	1.0510E-02	
Pu	1.3746E-05	2.3900E+02	3.2853E-03	3.2853E-03	
			3.3908E-01	1.3796E-02	0.076772%
		Mass, g			
Borax		2.2141E-02			
Calcite		1.9973E-01			
Celadonite		1.9764E-01			
Fluorapatite		2.3001E-03			
Max-Microcline		1.3757E+01			
Na4UO2(CO3)3		7.6472E-01			
Nontronite-K		0.0000E+00			
Nontronite-Na		5.0865E-01			
PuO2		3.7939E-03			
Pyrolusite		6.7110E-03			
Quartz		2.4989E+00			
Rutile		8.0414E-03			
Tenorite		2.2056E-05			
Total		1.7970E+01			

Workbook CELL2PASS.XLS, Sheet "Pass 2"

Fissile Material Content of Deposited Solids - Pass 2					
	Moles	MW	grams	g fissile	% mass fissile
U	1.9741E-03	2.3800E+02	4.6984E-01	1.4706E-02	
Pu	1.9180E-05	2.3900E+02	4.5840E-03	4.5840E-03	
			4.7442E-01	1.9290E-02	0.080058%
		Mass, g			
Borax		2.2185E-02			
Calcite		2.7939E-01			
Celadonite		1.9811E-01			
Fluorapatite		2.3014E-03			

Max-Microcline	1.9290E+01			
Na4UO2(CO3)3	1.0700E+00			
Nontronite-K	0.0000E+00			
Nontronite-Na	7.1291E-01			
PuO2	5.2936E-03			
Pyrolusite	6.7140E-03			
Quartz	2.5000E+00			
Rutile	8.0450E-03			
Tenorite	2.2098E-05			
Total	2.4095E+01			

Workbook CELL2PASS.XLS, Sheet "Pass Summary"

Deposition in Cell 2 From Three Passes for Reaction of LaBS pH 10 Effluent With Crushed Tuff						
(Each "pass" is one kg of water flowing through the system)						
		Uranium	Plutonium	Total Solids	Fissile	Fissile
		g	g	g	g	wt% of
						Total U+ Pu
	Pass 0	1.24E-01	1.24E-03	8.14E+00	5.13E-03	4.0877%
	Pass 1	3.36E-01	3.29E-03	1.80E+01	1.38E-02	4.0686%
	Pass 2	4.70E-01	4.58E-03	2.41E+01	1.93E-02	4.0660%

Workbook WP10CSNG.XLS, Sheet "Cell 1"

Phase/End-member	Log moles	Moles	Mass, g	Volume, cc		cc/mole
Goethite	-3.4	3.98E-04	3.54E-02	8.29E-03		20.819874
PuO2	-3.5205	3.02E-04	8.32E-02	7.19E-03		23.830443
Pyrolusite	-14.1338	7.35E-15	6.39E-13	1.26E-13	5.06	17.181178
Trevorite	-10.2399	5.76E-11	1.35E-08	2.88E-08		500
Smectite-di	-9.072	8.47E-10				
Beidellite-Ca	-91.6634	2.17E-92	7.96E-90	2.81E-90		129.52964
Beidellite-K	-88.7429	1.81E-89	6.74E-87	2.42E-87		133.70034
Beidellite-Mg	-92.236	5.81E-93	2.11E-90	7.15E-91		123.1911
Beidellite-Na	-88.3205	4.78E-89	1.76E-86	6.24E-87		130.54109
Montmor-Ca	-66.6862	2.06E-67	7.54E-65	1.03E-64		500.02428
Montmor-K	-63.5528	2.80E-64	1.04E-61	1.40E-61		500
Montmor-Mg	-67.0479	8.95E-68	3.25E-65	4.48E-65		500
Montmor-Na	-63.1412	7.22E-64	2.65E-61	3.61E-61		500
Nontronite-Ca	-12.5543	2.79E-13	1.18E-10	3.66E-11		131.09837
Nontronite-K	-9.6339	2.32E-10	1.00E-07	3.14E-08		135.27158
Nontronite-Mg	-13.1266	7.47E-14	3.15E-11	9.69E-12		129.76026
Nontronite-Na	-9.2114	6.15E-10	2.61E-07	8.12E-08		132.10927
			1.19E-01	1.55E-02		

WorkbookWP10CSNG.XLS, Sheet "Cell 1"

Phase/End-member	Log moles	Moles	Mass, g	Volume, cc		
Goethite	-3.3448	4.52E-04	4.02E-02	9.41E-03		20.820227
PuO2	-3.4298	3.72E-04	1.03E-01	8.86E-03		23.829701
Trevorite	-10.2401	5.75E-11	1.35E-08	2.88E-08		500
Smectite-di	-9.072	8.47E-10				
Beidellite-Ca	-91.6819	2.08E-92	7.62E-90	2.69E-90		129.52885
Beidellite-K	-88.7614	1.73E-89	6.46E-87	2.32E-87		133.70092
Beidellite-Mg	-92.2546	5.56E-93	2.03E-90	6.86E-91		123.19083
Beidellite-Na	-88.339	4.58E-89	1.68E-86	5.98E-87		130.53803
Montmor-Ca	-66.699	2.00E-67	7.32E-65	1.00E-64		500.005
Montmor-K	-63.5655	2.72E-64	1.01E-61	1.36E-61		499.98162
Montmor-Mg	-67.0607	8.70E-68	3.16E-65	4.35E-65		500
Montmor-Na	-63.1539	7.02E-64	2.57E-61	3.51E-61		500.00713
Nontronite-Ca	-12.5543	2.79E-13	1.18E-10	3.66E-11		131.1006
Nontronite-K	-9.6339	2.32E-10	1.00E-07	3.14E-08		135.27007
Nontronite-Mg	-13.1267	7.47E-14	3.15E-11	9.69E-12		129.76012
Nontronite-Na	-9.2114	6.15E-10	2.61E-07	8.12E-08		132.10979
			1.43E-01	1.83E-02		

Workbook WP10CSNG.XLS, Sheet "Carbon Steel 600 yr"

pH 10 solution from LaBS pkg reacting with carbon steel											
Anoxic Conditions		EQ6 Output File wp10CSNG.6o									
Package Inventory											
		moles	grams	wt% fissile							
	U	1.32E+02	3.13E+04	3.1300%							
	Pu	5.90E+02	1.41E+05	100.0000%							
	Flow Width	1.71E+02	cm	"shadow" of waste package							
	Flow Length	3.23E+02	cm	"shadow" of waste package							
	Flow Cross Section	5.52E+04	sq cm	same as slab deposit area							
Cell	Travel Time	Accumulated Solid For 1 kg of Water			Uranium			Plutonium		Fissile	
No.	Into Rock	Uranium	Plutonium	Total Solids	Uranium	Plutonium	U + Pu	Fissile	wt% of		
	d	Moles	Moles	g	g	g	g	g	U+Pu		
1	1.22E+01	0.00E+00	3.02E-04	1.19E-01	0.00E+00	7.21E-02	7.21E-02	7.21E-02	100.00%		
2	1.13E+03	0.00E+00	7.01E-05	2.41E-02	0.00E+00	1.68E-02	1.68E-02	1.68E-02	100.00%		
Total				1.43E-01	0.00E+00	8.88E-02	8.88E-02	8.88E-02			
Total Volume (cc)				1.83E-02							
Deposit on Steel Fragments											
Deposition	Infiltration Rate			Accumulation For The Deposition Period					Fissile	Slab Deposit**	
Time yr*	mm/yr	kg/yr	Total Solids	Total Solids	Uranium	Plutonium	U + Pu	Fissile	wt% of	Thickness	
			cc	g	g	g	g	g	U+Pu	cm	
*	600	1.00E-01	5.52E-01	6.05E+00	4.73E+01	0.00E+00	2.94E+01	2.94E+01	2.94E+01	100.00%	1.10E-04
*	600	1.00E+00	5.52E+00	6.05E+01	4.73E+02	0.00E+00	2.94E+02	2.94E+02	2.94E+02	100.00%	1.10E-03
*	400	5.00E+00	2.76E+01	2.02E+02	1.58E+03	0.00E+00	9.81E+02	9.81E+02	9.81E+02	100.00%	3.65E-03
*	300	1.00E+01	5.52E+01	3.03E+02	2.36E+03	0.00E+00	1.47E+03	1.47E+03	1.47E+03	100.00%	5.48E-03
*Equals the duration of pH 10 condition which is less at higher infiltrations due to flushing effects											
** The deposit is viewed as a slab of this thickness spread out over an area = to the package footprint											
The deposit could be accumulated in a smaller area (where there is iron)											

Workbook WP10CSNG.XLS, Sheet "Carbon Steel 600 yr"(Formulas Displayed)

	A	B	C	D	E	F	G	
1		pH 10 solution from LaBS pkg reacting with carbon steel						
2		Anoxic Conditions					EQ6 Output File wp10CSNG.6o	
3								
4		Package Inventory						
5				moles	grams	wt% fissile		
6			U	131.57	31313.66	0.0313		
7			Pu	589.92	140990.88	1		
8								
9			Flow Width	170.9	cm	"shadow" of waste package		
10			Flow Length	323	cm	"shadow" of waste package		
11			Flow Cross Section	=E10*E11	sq cm	same as slab deposit area		
12								
13		Cell	Travel Time		Accumulated Solid For 1 kg of Water			
14		No.	Into Rock	Uranium	Plutonium	Total Solids	Uranium	
15			d	Moles	Moles	g	g	
16		1	12.2	0	=Cell 1'D8	=Cell 1'E25	=E17*238	
17		2	1130	0	=Cell 2'D8-'Cell 1'D8	=Cell 2'E24-'Cell 1'E25	=E18*238	
18		Total				=SUM(G17:G18)	=SUM(H17:H18)	
19		Total Volume (cc)				=Cell 2'F24		
20								
21				Deposit on Steel Fragments				
22								
23			Deposition	Infiltration Rate			Accumulation For The Deposition Period	
24			Time yr*	mm/yr	kg/yr	Total Solids	Total Solids	
25						cc	g	
26		*	600	0.1	=\$E\$12*E27/10/1000	=F27*\$G\$20*\$D27	=\$G\$19*\$F27*\$D27	
27		*	600	1	=\$E\$12*E28/10/1000	=F28*\$G\$20*\$D28	=\$G\$19*\$F28*\$D28	
28		*	400	5	=\$E\$12*E29/10/1000	=F29*\$G\$20*\$D29	=\$G\$19*\$F29*\$D29	
29		*	300	10	=\$E\$12*E30/10/1000	=F30*\$G\$20*\$D30	=\$G\$19*\$F30*\$D30	

	H	I	J	K	L	M
1						
2						
3						
4						
5						
6						
7						
8						
9						
10						
11						
12						
13				Fissile		
14	Plutonium	U + Pu	Fissile	wt% of		
15	g	g	g	U+Pu		
16	=F17*239	=H17+I17	=(H17*\$G\$7+I17)	=K17/J17		
17	=F18*239	=H18+I18	=(H18*\$G\$7+I18)	=K18/J18		
18	=SUM(I17:I18)	=SUM(J17:J18)	=SUM(K17:K18)			
19						
20						
21						
22						
23					Fissile	Slab Deposit**
24	Uranium	Plutonium	U + Pu	Fissile	wt% of	Thickness
25	g	g	g	g	U+Pu	cm
26	=\$H\$19*\$F27*\$D27	=\$I\$19*\$F27*\$D27	=I27+J27	=(I27*\$G\$7+J27)	=L27/K27	=G27/\$E\$12
27	=\$H\$19*\$F28*\$D28	=\$I\$19*\$F28*\$D28	=I28+J28	=(I28*\$G\$7+J28)	=L28/K28	=G28/\$E\$12
28	=\$H\$19*\$F29*\$D29	=\$I\$19*\$F29*\$D29	=I29+J29	=(I29*\$G\$7+J29)	=L29/K29	=G29/\$E\$12
29	=\$H\$19*\$F30*\$D30	=\$I\$19*\$F30*\$D30	=I30+J30	=(I30*\$G\$7+J30)	=L30/K30	=G30/\$E\$12

I.6 Water Chemistry

For computations in which water is mixed into water already existing in the system under consideration, specifically into the solution inside a waste package or with an effluent from a waste package, EQ6 requires a composition of the water configured as a "special reactant" The following spread sheet shows this recalculation from the water analysis. Traces of additional elements have been added to enable calculations for these elements that are present in the waste or other materials, but were not reported in the water analysis.

Workbook WATERTAB.XLS, Sheet "Water"

J-13 water. Columns A-C: Adjusted for pH 7.6397 and log fO2 = -2.5390 to be consistent with thermodynamic data. Original molalities from Ref. 5.09; adjustments in EQ6 run j13avg20.6o. These data used for oxide fuel calculations.						
Col. E- G correspond to original data, balanced on Cl- and for log fO2 = -3.500						
These data were used for runs with glass waste before a method was devised to make a suitable adjustment to the raw data. The effect on the results is insignificant because the dissolution of the DHLW quickly dominates the chemistry.						
J-13 water	Molality	Mole Fr.		J-13 water	Molality	Mole Fr.
Na	1.99e-03	1.20e-05		Na	1.99e-03	1.20e-05
Si	1.02e-03	6.11e-06		Si	1.02e-03	6.11e-06
Ca	3.24e-04	1.95e-06		Ca	3.24e-04	1.95e-06
K	1.29e-04	7.74e-07		K	1.29e-04	7.74e-07
C	2.18e-03	1.31e-05		C	1.45e-04	8.69e-07
F	1.15e-04	6.89e-07		F	1.15e-04	6.89e-07
Cl	2.01e-04	1.21e-06		Cl	2.15e-04	1.29e-06
N	1.42e-04	8.53e-07		N	1.42e-04	8.53e-07
Mg	8.27e-05	4.97e-07		Mg	8.27e-05	4.97e-07
S	1.92e-04	1.15e-06		S	1.92e-04	1.15e-06
B	1.24e-05	7.44e-08		B	1.24e-05	7.44e-08
P	1.27e-06	7.63e-09		P	1.27e-06	7.63e-09
H	1.11e+02	6.67e-01		H	1.11e+02	6.67e-01
Al	1.48e-08	8.90e-11		O	5.55e+01	3.33e-01
Ba	1.00e-10	6.00e-13			1.67e+02	1.00e+00
Ce	1.00e-24	6.00e-27				
Cr	3.45e-07	2.07e-09				
Cu	1.00e-10	6.00e-13				
Cs	1.00e-10	6.00e-13				
Fe	1.15e-04	6.89e-07				
Gd	1.00e-14	6.00e-17				
La	1.00e-14	6.00e-17				
Li	1.00e-10	6.00e-13				
Mn	7.28e-07	4.37e-09				
Mo	1.00e-10	6.00e-13				
Nd	1.00e-14	6.00e-17				
Ni	1.00e-10	6.00e-13				
Pb	1.00e-10	6.00e-13				
Pu	1.00e-14	6.00e-17				

Sm	1.00e-10	6.00e-13				
Sr	1.00e-10	6.00e-13				
Ti	1.00e-10	6.00e-13				
U	1.00e-14	6.00e-17				
Zn	1.00e-10	6.00e-13				
Zr	1.00e-20	6.00e-23				
O	5.55e+01	3.33e-01				
	1.67e+02	1.00e+00				

I.7 Metal Chemistry

This section provides spreadsheets showing the calculation of the various metals as "special reactants" together with calculations of rates of degradation.

I.7.1 Steels**Workbook STEELTAB.XLS, Sheet "316SS"**

316L stainless steel, taken from p. I-5 of BBA000000-01717-0200-00002 REV 00, Ref. 5.92						
Element	At. Wt.	Wt%	g-Atoms	Atom Fr.	Mol. Wt.	
C	1.20e+01	3.00e-02	2.50e-03	1.37e-03		
N	1.41e+01	1.00e-01	7.11e-03	3.89e-03		
Si	2.81e+01	7.50e-01	2.67e-02	1.46e-02		
P	3.10e+01	4.50e-02	1.45e-03	7.96e-04		
S	3.21e+01	3.00e-02	9.36e-04	5.13e-04		
Cr	5.20e+01	1.70e+01	3.27e-01	1.79e-01		
Mn	5.49e+01	2.00e+00	3.64e-02	1.99e-02		
Fe	5.49e+01	6.55e+01	1.19e+00	6.54e-01		
Ni	5.87e+01	1.20e+01	2.04e-01	1.12e-01		
Mo	9.59e+01	2.50e+00	2.61e-02	1.43e-02		
		1.00e+02	1.83e+00	1.00e+00	5.48e+01	= "mol. wt." (weight of 1 "mole" of steel)

Workbook STEELTAB.XLS, Sheet "C-Steel"

Carbon Steel for baskets, from Design Analysis report BBA000000-01717-0200-00002 REV 00, Ref. 5.92						
Element	At. Wt.	Wt%	g-Atoms	Atom Fr.	Mol. Wt.	
Fe	5.49e+01	9.85e+01	1.79e+00	1.59e+03		
Mn	5.49e+01	9.00e-01	1.64e-02	1.45e+01		
S	3.21e+01	3.50e-02	1.09e-03	9.66e-01		
P	3.10e+01	3.50e-02	1.13e-03	1.00e+00		
Si	2.81e+01	2.75e-01	9.79e-03	8.67e+00		
C	1.20e+01	2.20e-01	1.83e-02	1.62e+01		
		1.00e+02	1.84e+00	1.63e+03	5.43e+01	= "mol. wt." (weight of 1 "mole" of steel)

Workbook STEELTAB.XLS, Sheet "B-Steel"

Borated Type 316 Steel for baskets, from Design Analysis report BBA000000-01717-0200-00002 REV 00, Ref. 5.92						
Element	At. Wt.	Wt%	g-Atoms	Atom Fr.	Mol. Wt.	
B	1.08e+01	1.28e+00	1.19e-01	6.18e-02		

C	1.20e+01	3.01e-02	2.51e-03	1.30e-03		
N	1.41e+01	1.00e-01	7.13e-03	3.71e-03		
Si	2.81e+01	7.52e-01	2.68e-02	1.39e-02		
P	3.10e+01	4.51e-02	1.46e-03	7.58e-04		
S	3.21e+01	3.01e-02	9.39e-04	4.89e-04		
Cr	5.20e+01	1.91e+01	3.67e-01	1.91e-01		
Mn	5.49e+01	2.01e+00	3.65e-02	1.90e-02		
Fe	5.49e+01	6.06e+01	1.10e+00	5.74e-01		
Ni	5.87e+01	1.35e+01	2.31e-01	1.20e-01		
Mo	9.59e+01	2.51e+00	2.61e-02	1.36e-02		
		1.00e+02	1.92e+00	1.00e+00	5.20e+01	= "mol. wt." (weight of 1 "mole" of steel)

Workbook STEELTAB.XLS, Sheet "304L"

304L Stainless Steel, Ref. 5.92					
Element	At. Wt.	Wt%	g-Atoms	Atom Fr.	Mol. Wt.
C	1.20e+01	3.00e-02	2.50e-03	1.37e-03	
Mn	5.49e+01	2.00e+00	3.64e-02	1.99e-02	
P	3.10e+01	4.50e-02	1.45e-03	7.94e-04	
S	3.21e+01	3.00e-02	9.36e-04	5.11e-04	
Si	2.81e+01	7.50e-01	2.67e-02	1.46e-02	
Cr	5.20e+01	1.90e+01	3.65e-01	2.00e-01	
Ni	5.87e+01	1.00e+01	1.70e-01	9.31e-02	
N	1.40e+01	1.00e-01	7.14e-03	3.90e-03	
Fe	5.58e+01	6.80e+01	1.22e+00	6.66e-01	
			1.83e+00		5.47e+01 = "mol. wt." (weight of 1 "mole" of steel)

I.7.2 Alloy Composition

Workbook STEELTAB.XLS, Sheet "625"

The atom fractions and "molecular weight" of this alloy have been figured in two ways because at the present time Nb is not in the EQ3/6 data base. Because it constitutes only a small percentage of the total and behaves chemically in a similar manner to Cr, it was not believed necessary to add this element to the data base.

Alloy 625							
Element	At. Wt.	Wt%	g-Atoms	Atom Fr.	Atom Fr. less Nb	Mol. Wt.	Mol. Wt. less Nb
Cr	5.20e+01	2.15e+01	4.13e-01	2.48e-01	2.54e-01		

Ni	5.87e+01	6.59e+01	1.12e+00	6.72e-01	6.89e-01				
Mo	9.59e+01	9.00e+00	9.38e-02	5.62e-02	5.76e-02				
Nb	9.29e+01	3.65e+00	3.93e-02	2.36e-02					
		1.00e+02	1.67e+00	1.00e+00	1.00e+00		5.99e+01		= "mol. wt." (weight of 1 "mole" of metal)
			1.63e+00					6.14e+01	= "mol. wt." (weight of 1 "mole" of metal)

I.7.3 Metal Corrosion Rates

Workbook STEELTAB.XLS, Sheet "Rates"

Rates of reaction for metals					
Material	Rate, um/yr	Rt, cm ³ /sec ¹	Density, g/cm ³	Rt, g/cm ² /s	Rt, mols/cm ² /s
304L*	2.50e+00	7.93e-12	7.90e+00	6.26e-11	1.15e-12
304L**	1.50e-01	4.76e-09	7.90e+00	3.76e-08	6.87e-10
Alloy 625***	2.54e+00	8.05e-12	8.44e+00	6.80e-11	1.13e-12
B-SS****	8.00e-01	2.54e-12	7.75e+00	1.97e-11	3.28e-13
C-steel *****	3.00e+01	9.51e-11	7.83e+00	7.45e-10	1.37e-11
¹ per cm ² of surface area					
* From Ref. 5.8, p. 12. Selected as reasonably conservative from the data presented.					
** Average of "general corrosion rate of" 0.1-0.2E-06 m/yr, Ref. 5.9, p. 4-2. This applies for near neutral solutions.					
*** No data available for relevant conditions. Rate conservatively assumed to be no more than 0.001 in /yr					
**** Ref. 5.8, p. 12					
***** Ref. 5.8, p. 27					

Algorithm for Successive Runs Simulating Flow and Transport

EQ6 is basically a batch code which does not have a built-in capacity for doing flow-through transport calculations. An automated system for performing repeated runs in EQ6 was developed. Using the automated system a series of EQ6 runs can be made exchanging a preset amount of water with fresh inlet water thus simulating a flushing through of infiltrating water. This is especially useful when the infiltration rate becomes much higher than 1mm per yr since it can simulate the dilution effect of the new water coming in. This section describes how this automated system works and lists the text files for all of its component parts. The text files are also included in the electronic files attachment (Section 9.2). Because this scheme rapidly produces a great deal of output, the algorithm was set up to retain only the most essential information. This is done by creating two files, initially named allin, which contains the input data for each of the successive runs, and allout, which contains the important results but does not twice repeat the input file portion of the normal output file, nor other information which occupies considerable space. It is also important to run a complete set of runs piecemeal, utilizing the last pickup file, from a file initially named allpick, in order to keep files small enough to retrieve the output into a buffer where it can be read. (It is impractical to print the entire file.) Therefore, the output from a "run" will be found in several files, each of which picks up where the previous one stopped.

The system works as follows:

Algorithm for Changing the Pickup File for Flow Through

In the algorithm, x = moles of solvent water at the start of the current run, y = moles of water at end of current run, and z = moles of water added by mixing in new J-13 water during the current run. "Current run" means the one used for the source of data to set up the next run in the sequence. z is delta moles of J-13 solution, as reported in the output file of EQ6, divided by an appropriate factor, e.g., 3. See the logic section below for an explanation.

The algorithm calculates $r = xy/(x+z)$ -- see logic below.

From the pickup file, p = moles aqueous is read from the last column of the first table listing chemical composition data.

From the pickup file, q = total moles is read from the middle column of the first table listing chemical composition data.

The algorithm then replaces p by rp/y , and replaces q by $q-p+rp/y$. [$r/y = x/(x+z)$]

The algorithm then adjusts the logarithmic basis species by taking a proportion:

- a. It reads the logarithmic species value from pickup file (except for H⁺ and species O₂ and thereafter). This is the log of the molality of the uncomplexed basis species. Here this value is called g .
- b. It takes the antilog, here called h , multiplies it by the reduction factor $x/(x+z)$ to get h' . takes the log of h' to get g' and replaces g by g' in the pickup file.

This procedure involves the assumption that the ratio of free to total aqueous species of an element at the end of the process of first admixing a solution in relatively large amounts, then removing a corresponding amount of the resulting solution, as the ratio would be if this process were performed during each step of reaction progress in EQ6. The resultant new set of logarithmic basis species need only be good enough to permit the Newton Raphson algorithm in EQ6 to converge.

Logic:

The objective is to change the pickup file to correspond to losses to the system that would result from outflow of solution produced by influx of a water solution, e.g., J-13 well water, from outside the system as changed by reaction within the system in such a way as to maintain the volume of influx equal, at least approximately, to the volume of efflux. To accomplish this:

1. From the output file, note the number of moles of J-13 added, e.g., delta J-13 divided by the mole fraction of oxygen in the solution that corresponds to free water (this excludes the oxygen tied up in sulfate, carbonate, etc.), and call this z .

Let z' be the number of moles of J-13 solution added. This needs to be modified by an appropriate factor, which for dilute solutions is $1/3$. This factor is the atom fraction of oxygen in pure water; for pure water the solution would be normalized to two gram atoms of H plus one gram atom of O to yield a normalization factor of $1/3$. In order to add the right number of moles of water into the system, relative to the infiltration rate which is entered as the moles of solution added per second (the product of $rk1$ and sk), by means of the mixing option in EQ6 the "moles" of solution must be multiplied by 3, which is done by means of specifying a value of 3 for fx in the input file. [Most of this added water is added to the moles of solvent water, the rest entering clays and other hydrous solids.] This means that the number in the output file for delta moles of solution is three times the moles of water added to the system. Hence, to make the appropriate changes to the pickup file, delta moles must be divided by 3. [There exist other ways of setting up the problem, e.g., using mole fractions of oxides rather than of elements; so long as internal consistency is maintained between the way the run is set up in the input file and the algorithm, correct results can be obtained.]

For more concentrated solutions the normalization factor must again be the ratio of moles of free water to moles of solution. The moles of free water may be determined by subtracting the gram atoms of sulfate, carbonate, water incorporated into aqueous complexes, etc. from the total number of gram atoms of oxygen in the solution. Thus, in this case, i.e. an inflowing concentrated solution, fx should be the ratio, moles of solution/moles of free water. Likewise, in making changes to the pickup file, delta moles must be divided by this factor. The default value in the algorithm is 3, but may be changed at run time.

The calculational scheme involves adding "new" solution, e.g., J-13 well water, as a special reactant, in keeping with the fluid mixing option in EQ6.

2. From the output file, note the number of moles of solvent water at the end of the preceding run, x , and the amount at the end of the current run, y .

3. Need is to subtract the amount of water added, minus the share of this added water that entered clays and other hydrous solids. In this way the water added is removed from the aqueous system, partly by entering solids and the rest by flowing out of the system.

4. The total water entering clays (and other solids) = amount of solvent water initially present + the amount of solvent water in J-13 added - amount of solvent water present at the end. This yields the total water entering clays as $x + z - y$.

5. Of the amount of water that enters solids the share that comes from newly added J-13 is $z/(x + z)$, the ratio of new solvent water to the total solvent water before solids are formed. Therefore, the amount of newly added water that enters solids is $z(x + z - y)/(x + z)$. To keep the total water in the system constant the remainder of the newly added water, s , needs to be removed.

6. Then, $s = z - z(x + z - y)/(x + z) = zy/(x + z)$. This amount in turn needs to be subtracted from the current amount of solvent water, y . Call this remainder r . After doing the algebra, we get $r = y - zy/(x + z) = xy/(x + z)$

7. From this analysis we conclude that the proper amount of water for the next step (run) is r , so the fraction of solvent water remaining is r/y . This leads to the conclusion that the correct amount of moles in the aqueous solution is obtained by multiplying moles aqueous by $r/y = x/(x + z)$.

8. The final objective is to change the pickup file. Needs here are to adjust values for "moles", "moles aqueous", and "logarithmic basis species".

9. From the pickup file call "moles aqueous" p . Then, following the conclusion in step 7, we get a new quantity, called $m = rp/y$. This is the new amount to enter in the "moles aqueous" column to replace p .

10. Next we need to correct the "moles" column. Call the entry here q , which is the sum of "moles aqueous" and moles solid. The number of moles of solid remains the same, and the aqueous portion is to be adjusted to equal m . Moles of solid is $q - p$. Thus, the new quantity should be $q - p + m = n$.

11. Repeat steps 9 & 10 for all elements, except for gases, e.g., $O_2(g)$.

12. Correct logarithmic basis species. These entries are the logarithms of the molalities of uncomplexed basis species. The logic is to decrease these molalities in the same proportion as used for decreasing the total moles of aqueous species. This is easily accomplished by reading a value of the logarithmic basis species, taking the antilog, multiplying by the reduction factor, taking the log, and entering the result as the new value of the logarithmic basis species.

bldinput.bat

```

echo "did not run bldinput" >sfile
count=1
bldinput
read status <sfile
if [ "$status" != "go" ]
then
    echo $status
    echo "job terminated"
    exit
fi
echo $count
while [ $count -lt 20 ]
do
    mv bldinput.out input
    eq6dR136.opt
    cat input >> allin
    cat pickup >> allpick
    cat output >> allout
    cat tab >> alltab
    ntxtinput
    read status <sfile
    if [ "$status" != "go" ]
    then
        echo $status
        echo "job terminated"
        exit
    fi
    count=`expr $count + 1`
    echo $count
done
exit

```

bldinput.in

```

root      date      creator      delmaxtime
autofloII 08/16/97    Automated    2.1e+08

#include <stdio.h>
#include <string.h>
#include <stdlib.h>
#include <math.h>
float  getfloat(char*,int,int);
void  setup(),bldpick(),infromstd(),infromlast(),
      strinsert(char*,char*,int,int);
int  locate0(char*,FILE*),locateall(char*,FILE*),tobar(char*,int);
float  duration,delmaxtime;
char  dummy[100],buffer[90],lookahead[90];
char  froot[20],cname[20],fname[20];
FILE  *fin,*fout,*fp,*ftemp,*fstd,*foutout,*finin,*fsfile;

void  main()
{int  i,j,k,flag;
fsfile=fopen("sfile","w");
fprintf(fsfile,"go\n");
flag=1;
fout=fopen("bldinput.out","w");/*file to be moved to input*/
if(flag==1) infromstd();
/*else infromlast();*/}

void  infromstd()
{int  i,j,k;

```

```

char tempstr[20],datestr[10];
fstd=fopen("input","r");/*template for initial input file*/
fin=fopen("bldinput.in","r");/*filename,creator,duration*/
fgets(dummy,100,fin);/*readthrough labels of setup data*/
fscanf(fin,"%s %s %s %f",froot,datestr,cname,&delmaxtime);
strcpy(fname,froot);
strcat(fname,"1.6i      ");
locate0("|EQ",fstd);
strinsert(dummy,fname,22,strlen(fname));
fputs(dummy,fout);
locate0("|Created",fstd);
strcat(cname,"      ");
strinsert(dummy,datestr,9,8);
strinsert(dummy,cname,30,strlen(cname));
fputs(dummy,fout);
locate0("| starting time",fstd);
i=tobar(dummy,1);
if(i<0)
    {printf("couldn't find |");
    exit(0);}
i=tobar(dummy,i+1);
if(i<0)
    {printf("couldn't find |");
    exit(0);}
i=tobar(dummy,i+1);
if(i<0)
    {printf("couldn't find |");
    exit(0);}
sprintf(tempstr,"%12.5e",delmaxtime);
k=strlen(tempstr);
j=tobar(dummy,i+1);
if(j<0)
    {printf("couldn't find |");
    exit(0);}
strncat(tempstr,"      ",j-i-1-k);
strinsert(dummy,tempstr,i+1,j-i-1);
fputs(dummy,fout);
while(fgets(dummy,90,fstd)!=NULL)fputs(dummy,fout);}

void strinsert(char inline[90],char insert[90],int start,int len)
{int i;
for(i=0;i<len;i++) inline[start+i]=insert[i];}

int locate0(char sstring[50],FILE *fp)
{int i=0;
while(fgets(dummy,90,fp)!=NULL)
    {if(strncmp(dummy,sstring,strlen(sstring))==0)return i;
    i++;
    fputs(dummy,fout);}
return 0;}

int tobar(char line[100],int start)
{int i;
i=start;
while((i<strlen(line))&&(line[i]!='|'))i++;
if(line[i]=='|')return i;
else return -1;}

```

nxtinput.bat

```

count=1
while [ $count -lt 23 ]
do
  mv bldinput.out input
  eq6dR136.opt
  cat input >> allin
  cat pickup >> allpick
  cat output >> allout
  cat tab >> alltab
  nxtinput
  read status <sfile
  if [ $status = "stop" ]
  then
    exit
  fi
  count=`expr $count + 1`
  echo $count
done
exit

```

nxtinput.c

```

#include <stdio.h>
#include <string.h>

#include <stdlib.h>
#include <math.h>
double getfloat(char*,int,int),gettobar(char*,int);
void setup(),bldpick(),infromstd(),infromlast(),
  convert(double,double,FILE*,FILE*),
  strinsert(char*,char*,int,int);
int locaterw(char*,FILE*,FILE*),locatero(char*,FILE*),
  locate2(char*,char*,FILE*),tobar(char*,int),
  puttobar(char*,char*,int),locatelof2(char*,char*,FILE*);
int finished=0;
double duration;
char dummy[100],tdummy[100];
char froot[20],cname[20],fname[20];
FILE *fout,*fpick,*fotemp,*fptemp,*fstd,*foutout,*finin,
  *fttemp,*fs,*fin;

void main()
{int i,j,k,flag;
fs=fopen("sfile","w");
fprintf(fs,"go\n");
flag=1;
fout=fopen("bldinput.out","w");/*file to be moved to input*/
infromlast();}

void infromlast()
{int i,j,k,dot;
char tempstr[30],carbstr[7],*cp,sstring[60],tempstr2[20];
double dmj13,msh2o,msh2ox,xx,yy,moles,dmoles,delmaxtime;
fin=fopen("bldinput.in","r");/*input parameters special to this case*/
fstd=fopen("input","r");/*template from last input file*/
fpick=fopen("pickup","r");/*old pickup file; extract section to bldinput.out*/
foutout=fopen("output","r");/*from last iteration to new input*/
finin=fopen("input","r");/*from last iteration to new input*/
fotemp=fopen("otemp","w");/*store intermediate segments from output*/
fptemp=fopen("ptemp","w");/*store intermediate segments from pickup*/
fgets(dummy,90,fin); /*readthrough labels*/

```

```

fscanf(fin,"%s %s %s %lf\n",
    tempstr,tempstr,tempstr,&delmaxtime);/*only 1 param used this prgrm*/
locatero("          Moles of solvent H2O",foutout);
msh2ox=getfloat(dummy,44,12); /*optional parameter from the first block*/
foutout=freopen("output","r",foutout);
strcpy(sstring,"          Reaction progress");
if(locatero(sstring,foutout)==-1) /*find output block of interest*/
    {printf("bad output file\n");
    exit(0);}
fputs(dummy,fotemp); /*and write it to temporary*/
while(fgets(dummy,90,foutout)!=NULL)
    {fputs(dummy,fotemp);
    if(strncmp(dummy,sstring,strlen(sstring))==0)
        {fotemp=freopen("otemp","w",fotemp);
        fputs(dummy,fotemp);}}
fotemp=freopen("otemp","r",fotemp);/*now reopen for use*/
if(locatero("c pickup file",fpick)==-1) /*start copying here*/
    {printf("bad pickup file\n");
    exit(0);}
fputs(dummy,fpotemp);
for(i=0;i<2;i++) /*readwrite through first "|EQ"*/
    {fgets(dummy,90,fpick);
    fputs(dummy,fpotemp);}
while(fgets(dummy,90,fpick)!=NULL) /*pickup to ptemp*/
    {fputs(dummy,fpotemp);
    if(strncmp(dummy,"|EQ",3)==0) /*read through without copying*/
        while(fgets(dummy,90,fpick)!=NULL)
            if(strncmp(dummy,"c pickup file",strlen("c pickup file"))==0)
                {fpotemp=freopen("ptemp","w",fpotemp);/*start copying over again*/
                fputs(dummy,fpotemp);
                for(i=0;i<2;i++)
                    {fgets(dummy,90,fpick);
                    fputs(dummy,fpotemp);}
                break;}}
fpotemp=freopen("ptemp","r",fpotemp); /*now reopen for use*/
if(locaterw("|EQ",fstd,fout)==-1)
    {printf("bad input file\n");
    exit(0);}
i=0;
while((i<strlen(dummy))&&(dummy[i]!='.'))i++;
dot=i;
i=0;
while((dummy[dot-i-1]<='9')&&(dummy[dot-i-1]>='0'))i++;
for(j=0;j<i;j++)tempstr[j]=dummy[dot-i+j];
tempstr[i]='\0';
k=atoi(tempstr);
sprintf(tempstr,"%u%s",k+1,".6i");
strinsert(dummy,tempstr,dot-i,strlen(tempstr));
fputs(dummy,fout);
fgets(dummy,90,fotemp);/*get ending value of zi from first line*/
xx=getfloat(dummy,48,22);
if(locaterw("| starting value of zi",fstd,fout)==-1)
    {printf("can't find starting zi in input file\n");
    exit(0);}
sprintf(tempstr,"%15.8lE",xx);
i=tobar(dummy,1);
strinsert(dummy,tempstr,i+1,strlen(tempstr));
fputs(dummy,fout); /*and put into input*/
fgets(dummy,90,fstd);
fputs(dummy,fout);
fgets(tdummy,90,fstd);/*this takes us to entry for starting time*/
if(locatero("          Time increased from",fotemp)==-1)
    {printf("can't find last ending time in output\n");
    exit(0);}
fgets(dummy,90,fotemp);/*this line will have end time of last run*/

```

```

xx=getfloat(dummy,31,12);
sprintf(tempstr,"%11.51E",xx);
i=tobar(tdummy,1);
if(i==--1)
  {printf("cant find slot for starttime\n");
  exit(0);}
strinsert(tdummy,tempstr,i+1,strlen(tempstr));
i=tobar(tdummy,i+1);
i=tobar(tdummy,i+1);
if(i==--1)
  {fs=freopen("sfile","w",fs);
  printf("cant find slot for maxtime\n");
  exit(0);}
/*yy=gettobar(tdummy,i+1); */
sprintf(tempstr,"%12.41E",xx+delmaxtime);
strinsert(tdummy,tempstr,i+1,strlen(tempstr));
fputs(tdummy,fout); /*and put into input*/
fotemp=freopen("otemp","r",fotemp); /*last read was beyond current interest*/
if(locatero("      Reactant                Moles      Delta
moles",fotemp)==-1)
  {printf("cant find values for reactants in the output file\n");
  exit(0);}
fgets(tdummy,90,fotemp);
fgets(tdummy,90,fotemp); /*get to first reactant in otemp*/
while((finished==0)&&(strncmp(tdummy,"\n",1)!=0)) /*loop to do all reactants*/
  {moles=getfloat(tdummy,29,10);
  dmoles=getfloat(tdummy,42,10);
  locaterw("| moles remaining",fstd,fout); /*next reactant*/
  sprintf(tempstr,"%10.41E",moles);
  strinsert(dummy,tempstr,20,strlen(tempstr));
  if(strncmp(tdummy," J-13 water",12)!=0)
    {sprintf(tempstr2,"%10.41E",dmoles);
    strinsert(dummy,tempstr2,58,strlen(tempstr2));}
  else
    {dmj13=dmoles;
    finished=1;} /*Water is the last reactant*/
  fputs(dummy,fout);
  fgets(tdummy,90,fotemp);}
if(locatero("      Moles of solvent H2O",fotemp)==-1)
  {fprintf(fs,"cant find moles water in output\n");
  exit(0);}
msh2o=getfloat(dummy,44,12);
k=locatero(" --- The reaction path has terminated normally",fotemp);
if(k==--1)
  {fputs("abnormal reaction path termination\n",fs);
  exit(0);}
fotemp=freopen("otemp","r",fotemp); /*back to the top again*/
if((k=locate2(" CO3--", " HCO3-",fotemp))==1) strcpy(carbstr,"| CO3--");
else if (k==2) strcpy(carbstr,"| HCO3-");
fttemp=fopen("ttemp","w"); /*will later attach to input*/
if(locatelof2("| CO3--", "| HCO3-",fttemp)==-1) /*also copies ptemp to ttemp*/
  {fprintf(fs,"cant find line to insert carbonates in pickup\n");
  exit(0);}
strinsert(dummy,carbstr,0,strlen(carbstr));
fputs(dummy,fttemp);
while(fgets(dummy,90,fttemp)!=NULL)fputs(dummy,fttemp); /*rest of ptemp to
ttemp*/
fttemp=freopen("ttemp","r",fttemp);
if(locaterw("c pickup file",fstd,fout)==-1) /*transfer the relevant remainder
of the template*/
  {fprintf(fs,"cant find start for pickup info\n");
  exit(0);}
convert(msh2o,dmj13/3,fstd,fttemp);}

int locatelof2(char sstring1[50],char sstring2[50],FILE *fp)

```

```

(int found1=0,found2=0;
while((found1==0)&&(found2==0))
  {if(fgets(dummy,90,fp)==NULL)return -1;
  if(found1==0)
    if(strncmp(dummy,sstring1,strlen(sstring1))==0)
      found1=1;
  if(found2==0)
    if(strncmp(dummy,sstring2,strlen(sstring2))==0)
      found2=1;
  if((found1==0)&&(found2==0))fputs(dummy,fttemp);}
if((found1==0)&&(found2==0))return -1;
else return 0;}

void strinsert(char inline[90],char insert[90],int start,int len)
{int i;
for(i=0;i<len;i++) inline[start+i]=insert[i];}

int locate2(char sstring1[50],char sstring2[50],FILE *fp)
{int i,found1=0,found2=0;
double x1=0,x2=0;
char buffer[100];
while((fgets(dummy,90,fp)!=NULL)&&((found1==0)|| (found2==0)))
  {strcpy(buffer,dummy);
  if(found1==0)
    if(strncmp(dummy,sstring1,strlen(sstring1))==0)
      {found1=1;
      x1=getfloat(dummy,28,12);}
  if(found2==0)
    if(strncmp(dummy,sstring2,strlen(sstring2))==0)
      {found2=1;
      x2=getfloat(dummy,28,12);}}
if(x1<x2) return 2;
else return 1;}

int locatero(char sstring[60],FILE *fp)/*read only*/
{while(fgets(dummy,90,fp)!=NULL)
  if(strncmp(dummy,sstring,strlen(sstring))==0)return 1;
return -1;}

int locaterw(char sstring[60],FILE *fpin,FILE *fpout)/*read&write*/
{while(fgets(dummy,90,fpin)!=NULL)
  {if(strncmp(dummy,sstring,strlen(sstring))==0)return 1;
  fputs(dummy,fpout);}
return -1;}

void convert(double x,double z,FILE *fins,FILE *finp)
{int i,count=0;
double u,v,w,r;
char buffer[100],temp[50],temp2[50];
r=x/(x+z);
if(locaterw("| elements, moles",finp,fout)==-1)/*readwrite to this point*/
  {printf("cant locate place to put new values of reagents in input\n");
  exit(0);}
fputs(dummy,fout);
fgets(buffer,90,finp);
fputs(buffer,fout);
fgets(buffer,98,finp);
while(strncmp(buffer,"|-----",8)!=0)
  {w=getfloat(buffer,55,21);
  v=w*r;
  u=getfloat(buffer,30,21)-w*(1-r);
  sprintf(temp,"%22.151E",u);
  strinsert(buffer,temp,29,strlen(temp));
  sprintf(temp,"%22.151E",v);
  strinsert(buffer,temp,54,strlen(temp));

```

```

    fputs(buffer, fout);
    fgets(buffer, 90, finp);
    count++;}
fputs(buffer, fout);
for(i=0;i<2;i++)
    {fgets(buffer, 100, finp); /*readthrough to species table*/
    fputs(buffer, fout);}
for(i=0;i<count;i++)
    {fgets(buffer, 100, finp);
    w=getfloat(buffer, 56, 22);
    sprintf(temp, "%+20.151E", w+log10(r));
    strinsert(buffer, temp, 56, strlen(temp));
    fputs(buffer, fout);}
while(fgets(buffer, 100, finp)!=NULL) fputs(buffer, fout);}

```

```

double getfloat(string, start, len)
char string[100];
int start, len;
{char temp[30];
strncpy(temp, string+start, len);
temp[len]='\0';
return atof(temp);}

```

```

double gettoabar(char line[100], int start)
{int i;
char temp[30];
i=start;
while((i<strlen(line))&&(line[i]!='|'))
    {temp[i-start]=line[i];
    i++;}
temp[i]='\0';
if(line[i]!='|')return -1;
return atof(temp);}

```

```

int puttobar(char line[100], char string[30], int start)
(int i, k;
i=start;
k=strlen(string);
while((i<strlen(line))&&(line[i]!='|')&&(i-start<k))
    {line[i]=string[i-start];
    i++;}
if(line[i]=='|')return i;
else return -1;}

```

```

int tobar(char line[100], int start)
(int i;
i=start;
while((i<strlen(line))&&(line[i]!='|'))i++;
if(line[i]=='|')return i;
else return -1;}

```

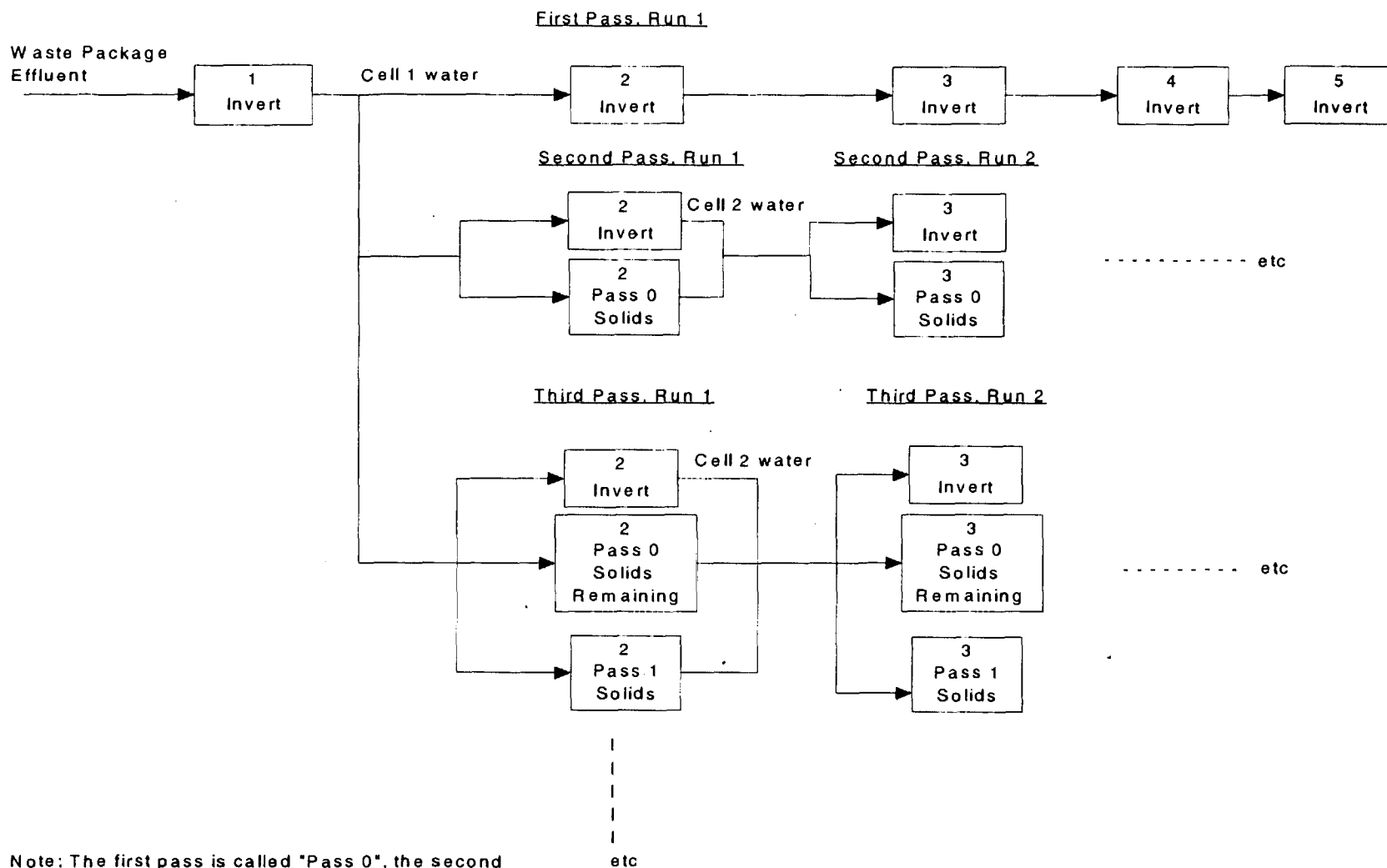
Description of the Modeling Approach between Effluent from the Waste Package and Invert or Rock, Using EQ6

The approach to modeling the reaction of waste package effluent with invert materials uses a feature of the EQ6 code which models an "open system". This feature follows an initial one kilogram of water as it passes through a reacting material. The water reacts with the reactant and solids are precipitated. In EQ6 the precipitated solids are "assigned" to a "physically removed subsystem" where they no longer react with the water. This is done periodically by the code as the movement of the water (simulated as time or "reaction progress") proceeds. This simulates the movement of the specific kg of water through the system, leaving behind it the precipitated material.

The "open system" feature is used for several successive runs to simulate successive kg quantities of water reacting with the invert and with the precipitated solids left behind by the previous kg of water. The scheme of runs is depicted in Figure III-1. Each successive kg of water contacting the solid is called a "pass". The first pass is a single EQ6 run as an open system. During the first pass the results show the history of the water chemistry and the solids deposited down the flow path. An effluent resulting from dissolution of waste package contents is used as the water for the first pass. This reacts with invert material (either crushed tuff or a concrete made with tuff as an aggregate). The results of the first pass are then used to define discrete periods of the reaction (also corresponding to time and distance) called "cells". The cells are defined either by a marked change in mineralogy or reasonable logarithmic time interval if no changes of mineralogy are seen for a long period. The reaction rates are quite slow and the mineralogy changes only a relatively few times. Therefore five cells or less is generally a reasonable discretization.

To simulate a successive kg of water several EQ6 runs are needed (First Pass, Run1; Second Pass, Run2; etc.). The starting water for Second Pass, Run 1 is taken as the water exiting the first cell of the First Pass in which there was no precipitation. In some instances there is no region where there is no precipitation. In this case the starting water for the second pass is waste package effluent again. Figure III-1 shows the case where there is no precipitation in Cell 1. The input water is introduced into the next cell (Cell 2 in the case shown in Figure III-1) and reacted with invert material and the solids that were deposited in that cell during the first pass. The code is only run for the time period corresponding to Cell 2. In the second pass, Run2, water from the second pass, Run 1 (from Cell 2) is reacted with invert material and Cell 3, first pass solids. The second pass, Run 2 proceeds for the time period corresponding to Cell 3. A similar progression is used for the rest of the second pass. The third pass follows the same pattern as shown in Figure III-1. Several EQ6 runs can then be used to simulate the buildup of solids by successive kg quantities of water passing through the invert which react with invert and residual solids left by previous kgs of water. The total material present is then the sum of previous reactants remaining and new deposited material.

Several conservative assumptions are applied to this model, notably Assumptions 5.16, 5.17, 5.18, and 5.19.



Note: The first pass is called "Pass 0", the second is called "Pass 1", the third "Pass 2" etc. in the computer runs.

Figure III-1 Model Scheme for EQ6 Calculations